Justus-Liebig-Universität Gießen

Fachbereich Agrarwissenschaften, Ökotrophologie und Umweltmanagement

Institut für Phytopathologie und Angewandte Zoologie

„Local and systemic defence signalling in plants"

Habilitationsschrift

Zur Erlangung der Lehrbefähigung für das Fach Molekulare Pflanzenphysiologie und

Molekulare Phytopathologie

Im Fachbereich Agrarwissenschaften, Ökotrophologie und Umweltmanagement

Der Justus-Liebig-Universität Gießen

Vorgelegt von

Dr. rer. nat. Frank Gaupels

München 2015

Local and systemic defence signalling in plants

Publications – Part 1. Functions of NO and ONOO⁻ in defence signalling

NO signals in the haze – Nitric oxide signalling in plant defence

Upstream and downstream signals of NO in pathogen defence

Detection of peroxynitrite accumulation in *Arabidopsis thaliana* during the hypersensitive defense response

Differential inhibition of *Arabidopsis* superoxide dismutases by peroxynitrite-mediated tyrosine nitration

Nitric oxide, antioxidants and prooxidants in plant defence responses

Publications – Part 2. Local and systemic defence responses of the phloem

A combinatory approach for analysis of protein sets in barley sieve-tube samples using EDTA-facilitated exudation and aphid stylectomy

Adaptation of aphid stylectomy for analyses of proteins and mRNAs in barley phloem sap

Nitric oxide generation in *Vicia faba* phloem cells reveals them to be sensitive detectors as well as possible systemic transducers of stress signals

Looking deep inside: detection of low-abundance proteins in leaf extracts of *Arabidopsis* and phloem exudates of pumpkin

Deciphering systemic wound responses of the pumpkin extrafascicular phloem by metabolomics and stable isotope-coded protein labeling

The extrafascicular phloem is made for fighting

General introduction

Local pathogen-induced defence signalling

Throughout their lifetime plants are attacked by a multitude of pathogens and herbivores. Apart from preformed barriers plants also dispose of very effective inducible defence mechanisms, which rely on successful recognition of the invading organism. A first layer of defence is activated upon perception of general microbe-associated molecular patterns (MAMPs) such as fungal chitin oligomers and bacterial lipopolysaccharides and flagellin (Boller and Felix, 2009). These elicitors bind to pattern-recognition receptors (PRRs) in the plant cell membrane leading to the establishment of pattern-triggered immunity (PTI). Early signalling involves calcium, reactive oxygen species (ROS), nitric oxide (NO) mitogen-activated protein (MAP) kinases and ethylene (Boller and Felix, 2009; Garcia-Brugger et al., 2006; Zipfel, 2014). However, some pathogens have developed means of escaping detection either by masking elicitors in their extracellular matrix or by injecting virulence proteins (effectors) into the host cell, which suppress signal cascades down-stream of the PRRs (Cui et al., 2014; Spoel and Dong, 2012). In the course of a second layer of activated pathogen resistance plants can perceive the pathogen's effector molecules, which then turn into avirulence (avr) factors, by intracellular resistance (R) receptors. The highly species-specific R-gene-mediated resistance is also known as effector-triggered immunity (ETI) (Cui et al., 2014; Spoel and Dong, 2012).

One hallmark of ETI is the hypersensitive response (HR) often mounting in programmed cell death (PCD). According to current knowledge SA interacts with ROS and NO during execution of HR-PCD in infected cells and induction of antimicrobial pathogenesis-related (*PR*) genes in neighbouring cells (Coll et al., 2011; Wu et al., 2014). Non-Expressor of PR1 (NPR1) is the central redox switch for SA-mediated defence responses. Upon pathogen-triggered cellular redox changes NPR1 monomers are released from cytoplasmic oligomers, and are translocated into the nucleus. The fate of nuclear NPR1 monomers is determined by the prevailing SA concentrations. High SA levels at the local infection site promote cell death through binding of the SA receptor NPR3 to NPR1, which is then degraded by the proteasome. Intermediate SA levels in nearby uninfected cells, however, favours dissociation of the SA receptor NPR4 from NPR1, cell survival and *PR* gene expression (Fu and Dong, 2013).

The roles of NO and ONOO$^-$ in HR cell death

During the past 20 years NO has emerged as an important player in ETI and HR-PCD signalling. Experiments amongst others with soybean cell cultures, Arabidopsis and

tobacco have consistently shown simultaneous synthesis of NO and H_2O_2 at approx. 4h after inoculation with different avirulent pathovars of *Pseudomonas syringae* (Delledonne et al., 1998; Scheler et al., 2013b; Wang et al., 2013). Synthesis of NO by a nitric oxide synthase (NOS)-like activity was essential for induction of HR-PCD as demonstrated by use of NO scavengers and mammalian NOS inhibitors - although also nitrate reductase (NR) contributed to the NO burst (Leitner et al., 2009a).

NO can exert signalling functions through binding to proteins via S-nitrosylation of cysteine (Cys) residues, which is mediated by the endogenous NO donor S-nitrosoglutathione (GSNO) and is under control of GSNO reductase (GSNOR) (Gaupels et al., 2011a; Kovacs and Lindermayr, 2013; Spoel and Loake, 2011). Recently, Tada et al. (2008) found that NPR1 is S-nitrosylated in *Arabidopsis* upon infection with avirulent *Pseudomonas syringae* pv. *maculicola* (*avrRpt2*). Monomerization and nuclear localization of NPR1 as well as subsequent *PR1* expression was suppressed by binding of NO to Cys156 but induced by action of the two thioredoxins TRX-h-3 and -5 (Kneeshaw et al., 2014; Tada et al., 2008) implying that S-nitrosylation is a reversible protein modification like phosphorylation. However, the exact mechanism of NPR1 regulation by S-nitrosylation and thioredoxin activity is still debated (Gaupels et al., 2011a; Lindermayr et al., 2010). New evidence hints at an additional role of NO in regulating *PR* gene expression by binding to the transcription factor TGA1. S-nitrosylation of Cys260 and -266 enhanced binding of TGA1 to DNA in the presence of NPR1 (Lindermayr et al., 2010). The biological significance of these *in vitro* results still awaits verification *in vivo*.

Meanwhile it is widely accepted that the cooperative action of NO and H_2O_2 is needed for full expression of a HR but the exact mode of cross-talk between these redox signals remains to be deciphered (Leitner et al., 2009; Wang et al., 2013). During HR-PCD NADPH oxidases are major sources of O_2^-, which then dismutates to H_2O_2 either spontaneously or catalysed by superoxide dismutases (SODs) (Scheler et al., 2013; Wang et al., 2013). NO facilitates accumulation of H_2O_2 by inhibition of the antioxidant enzymes catalase and ascorbate peroxidase (APX; Figure 1A) (Gross et al., 2013). For instance, cytosolic APX was S-nitrosylated during H_2O_2-induced PCD in tobacco suspension cell culture (de Pinto et al., 2013). Notably, NO synthesis is induced by H_2O_2 placing both signals in a positive feedback-loop (Gross et al., 2013). On the other hand, NO can also have antagonistic effects on H_2O_2 signalling. The NADPH oxidase Respiratory Burst Oxidase Homolog D (RBOHD) was S-nitrosylated at Cys890 in Arabidopsis challenged by avirulent *Pseudomonas syringae*, which caused inhibition of enzyme activity and a reduction in O_2^- levels at later stages of the HR (Yun et al., 2011). According to a model proposed by the authors of this study, prolonged exposure to increasing levels of NO

derivatives such as GSNO in the course of the plant pathogen interaction terminates the RBOHD-driven oxidative burst as a measure against runaway-cell death (Yun et al., 2011).
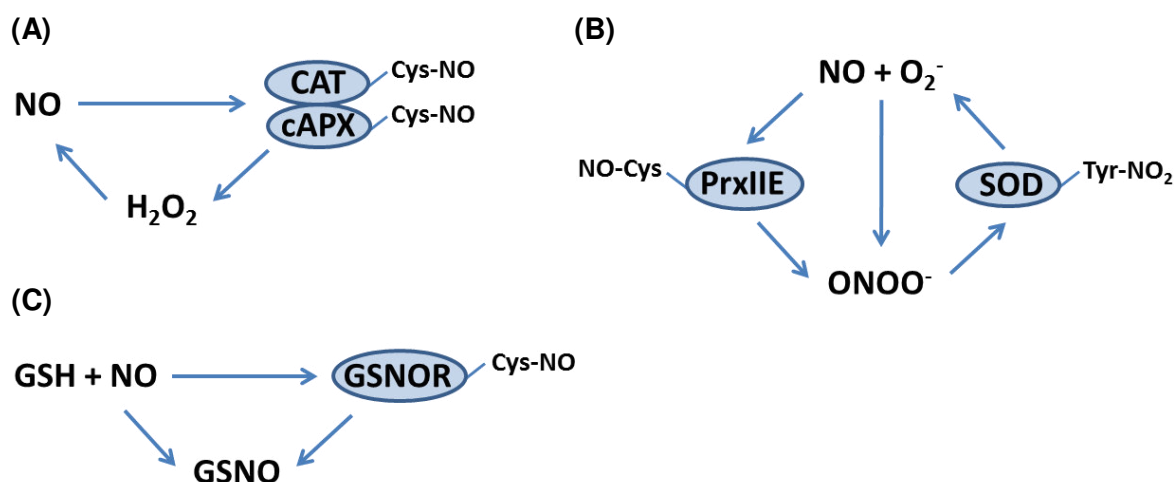

Figure 1 Amplification mechanisms in the interactions between NO, ROS and redox enzymes. **(A)** NO inhibits CAT and cytosolic APX by S-nitrosylation. Subsequent accumulation of H_2O_2, in turn, could amplify NO synthesis. **(B)** NO reacts with O_2^- to give $ONOO^-$, which might facilitate further accumulation of O_2^- by nitration-mediated inhibition of specific SOD isoforms (as shown for MSD1, FSD3 and CSD3 of Arabidopsis). Formation of $ONOO^-$ is enhanced by S-nitrosylation and inactivation of PrxIIE. **(C)** Accumulation of GSNO results from the reaction of reduced glutathione (GSH) with NO and is favoured by a simultaneous down-regulation of GSNOR through S-nitrosylation.

NO and O_2^- react with diffusion-limited kinetics thereby forming peroxynitrite ($ONOO^-$), which modifies proteins by nitration (NO_2 adduct) of tyrosine or tryptophane residues (Arasimowicz-Jelonek and Floryszak-Wieczorek, 2011; Gaupels et al., 2011a; Gaupels et al., 2011b). Tyrosine (Tyr)-nitrated proteins can be detected by immuno-blot analysis with anti-nitrotyrosine antibodies. Formation of $ONOO^-$ during the HR of Arabidopsis against avirulent bacteria was followed photometrically employing the fluorescent dye HKGreen-2 in a leaf disc assay. Fluorescence did not increase at 1-2 h but 3-8 h post infection coincident with the increase in ROS, NO and PCD (Gaupels et al., 2011b). The specificity of the probe was confirmed with the $ONOO^-$ scavenger urate. Cellular $ONOO^-$ levels are dependent on the rate of O_2^- and NO synthesis and the presence and activity of scavengers. Peroxiredoxin IIE (PrxIIE) degrades primarily $ONOO^-$ to NO_3^- and is a known target protein of NO during the bacteria-triggered HR in *Arabidopsis* (Romero-Puertas et al., 2008). S-nitrosylation caused inhibition of enzyme activity and a concomitant increase in levels of Tyr-nitrated proteins (Romero-Puertas et al., 2007). Hence, PrxIIE represents a prime example of cross-talk between two nitrogen oxide species, namely NO and $ONOO^-$ (Figure 1B).

To date, very little is known about putative physiological functions of $ONOO^-$. A current *in vitro* study provided evidence that isoforms of *Arabidopsis* superoxide dismutase

(SOD) might be differentially targeted by NO derivatives (Holzmeister et al., 2014). Cys-containing SOD isoforms were not affected by GSNO whereas $ONOO^-$ partially inhibited 3 of the 5 SODs containing at least one Tyr residue. Treatment with 0.5 mM $ONOO^-$ reduced the activity of mitochondrial Mn^{2+}-SOD1 (MSD1) by 90% but of peroxisomal Cu^{2+}-SOD3 (CSD3) and chloroplastic Fe^{2+}-SOD3 (FSD3) only by about 30% (Holzmeister et al., 2014). Site-directed mutagenesis revealed that MSD1 was inactivated through nitration of Tyr63. Modulation of SODs by tyrosine nitration has possible implications for the pathogen-induced PCD. Accumulation of O_2^- due to inhibition of SODs would further amplify the formation of $ONOO^-$ in the presence of NO (Figure 1B) (Holzmeister et al., 2014). The consequential shift from nitrosative compounds such as NO and N_2O_3 towards the nitrative compounds $ONOO^-$ and NO_2 (nitrogen dioxide) was proposed to be associated with cell protection from nitrosative stress (Thomas et al., 2008). Alternatively, the lack of SOD activity could also cause oxidative damage to mitochondria, which is a well-known early event in PCD initiation (Wang et al., 2013). If one of these hypothetical scenarios occurs *in vivo* will be unveiled in future research.

In sum, NO, ROS, redox-regulatory proteins and antioxidants form a complex signal network for induction of HR (Groß et al., 2013). NO interacts with ROS both directly as well as indirectly. The chemical reaction of NO with ROS releases new signal molecules such as $ONOO^-$ with properties and specificities different from their precursors. Another important function of NO is the amplification of the oxidative burst by inhibition of antioxidant enzymes and at the later stage of the HR dampening of ROS production by inhibition of NADPH oxidases. And there is more to come. Very recently, it was discovered that GSNOR can be inhibited by S-nitrosylation (Figure 1C) (Frungillo et al., 2014) further illustrating the complexity and interconnectedness of signal webs involving ROS, NO and redox enzymes.

The phloem

The phloem is a unique plant tissue highly specialized in distributing photoassimilates from photosynthetic active source leaves to sinks such as roots, young leaves and meristems. Sieve tubes are the transport conduits of the phloem consisting of an array of elongated cells called sieve elements (SEs) which are connected by largely perforated sieve plates. The enucleate SEs are supplied with nutrients and other vital compounds by the metabolically highly active companion cells (CCs) via characteristic pore/plasmodesma units. However, there are only few plasmodesmata between SE/CC-complexes and surrounding cells implying that most of the macromolecules and membrane-impermeable

small molecules present in the sieve tubes likely originate from CCs (Atkins et al., 2011; Lucas et al., 2013; Turnbull and Lopez-Cobollo, 2013; van Bel, 2003).

Contrary to old text-book knowledge, the phloem is not just a transport conduit for nutrients but it also synthesizes and translocates a large number of signals and defensive compounds as discussed in the following chapters. For a better understanding of phloem functions it would be necessary to raise a complete inventory of the structures and molecules present in the CCs and SEs. Unfortunately, the phloem is difficult to investigate because it is delicate and deeply embedded in other tissues. One very useful microscopy technique was invented by Michael Knoblauch and his colleagues (Knoblauch and van Bel, 1998). They produced shallow cortical cuts into the midveins of *Vicia faba* leaves for observation of living phloem. Previously, preparation of vascular tissues for microscopy produced wounding- and fixation-related artefacts. The new method allowed for the first time a detailed description of structures and physiological processes in undisturbed, actually transporting phloem (Knoblauch and van Bel, 1998).

Sampling of exudates from sieve tubes is complicated due to efficient occlusion mechanisms by callose plugging of the sieve plates. Facilitated exudation by placing cut plants in a solution with the calcium-scavenger EDTA for preventing callose formation is quick and easy but prone to artefacts (Dinant and Kehr, 2013). Stylectomy is a more elegant way of phloem sampling at least for monocots (Doering-Saad et al., 2002; Fisher et al., 1992; Gaupels et al., 2008a; Gaupels et al., 2008c). Aphid stylets are cut under the binocular e.g. using a radiofrequency microcautery unit and exuding droplets of pure SE content are collected for analysis. Recent improvements of stylectomy allows now sampling of up to 10 µL phloem sap per day as compared to nL yields of former set-ups (Gaupels et al., 2008a; Gaupels et al., 2008c). This way, more than 250 proteins were visualized in barley phloem sap sampled by stylectomy, and a total of 120 proteins were identified by mass spectrometry in rice and barley (Aki et al., 2008; Gaupels et al., 2008a).

Advanced techniques are required for analysis of the rather low concentrations of proteins, mRNAs and small molecules in sieve tube exudates. For example, cDNA-amplified fragment length polymorphism (cDNA-AFLP) was adapted for identification of barley phloem mRNA while rice phloem proteins were identified by nano-scale proteomics (Aki et al., 2008; Gaupels et al., 2008a). In exudates from cut stems and petioles of cucurbits the highly abundant Phloem Protein1 and -2 (PP1/PP2) interfere with protein analysis by electrophoresis and mass spectrometry because they mask similar-sized proteins and tend to precipitate upon oxidation. Therefore, we applied ProteoMiner beads for depletion of high- and enrichment of low-abundance proteins (Fröhlich et al., 2012; Gaupels et al., 2012). Wound-regulated changes in protein composition were subsequently

analyzed by gel-free stable isotope-coded protein labelling (ICPL). This way, we identified more than 320 proteins, of which 51 proteins were wound-regulated (Gaupels et al., 2012).

Altogether, analyses of phloem exudates from various plants suggest a complex set of non-assimilate compounds within the sieve tubes including proteins, RNA species, carbohydrates, and a multitude of small metabolites which have putative functions in sieve tube maintenance and defence against phloem-feeding insects and pathogens (AJ and Gaupels, 2004; Atkins et al., 2011; Gaupels et al., 2008b; Gaupels et al., 2012; Lin et al., 2009; Lucas et al., 2013; Turnbull and Lopez-Cobollo, 2013; van Bel, 2003). Although historically SEs were thought to be almost empty pipes optimized for transport functions new findings have revised this picture. Meanwhile it is well-established that this cell type disposes of an endoplasmatic reticulum (ER) and a parietal cytoskeleton (Hafke et al., 2013; Knoblauch and van Bel, 1998). Several proteins in pumpkin phloem exudates were related to membrane trafficking and vesicle transport (Fröhlich et al., 2012; Gaupels et al., 2012). Moreover, evidence is accumulating that at least in the cucurbit-specific extrafascicular phloem SEs have a functional machinery for protein translation, transport, modification and degradation (Fröhlich et al., 2012; Gaupels et al., 2012; Lin et al., 2009). This has also possible implications for defence responses and signal transduction in the phloem, e.g. the ER seems to serve as internal calcium store and mRNAs in the SEs are not necessarily signals as postulated before but could be translated into proteins. Cytoskeleton-mediated vesicle transport might even permit signal transport against the assimilation stream (Aoki et al., 2005).

Systemic signalling via the phloem

Long-distance signalling is essential for whole plant integration of photosynthesis, leaf movement, shade avoidance, flowering and other processes. Until now only a few signals have been demonstrated to be transported in the sieve tubes and exert their effects in systemic tissues. For instance, the protein FLOWERING LOCUS T is involved in floral induction while mRNAs of the genes *GIBBERRELIC ACID INSENSITIVE* and *KNOTTED-like* regulate leaf development (Corbesier et al., 2007; Haywood et al., 2005). Systemic signalling is also very common in plant defence against pathogens and herbivorous insects. Local induction of PTI as well as ETI can result in spreading of resistance to distal plant parts. The so-called systemic acquired resistance (SAR) is dependent on SA and NPR1 in the remote but not in the locally infected tissues (Dempsey and Klessig, 2012; Fu and Dong, 2013; Gaupels and Vlot, 2013). After the initial local infection plants are in a primed (alarmed) state and can trigger more efficiently pathogen defence mechanisms upon secondary infections of distal plant parts (Conrath, 2011). This enhanced immunity is

long-lasting and might even be inherited to the progeny via chromatin modifications (Conrath, 2011; Jaskiewicz et al., 2011; Spoel and Dong, 2012).

Similar to pathogen-triggered responses leaf damage by insect feeding triggers a systemic wound response (SWR) upon local perception of herbivore-associated molecular patterns (HAMPs) or damage-associated molecular patterns (DAMPs) by specific PRRs (Heil and Land, 2014; Wu and Baldwin, 2010). DAMPs are also released from pathogen infected tissues which could explain the observed overlap between herbivore- and pathogen-triggered responses (Heil and Land, 2014). Both local as well as systemic wound responses are dependent on JA (Gaupels and Vlot, 2013; Schilmiller and Howe, 2005; Wasternack, 2007). Disruption of phloem transport by heat or cold girdling of the stem provided evidence that systemic defence responses are dependent on phloem-bound signalling (Gaupels and Vlot, 2013). Based on these results many attempts have been undertaken in the past years to decipher SAR and SWR signalling processes. For that matter, the identification of phloem-transmitted systemic defence signals should meet the following criteria (Gaupels and Vlot, 2013): candidate compounds should (i) accumulate in sieve tube exudates after local stress, (ii) demonstrate phloem-mobility, and (iii) induce stress resistance systemically if exogenously applied or over-expressed.

To date, the known SAR signals which meet all these criteria are methyl salicylate (MeSA), azelaic acid (AzA), an unknown glycerol-3-phosphate-derived factor (G3P*) and dehydroabietenal (DA) (Shah et al., 2014). Park et al. (2007) uncovered methylated salicylate (SA) as an essential systemic SAR signal. MeSA was found in phloem exudates from virus-infected tobacco leaves. During establishment of SAR MeSA is produced from SA at the infection site by SA-Methyltransferase1 (SAMT1), transported in the sieve tubes and re-converted to SA in systemic leaves by the MeSA esterase SABP2 (SA-Binding Protein2) (Park et al., 2007). Later, it was reported that SAR can be induced in MeSA-deficient mutants and that MeSA signalling might be influenced by growth conditions, particularly by the light period (Attaran et al., 2009; Liu et al., 2011). The lipid-derived AzA has been implicated in systemic priming of SA-dependent defence signalling (Jung et al., 2009). AzA accumulated in petiole exudates after primary inoculation with avirulent bacteria and induced defence priming if locally applied to a leaf. The phloem-mobility was confirmed by detection of deuterium-labelled AzA in phloem sap and in distal leaves after local administration to one leaf (Jung et al., 2009). However, it is still debated how efficient AzA is transported in the phloem (Shah et al., 2014). The priming effect of AzA was dependent on the environmental conditions like reported also for MeSA (Liu et al., 2011; Shah et al., 2014).

Thus, there is still not a single essential signal known, which can alone and under all conditions induce SAR. A possible reason for this would be that parallel systemic

9

cascades or web of signals rather than a single signal evoke SAR (Gaupels and Vlot, 2013). This hypothesis is supported by recent publications on possible interactions of AzA with G3P* and DA (Shah et al., 2014). AzA induces SAR via G3P*, which might promote the conversion of MeSA to SA in systemic tissues (Gao et al., 2014). Systemic signal transmission by AzA and G3P* is dependent on the lipid transfer proteins Defective in Induced Resistance1 (DIR1) and Acelaic Acid Induced1 (AZI1) (Chanda et al., 2011; Yu et al., 2013). DA is a potent inducer of SAR in various plants. It is mobile in the phloem as evidenced by using an isotope derivative and stimulates SA signalling in systemic leaves (Chaturvedi et al., 2012). DA is hydrophobic and, therefore, can move in the sieve tubes only if bound to a high molecular weight complex containing DIR1. The synergistic action of AzA, G3P*, DA, DIR1 and AZI1 is required for the full extent of SAR (Shah et al., 2014; Yu et al., 2013).

During establishment of SWR JA derivatives were shown to be produced and transported in the phloem (Gaupels and Vlot, 2013). In an elegant set of grafting experiments with Arabidopsis mutants defective in JA biosynthesis or perception it was demonstrated that production of JA in the wounded leaf and perception of JA in systemic leaves is pivotal for induction of SWR (Li et al., 2002). The 18-amino-acid peptide systemin has been found exclusively in *Solanaceae*. The respective precursor PROSYSTEMIN is expressed in phloem parenchyma cells and systemin was hypothesized to interact with JA in a signal amplification loop within the phloem (Ryan and Moura, 2002). In Arabidopsis a family of peptides similar to systemin called *At*Pep1 to -6 is involved in stress defence signalling (Ryan et al., 2007). Expression of the precursor genes *PROPEP1-6* is up-regulated by wounding, methyl JA and ethylene (Yamaguchi et al., 2006). AtPeps and the corresponding receptors PEPR1-4 participate in the amplification of PTI (Bartels et al., 2013). If the peptides move long distances via the phloem similar to systemin was not yet investigated.

Local leaf wounding triggers rapid systemic signalling by membrane depolarization waves. The electrical signals move in the phloem and are dependent on Glutamate-Receptor-Like (GLR), which are putative calcium channels or pumps (Salvador-Recatala et al., 2014). Expression of marker genes for JA signalling in distal unwounded leaves correlated with phloem-based progression of the electrical signal and was attenuated in GLR-defective mutants (Mousavi et al., 2013; Salvador-Recatala et al., 2014). It would be interesting to learn more about the involved receptors and amplification mechanisms in the cooperative wound signalling by electric signals, JA and systemin (Koo et al., 2009). While electric signals have the advantage of being rapid the JA-systemin feedback loop might be important for improving signal specificity and duration. Other candidate SWR signals

include hydraulic xylem-transmitted signals, ethylene, abscisic acid (ABA), ROS and NO (Schilmiller and Howe, 2005; Wasternack, 2007; Miller et al., 2009).

Phloem-internal and systemic signalling by NO and ROS

NO is a general messenger in plant stress responses. For instance, NO accumulation was detected upon wounding and treatment with ozone, UV-B, heat, salt and hyperosmotic stress in various plant species (Besson-Bard et al., 2008; Leitner et al., 2009b; Mur et al., 2013). In plant defence against pathogens NO plays well-documented roles during the HR-PCD as well as in papilla formation during barley/powdery mildew-interactions (Mur et al., 2013). Although arginine-consuming NO production has been measured in various plant species, so far, no plant nitric oxide synthase (NOS) could be identified (Besson-Bard et al., 2008; Leitner et al., 2009). Other researchers found that nitrite is a source of NO in plants, derived either non-enzymatically at low pH or via nitrate reductase (NR) activity (Besson-Bard *et al.*, 2008; Leitner et al., 2009). Often NO has been shown to interact with ROS (Gross et al., 2013; Scheler et al., 2013). This was also observed during ozone exposure. Microarray analyses comparing Arabidopsis genes induced by fumigation with the reactive oxygen derivative ozone and treatment with the NO donor sodiumnitroprusside revealed a high overlap of about 75% between both data sets. From this result the authors concluded that NO functions as a major signal in the plant reaction to ozone exposure (Ahlfors et al., 2009).

In view of its high mobility, nitric oxide (NO) has been proposed to be a systemic stress signal (van Bel and Gaupels, 2004; Durner and Klessig, 1999; Gaupels and Vlot, 2013). Supportive of this suggestion was the detection of NO in vascular tissues. Using the fluorochrome 4,5-diamino-fluorescein diacetate (DAF-2 DA), NO was found in vascular bundles where it functioned in senescense, cell wall lignifications, salt stress response and pathogen defence (Corpas et al., 2004; Valderrama et al., 2007). Moreover, in a detailed microscopic study of the living intact phloem we could demonstrate NO synthesis in CCs of *Vicia faba* (Figure 2) (Gaupels et al., 2008b). The pathogen resistance and stress signals SA and H_2O_2 induced a strong NO-specific DAF fluorescence, which was dependent on calcium and could be blocked by inhibitors of NOS but not NR and by inhibitors of the mitochondrial electron transport chain. Significantly, NO was microscopically detected in SEs suggesting systemic transport of NO or NO-binding compounds (Figure 2B, C) (Gaupels et al., 2008b).

Since NO is produced in the phloem one would expect phloem proteins to be modified by S-nitrosylation and/or nitration under stress conditions. In fact, by western blot analyzes with nitrotyrosine antibodies we found accumulation of nitrated proteins in

phloem exudates of pumpkin plants which were watered with 10 mM H_2O_2 (Gaupels et al., 2008b). Additionally, wounding, the resistance inducer BION (50 mg/l soil), heat (40 °C), UV-B (100 mW/m^2), ozone (80 ppb) and salt (100 mM) turned out to be effective inducers of protein nitration in the pumpkin phloem (unpublished results). Similarly, Valderrama et al. (2007) visualized nitrated and S-nitrosylated proteins in the vascular tissue of salt-stressed olive plants with antibodies and new fluorescence probes. In neither of the latter studies NO-binding phloem proteins have been identified.
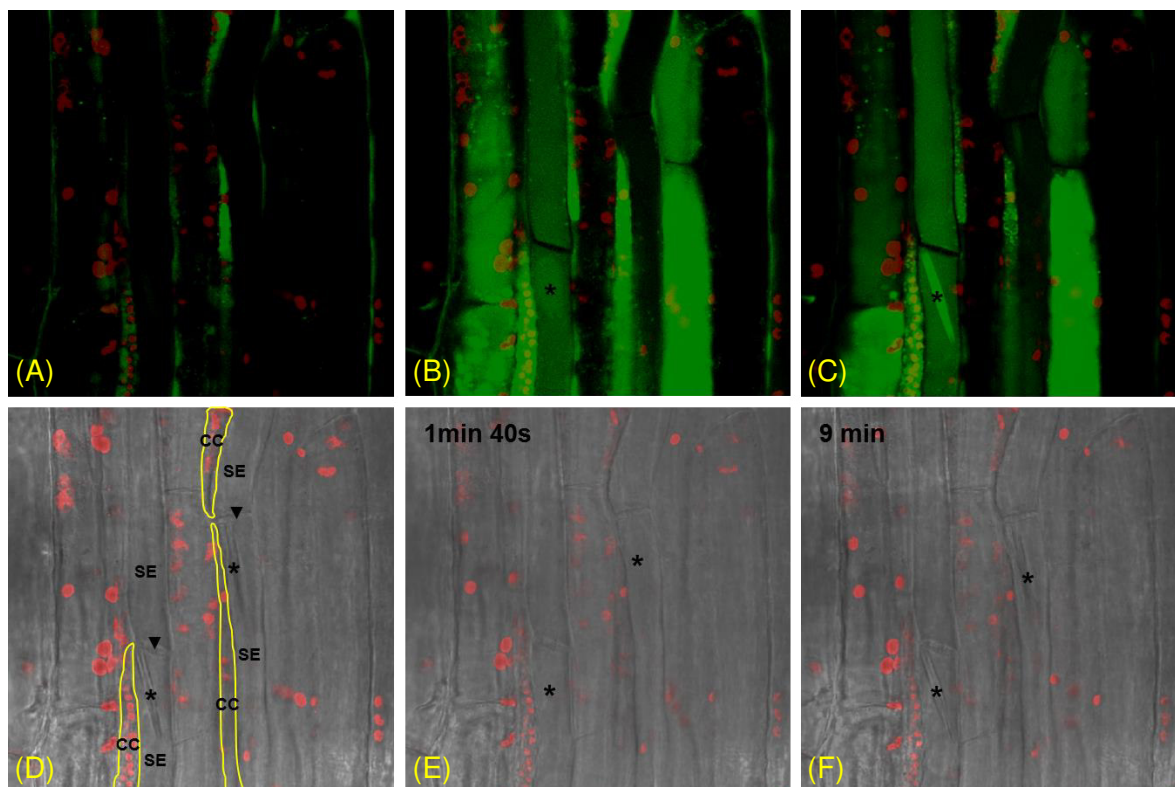

Figure 2 NO production in the phloem of *Vicia faba* in response to H_2O_2. NO was detected by confocal laser scanning microscopy using the fluorescent dye 4,5-diaminofluorescein diacetate (DAF-2 DA). **(A–C)** Digital overlay of DAF fluorescence (green) and autofluorescence of chloroplasts (red); **(D–F)** Overlay of transmission image and autofluorescence of chloroplasts. Condensed Ca^{2+}-sensitive forisomes (asterisks) and sieve plates (black arrow heads) are indicated. **(D)** Companion cell (CC) borders are delineated by yellow lines. **(A, D)** Control images (DAF fluorescence vs. transmission) before treatment with H_2O_2. **(B, C)** Emergence of DAF fluorescence 1 min 40 s and 9 min after treatment with 1 mM H_2O_2. **(C)** Sensitivity of photomultipliers down-regulated. The forisomes disperse **(B, E)** and recondense **(C, F)** in response to H_2O_2 treatment indicative of Ca^{2+} influx into the sieve elements (SEs). Figure modified after Gaupels *et al.*, 2008.

To date, mounting evidence suggests the involvement of NO signaling in SAR. Injection of NO donors into tobacco leaves reduced the size of lesions caused by tobacco mosaic virus on treated and systemic non-treated leaves (Song and Goodman, 2001). Also, local treatment with NOS inhibitors or an NO scavenger attenuated SAR in distal leaves (Song and Goodman, 2001). Rusterucci *et al.* (2007) recently found that GSNO might act as a systemic signal. *Arabidopsis* antisense lines of the GSNO catabolizing

GSNO reductase (GSNOR) displayed elevated resistance and constitutive SAR against *Peronospora parasitica*. These researchers also observed that GSNOR was primarily located in CCs and proposed that inhibition of GSNOR, leading to the accumulation and transport of GSNO in the sieve tubes, may be an important factor in the generation of SAR (Rusterucci et al., 2007). In systemic leaves GSNO could induce resistance gene expression according to its local effect on tobacco leaves (Durner et al., 1998).

However, contrary to the above findings another study found that T-DNA insertion mutants of *AtGSNOR1* displayed decreased SA levels and affected *R* gene-dependent, basal as well as non-host resistance (Feechan et al., 2005). The issue has been finally settled by a careful investigation of SAR in Arabidopsis plants treated with NO and ROS donors and mutants with altered NO and ROS levels (Wang et al., 2014). Experiments with two different NO donors revealed that NO induced systemic immunity against virulent *Pseudomonas syringae* pv. *tomato* DC3000 in a dose-dependent manner. Injection of 100 µM DETA-NONOate triggered much stronger immunity in distal leaves than higher concentrations. Accordingly, SAR was suppressed in *gsnor1* mutants, which accumulate high levels of NO (Wang et al., 2014). In comparison, the intermediate NO levels in GSNOR antisense plants with only partially reduced GSNOR activity would rather stimulate SAR analogous to intermediate NO donor concentrations. ROS donors stimulated systemic immunity in a similar fashion like NO donors. Moreover, ROS-induced SAR was compromised in NO-deficient mutants while on the other hand NO-induced SAR was compromised in ROS-deficient mutants suggesting that both redox signals cooperate in a positive feedback loop. In relation to other known SAR signals NO and ROS were shown to be upstream of AzA and G3P* but probably independent of SA and NPR1 (Wang et al., 2014).

In addition to SAR ROS and NO have been implicated in systemic responses to various abiotic stresses. Adaptation processes of plants exposed to adverse environmental conditions were collectively termed systemic acquired acclimation (SAA) (Karpinski et al., 1999). In Arabidopsis transgenic plants expressing the luciferase reporter gene under control of the ROS-inducible *ZAT12* promoter it was discovered that local wounding, excess light, heat and salt caused a rapidly spreading wave of H_2O_2 production, which was dependent on RBOHD activity and calcium (Miller et al., 2009; Suzuki et al., 2013). The H_2O_2-calcium autopropagation wave as well as ABA and electrical signalling were all suppressed in *rbohD* mutants. In a similar approach using transgenic Arabidopsis expressing the reporter gene *LUCIFERASE* under control of the H_2O_2-inducible *APX2* promoter Karpinski et al. (1999) uncovered a crucial function of bundle sheath cells (BSCs) surrounding the vascular tissue in eliciting SAA to excess light stress. The authors

proposed that H_2O_2 and ABA act as systemic signals moving in the phloem and that APX activity in the BSCs regulates H_2O_2 levels (Fryer et al., 2003; Karpinski et al., 1999).

In this context it is important that low concentrations of 100 and even 10 µM H_2O_2 induced rapid NO synthesis in the phloem of *Vicia faba* whereas in other tissues no or only weak NO was detected. Hence, the phloem seems to be particularly sensitive to H_2O_2 and is well-equipped with NO generating enzymes (Gaupels et al., 2008b). Within the SEs GSNO was proposed to act as a phloem-mobile carrier of NO during SAR and SWR in *Arabidopsis* (Espunya et al., 2012; Rusterucci et al., 2007). After leaf wounding accumulation of GSNO in the systemic leaf started in the main vein and spread throughout the leaf blade. If GSNO was transported over long distances or synthesized by the phloem is not known. As mentioned before GSNOR is mainly localized in CCs (Rusterucci et al., 2007) and can be inhibited by S-nitrosylation (Frungillo et al., 2014), which makes this enzyme an excellent candidate modulator of systemic stress signalling by NO/GSNO.
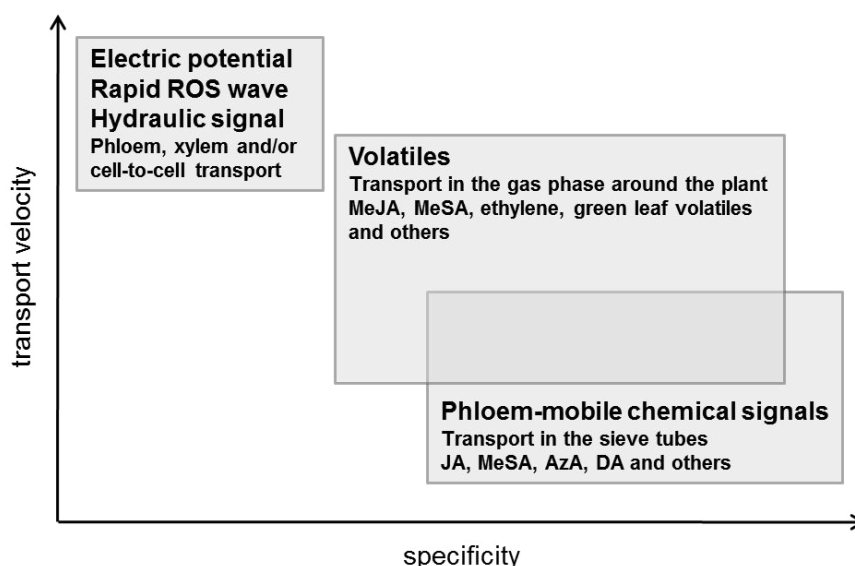

Figure 3 Hypothetical model ranking systemic signals according to their transport velocity and signal specificity. Figure modified after Gaupels and Vlot, 2013.

The operation mode of NO in systemic stress signalling has not yet been elucidated but might include the regulation of antioxidant enzymes like previously described for HR and other local defence responses (Wendehenne et al., 2014). APX isoforms are the main H_2O_2-scavenging enzymes in BSCs and SEs, which do not contain CAT. We speculate that NO or GSNO inhibit (by S-nitrosylation) APX in the SEs as well as APX and CAT in CCs and BSCs thereby amplifying and propagating the ROS wave. In line with this hypothesis SAA was increased in a heat shock-treated apx1 mutant compared to wild-type plants. In sum, the systemically moving ROS-calcium loop probably induces concomitant NO production, which further drives ROS accumulation by inhibition of antioxidant

enzymes along the signalling route. Although not yet proven we assume that these systemic signals move in the phloem.

Notably, SAA exhibited a certain degree of stress-specificity. All treatments triggered the rapid ROS production wave but heat stress additionally induced ABA and wounding JA (and ABA) signalling as inferred from transcriptomic data (Suzuki et al., 2013). From these results it can be concluded that multiple signalling events are initiated after stress perception by the plant (Figure 3). Rapid general stress signalling involves ROS, calcium, NO and electropotential waves, which might function in early JA signalling and in regulating the shift from primary to secondary metabolism. Later, slow-moving messengers would provide distal plant parts with additional stress-specific information. Release of volatile compounds such as ethylene, methyl jasmonate (MeJA) and MeSA could represent a third way of systemic signal transduction, which would be more independent of phloem connections and could even spread to neighbouring plants.

Local and systemic defence responses of the phloem

The plant vascular system consists of phloem, xylem and parenchyma cells. Xylem vessels and phloem sieve tubes are essential for uptake of water and minerals and distribution of photoassimilates throughout the plant. In addition, the vascular conduits are transport routes for signals involved in systemic regulation of developmental, physiological and defence-related processes (Lucas et al., 2013). Hence, the intact vascular tissue is essential for plant growth and survival. However, due to its high nutrient content this tissue is an attractive target for insect and pathogen attack. The vascular bundles are also utilised by viruses and pathogens as systemic highways for infection of distal plant parts. Recently, it was shown that virulent *Pseudomonas syringae* pv. *syringae* DC3000 moved in the xylem of *Nicotiana benthamiana* colonising the apoplast along the vasculature and systemic leaves (Misas-Villamil et al., 2011). In *Arabidopsis* spread of the bacterial wilt pathogen *Ralstonia solanacearum* in the xylem induced expression of the transcription factor WRKY27 in the phloem (Mukhtar et al., 2008). In this plant/pathogen interaction WRKY27 acted as a negative regulator of defence gene expression. Furthermore, the bacterial elicitor lipopolysaccharide was found to be xylem-mobile (Zeidler et al., 2010).

These findings imply that vascular tissues are encountered by various invaders and therefore must have the cellular equipment for efficient perception of pathogen- and herbivore-derived elicitors. Accordingly, application of the fungal elicitor chitooctaose and the defence signals SA and H_2O_2 to the bare-lying intact phloem induced NO production in CCs of *Vicia faba* probably indicative for induction of PTI (Gaupels et al. 2008). Notably, JA, SA, NO and H_2O_2 were all found to be synthesised in phloem and parenchyma cells

serving both in phloem-internal and systemic defence signalling (van Bel & Gaupels 2004; Gaupels and Vlot, 2013). Although the importance of the phloem in systemic signalling is well-recognized, much less is known about local and systemic defence mechanisms of the phloem. Below it will be discussed that the phloem can even serve as a defensive structure.

If sieve tubes are damaged e.g. by insect feeding the resulting turgor loss induces rapid plugging of sieve plates by calcium-dependent callose formation and by specialized Sieve Element Occlusion (SEO) proteins including forisomes of *Fabaceae* (Furch et al., 2010; Knoblauch et al., 2014). This way, the loss of valuable nutrients by exudation of phloem content from the wound site can be prevented. It is an interesting notion that sieve plate plugging does not only occur in damaged but also in distal sieve tubes. For instance, wounding of one leaf by squeezing or burning triggered callose formation in the phloem of a systemic leaf as seen in *Vicia faba* and pumpkin. The local stress was systemically communicated by an electropotential wave propagating along the phloem (Furch et al., 2010). Callose formation was probably also responsible for a 40% reduction in phloem sap yield from stylectomy after infection of barley leaves with *Blumeria graminis* f.sp. *hordei* (barley powdery mildew), which does not damage the phloem (Gaupels et al., 2008c). Sieve tube occlusion in (systemic) non-damaged phloem could (I) reduce the availability of phloem content for pathogens or insects and (II) could cause accumulation of defensive compounds in the phloem for better fighting secondary attack of a distal leaf.

Many defence-related macromolecules were identified in phloem exudates providing some insights in the phloem defence strategy (Kehr, 2006). The highly diverse set of proteinase inhibitors is directed against digestive proteinases of phloem-sucking and – biting insects. Defensive lectins bind chitin and are effective against insects as well as pathogens. In pumpkin phloem exudates the lectin Phloem Protein2 (PP2) represents a major defence-related protein. Widely occuring are also JA-producing and JA-inducible proteins such as the prominent phloem protein Jasmonate-Inducible Protein23 of barley (Gaupels et al., 2008a). These proteins are important elements of the preformed phloem defence (Gaupels et al., 2012).

To date, however, not much is known about inducible defence mechanisms of the phloem. Therefore, we investigated by metabolomic and proteomic approaches systemic responses of the phloem to leaf wounding (Gaupels et al., 2012). Pumpkin was chosen as the experimental plant because cucurbits allow easy sampling of large exudate volumes from cut petioles and stems. It was recently discovered that these exudates do not originate from the "regular" fascicular (bundle) phloem (FP) but from the cucurbit-specific extrafascicular phloem (EFP), which is a network of phloem strands outside of vascular bundles (Gaupels et al., 2012; Zhang et al., 2010). The EFP does not transport assimilates

but is a defensive structure similar to latex-containing laticifers in other plants (Gaupels and Ghirardo, 2013). SDS-PAGE revealed clear differences in the protein composition between exudates from the EFP – termed phloem latex hereafter – and pure phloem sap collected by stylectomy (Gaupels et al., 2012). However, the approx. 50% overlap of so-far identified phloem proteins from rice, rape and castor bean with known phloem latex proteins suggested that some of the wound responses observed in the EFP could be activated also in the FP (Lin et al., 2009).

As an early consequence of leaf wounding the exudate volume decreased transiently probably due to partial sieve tube occlusion by callose. The wound-signal JA and the biologically active derivative JA-isoleucine accumulated after 30 – 60 min in phloem latex collected from systemic petioles and stem sections (Gaupels et al., 2012). Similar kinetics of JA signalling have been reported previously in wounded and systemic leaves of tomato and are indicative for the onset of a SWR (Koo et al., 2009). Metabolomics by gas chromatography-coupled mass spectrometry and proteomics by isotope-coded protein labelling (ICPL) indicated that the energy metabolism in the EFP is enhanced upon wounding. Between 3 and 24 h after wounding glucose-6-phosphate (Glc-6-P) is channelled preferentially into glycolysis and citrate cycle for increasing energy supply whereas pentosephosphate pathway (via Glc-6-phosphate dehydrogenase, G6PDH) and synthesis of cell wall components were down-regulated. A 14-3-3 protein and two Sucrose Non-Fermenting1 (SNF1)-related protein kinases might act as central regulators of energy metabolism during stress responses.

ICPL proteomics revealed changes in abundance of several proteins functioning in signalling and defence. The levels of 18 kDa-cyclophilin (CYP18) and Phloem Protein16-1 (PP16-1) were increased but PP2 was transiently decreased after leaf damage. Regulation of these proteins was confirmed by SDS-PAGE and western blot analysis. Silverleaf Whitefly-Induced protein1 (SLW1) is known to be inducible by phloem-sucking insects and JA (van de Ven et al., 2000). The pumpkin CYP18 is highly similar to *Arabidopsis* CYP18-3, which was shown to be 3.5-fold induced in response to wounding (Chou and Gasser, 1997). Moreover, our preliminary results suggest that CYP18 expression in the pumpkin EFP can also be triggered by treatment with MeJA (unpublished results). Thus, both SLW1 as well as CYP18 are candidate marker proteins for JA signalling in the EFP. PP2 is a defensive lectin, which is carbonylated (oxidized) under unstressed conditions but reduced and probably mobilized in the phloem after wounding (Gaupels et al., 2012). We hypothesize that this lectin binds to chitin molecules of attacking insects thereby clogging their mouth parts. Notably, a decrease in PP2 abundance was also observed in upper plant parts when only two lower leaves were wounded indicating that phloem internal defence mechanisms are induced systemically probably by phloem-mobile JA.

This is the first detailed report about the wound-inducible defence response of the phloem. In sum, systemic wound responses of the pumpkin EFP are regulated by JA and redox signalling and involve partial sieve tube occlusion, enhanced energy metabolism, and expression of defence-related proteins. The exact sequence and mechanism of interactions between the signals will be addressed in future studies.

Conclusions

Signalling during induced defence responses of plants to biotic and abiotic stresses is often multi-layered and rather complex. By developing signal networks the plant maintains high flexibility, which is necessary for adequate reactions to ever-changing environmental conditions and a multitude of different pathogens. Redox signalling is a good example of how a seemingly rather simple set of signalling components can result in high complexity. Starting from O_2^-, NO and some redox enzymes chemical reactions between both radicals and interactions of the reactive intermediates with redox enzymes can result in an extreme versatility of possible messenger molecules. Protein S-nitrosylation is only one mechanism of signal transduction by NO. The significance of this protein modification in plant defence responses, particularly in the HR-PCD is well established and functions of some NO target proteins were already successfully characterized. However, the involvement of $ONOO^-$, NO_2 and protein nitration in defence signalling is just starting to be investigated.

ROS and NO derivatives such as GSNO can move from the initial site of stress encounter to distal plant parts, thereby participating in the induction of systemic stress immunity. In this context it is important that the phloem can synthesize NO and might be the transport route for a rapid ROS-calcium-NO autopropagation wave. In this signal interaction NO might facilitate ROS accumulation by inhibiting antioxidant enzymes as it has been observed during the HR-PCD. H_2O_2, in turn, was shown to be a potent inducer of NO production in the phloem (Figure 4A). Perhaps the intensity of the initial stimulus decides if local amplification turns into systemic propagation of redox signalling. Similar apparent translocation velocities suggest also a link between rapid redox signalling and electrical signals. Such amplification loops currently emerge as a widespread phenomenon in systemic defence signalling.

Particularly, the reactive molecules H_2O_2 and NO would be lost during long-distance transport due to dilution and scavenging and, for this reason, must be constantly synthesized en route. In general, systemic signal propagation waves can move cell-to-cell in all tissues but are most efficiently transmitted in the vasculature, particularly in the phloem (Figure 4B). Communication between distal plant parts often involves sequential and parallel signalling events. For instance, systemic wound responses are regulated by

electrical signals, ROS wave and JA. By flexibly combining partly independent signalling pathways the plant might optimize both speed as well as specificity of the defence response. Future research will have the challenging task of defining the molecular basis of signal interactions within the phloem.
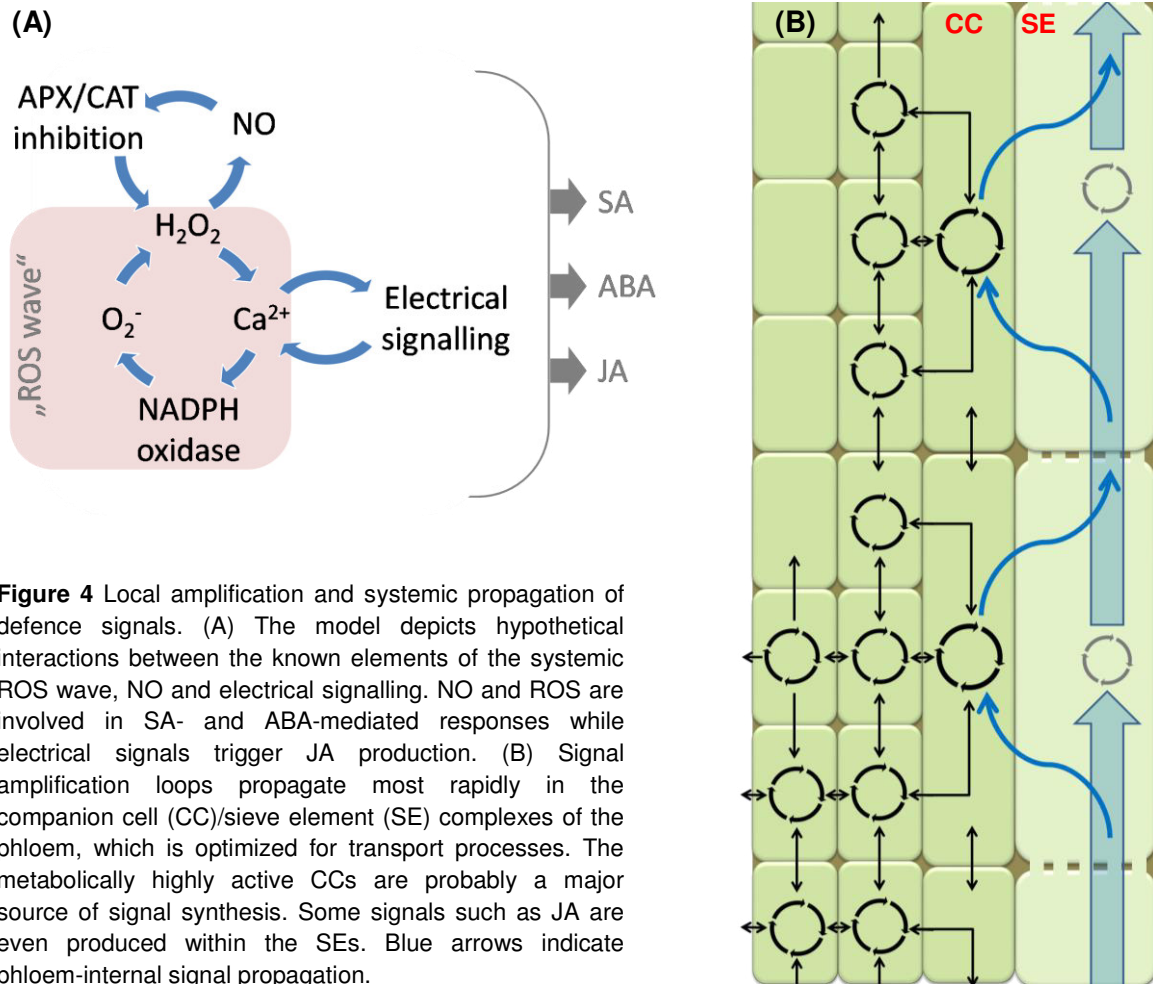

Figure 4 Local amplification and systemic propagation of defence signals. (A) The model depicts hypothetical interactions between the known elements of the systemic ROS wave, NO and electrical signalling. NO and ROS are involved in SA- and ABA-mediated responses while electrical signals trigger JA production. (B) Signal amplification loops propagate most rapidly in the companion cell (CC)/sieve element (SE) complexes of the phloem, which is optimized for transport processes. The metabolically highly active CCs are probably a major source of signal synthesis. Some signals such as JA are even produced within the SEs. Blue arrows indicate phloem-internal signal propagation.

An intact and functional phloem is essential for plant performance and survival. Therefore, it is also of agronomical importance to analyse in detail inducible defence mechanisms of the phloem. A pioneering proteomic and metabolomic investigation of phloem wound responses has revealed some interesting wound-regulated phloem proteins including PP2 and CYP18. Both proteins were detected in phloem exudates from a number of different plant species including barley, rice, potato, castor bean and others. Therefore, studying the functions of PP2 and Cyp18 and increasing protein levels by breeding or biotechnological approaches could be a reasonable strategy for improving crop resistance to herbivorous and phloem-sucking insects, which cause major yield losses all over the world.

References

Ahlfors, R., Brosche, M., Kollist, H. and Kangasjarvi, J., 2009. Nitric oxide modulates ozone-induced cell death, hormone biosynthesis and gene expression in Arabidopsis thaliana. Plant J, 58(1): 1-12.

Aki, T., Shigyo, M., Nakano, R., Yoneyama, T. and Yanagisawa, S., 2008. Nano scale proteomics revealed the presence of regulatory proteins including three FT-Like proteins in phloem and xylem saps from rice. Plant Cell Physiol, 49(5): 767-90.

Aoki, K., Suzui, N., Fujimaki, S., Dohmae, N., Yonekura-Sakakibara, K., Fujiwara, T., Hayashi, H., Yamaya, T., Sakakibara, H., 2005. Destination-selective long-distance movement of phloem proteins. Plant Cell, 17(6): 1801-14.

Arasimowicz-Jelonek, M. and Floryszak-Wieczorek, J., 2011. Understanding the fate of peroxynitrite in plant cells - From physiology to pathophysiology. Phytochemistry, 72(8): 681-8.

Atkins, C.A., Smith, P.M. and Rodriguez-Medina, C., 2011. Macromolecules in phloem exudates--a review. Protoplasma, 248(1): 165-72.

Attaran, E., Zeier, T.E., Griebel, T. and Zeier, J., 2009. Methyl salicylate production and jasmonate signaling are not essential for systemic acquired resistance in Arabidopsis. Plant Cell, 21(3): 954-71.

Bartels, S., Lori, M., Mbengue, M., van Verk, M., Klauser, D., Hander, T., Böni, R., Robatzek, S., Boller, T., 2013. The family of Peps and their precursors in Arabidopsis: differential expression and localization but similar induction of pattern-triggered immune responses. J Exp Bot, 64(17): 5309-21.

Besson-Bard, A., Pugin, A. and Wendehenne, D., 2008. New insights into nitric oxide signaling in plants. Annu Rev Plant Biol, 59: 21-39.

Boller, T. and Felix, G., 2009. A renaissance of elicitors: perception of microbe-associated molecular patterns and danger signals by pattern-recognition receptors. Annu Rev Plant Biol, 60: 379-406.

Chanda, B., Xia, Y., Mandal, M.K., Yu, K., Sekine, K.T., Gao, Q.M., Selote, D., Hu, Y., Stromberg A., Navarre, D., Kachroo, A., Kachroo, P., 2011. Glycerol-3-phosphate is a critical mobile inducer of systemic immunity in plants. Nat Genet, 43(5): 421-7.

Chaturvedi, R., Venables, B., Petros, R.A., Nalam, V., Li, M., Wang, X., Takemoto, L.J., Shah, J., 2012. An abietane diterpenoid is a potent activator of systemic acquired resistance. Plant J, 71(1): 161-72.

Chou, I.T. and Gasser, C.S., 1997. Characterization of the cyclophilin gene family of Arabidopsis thaliana and phylogenetic analysis of known cyclophilin proteins. Plant molecular biology, 35(6): 873-92.

Coll, N.S., Epple, P. and Dangl, J.L., 2011. Programmed cell death in the plant immune system. Cell Death Differ, 18(8): 1247-56.

Conrath, U., 2011. Molecular aspects of defence priming. Trends Plant Sci, 16(10): 524-31.

Corbesier, L. et al., 2007. FT protein movement contributes to long-distance signaling in floral induction of Arabidopsis. Science, 316(5827): 1030-3.

Corpas, F.J., Barroso, J.B., Carreras, A., Quirós, M., León, A.M., Romero-Puertas, M.C., Esteban, F.J., Valderrama, R., Palma, J.M., Sandalio, L.M., Gómez, M., del Río, L.A., 2004. Cellular and subcellular localization of endogenous nitric oxide in young and senescent pea plants. Plant Physiol, 136(1): 2722-33.

Cui, H., Tsuda, K. and Parker, J.E., 2014. Effector-Triggered Immunity: From Pathogen Perception to Robust Defense. Annu Rev Plant Biol.

de Pinto M.C., Locato, V., Sgobba, A., Romero-Puertas, M. del C., Gadaleta, C., Delledonne, M., De Gara, L., 2013. S-nitrosylation of ascorbate peroxidase is part of programmed cell death signaling in tobacco Bright Yellow-2 cells. Plant Physiol, 163(4): 1766-75.

Delledonne, M., Xia, Y., Dixon, R.A. and Lamb, C., 1998. Nitric oxide functions as a signal in plant disease resistance. Nature, 394(6693): 585-8.

Dempsey, D.A. and Klessig, D.F., 2012. SOS - too many signals for systemic acquired resistance? Trends Plant Sci, 17(9): 538-45.

Dinant, S. and Kehr, J., 2013. Sampling and analysis of phloem sap. Methods Mol Biol, 953: 185-94.

Doering-Saad, C., Newbury, H.J., Bale, J.S. and Pritchard, J., 2002. Use of aphid stylectomy and RT-PCR for the detection of transporter mRNAs in sieve elements. J Exp Bot, 53(369): 631-7.

Durner, J. and Klessig, D.F., 1999. Nitric oxide as a signal in plants. Curr Opin Plant Biol, 2(5): 369-74.

Durner, J., Wendehenne, D. and Klessig, D.F., 1998. Defense gene induction in tobacco by nitric oxide, cyclic GMP, and cyclic ADP-ribose. Proc Natl Acad Sci U S A, 95(17): 10328-33.

Espunya, M.C., De Michele, R., Gomez-Cadenas, A. and Martinez, M.C., 2012. S-Nitrosoglutathione is a component of wound- and salicylic acid-induced systemic responses in Arabidopsis thaliana. J Exp Bot, 63(8): 3219-27.

Feechan, A., Kwon, E., Yun, B.W., Wang, Y., Pallas, J.A., Loake, G.J., 2005. A central role for S-nitrosothiols in plant disease resistance. Proc Natl Acad Sci U S A, 102(22): 8054-9.

Fisher, D.B., Wu, Y. and Ku, M.S., 1992. Turnover of soluble proteins in the wheat sieve tube. Plant Physiol, 100(3): 1433-41.

Fröhlich, A., Gaupels, F., Sarioglu, H., Holzmeister, C., Spannagl, M., Durner, J., Lindermayr, C., 2012. Looking deep inside: detection of low-abundance proteins in leaf extracts of Arabidopsis and phloem exudates of pumpkin. Plant Physiol, 159(3): 902-14.

Frungillo, L., Skelly, M.J., Loake, G.J., Spoel, S.H. and Salgado, I., 2014. S-nitrosothiols regulate nitric oxide production and storage in plants through the nitrogen assimilation pathway. Nat Commun, 5: 5401.

Fryer, M.J., Ball, L., Oxborough, K., Karpinski, S., Mullineaux, P.M., Baker, N.R., 2003. Control of Ascorbate Peroxidase 2 expression by hydrogen peroxide and leaf water status during excess light stress reveals a functional organisation of Arabidopsis leaves. Plant J, 33(4): 691-705.

Fu, Z.Q. and Dong, X., 2013. Systemic acquired resistance: turning local infection into global defense. Annu Rev Plant Biol, 64: 839-63.

Furch, A.C., Zimmermann, M.R., Will, T., Hafke, J.B. and van Bel, A.J., 2010. Remote-controlled stop of phloem mass flow by biphasic occlusion in Cucurbita maxima. J Exp Bot, 61(13): 3697-708.

Gao, Q.M., Kachroo, A. and Kachroo, P., 2014. Chemical inducers of systemic immunity in plants. J Exp Bot, 65(7): 1849-55.

Garcia-Brugger, A., Lamotte, O., Vandelle, E., Bourque, S., Lecourieux, D., Poinssot, B., Wendehenne, D., Pugin, A., 2006. Early signaling events induced by elicitors of plant defenses. Mol Plant Microbe Interact, 19(7): 711-24.

Gaupels, F., Buhtz, A., Knauer, T., Deshmukh, S., Waller, F., van Bel, A.J., Kogel, K.H., Kehr, J., 2008a. Adaptation of aphid stylectomy for analyses of proteins and mRNAs in barley phloem sap. J Exp Bot, 59(12): 3297-306.

Gaupels, F., Furch, A.C., Will, T., Mur, L.A., Kogel, K.H., van Bel, A.J., 2008b. Nitric oxide generation in Vicia faba phloem cells reveals them to be sensitive detectors as well as possible systemic transducers of stress signals. New Phytol, 178(3): 634-46.

Gaupels, F. and Ghirardo, A., 2013. The extrafascicular phloem is made for fighting. Front Plant Sci, 4: 187.

Gaupels, F., Knauer, T. and van Bel, A.J., 2008c. A combinatory approach for analysis of protein sets in barley sieve-tube samples using EDTA-facilitated exudation and aphid stylectomy. J Plant Physiol, 165(1): 95-103.

Gaupels, F., Kuruthukulangarakoola, G.T. and Durner, J., 2011a. Upstream and downstream signals of nitric oxide in pathogen defence. Curr Opin Plant Biol, 14(6): 707-14.

Gaupels, F., Sarioglu, H., Beckmann, M., Hause, B., Spannagl, M., Draper, J., Lindermayr, C., Durner, J., 2012. Deciphering systemic wound responses of the pumpkin extrafascicular phloem by metabolomics and stable isotope-coded protein labeling. Plant Physiol, 160(4): 2285-99.

Gaupels, F., Spiazzi-Vandelle, E., Yang, D. and Delledonne, M., 2011b. Detection of peroxynitrite accumulation in Arabidopsis thaliana during the hypersensitive defense response. Nitric Oxide, 25(2): 222-8.

Gaupels, F. and Vlot, A.C., 2013. Plant Defense and Long-Distance Signaling in the Phloem. In: G.A. Thompson and A.J.E. van Bel (Editors), Phloem: Molecular Cell Biology, Systemic Communication, Biotic Interactions. Wiley-Blackwell, Hoboken, pp. 227-247.

Gross, F., Durner, J. and Gaupels, F., 2013. Nitric oxide, antioxidants and prooxidants in plant defence responses. Front Plant Sci, 4: 419.

Hafke, J.B., Ehlers, K., Föller, J., Höll, S.R., Becker, S., van Bel, A.J., 2013. Involvement of the sieve element cytoskeleton in electrical responses to cold shocks. Plant Physiol, 162(2): 707-19.

Haywood, V., Yu, T.S., Huang, N.C. and Lucas, W.J., 2005. Phloem long-distance trafficking of GIBBERELLIC ACID-INSENSITIVE RNA regulates leaf development. Plant J, 42(1): 49-68.

Heil, M. and Land, W.G., 2014. Danger signals - damaged-self recognition across the tree of life. Front Plant Sci, 5: 578.

Holzmeister, C., Gaupels, F., Geerlof, A., Sarioglu, H., Sattler, M., Durner, J. and Lindermayr, C., 2014. Differential inhibition of Arabidopsis superoxide dismutases by peroxynitrite-mediated tyrosine nitration. J Exp Bot, pii: eru458.

Jaskiewicz, M., Conrath, U. and Peterhansel, C., 2011. Chromatin modification acts as a memory for systemic acquired resistance in the plant stress response. EMBO Rep, 12(1): 50-5.

Jung, H.W., Tschaplinski, T.J., Wang, L., Glazebrook, J. and Greenberg, J.T., 2009. Priming in systemic plant immunity. Science, 324(5923): 89-91.

Karpinski, S., Reynolds, H., Karpinska, B., Wingsle, G., Creissen, G., Mullineaux, P., 1999. Systemic signaling and acclimation in response to excess excitation energy in Arabidopsis. Science, 284(5414): 654-7.

Kehr, J., 2006. Phloem sap proteins: their identities and potential roles in the interaction between plants and phloem-feeding insects. J Exp Bot, 57(4): 767-74.

Kneeshaw, S., Gelineau, S., Tada, Y., Loake, G.J. and Spoel, S.H., 2014. Selective protein denitrosylation activity of Thioredoxin-h5 modulates plant Immunity. Mol Cell, 56(1): 153-62.

Knoblauch, M., Froelich, D.R., Pickard, W.F. and Peters, W.S., 2014. SEORious business: structural proteins in sieve tubes and their involvement in sieve element occlusion. J Exp Bot, 65(7): 1879-93.

Knoblauch, M. and van Bel, A.J.E., 1998. Sieve tubes in action. Plant Cell, 10: 35-50

Koo, A.J., Gao, X., Jones, A.D. and Howe, G.A., 2009. A rapid wound signal activates the systemic synthesis of bioactive jasmonates in Arabidopsis. Plant J, 59(6): 974-86.

Kovacs, I. and Lindermayr, C., 2013. Nitric oxide-based protein modification: formation and site-specificity of protein S-nitrosylation. Front Plant Sci, 4: 137.

Leitner, M., Vandelle, E., Gaupels, F., Bellin, D. and Delledonne, M., 2009. NO signals in the haze: nitric oxide signalling in plant defence. Curr Opin Plant Biol, 12(4): 451-8.

Li, L., Li, C., Lee, G.I. and Howe, G.A., 2002. Distinct roles for jasmonate synthesis and action in the systemic wound response of tomato. Proc Natl Acad Sci U S A, 99(9): 6416-21.

Lin, M.K., Lee, Y.J., Lough, T.J., Phinney, B.S. and Lucas, W.J., 2009. Analysis of the pumpkin phloem proteome provides insights into angiosperm sieve tube function. Mol Cell Proteomics, 8(2): 343-56.

Lindermayr, C., Sell, S., Muller, B., Leister, D. and Durner, J., 2010. Redox regulation of the NPR1-TGA1 system of Arabidopsis thaliana by nitric oxide. Plant Cell, 22(8): 2894-907.

Liu, P.P., von Dahl, C.C. and Klessig, D.F., 2011. The extent to which methyl salicylate is required for signaling systemic acquired resistance is dependent on exposure to light after infection. Plant Physiol, 157(4): 2216-26.

Lucas, W.J., Groover, A., Lichtenberger, R., Furuta, K., Yadav, S.R., Helariutta, Y., He, X.Q., Fukuda, H., Kang, J., Brady, S.M., Patrick, J.W., Sperry, J., Yoshida, A., López-Millán, A.F., Grusak, M.A., Kachroo, P., 2013. The plant vascular system: evolution, development and functions. J Integr Plant Biol, 55(4): 294-388.

Miller, G., Schlauch, K., Tam, R., Cortes, D., Torres, M.A., Shulaev, V., Dangl, J.L., Mittler, R., 2009. The plant NADPH oxidase RBOHD mediates rapid systemic signaling in response to diverse stimuli. Sci Signal, 2(84): ra45.

Misas-Villamil, J.C., Kolodziejek, I. and van der Hoorn, R.A., 2011. Pseudomonas syringae colonizes distant tissues in Nicotiana benthamiana through xylem vessels. Plant J, 67(5): 774-82.

Mousavi, S.A., Chauvin, A., Pascaud, F., Kellenberger, S. and Farmer, E.E., 2013. GLUTAMATE RECEPTOR-LIKE genes mediate leaf-to-leaf wound signalling. Nature, 500(7463): 422-6.

Mukhtar, M.S., Deslandes, L., Auriac, M.C., Marco, Y. and Somssich, I.E., 2008. The Arabidopsis transcription factor WRKY27 influences wilt disease symptom development caused by Ralstonia solanacearum. Plant J, 56(6): 935-47.

Mur, L.A., Mandon, J., Persijn, S., Cristescu, S.M., Moshkov, I.E., Novikova, G.V., Hall, M.A., Harren, F.J., Hebelstrup, K.H., Gupta, K.J., 2013. Nitric oxide in plants: an assessment of the current state of knowledge. AoB Plants, 5: pls052.

Park, S.W., Kaimoyo, E., Kumar, D., Mosher, S. and Klessig, D.F., 2007. Methyl salicylate is a critical mobile signal for plant systemic acquired resistance. Science, 318(5847): 113-6.

Romero-Puertas, M.C., Campostrini, N., Mattè, A., Righetti, P.G., Perazzolli, M., Zolla, L., Roepstorff, P., Delledonne, M., 2008. Proteomic analysis of S-nitrosylated proteins in Arabidopsis thaliana undergoing hypersensitive response. Proteomics, 8(7): 1459-69.

Romero-Puertas, M.C., Laxa, M., Mattè, A., Zaninotto, F., Finkemeier, I., Jones, A.M., Perazzolli, M., Vandelle, E., Dietz, K.J., Delledonne, M., 2007. S-nitrosylation of peroxiredoxin II E promotes peroxynitrite-mediated tyrosine nitration. Plant Cell, 19(12): 4120-30.

Rusterucci, C., Espunya, M.C., Diaz, M., Chabannes, M. and Martinez, M.C., 2007. S-nitrosoglutathione reductase affords protection against pathogens in Arabidopsis, both locally and systemically. Plant Physiol, 143(3): 1282-92.

Ryan, C.A., Huffaker, A. and Yamaguchi, Y., 2007. New insights into innate immunity in Arabidopsis. Cell Microbiol, 9(8): 1902-8.

Ryan, C.A. and Moura, D.S., 2002. Systemic wound signaling in plants: a new perception. Proc Natl Acad Sci U S A, 99(10): 6519-20.

Salvador-Recatala, V., Tjallingii, W.F. and Farmer, E.E., 2014. Real-time, in vivo intracellular recordings of caterpillar-induced depolarization waves in sieve elements using aphid electrodes. New Phytol, 203(2): 674-84.

Scheler, C., Durner, J. and Astier, J., 2013a. Nitric oxide and reactive oxygen species in plant biotic interactions. Curr Opin Plant Biol, 16(4): 534-9.

Schilmiller, A.L. and Howe, G.A., 2005. Systemic signaling in the wound response. Current Opin Plant Biol, 8(4): 369-77.

Shah, J., Chaturvedi, R., Chowdhury, Z., Venables, B. and Petros, R.A., 2014. Signaling by small metabolites in systemic acquired resistance. Plant J, 79(4): 645-58.

Song, F. and Goodman, R.M., 2001. Activity of nitric oxide is dependent on, but is partially required for function of, salicylic acid in the signaling pathway in tobacco systemic acquired resistance. Mol Plant Microbe Interact, 14(12): 1458-62.

Spoel, S.H. and Dong, X., 2012. How do plants achieve immunity? Defence without specialized immune cells. Nature reviews. Immunology, 12(2): 89-100.

Spoel, S.H. and Loake, G.J., 2011. Redox-based protein modifications: the missing link in plant immune signalling. Curr Opin Plant Biol, 14(4): 358-64.

Suzuki, N., Miller, G., Salazar, C., Mondal, H.A., Shulaev, E., Cortes, D.F., Shuman, J.L., Luo, X., Shah, J., Schlauch, K., Shulaev, V., Mittler, R., 2013. Temporal-spatial interaction between reactive oxygen species and abscisic acid regulates rapid systemic acclimation in plants. Plant Cell, 25(9): 3553-69.

Tada, Y., Spoel, S.H., Pajerowska-Mukhtar, K., Mou, Z., Song, J., Wang, C., Zuo, J., Dong, X., 2008. Plant immunity requires conformational changes [corrected] of NPR1 via S-nitrosylation and thioredoxins. Science, 321(5891): 952-6.

Thomas, D.D., Ridnour, L.A., Isenberg, J.S., Flores-Santana, W., Switzer, C.H., Donzelli. S., Hussain, P., Vecoli, C., Paolocci, N., Ambs, S., Colton, C.A., Harris, C.C., Robert, D.D., Wink, D.A., 2008. The chemical biology of nitric oxide: implications in cellular signaling. Free Radical Biol Med, 45(1): 18-31.

Turnbull, C.G. and Lopez-Cobollo, R.M., 2013. Heavy traffic in the fast lane: long-distance signalling by macromolecules. New Phytol, 198(1): 33-51.

Valderrama, R., Corpas, F.J., Carreras, A., Fernández-Ocaña, A., Chaki, M., Luque, F., Gómez-Rodríguez, M.V., Colmenero-Varea, P., Del Río, L.A., Barroso, J.B., 2007. Nitrosative stress in plants. FEBS Lett, 581(3): 453-61.

van Bel, A.J., 2003. Transport phloem: low profile, high impact. Plant Physiol, 131(4): 1509-10.

van Bel and Gaupels, F., 2004. Pathogen-induced resistance and alarm signals in the phloem. Mol Plant Pathol, 5(5): 495-504.

van de Ven, W.T., LeVesque, C.S., Perring, T.M. and Walling, L.L., 2000. Local and systemic changes in squash gene expression in response to silverleaf whitefly feeding. Plant Cell, 12(8): 1409-23.

Wang, C., El-Shetehy, M., Shine, M.B., Yu, K., Navarre, D., Wendehenne, D., Kachroo, A., Kachroo, P., 2014. Free radicals mediate systemic acquired resistance. Cell reports, 7(2): 348-55.

Wang, Y., Lin, A., Loake, G.J. and Chu, C., 2013. H2O2-induced leaf cell death and the crosstalk of reactive nitric/oxygen species. J Integr Plant Biol, 55(3): 202-8.

Wasternack, C., 2007. Jasmonates: an update on biosynthesis, signal transduction and action in plant stress response, growth and development. Ann Bot, 100(4): 681-97.

Wendehenne, D., Gao, Q.M., Kachroo, A., Kachroo, P., 2014. Free radical-mediated systemic immunity in plants. Curr Opinion Plant Biol, 20: 127-34.

Wu, J. and Baldwin, I.T., 2010. New insights into plant responses to the attack from insect herbivores. Ann Review Genetics, 44: 1-24.

Wu, L., Chen, H., Curtis, C. and Fu, Z.Q., 2014. Go in for the kill. Virulence, 5(7): 710-21.

Yamaguchi, Y., Pearce, G. and Ryan, C.A., 2006. The cell surface leucine-rich repeat receptor for AtPep1, an endogenous peptide elicitor in Arabidopsis, is functional in transgenic tobacco cells. Proc Natl Acad Sci U S A, 103(26): 10104-9.

Yu, K., Soares, J.M., Mandal, M.K., Wang, C., Chanda, B., Gifford, A.N., Fowler, J.S., Navarre, D., Kachroo, A., Kachroo, P., 2013. A feedback regulatory loop between G3P and lipid transfer proteins DIR1 and AZI1 mediates azelaic-acid-induced systemic immunity. Cell reports, 3(4): 1266-78.

Yun, B.W., Feechan, A., Yin, M., Saidi, N.B., Le Bihan, T., Yu, M., Moore, J.W., Kang, J.G., Kwon, E., Spoel, S.H., Pallas, J.A., Loake, G.J., 2011. S-nitrosylation of NADPH oxidase regulates cell death in plant immunity. Nature, 478(7368): 264-8.

Zeidler, D., Dubery, I.A., Schmitt-Kopplin, P., Von Rad, U. and Durner, J., 2010. Lipopolysaccharide mobility in leaf tissue of Arabidopsis thaliana. Mol Plant Pathol, 11(6): 747-55.

Zhang, B., Tolstikov, V., Turnbull, C., Hicks, L.M. and Fiehn, O., 2010. Divergent metabolome and proteome suggest functional independence of dual phloem transport systems in cucurbits. Proc Natl Acad Sci U S A, 107(30): 13532-7.

Zipfel, C., 2014. Plant pattern-recognition receptors. Trends Immun, 35(7): 345-51.

Publications – Part 1. Functions of NO and ONOO⁻ in defence signalling

Leitner, M., Vandelle, E., Gaupels, F., Bellin, D. and Delledonne, M. 2009. NO signals in the haze: nitric oxide signalling in plant defence. Curr Opin Plant Biol, 12(4): 451-8.

Gaupels, F., Kuruthukulangarakoola, G.T. and Durner, J. 2011. Upstream and downstream signals of nitric oxide in pathogen defence. Curr Opin Plant Biol, 14(6): 707-14.

Gaupels, F., Spiazzi-Vandelle, E., Yang, D. and Delledonne, M. 2011. Detection of peroxynitrite accumulation in Arabidopsis thaliana during the hypersensitive defense response. Nitric Oxide, 25(2): 222-8.

Holzmeister, C., Gaupels, F., Geerlof, A., Sarioglu, H., Sattler, M., Durner, J. and Lindermayr, C. 2014. Differential inhibition of Arabidopsis superoxide dismutases by peroxynitrite-mediated tyrosine nitration. J Exp Bot, pii: eru458.

Gross, F., Durner, J. and Gaupels, F. 2013. Nitric oxide, antioxidants and prooxidants in plant defence responses. Front Plant Sci, 4: 419.

ELSEVIER

NO signals in the haze
Nitric oxide signalling in plant defence

Margit Leitner, Elodie Vandelle, Frank Gaupels, Diana Bellin and Massimo Delledonne

Nitric oxide (NO) is gaining increasing attention as a regulator of diverse (patho-)physiological processes in plants. Although this molecule has been described as playing a role in numerous conditions, its production, turnover and mode of action are poorly understood. Recent studies on NO production have tended to highlight the questions that still remain unanswered rather than telling us more about NO metabolism. But regarding NO signalling and functions, new findings have given an impression of the intricacy of NO-related signalling networks. Different targets of protein *S*-nitrosylation have been characterised and enzymatic routes controlling this posttranslational modification are emerging, along with their physiological implications. Evidence is also accumulating for protein tyrosine nitration and cGMP as important components of NO-related signal transduction.

Address
Università degli Studi di Verona, Dipartimento di Biotecnologie, Strada Le Grazie 15, 37134 Verona, Italy

Corresponding author: Delledonne, Massimo (massimo.delledonne@univr.it)

Introduction

Nitric oxide (NO) is a small gaseous radical with diverse signalling functions. In plants, NO was first found to play a crucial role in mediating defence reactions against bacterial pathogens [1] and is now well known to influence numerous physiological processes throughout the entire plant life cycle. To name a few, NO is involved in germination, leaf expansion, lateral root development, flowering, stomatal closure, cell death and defence against biotic and abiotic stresses [2•]. Whereas descriptions of NO-mediated processes are accumulating, the plant signalling pathways governed by NO are still largely unknown. NO-related signalling can be attributed to various NO derivatives, collectively referred to as reactive nitrogen species (RNS). RNS comprise not only the NO radical (NO•) and its nitroxyl (NO−) and nitrosonium (NO+) ions, but also peroxynitrite (ONOO−), *S*-nitrosothiols, higher oxides of nitrogen and dinitrosyl–iron complexes; in short, all NO derivatives that can effect NO-dependent modifications [3]. Hence, the term NO-related signalling is used here to summarise effects caused by all these RNS.

In principle, NO-related functions are subject to different levels of control. Production and turnover regulate NO bioavailability; once the NO level increases in the system, it can affect signalling either directly via protein modifications or indirectly via activation of second messengers. In animals, second messengers, such as cGMP, are well-characterised components of NO signal transduction, whereas studies of NO-dependent posttranslational modifications are more recent. However, in research conducted in plants, knowledge of the cGMP-dependent pathways is restricted to data gained using pharmacological approaches. By contrast, the impact of NO-dependent protein modifications, especially of *S*-nitrosylation, is the best studied mode of action in plants to date.

Among the diverse physiological processes affected by NO, available data predominantly explain signalling related to plant defence responses—which is the focus of this review.

Regulation of NO bioavailability
No simple answers to the question how NO is produced in plants

Three routes to yield NO have been described in plants: non-enzymatic conversion of nitrite to NO in the apoplast, nitrate reductase (NR)-dependent NO formation and NO synthase (NOS)-like activity, that is arginine-dependent NO formation. These pathways have been reviewed in detail [2•,4•]. In a nutshell: since the enzymatic source(s) of NO in plant stress responses remains elusive, unbiased genetic tools are still lacking for non-invasive manipulations of NO levels *in planta*. Despite numerous studies using pharmacological tools demonstrated NOS-like activity in plants, the identity of the enzymes involved remains unknown. The only postulated plant NOS (AtNOA1/RIF1) has recently been shown to have no NOS activity [5••]. Instead, it is a chloroplast-targeted GTPase essential for proper ribosome assembly [6•]. Mutation in this gene leads to reduced NO accumulation, probably because of its rapid

Table 1

Characterised mutants and transgenics with altered NO levels.

Gene	Description	Mod.	Species	NO level	related phenotype	Ref.
Noa1/Rif1	Nitric oxide associated1/resistant to fosmidomycin 1; chloroplastic GTPase	m	At	−	ROS accumulation	[5••,6•]
		s	At	+	−	[5••,6•]
Nia1 Nia2	Nitrate reductase	m	At	−	Reduced amino acid and nitrite levels	[8]
NiR	Nitrite reductase	as	Nt	+	Nitrite accumulation	[12]
Argah1 and 2	Arginine amidohydrolase; arginase	m	At	+	L-Arginine accumulation	[9]
Nox1/cue1	NO overproducer 1/chlorophyll a/b binding protein underexpressed 1; PEP phosphate translocator	m	At	+	L-Arginine accumulation	[10]
Rcd1	Radical-induced cell death1; unknown function.	m	At	+	ROS accumulation	[13]
Gsnor1/hot5	GSNO reductase	m	At	+	Accumulation of S-nitroso species and nitrate	[11•,19,20]
		as	At	+		
		s	At	−	−	[11•,19]
Vsr3	Vacuolar sorting receptor	as	At	+	ROS accumulation	[14]
Hb1	Ns haemoglobin	as	At, Ms	+	−	[17]
		s	At, Ms	−	Nitrate accumulation	[17]
Hmp	Bacterial flavohaemoglobin	s	At	−	Nitrate accumulation	[18]

as, antisense; At, Arabidopsis thaliana; GSNO, S-nitrosoglutathione; Mod., gene modification; Ms, Medicago sativa; m, mutant; Nt, Nicotiana tabacum; Ns, non-symbiotic; PEP, phosphoenolpyruvate; Ref., references; ROS, reactive oxygen species; s, sense.

reaction with the elevated amounts of ROS observed in the *Atnoa1* mutant [5••].

By contrast, NO can clearly be produced by NR activity [7]. However, NR deficiency also leads to impaired nitrogen assimilation, thus generally influencing primary and secondary metabolism. Indeed, Arabidopsis *nia1 nia2* double mutants display decreased levels of both nitrite and amino acids [8]. Hence, direct effects due to impaired NO biosynthesis are difficult to distinguish from those caused by metabolic alterations. In several other mutants, increased NO accumulation correlates with concentrations of putative substrates for NO biosynthesis (Table 1): (1) Arginase-deficient *Atargah 1-1* and *2-1* as well as *Atnox1/cue1*, defective in a phosphoenolpyruvate phosphate translocator, display elevated levels of L-arginine [9,10]; (2) *Atgsnor1-3/hot5-2*, defective in the *S*-nitrosoglutathione reductase, accumulates nitrate and (3) an antisense *NiR* (nitrite reductase) tobacco accumulates nitrite [11•,12]. Recently, the Arabidopsis *rcd1*, a mutant sensitive to ozone and *VSR3* (vacuolar sorting receptor 3) antisense transgenic were shown to overaccumulate NO and ROS, extending the list of genetically modified plants with altered NO and/or ROS homeostasis [13,14]. In summary, none of these NO-related mutants is exclusively affected in NO production. Their complex and pleiotropic phenotypes make genetic study of NO function difficult. The significance of using genetic tools for studying NO-related signalling *in vivo* is underlined by recent reports demonstrating the strict co-localisation of NO sources (i.e. NOSs) and *S*-nitrosylation in mammalian systems [15,16]. Therefore, the identification and

characterisation of NO-producing enzymes in plants, other than NR, remain equally challenging and mandatory tasks.

Different paths lead to RNS and their turnover
Relative to the elusive routes of NO production, mechanisms regulating bioavailable RNS are comparatively well characterised. As outlined above, different RNS contribute to NO-related signalling. Accordingly, a network of RNS transformation and turnover balances the bioavailability of these signal compounds. These pathways are illustrated here using three examples. NO can be metabolised to nitrate by non-symbiotic haemoglobins, like Arabidopsis Hb1, which acts as an NO dioxygenase using NADPH as an electron donor (Figure 1, [17]). However, the NO-reducing activity of Arabidopsis Hb1 is rather low, although physiologically relevant under hypoxic stress [17]. NO also reacts with GSH to form *S*-nitrosylated glutathione (GSNO), which can release NO or function as a transnitrosylating agent; it is thus considered a reactive nitrogen species (RNS) and natural reservoir of NO. The enzyme controlling GSNO levels is GSNO reductase (GSNOR). It reduces GSNO to oxidised glutathione and NH_3. Though highly specific for GSNO, GSNOR seems to also influence levels of protein *S*-nitrosylation [19]. In Arabidopsis, mutation of GSNOR (*gsnor1-3/hot5-2*) causes increased basal levels of NO and *S*-nitroso species. The mutant plants not only have impaired resistance to biotic and abiotic stresses, but also show reduced growth, fertility and reproduction. This complex phenotype underlines the vital role of functional RNS homeostasis in diverse physiological processes

Figure 1
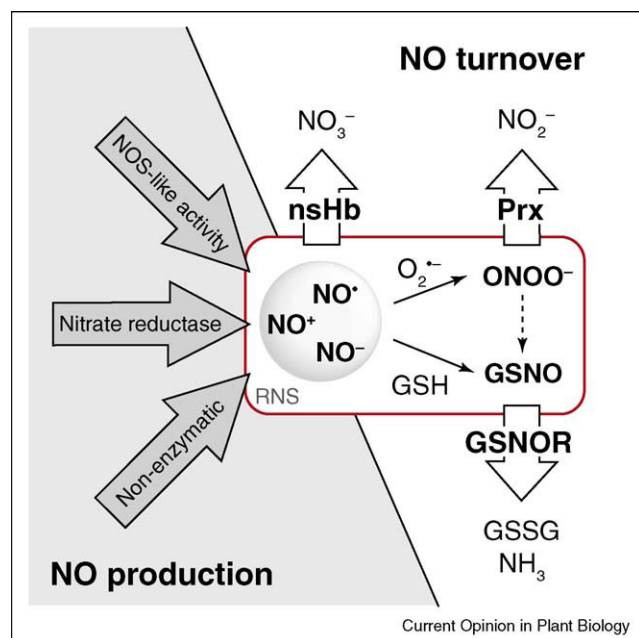
Routes of NO production and turnover. Three pathways of NO production are thought to exist in plants: NOS-like activity of (an) unidentified protein(s), NO production by nitrate reductase and non-enzymatic conversion of nitrite to NO under acidic conditions. Three main routes lead to NO turnover: NO scavenging by non-symbiotic haemoglobins, transformation of NO to GSNO and degradation by GSNOR and reaction of NO with superoxide to form peroxynitrite, which is detoxified by peroxiredoxins. Abbreviations: GSNO, *S*-nitrosoglutathione; GSNOR, *S*-nitrosoglutathione reductase; NOS, nitric oxide synthase; nsHb, non-symbiotic haemoglobin; Prx, peroxiredoxin; RNS, reactive nitrogen species.
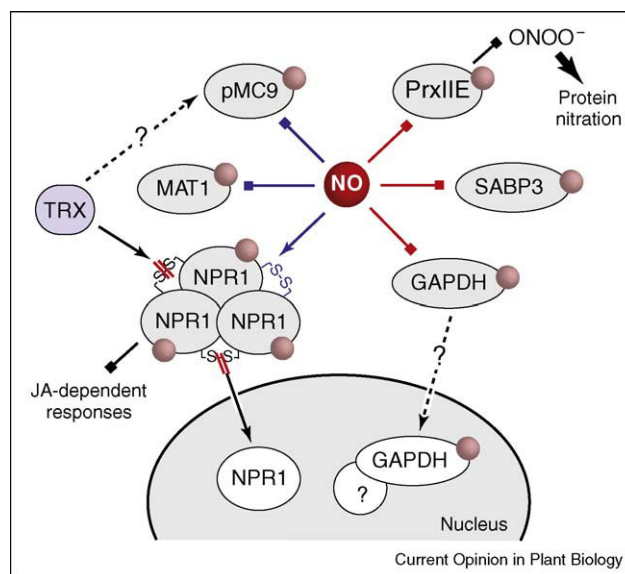
Figure 2

Characterised targets of protein *S*-nitrosylation in plants. *S*-nitrosylation under physiological conditions (basal NO tone, blue arrows) is assumed to inhibit MAT1 and pMC9 and to facilitate oligomer formation of NPR1. Induced NO production (i.e. defence-related NO burst; red arrows) leads to *S*-nitrosylation of GAPDH, SABP3 and PrxIIE. GAPDH activity is blocked upon *S*-nitrosylation and the protein is thought to translocate to the nucleus. *S*-nitrosylation of SABP3 leads to the loss of the enzyme's SA-binding capacity as well as inhibition of its carbonic anhydrase activity. Also PrxIIE activity is inhibited by *S*-nitrosylation, which leads to increased peroxynitrite levels and protein nitration. Under induced conditions, thioredoxins counteract *S*-nitrosylation of NPR1, leading to monomer release and translocation of this transcription co-factor to the nucleus. Dashed lines indicate hypothetical interactions, *S*-nitrosylation is symbolised by red bullets. Abbreviations: GAPDH, glyceraldehyde 3-phosphate dehydrogenase; JA, jasmonic acid; MAT1, methionine adenosyltransferase 1; NPR1, non-expressor of pathogenesis-related protein 1; pMC9, prometacaspase 9; PrxIIE, peroxiredoxin II E; SABP3, salicylic acid binding protein 3; TRX, thioredoxin.

[11[•],20,21]. Finally, NO rapidly reacts with superoxide (O_2^-) to form peroxynitrite ($ONOO^-$), a potent oxidising and nitrating species. This non-enzymatic reaction is tightly controlled by the (enzymatic) formation of its precursors. $ONOO^-$ can, in turn, be detoxified by some peroxiredoxins. For example, Arabidopsis PrxIIE possesses peroxynitrite reductase activity (Figure 1) [22[••]] and therefore controls the bioavailability of $ONOO^-$.

Hence, a complex interplay between RNS becomes evident: by removing NO, other RNS can be formed, presumably with altered signalling functions ([23], cf. Figure 1 and below). Moreover, peroxiredoxin II E is inhibited by *S*-nitrosylation, causing increased $ONOO^-$-mediated protein tyrosine nitration. This demonstrates that enzyme regulation by NO can facilitate accumulation of another RNS.

NO-associated protein modifications
RNS can directly react with diverse biomolecules [3]. Amongst them, proteins can be modified by RNS through reactions with different amino acids or prosthetic groups.

More specifically, the main NO-associated protein modifications in the biological context are the covalent modifications of cysteine (*S*-nitrosylation) and tyrosine (tyrosine 3-nitration) residues and NO binding to transition metals (metal nitrosylation). To date, the best characterised of these is cysteine *S*-nitrosylation.

Protein *S*-nitrosylation
S-nitrosylation refers to the covalent attachment of an NO moiety to the thiol side chain of cysteine [24]. Although proteomic approaches identified numerous candidates in plants [25,26], only a few confirmed functional modifications have been reported (Figure 2). Nevertheless, beginning characterisation of modified proteins now reveals the physiological significance of *S*-nitrosylation.

S-nitrosylation contributes to gene regulation
NO-dependent gene regulation strongly depends on the plant organ and the inducing stimulus, reinforcing the

need to consider downstream regulatory networks [27]. Changes in gene expression have been intensively studied using different NO donors (reviewed by [28]), though the regulatory basis leading to these changes remains unknown. Common regulatory elements in differentially expressed genes could be identified using bioinformatics tools [29]. These theoretical considerations have recently been substantiated by experimental data that documented the control of NO over transcription factors [30,31••]. In particular, finding NPR1, a crucial component of disease resistance and signal cross-talk, to be regulated via S-nitrosylation added an important clue to understanding NO's signalling functions [31••]. The subcellular localisation of NPR1, and thus its transcription co-factor activity, is controlled by S-nitrosylation. Intermolecular disulphide bridges sustain NPR1 oligomers, which are retained in the cytosol. Intriguingly, S-nitrosylation facilitates oligomerisation of NPR1, whereas thioredoxins support reductive monomer release, a reaction that is boosted by SA (Figure 2). After identifying the crucial components, the next challenge will be to investigate how this intricate balance is achieved.

S-nitrosylation modulates phytohormonal signalling

NPR1 not only mediates defence gene expression, but also contributes to the suppression of JA-dependent responses in the cytosol in a so far unknown mode [32]. S-nitrosylation could thus contribute to the well-documented negative cross-talk between SA and JA signalling pathways. Moreover, allene oxide cyclase, a JA biosynthetic enzyme, has been shown to be S-nitrosylated during the hypersensitive response [26], which potentially represents another mechanism regulating oxylipin levels. In this connection, S-nitrosylation of salicylic acid binding protein 3 (SABP3) may also interfere with signal cross-talk by affecting lipid-derived signalling components as both carbonic anhydrase activity and SA-binding capacity of SABP3 are inhibited by S-nitrosylation [33]. Besides its apparent influence on SA/JA cross-talk, NO also affects ethylene, abscisic acid (ABA) and auxin signalling [34,35•,36]. S-nitrosylation of methionine adenosyltransferase 1 (MAT1; involved in ethylene biosynthesis) inhibits ethylene production [34], whereas NO is required for downstream responses to auxin and ABA [35•,36]. The interplay between different phytohormones and NO during innate immune reactions is an outstanding example of the emerging mutual influences and of how NO plays its regulatory role in vital functions of plants. ABA-dependent and SA-dependent stomatal closure upon pathogen recognition is mediated by NO; the virulence factor coronatine, a structural and functional mimic of JA, can reverse the effect and lead to stomatal reopening. These data implicate the involvement of at least three phytohormones (or mimics thereof) in pathogen-induced stomatal movements and suggest NO as a key mediator of these hormone responses [35•]. Although the role of NO in stomatal closure remains to be defined, S-nitrosylation of K^+ outward rectifying chan-

nels supports a potential role of this posttranslational modification in modulating stomatal movements [37].

S-nitrosylation controls cell death

NO's control over Arabidopsis metacaspase 9, a potential executioner of programmed cell death [38•], is another intriguing example of how NO exerts its physiological functions through S-nitrosylation. Data indicate that this modification keeps the zymogen inactive under normal physiological conditions, inhibiting the autoproteolytic activity of prometacaspase 9. S-nitrosylation of Arabidopsis cytosolic glyceraldehyde 3-phosphate dehydrogenase (GAPDH) could also play a role in the regulation of cell death, as it causes GAPDH inactivation and potentially induces translocation to the nucleus [39]. In animal systems, S-nitrosylated GAPDH binds to and stabilises Siah1 (an E3 ubiquitin ligase), followed by translocation to the nucleus, where Siah1 degrades nuclear proteins. These events finally lead to apoptosis [40]. A similar scenario, though conceivable, still remains to be demonstrated in plant cells. S-nitrosylation seems to have opposing roles in controlling programmed cell death: on the one hand, S-nitrosylation promotes the execution of programmed cell death by altering GAPDH function and on the other hand, S-nitrosylation of prometacaspase 9 keeps this putative executioner of cell death inactive. However, the kinetics of these signalling reactions suggests the involvement of enzymatic mechanisms [41]. Hence, activation of metacaspase 9 under conditions of increased NO production may depend on enzymatic denitrosylation. In this context, thioredoxins clearly deserve attention in the future ([42•], cf. NPR1).

This overview of S-nitrosylation already gives an impression of the emerging complexity of NO-dependent signalling in plants. But there is more to come: Arabidopsis PrxIIE has been found to be S-nitrosylated during the hypersensitive disease resistance response, resulting in not only inhibition of its hydroperoxide-reducing peroxidase activity, but also reduction of its ability to detoxify $ONOO^-$ [22••]. This inhibition leads to increased $ONOO^-$-dependent nitrotyrosine formation. Thus, S-nitrosylation can modulate a central point of convergence for ROS-dependent and NO-dependent signalling pathways in response to several stresses by deactivating a crucial component of the cellular antioxidant system.

Protein tyrosine nitration

Protein tyrosine nitration results from a chemical reaction, in which $ONOO^-$ adds a nitro group in *ortho* position to the aromatic ring of tyrosine residues [43,44]. The added nitro group can alter protein function and conformation when placed on a relevant tyrosine residue and can increase the proteins' susceptibility to proteolysis [45,46].

In animals, nitration of tyrosine residues is often considered a marker for certain pathological conditions, but

has recently been suggested to be relevant to redox signalling [47*,48]. In plants, tyrosine nitration appears to be physiologically relevant during biotic and abiotic stresses [22**,49,50]. However, any physiological reaction must meet certain criteria to be considered a signalling process: (i) the signal compound is produced at strictly controlled rates; (ii) the induced reaction is reversible and/or the effects transient; (iii) the resulting modification (e.g. of a target protein) causes alterations of cell function(s). On the basis of these criteria, what arguments can be put forward to qualify tyrosine nitration as a signalling process in plants? (i) ONOO$^-$ production is not under direct enzymatic control, but nonetheless seems to be tightly regulated (see 'Regulation of NO bioavailability'). The transient increase of ONOO$^-$ levels in elicitor challenged tobacco cell culture supports this notion [50]. (ii) Recent studies report a transient increase of tyrosine-nitrated proteins during the disease resistance response [22**,50,51]. (iii) The only indications for functional modifications by tyrosine nitration come from the animal kingdom, where both enzyme inhibition and activation have been reported [52–54]. In plants, only one study provided an indirect proof of inhibition of glutathione *S*-transferase by RNS that correlated with increased nitro-tyrosine levels [55]. We have recently conducted a proteomic study to identify tyrosine nitrated proteins in Arabidopsis plants challenged with an incompatible bacterial pathogen [51]. Interestingly, several of the proteins with increased nitration levels during the hypersensitive resistance response are also nitrated in unchallenged plants. Thus, tyrosine nitration could play a role under physiological as well as stress conditions. Independently, we found that NtMEK2, a tobacco MAPKK, can be nitrated *in vitro*, resulting in loss of its activity (E Vandelle *et al.*, unpublished). In animal systems, ONOO$^-$ is known to interfere with phosphorylation cascades via nitration of relevant tyrosine residues in target proteins, mimicking or preventing tyrosine phosphorylation [47*]. Furthermore, several protein kinases, comprising all components of the MAPK module [47*], have been shown to be modulated by tyrosine nitration, being either activated [56,57] or inhibited [58,59]. On the basis of these findings, regulatory mechanisms controlling the MAPK module by tyrosine nitration are also plausible in plants, again pointing to RNS as crucial modulators of signal transduction.

Taken together, the above-mentioned data support our view that tyrosine nitration is a physiologically relevant posttranslational modification in plants.

Metal nitrosylation
NO can react with most transition metals, but its interactions with iron are probably the most relevant biologically [41,60]. The most prominent examples for modulation of enzymatic activity by NO in animals are associated with haem nitrosylation, such as inhibition of cytochrome *c* oxidase and NOS, regulation of diverse cytochrome P450s and activation of soluble guanylate cyclase (sGC). sGC is the prototypic NO sensor and NO-modified protein in animals [61]. sGC is activated via haem nitrosylation and is responsible for the majority of physiological responses to NO. By contrast, virtually nothing is known about this NO-dependent modification in plants. The only exceptions are plant haemoglobins (cf. 'Regulation of NO bioavailability'). However, in this case the occurring reaction constitutes an NO scavenging mechanism and not a modification of enzymatic function. On the basis of chemical considerations, plant cytochrome P450s seem likely targets of metal nitrosylation. Given the functional diversity of plant cytochrome P450s, intriguing connections between NO-related signalling and different metabolic processes could emerge.

The missing link to cGMP
In animals, NO can initiate its biological effects through the activation of sGC and associated increase in the levels of the second messenger cGMP. Both a transient increase in cGMP and its involvement in several processes have also been demonstrated in plants [62]. Indeed, pharmacological and biochemical approaches showed that cGMP is involved in NO-dependent signalling, gene transcription modulation, root growth and gravitropism, pollen tube growth and orientation, hormone-dependent responses, stomatal opening and responses to biotic and abiotic stresses. Hence, the physiological role of this second messenger is unequivocally recognised. Although several potential GCs have been identified using bioinformatics tools, their relevance as cGMP sources still awaits demonstration. In fact, the overexpression of AtGC1 in *E. coli* [63] and activity analysis of the putative GC catalytic centre of the brassinosteroid receptor AtBRI1 *in vitro* [64] showed only low activity compared with the animal sGC [65], questioning their relevance as plant GCs. Supporting this observation, despite the capacity of these proteins to produce cGMP from GTP *in vitro*, our experiments did not reveal any increase in cGMP level in Arabidopsis plants overexpressing AtGC1 (J Hussain *et al.*, unpublished data). By contrast, we have produced Arabidopsis plants expressing the α-subunit and β-subunit of mammalian sGC that display an up to 40-fold increase in cGMP levels compared with wild-type plants (J Hussain *et al.*, unpublished). This has made a genetic tool available to study the impact of this second messenger in plants. The endogenous cGMP production systems, however, remain unclear.

Conclusions
We continue to gain new knowledge on NO-related signalling. However, the data available are still far from offering a comprehensive and consistent picture of NO function in plants. The lack of genetic tools substantially hinders research on NO production and functions. New findings, however, underline the importance of NO in plant cell physiology and the complexity of NO-related

signalling networks. Particularly, the impact of *S*-nitrosylation on protein function has been clearly demonstrated, plus different modes of NO-mediated signalling are gaining increasing attention. On the basis of the current status of research we can expect the functional relevance of other NO-mediated posttranslational modifications and/or second messengers to be demonstrated soon.

Acknowledgement

References and recommended reading

Papers of particular interest, published within the period of review, have been highlighted as:

- of special interest
- •• of outstanding interest

1. Delledonne M, Xia Y, Dixon RA: **Lamb C: nitric oxide functions as a signal in plant disease resistance**. *Nature* 1998, **394**:585-588.

2. Wilson ID, Neill SJ, Hancock JT: **Nitric oxide synthesis and**
• **signalling in plants**. *Plant Cell Environ* 2008, **31**:622-631.
This review, together with [4•], gives a more detailed overview of NO production in plants and some aspects of signalling that are not covered here due to space limitations.

3. Nathan C: **The moving frontier in nitric oxide-dependent signalling**. *Sci STKE* 2004, **2004**:pe52.

4. Besson-Bard A, Pugin A, Wendehenne D: **New insights into**
• **nitric oxide signaling in plants**. *Annu Rev Plant Biol* 2008, **59**:21-39.
As [2•], this review describes NO signalling and production in plants in more detail; both references also contain extensive bibliographies.

5. Moreau M, Lee GI, Wang Y, Crane BR, Klessig DF: **AtNOS/**
•• **AtNOA1 is a functional *Arabidopsis thaliana* cGTPase and not a nitric-oxide synthase**. *J Biol Chem* 2008, **283**:32957-32967.
After a long controversy, this study finally demonstrated that AtNOS1/AtNOA1 is not a nitric oxide synthase, but a chloroplastic GTPase involved in proper ribosome assembly.

6. Flores-Pérez U, Sauret-Güeto S, Gas E, Jarvis P, Rodríguez-
• Concepción M: **A mutant impaired in the production of plastome-encoded proteins uncovers a mechanism for the homeostasis of isoprenoid biosynthetic enzymes in Arabidopsis plastids**. *Plant Cell* 2008, **20**:1303-1315.
Together with [4•], this study ended the controversy about AtNOS1/AtNOA1/AtRif1. The gene was identified independently in a screening for fosmidomycin resistance. Levels of methylerythritol pathway enzymes are upregulated in the mutant.

7. Bright J, Desikan R, Hancock JT, Weir IS, Neill SJ: **ABA-induced NO generation and stomatal closure in Arabidopsis are dependent on H_2O_2 synthesis**. *Plant J* 2006, **45**:113-122.

8. Modolo LV, Augusto O, Almeida IMG, Pinto-Maglio CAF, Oliveira HC, Seligman K, Salgado I: **Decreased arginine and nitrite levels in nitrate reductase-deficient Arabidopsis thaliana plants impair nitric oxide synthesis and the hypersensitive response to Pseudomonas syringae**. *Plant Sci* 2006, **171**:34-40.

9. Flores T, Todd CD, Tovar-Mendez A, Dhanoa PK, Correa-Aragunde N, Hoyos ME, Brownfield DM, Mullen RT, Lamattina L, Polacco JC: **Arginase-negative mutants of Arabidopsis exhibit increased nitric oxide signaling in root development**. *Plant Physiol* 2008, **147**:1936-1946.

10. He Y, Tang R-H, Hao Y, Stevens RD, Cook CW, Ahn SM, Jing L, Yang Z, Chen L, Guo F *et al.*: **Nitric oxide represses the Arabidopsis floral transition**. *Science* 2004, **305**:1968-1971.

11. Lee U, Wie C, Fernandez BO, Feelisch M, Vierling E: **Modulation of**
• **nitrosative stress by S-nitrosoglutathione reductase is critical for thermotolerance and plant growth in Arabidopsis**. *Plant Cell* 2008, **20**:786-802.

Mutations in Atgsnor lead to impaired heat acclimation. The detailed characterisation of the mutant phenotype illustrates that altered NO homeostasis not only impacts stress resistance, but also influences various developmental processes.

12. Morot-Gaudry-Talarmain Y, Rockel P, Moureaux T, Quilleré I, Leydecker MT, Kaiser WM, Morot-Gaudry JF: **Nitrite accumulation and nitric oxide emission in relation to cellular signaling in nitrite reductase antisense tobacco**. *Planta* 2002, **215**:708-715.

13. Ahlfors R, Brosché M, Kollist H, Kangasjärvi J: **Nitric oxide modulates ozone-induced cell death, hormone biosynthesis and gene expression in *Arabidopsis thaliana***. *Plant J* 2009, **58**:1-12.

14. Avila EL, Brown M, Pan S, Desikan R, Neill SJ, Girke T, Surpin M, Raikhel NV: **Expression analysis of Arabidopsis vacuolar sorting receptor 3 reveals a putative function in guard cells**. *J Exp Bot* 2008, **59**:1149-1161.

15. Iwakiri Y, Satoh A, Chatterjee S, Toomre DK, Chalouni CM, Fulton D, Groszmann RJ, Shah VH, Sessa WC: **Nitric oxide synthase generates nitric oxide locally to regulate compartmentalized protein S-nitrosylation and protein trafficking**. *Proc Natl Acad Sci USA* 2006, **103**:19777-19782.

16. Harris LK, McCormick J, Cartwright JE, Whitley GSJ, Dash PR: **S-nitrosylation of proteins at the leading edge of migrating trophoblasts by inducible nitric oxide synthase promotes trophoblast invasion**. *Exp Cell Res* 2008, **314**:1765-1776.

17. Perazolli M, Dominici P, Romero-Puertas MC, Zago E, Zeier J, Sonoda M, Lamb C, Delledonne M: **Arabidopsis nonsymbiotic hemoglobin AHb1 modulates nitric oxide bioactivity**. *Plant Cell* 2004, **16**:2785-2794.

18. Zeier J, Delledonne M, Mishina T, Severi E, Sonoda M, Lamb C: **Genetic elucidation of nitric oxide signaling in incompatible plant–pathogen interactions**. *Plant Physiol* 2004, **136**:2875-2886.

19. Liu L, Hausladen A, Zeng M, Que L, Heitman J, Stamler JS: **A metabolic enzyme for S-nitrosothiol conserved from bacteria to humans**. *Nature* 2001, **410**:490-494.

20. Feechan A, Kwon E, Yun B-W, Wang Y, Pallas JA, Loake GJ: **A central role for S-nitrosothiols in plant disease resistance**. *Proc Natl Acad Sci USA* 2005, **102**:8054-8059.

21. Rustérucci C, Espunya MC, Díaz M, Chabannes M, Martínez MC: **S-nitrosoglutathione reductase affords protection against pathogens in Arabidopsis, both locally and systemically**. *Plant Physiol* 2007, **143**:1282-1292.

22. Romero-Puertas MC, Laxa M, Mattè A, Zaninotto F, Finkemeier I,
•• Jones AME, Perazolli M, Vandelle E, Dietz K-J, Delledonne M: **S-nitrosylation of peroxiredoxin II E promotes peroxynitrite-mediated tyrosine nitration**. *Plant Cell* 2007, **19**:4120-4130.
Peroxiredoxin II E is involved in peroxynitrite detoxification. This activity is inhibited by *S*-nitrosylation of the enzyme, which leads to increased protein nitration by peroxynitrite. The combined functions of hydroperoxide and peroxynitrite detoxification suggest that PrxIIE modulates both ROS and NO signalling.

23. Delledonne M, Zeier J, Marocco A, Lamb C: **Signal interactions between nitric oxide and reactive oxygen intermediates in the plant hypersensitive disease resistance response**. *Proc Natl Acad Sci USA* 2001, **98**:13454-13459.

24. Stamler JS, Lamas S, Fang FC: **Nitrosylation: the prototypic redox-based signaling mechanism**. *Cell* 2001, **106**:675-683.

25. Lindermayr C, Saalbach G, Durner J: **Proteomic identification of S-nitrosylated proteins in Arabidopsis**. *Plant Physiol* 2005, **137**:921-930.

26. Romero-Puertas MC, Campostrini N, Mattè A, Righetti PG, Perazolli M, Zolla L, Roepstorff P, Delledonne M: **Proteomic analysis of S-nitrosylated proteins in Arabidopsis thaliana undergoing hypersensitive response**. *Proteomics* 2008, **8**:1459-1469.

27. Ferrarini A, De Stefano M, Baudouin E, Pucciariello C, Polverari A, Puppo A, Delledonne M: **Expression of Medicago truncatula genes responsive to nitric oxide in pathogenic and symbiotic conditions**. *Mol Plant Microbe Interact* 2008, **21**:781-790.

28. Grün S, Lindermayr C, Sell S, Durner J: **Nitric oxide and gene regulation in plants**. *J Exp Bot* 2006, **57**:507-516.

29. Palmieri MC, Sell S, Huang X, Scherf M, Werner T, Durner J, Lindermayr C: **Nitric oxide-responsive genes and promoters in Arabidopsis thaliana: a bioinformatics approach**. *J Exp Bot* 2008, **59**:177-186.

30. Serpa V, Vernal J, Lamattina L, Grotewold E, Cassia R, Terenzi H: **Inhibition of AtMYB2 DNA-binding by nitric oxide involves cysteine S-nitrosylation**. *Biochem Biophys Res Commun* 2007, **361**:1048-1053.

31. Tada Y, Spoel SH, Pajerowska-Mukhtar K, Mou Z, Song J,
•• Wang C, Zuo J, Dong X: **Plant immunity requires conformational charges of NPR1 via S-nitrosylation and thioredoxins**. *Science* 2008, **321**:952-956.
S-nitrosylation is involved the control of NPR1 oligomerisation and localisation and thus influences the activation of SA-dependent defence responses.

32. Spoel SH, Koornneef A, Claessens SMC, Korzelius JP, Van Pelt JA, Mueller MJ, Buchala AJ, Métraux J-P, Brown R, Kazan K *et al.*: **NPR1 modulates cross-talk between salicylate- and jasmonate-dependent defense pathways through a novel function in the cytosol**. *Plant Cell* 2003, **15**:760-770.

33. Wang Y-Q, Feechan A, Yun B-W, Shafiei R, Hofmann A, Taylor P, Xue P, Yang F-Q, Xie Z-S, Pallas JA *et al.*: **S-nitrosylation of AtSABP3 antagonizes the expression of plant immunity**. *J Biol Chem* 2009, **284**:2131-2137.

34. Lindermayr C, Saalbach G, Bahnweg G, Durner J: **Differential inhibition of Arabidopsis methionine adenosyltransferases by protein S-nitrosylation**. *J Biol Chem* 2006, **281**:4285-4291.

35. Melotto M, Underwood W, Koczan J, Nomura K, He SY: **Plant
• stomata function in innate immunity against bacterial invasion**. *Cell* 2006, **126**:969-980.
The authors show that NO is involved in SA-dependent and ABA-dependent stomatal closure upon pathogen recognition. The virulence factor coronatine is involved in reopening of stomata and thus circumvention of this mechanism of innate immunity. This study gives an impressive example of the intricate interplay of different signals.

36. Correa-Aragunde N, Graziano M, Lamattina L: **Nitric oxide plays a central role in determining lateral root development in tomato**. *Planta* 2004, **218**:900-905.

37. Sokolovski S, Blatt MR: **Nitric oxide block of outward-rectifying K+ channels indicates direct control by protein nitrosylation in guard cells**. *Plant Physiol* 2004, **136**:4275-4284.

38. Belenghi B, Romero-Puertas MC, Vercammen D, Brackenier A,
• Inzé D, Delledonne M, Van Breusegem F: **Metacaspase activity of Arabidopsis thaliana is regulated by S-nitrosylation of a critical cysteine residue**. *J Biol Chem* 2007, **282**:1352-1358.
The authors provide evidence for the inhibition of autoproteolytic activity of prometacaspase 9 by S-nitrosylation, whereas the mature protease is not inhibited by NO. Thus, steady-state S-nitrosylation in unchallenged plants may be a mechanism to keep executioners of programmed cell death inactive.

39. Holtgrefe S, Gohlke J, Starmann J, Druce S, Klocke S, Altmann B, Wojtera J, Lindermayr C, Scheibe R: **Regulation of plant cytosolic glyceraldehyde 3-phosphate dehydrogenase isoforms by thiol modifications**. *Physiol Plant* 2008, **133**:211-228.

40. Hara MR, Agrawal N, Kim SF, Cascio MB, Fujimuro M, Ozeki Y, Takahashi M, Cheah JH, Tankou SK, Hester LD *et al.*: **S-nitrosylated GAPDH initiates apoptotic cell death by nuclear translocation following Siah1 binding**. *Nat Cell Biol* 2005, **7**:665-674.

41. Forman HJ, Fukuto JM, Miller T, Zhang H, Rinna A, Levy S: **The chemistry of cell signaling by reactive oxygen and nitrogen species and 4-hydroxynonenal**. *Arch Biochem Biophys* 2008, **477**:183-195.

42. Benhar M, Forrester MT, Hess DT, Stamler JS: **Regulated protein
• denitrosylation by cytosolic and mitochondrial thioredoxins**. *Science* 2008, **320**:1050-1054.
The authors demonstrated that thioredoxins act as denitrosylating enzymes in animal systems. Besides their role in protection against oxidative damage, thioredoxins potentially contribute to NO-related signal transduction by modulating basal and stimulus induced denitrosylation.

43. Radi R: **Nitric oxide, oxidants, and protein tyrosine nitration**. *Proc Natl Acad Sci USA* 2004, **101**:4003-4008.

44. Rubbo H, Radi R: **Protein and lipid nitration: role in redox signaling and injury**. *Biochim Biophys Acta* 2008, **1780**:1318-1324.

45. Grune T, Blasig IE, Sitte N, Roloff B, Haseloff R, Davies KJA: **Peroxynitrite increases the degradation of aconitase and other cellular proteins by proteasome**. *J Biol Chem* 1998, **273**:10857-10862.

46. Souza JM, Choi I, Chen Q, Weisse M, Daikhin E, Yudkoff M, Obin M, Ara J, Horwitz J, Ischiropoulos H: **Proteolytic degradation of tyrosine nitrated proteins**. *Arch Biochem Biophys* 2000, **380**:360-366.

47. Monteiro HP, Arai RJ, Travassos LR: **Protein tyrosine
• phosphorylation and protein tyrosine nitration in redox signaling**. *Antioxid Redox Signal* 2008, **10**:843-890.
This review presents a very good survey of the competition/cooperation between tyrosine phosphorylation and tyrosine nitration in animals. Emphasis is placed on the role of nitration in modulating phosphorylation-mediated cellular events by mimicking or inhibiting tyrosine-phosphorylation.

48. Aulak KS, Koeck T, Crabb JW, Stuehr DJ: **Proteomic method for identification of tyrosine-nitrated proteins**. *Methods Mol Biol* 2004, **279**:151-165.

49. Corpas FJ, Chaki M, Fernandez-Ocana A, Valderrama R, Palma JM, Carreras A, Begara-Morales JC, Airaki M, del Rio LA, Barroso JB: **Metabolism of reactive nitrogen species in pea plants under abiotic stress conditions**. *Plant Cell Physiol* 2008, **49**:1711-1722.

50. Saito S, Yamamoto-Katou A, Yoshioka H, Doke N, Kawakita K: **Peroxynitrite generation and tyrosine nitration in defense responses in tobacco BY-2 cells**. *Plant Cell Physiol* 2006, **47**:689-697.

51. Cecconi D, Orzetti S, Vandelle E, Rinalducci S, Zolla L, Delledonne M: **Protein nitration during defence response in Arabidopsis thaliana**. *Electrophoresis* 2009, doi:10.1002/elps.200800826.

52. Neumann H, Hazen JL, Weinstein J, Mehl RA, Chin JW: **Genetically encoding protein oxidative damage**. *J Am Chem Soc* 2008, **130**:4028-4033.

53. Wong PSY, Eiserich JP, Reddy S, Lopez CL, Cross CE, van der Vliet A: **Inactivation of glutathione S-transferases by nitric oxide-derived oxidants: exploring a role for tyrosine nitration**. *Arch Biochem Biophys* 2001, **394**:216-228.

54. Cassina AM, Hodara R, Souza JM, Thomson L, Castro L, Ischiropoulos H, Freeman BA, Radi R: **Cytochrome c nitration by peroxynitrite**. *J Biol Chem* 2000, **275**:21409-21415.

55. Gong Y-W, Yuan Y-J: **Nitric oxide mediates inactivation of glutathione S-transferase in suspension culture of Taxus cuspidata during shear stress**. *J Biotechnol* 2006, **123**:185-192.

56. Zhang P, Wang Y-Z, Kagan E, Bonner JC: **Peroxynitrite targets the epidermal growth factor receptor, Raf-1, and MEK independently to activate MAPK**. *J Biol Chem* 2000, **275**:22479-22486.

57. Pinzar E, Wang T, Garrido MR, Xu W, Levy P, Bottari SP: **Angiotensin II induces tyrosine nitration and activation of ERK1/2 in vascular smooth muscle cells**. *FEBS Lett* 2005, **579**:5100-5104.

58. Schieke S, Briviba K, Klotz L-O, Sies H: **Activation pattern of mitogen-activated protein kinases elicited by peroxynitrite: attenuation by selenite supplementation**. *FEBS Lett* 1999, **448**:301-303.

59. Kinjo N, Kawanaka H, Akahoshi T, Yamaguchi S, Yoshida D, Anegawa G, Konishi K, Tomikawa M, Tanoue K, Tarnawski A *et al.*: **Significance of ERK nitration in portal hypertensive gastropathy and its therapeutic implications**. *Am J Physiol Gastrointest Liver Physiol* 2008, **295**:G1016-1024.

60. Cooper CE: **Nitric oxide and iron proteins**. *Biochim Biophys Acta* 1999, **1411**:290-309.

61. Poulos TL: **Soluble guanylate cyclase**. *Curr Opin Struct Biol* 2006, **16**:736-743.

62. Meier S, Gehring C: **Emerging roles in plant biotechnology for the second messenger cGMP—guanosine 3′, 5′-cyclic monophosphate**. *Afr J Biotechnol* 2006, **5**:1687-1692.

63. Ludidi N, Gehring C: **Identification of a novel protein with guanylyl cyclase activity in *Arabidopsis thaliana***. *J Biol Chem* 2003, **278**:6490-6494.

64. Kwezi L, Meier S, Mungur L, Ruzvidzo O, Irving H, Gehring C: **The Arabidopsis thaliana brassinosteroid receptor (AtBRI1) contains a domain that functions as a guanylyl cyclase *in vitro***. *PLoS ONE* 2007, **2**:e449.

65. Winger JA, Marletta MA: **Expression and characterization of the catalytic domains of soluble guanylate cyclase: interaction with the heme domain**. *Biochemistry* 2005, **44**:4083-4090.

ELSEVIER

Upstream and downstream signals of nitric oxide in pathogen defence

Frank Gaupels[1], Gitto Thomas Kuruthukulangarakoola[1] and Jörg Durner[1,2]

Nitric oxide (NO) is now recognised as a crucial player in plant defence against pathogens. Considerable progress has been made in defining upstream and downstream signals of NO. Recently, MAP kinases, cyclic nucleotide phosphates, calcium and phosphatidic acid were demonstrated to be involved in pathogen-induced NO-production. However, the search for inducers of NO synthesis is difficult because of the still ambiguous enzymatic source of NO. Accumulation of NO triggers signal transduction by other second messengers. Here we depict NON-EXPRESSOR OF PATHOGENESIS-RELATED 1 and glyceraldehyde-3-phosphate dehydrogenase as central redox switches translating NO redox signalling into cellular responses. Although the exact position of NO in defence signal networks is unresolved at last some NO-related signal cascades are emerging.

Addresses
[1] Institute of Biochemical Plant Pathology, Helmholtz Zentrum München, German Research Center for Environmental Health, 85764 Munich/Neuherberg, Germany
[2] Chair of Biochemical Plant Pathology, Technische Universität München, 85354 Freising, Germany

Corresponding authors: Gaupels, Frank
(frank.gaupels@helmholtz-muenchen.de), Durner, Jörg
(durner@helmholtz-muenchen.de)

Introduction

Nitric oxide (NO) mediates a plethora of physiological functions in plants, animals and microbes. Apart from its physiological role, NO can mediate defence responses in plants against invading pathogens [1]. Endogenous messenger molecules and signalling cascades induced by pathogenic elicitors trigger an increase in NO levels in plant. However, an exact source of NO production during defence response has yet to be elucidated [2,3]. Increasing cellular NO levels mediate NO-based signalling processes either by directly modifying proteins or through the activation of second messengers. NO has been demonstrated to interact with second messengers such as phosphatidic acid (PA) and cyclic guanosine monophosphate (cGMP) [4,5]. S-nitrosylation and tyrosine nitration are the two NO-dependent direct protein modifications involved in plant defence signalling. Biochemical and pharmacological studies have indicated that S-nitrosylation is a significant signalling event in determining the fate of plant–pathogen interaction and is the best-studied NO-based modification in plants. This review discusses recent developments in understanding NO-related signalling processes in pathogen defence responses.

NO synthesis

Mammalian nitric oxide synthase (NOS)-like activity is regarded as a major enzymatic source of NO during plant–pathogen interactions [2]. Despite this fact not much progress has been made in identifying a plant gene coding for a NOS-like enzyme [1–3]. Only in the unicellular green alga *Ostreococcus tauri* has a NOS been characterised, without any known homologues in higher plants [6•]. Interestingly, nitrate reductase (NR), which was also reported to be — directly or indirectly — involved in NO accumulation during defence responses can be inhibited by NO. In *Chlamydomonas reinhardtii* nitrate assimilation was found to be under control of the soluble guanylate cyclase (sGC) CYG56 [7••]. Ammonium accumulation induced NO production by a NOS-like enzyme activity and NO-dependent activation of CYG56, which repressed the NR-coding gene *NIA1*. Accordingly, injection of NO donors partially inhibited while NOS inhibitors increased NR activity in wheat leaves [8]; however, in this study enzyme activity rather than gene expression was affected by NO. Recently, an *Arabidopsis thaliana* copper amine oxidase (CuAO1) was reported to produce NO from polyamines upon treatment with abscisic acid (ABA) [9]. The biological significance of these findings in the context of pathogen defence is unclear.

Signals upstream of NO synthesis

A role for NO in plant defence against pathogens is well established and several elicitors of NO synthesis have been identified in the past. However, detailed knowledge about signal cascades upstream of NO is still lacking. Calcium/calmodulin is the only signal or co-factor that was frequently reported to be essential for NO production upon pathogen challenge [5,10]. On the basis of recent findings, herein we speculate on signalling cascades from pathogen perception to calcium-dependent NO production.

Extracellular ATP and phosphatidic acid

Extracellular adenosine triphosphate (eATP) is involved in pathogen defence signalling but extracellular receptors and exact mechanisms are unknown [4,11]. Downstream signals of eATP include calcium, reactive oxygen species (ROS) and NO [4]. Interestingly, exogenous treatment of suspension-cultured tomato cells with ATP induced rapid formation of PA from membrane phospholipids within minutes and accumulation of NO [12•]. It was further demonstrated that the induction of NO synthesis by eATP was dependent on PA and a rise in cytosolic calcium. Moreover, PA bound and activated ROS-producing respiratory burst oxidase homologue (RBOH) D and F isoforms of *Arabidopsis* in ABA-mediated stomatal closure [13]. Thus, eATP, PA, ROS and calcium are likely to be elements of one signalling cascade in the induction of NO. The exact position of calcium in this sequence remains to be determined (Figure 1).

Cyclic nucleotides and calcium

Until recently, cyclic nucleotide phosphate (cNMP) signalling has been regarded to be downstream of NO (see below). Strikingly, research in the group of GA Berkowitz provided evidence that cNMPs are also important players in plant defence signalling upstream of calcium and NO [5]. The receptor AtPepR1 for *Arabidopsis* AtPep signal peptides was found to be a functional guanylate cyclase (GC) producing the second messenger cGMP from guanosine triphosphate [14]. The GC domain was embedded in the cytosolic kinase region of the leucine-rich repeat receptor-like kinase (LRR-RLKS). It was shown that cytosolic calcium influx and defence gene induction after treatment with cGMP, AtPep3 or flagellin was dependent on AtPepR1 and cyclic nucleotide gated channel 2 (CNGC2) [14]. Similarly, upon challenge with avirulent *Pseudomonas syringae* or pathogen-derived lipopolysaccharides a rapid rise in cyclic adenosine monophosphate (cAMP) levels triggered a CNGC2-mediated calcium influx, confirming the central role of calcium in cNMP signalling. The rise in cytosolic calcium was followed by NO and ROS generation and hypersensitive response (HR) [15••].

Using inhibitors of adenylyl cyclase and cAMP-degrading phosphodiesterase demonstrated that pathogen-induced NO production was dependent on cAMP-induced calcium influx. Hence a picture develops, in which perception of a pathogen/elicitor triggers cNMP production by the nucleotide cyclase domain of the receptor. Subsequently, cNMPs would elicit a CNGC2-mediated calcium transient, calcium-dependent NO and ROS synthesis and finally defence gene expression [5] (Figure 1).

MAP kinase signalling

Mitogen-activated protein kinases (MAPK) translate external stress stimuli into a cellular response. Recently, it was discovered that MAPK cascades regulate the

Figure 1
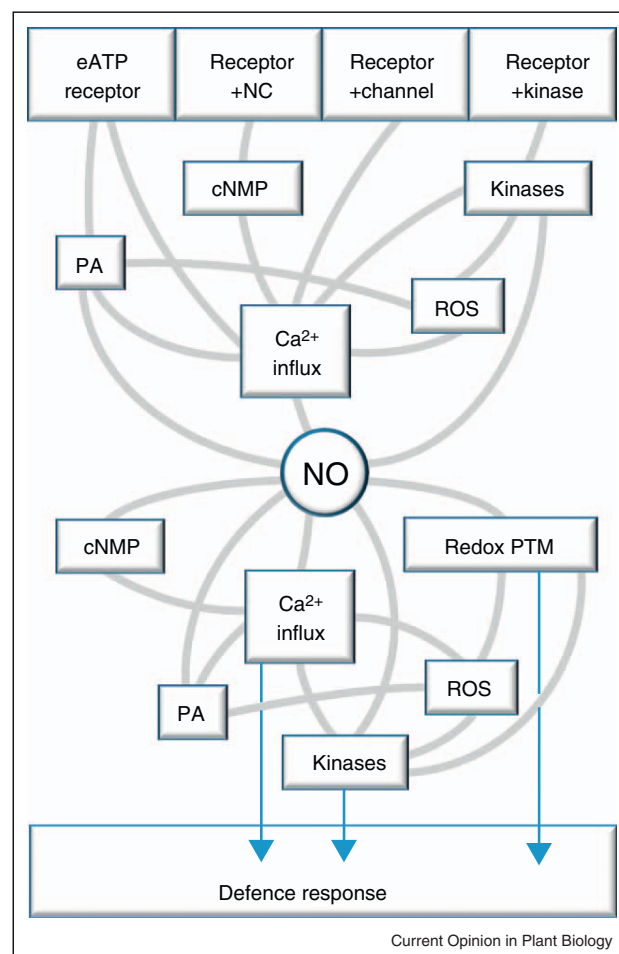
Hypothetical interaction map of upstream and downstream signals of NO in pathogen defence. Lines indicate direct or indirect interactions as described in the publications discussed in this review. The upper part of the figure schematically depicts the yet unknown eATP receptor and receptors linked to nucleotide cyclase (+NC), ion/calcium channel (+channel) or kinase (+kinase) as potential starting points for defence signalling. Kinases include MAP kinase cascades and (Ca^{2+}-dependent) protein kinases. Second messengers upstream and downstream of NO form signal cascades and networks ultimately inducing a defence response (arrows). For instance, calcium (Ca^{2+}), MAP kinases and redox-post-translational modifications (PTM) of NPR1/TGA1 are known inducers of pathogenesis-related genes.

concerted production of NO and ROS during the onset of HR (Figure 1). In a study with *Nicotiana benthamiana*, transient expression of a constitutively active form of the MAPK kinase MEK2 (MEK2^{DD}) caused phosphorylation of the MAPK SIPK/NTF4, NO and ROS burst and cell death [16]. NO synthesis was dependent on NITRIC OXIDE ASSOCIATED 1, and ROS was produced by RBOHB. The latter was also induced by the MEK1–NTF6 cascade [16]. Accordingly, silencing of both MAPK cascades suppressed NO/ROS accumulation and HR cell

death upon treatment with the fungal elicitor INF1. One proposed mode of interaction between MAPKs and NO/ROS signalling is the activation of the flavin biosynthesis enzyme RibA by MEK2–SIPK/NTF4 [17]. Activated RibA would then supply flavin for the prosthetic groups of NO and ROS-producing flavoenzymes such as NOS-like, NR and RBOH.

Signals downstream of NO synthesis

Work with NO donors and NO-related mutants provided insight into NO-induced signalling but knowledge on interactions between the identified signals is still limited. Notably, some of the signals described above as inducers of NO synthesis were also reported to act downstream of NO, underlining the complexity of NO-related signal webs (Figure 1).

Emerging NO-induced second messengers

In animals, one of the best-studied targets of NO is the haem domain of soluble GC (sGC). Metal nitrosylation of this domain strongly induces cGMP production. Significantly, NO elicited a rapid rise in cGMP levels within seconds in transgenic rice protoplasts and *Arabidopsis* plants expressing the cGMP fluorescent sensor δ FlincG suggesting that sGC enzymes are present in higher plants although no sGC has been identified to date [18]. In the algal protist *C. reinhardtii* NO-activation of the sGC CYG56 in response to ammonium accumulation caused cGMP-mediated suppression of *NIA1* (see above [7••]).

PA is one of the signals that probably acts both upstream and downstream of NO. The elicitors xylanase and chitosan induced PA synthesis and ROS accumulation [19,20]. The ROS burst and xylanase-induced cell death were diminished by applying a scavenger of NO (cPTIO) and inhibitors of the PA biosynthesis enzyme phospholipase C. Further downstream signals of NO comprise calcium [10,21] and MAP kinases, which might be regulated via redox modifications [1] or by an unknown mode of interaction with S-nitrosylated glyceraldehyde-3-phosphate dehydrogenase (GAPDH) [22].

S-nitrosylation

Cysteine S-nitrosylation is a post-translational modification involving the reversible covalent binding of NO to the cysteine residue of proteins to form S-nitrosocysteine. In *Arabidopsis*, many potential protein candidates carrying NO-sensitive cysteine residues have already been reported [23–25].

NPR1 (non-expressor of PR1) is a central SA-responsive transcription co-activator of pathogenesis-related gene 1 (*PR1*) — it was first identified in *Arabidopsis*. NPR1 is an oligomer localised in the cytoplasm. During SA-induced disease resistance, the oligomer dissociates into monomers which then move into the nucleus [26]. While the monomerisation reaction of NPR1 was shown to be

catalysed by thioredoxin, oligomerisation is facilitated by S-nitrosylation [27]. However, accumulation of NPR1 in the nucleus increased significantly when *Arabidopsis* mesophyll protoplasts were treated with the physiological NO donor, S-nitrosoglutathione (GSNO) [28••]. Though the above two studies appear to be contradictory, it is likely that S-nitrosylated NPR1 might be serving as an intermediate between the more oxidised (oligomer) and reduced (monomer) forms. Reversible and dynamic nature of S-nitrosylated NPR1 can be more effective in sensing the changing redox microenvironment and maintain the NPR1 equilibrium in the cytoplasm [27]. In the nucleus, NPR1 interacts with the transcription factor TGA1 (TGACG motif binding factor) and binds to the promoter region to activate PR gene expression [29]. *In vitro* studies using GSNO have shown that both NPR1 and TGA1 are prone to S-nitrosylation reduction, which favoured DNA binding and TGA1 stability [28••]. Thus, S-nitrosylation might be crucial in regulating SA-induced plant immunity.

SA-binding protein 3 (SABP3), another key element in SA signalling, can positively regulate the plant defence response through SA-activated carbonic anhydrase (CA) activity. S-nitrosylation of SABP3 in *Arabidopsis* reduced the SA binding and CA activity of this protein [30•]. Also, S-nitrosylation of SABP3 increased with increasing cellular S-nitrosothiol (SNO) levels. S-nitrosylation of SABP3 could be either a negative feedback loop that modulates the plant defence response or a pathogen-induced suppression of HR. Nevertheless, these results suggest involvement of S-nitrosylation in the HR.

In line with this, GAPDH, peroxyredoxin II E (PrxII E) and *Arabidopsis* type II metacaspase 9 (AtMC9) were reported as S-nitrosylated proteins involved in the HR (reviewed by [1]). Glycine decarboxylase complex (GDC) is a key enzyme in the mitochondrial photorespiratory C2 cycle in C3 plants. Inhibition of GDC activity results in ROS accumulation and elevates cell death symptoms [25]. When treated with GSNO, GDC was shown to be S-nitrosylated at several cysteine residues that resulted in the inhibition of its activity [25]. In addition, hairpin bacterial elicitor induced a NO burst that inhibited the GDC activity [25]. Thus, NO-mediated inhibition of the mitochondrial enzyme GDC can induce ROS accumulation and dysfunctioning of mitochondria and subsequent initiation of HR cell death.

As a physiologically relevant signalling process, S-nitrosylation must be strictly regulated. GSNO is the physiological NO molecule that mediates direct protein S-nitrosylation. GSNO reductase (GSNOR) is an enzyme that can regulate SNO homeostasis through the breakdown of GSNO into oxidised glutathione and ammonia. An *Arabidopsis* allelic missense mutant of GSNOR showed high SNO levels and anti-cell death phenotype when

treated with paraquat, a non-selective herbicide that induces cell death in a ROS-based signalling pathway [31]. Consistent with this result, wild-type plants treated with NO donors showed the anti-cell death to paraquat phenotype [31]. These results suggest that higher SNO levels might be disturbing ROS sensitivity of the plant, which is negatively regulating the defence responses. This could also be the reason for altered phenotype and poor germination in these mutant plants. However, studies to find the function of GSNO/GSNOR in plant defence have produced contradictory results [32–34]. Other regulatory mechanisms that confer the S-nitrosylation specificity have been described in animal studies [35].

GAPDH

First known as a glycolytic enzyme present in all living organisms, GAPDH has recently been found to participate in various stress responses [36,37]. GAPDH is an important example of a redox-regulated protein. Its catalytic activity is inhibited upon oxidation, S-nitrosylation of specific cysteine residues in the active centre and also by tyrosine nitration as shown for *Arabidopsis* cytosolic GAPDHs [38,39•].

Redox modifications not only affect GAPDH activity but also can profoundly change protein functions. Accordingly, in rat brain cells S-nitrosylation facilitated binding of GAPDH to the nuclear-targeted Siah1 (an E3 ubiquitin ligase), transfer of the GAPDH/Siah1 complex into the nucleus and degradation of nuclear proteins which ultimately induced apoptosis [36,37,40]. In the nucleus S-nitrosylated GAPDH was additionally capable of targeted (trans-) nitrosylation of specific nuclear proteins; being the first identified nitrosylase [35,41••]. Although no similar role of GAPDH is known in plants, nevertheless it was observed that GAPDH moved into the nucleus where it bound to DNA [38] (Figure 2).

In plants, emerging evidence implies involvement of GAPDH in redox signalling. Two *Arabidopsis* cytosolic GAPDH isoforms (GAPC1 and GAPC2) were translocated to the mitochondrial outer membrane after treatment with hydrogen peroxide (H_2O_2) [42]. Together with other glycolytic enzymes they contributed to the supply of pyruvate for stress-induced respiration preventing toxic ROS accumulation [43]. In support of these findings, GAPC1-deficient plants displayed mitochondrial dysfunction and increased oxidative stress [44]. Moreover, H_2O_2 treatment triggered expression of a chloroplastic GAPDH (GAPA) [45] while overexpression of GAPA reduced heat (44°C)-induced ROS accumulation and cell death in transgenic *Arabidopsis*. Thus, we hypothesise that the role of GAPDH in the antioxidant system of the cell is enhanced by mild ROS stress, whereas high levels of ROS and NO would inhibit GAPDH activity. This would possibly cause ROS accumulation in chloroplasts and mitochondria leading to cell death (Figure 2).

Many more functions of GAPDH in stress responses have been discovered in various organisms. For example S-nitrosylated GAPDH can mediate haem insertion into inducible NOS while H_2O_2-oxidised (as well as S-nitrosylated) GAPDH interacts with MAP kinase signalling [22,36,37,46].

Protein nitration

Protein nitration is the covalent binding of a nitro adduct ($R-NO_2$) to aromatic amino acids such as tyrosine and tryptophan. This protein modification is thought to be mediated predominantly by peroxynitrite (ONOOH/$ONOO^-$) and its reactive derivatives nitrogen dioxide (NO_2/$^\bullet NO_2$) and nitrosoperoxocarbonate ($ONOOCO_2^-$). Peroxynitrite arises from the diffusion-limited reaction of NO with superoxide (O_2^-). However, recently it was found that nitrite in conjunction with haem peroxidases and H_2O_2 could act as a nitrating agent (for recent reviews on protein nitration see [47–50]).

Formation of the short-lived peroxynitrite during plant defence responses was investigated by employing the fluorescent probes HKGreen-2 and aminophenyl fluoresceine (APF). In a HKGreen-2-based leaf disc assay, a rise in peroxynitrite levels was detected at 3–6 h after infection of *Arabidopsis* leaves with avirulent *P. syringae* [51] Similarly, APF fluorescence reached a maximum at 6 h after treatment of tobacco cells with the elicitor INF1 [52]. In both experimental systems peroxynitrite accumulation correlated with the onset of HR and an increase in protein tyrosine nitration [51–53].

Since nitration is a covalent protein modification, western blot analyses, immunoprecipitation and mass spectrometry (MS) are suitable for detection and identification of nitrated proteins [47]. In a first study, tyrosine-nitrated proteins were identified in extracts from *P. syringae*-infected *Arabidopsis* leaves combining two-dimensional electrophoresis, anti-nitrotyrosine western blots and MS [53]. Notably, 11 of 12 nitrated proteins were located in the chloroplasts. Nitration and oxidation of chloroplast proteins were further corroborated by analyses of *Arabidopsis* leaves exposed to high light stress [54•]. In this study an optimised LC–MS/MS (liquid chromatography coupled to tandem MS) technique facilitated the identification of 126 tyrosine-nitrated and 12 tryptophan-nitrated peptides from chloroplast protein preparations, suggesting chloroplasts as a prime site of nitrosative and oxidative stress.

Further tyrosine-nitrated proteins were identified in untreated sunflower (21 proteins) and *Arabidopsis* plants [39•,55]. In the latter study, anti-nitrotyrosine antibodies were employed for immunoprecipitation and identification of 127 nitrated proteins by LC–MS/MS. Interestingly, 35% of the identified proteins were already known to be nitrated, suggesting that the presented list of candidate proteins could serve as a basis for future studies

Figure 2
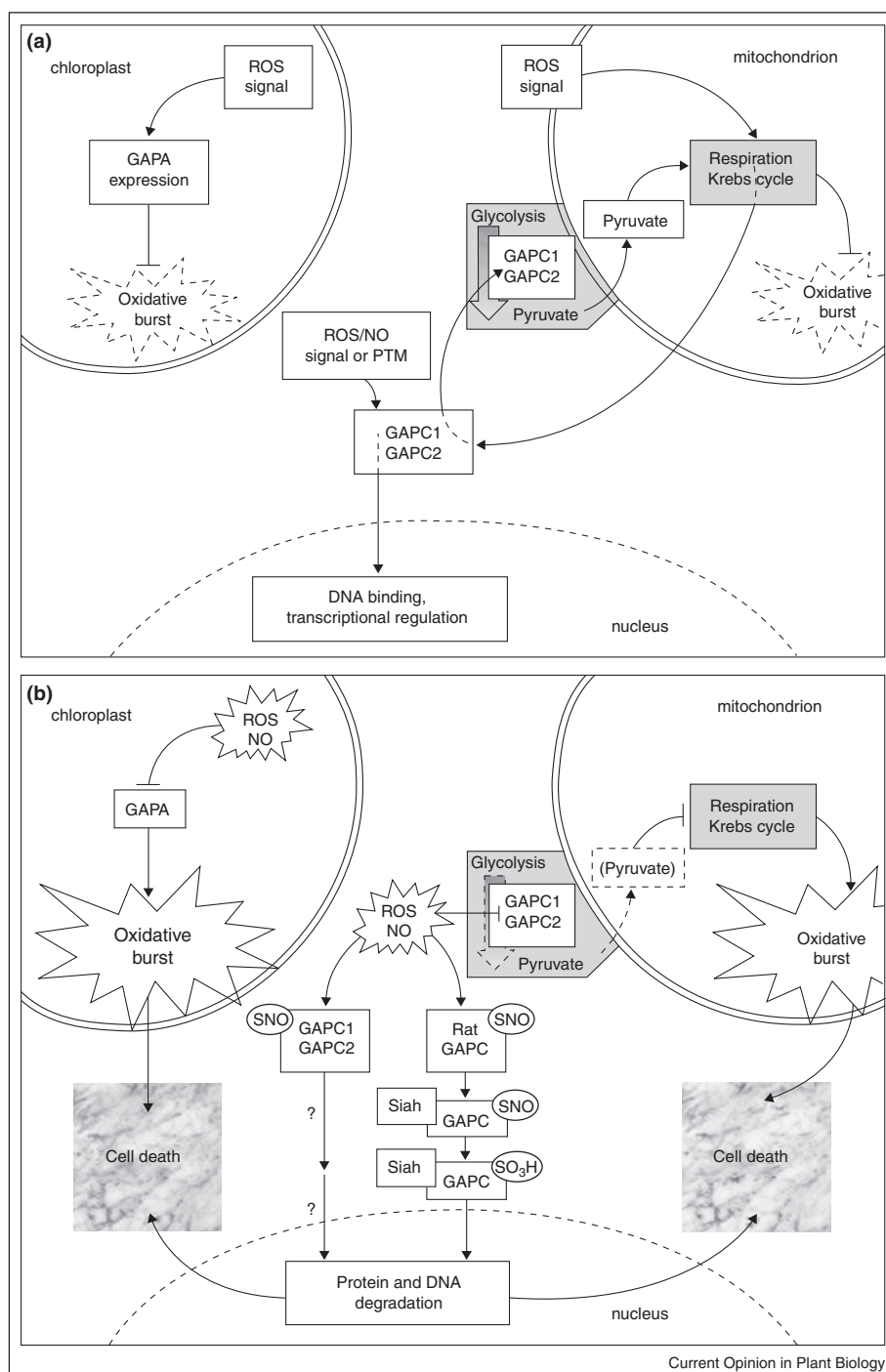
Interaction of GAPDH with ROS and NO in antioxidant defence, stress signalling and cell death. **(a)** Functions of GAPDH under conditions of mild oxidative stress/redox signalling. ROS trigger expression of a chloroplastic GAPDH (GAPA, At4g26650) which prevents oxidative burst and cell death under heat stress conditions. A ROS-mediated increase in respiration induced translocation of cytosolic GAPDHs (GAPC1, At3g04120 and GAPC2, At1g13440) to the outer mitochondrial membrane. Glycolysis-derived pyruvate minimized mitochondrial ROS production by maintaining functional respiration. Oxidative stress signalling or post-translational modifications (PTM) by ROS/NO might facilitate translocation of GAPCs into the nucleus and transcriptional regulation. **(b)** Functions of GAPDH under heavy oxidative stress conditions. Inhibition of GAPA and GAPC would cause an oxidative burst in chloroplasts and mitochondria and ultimately cell death. In rat cells S-nitrosylation and irreversible sulfonation (–SNO or –SO$_3$H adduct at active centre cysteine) of GAPDH and interaction of GAPDH with the ubiquitin ligase Siah induces cell death. It is unknown if NO-modified and ROS-modified GAPC1 and GAPC2 of *Arabidopsis* partake in cell death signalling.

on protein nitration. However, because of the low stability of the nitro adduct under the chosen experimental conditions, no *in vivo* nitration sites could be identified [39[•]]. In fact, to date only one publication reports on the identification of *in vivo* nitration sites [53], nothing is known about *in vivo* effects of nitration on protein functions and only few data showed effects of peroxynitrite on enzyme activities *in vitro* [39[•],56]. Hence, most of the candidate nitrated proteins are still awaiting confirmation.

Although several interesting candidates with assigned functions in defence/stress responses and redox regulation were discovered [39[•],55], the role of nitrated proteins in defence signalling is still obscure. Recent speculations include competition of tyrosine nitration with tyrosine phosphorylation (e.g. in kinase signalling cascades [1,48]), (de-) activation of redox-sensitive transcription factors as well as regulation of enzymes involved in redox homeostasis and signal generation.

As for S-nitrosylation, one prerequisite for signalling by nitration would be that this protein modification is regulated and reversible. Remarkably, plants contain a large stock of natural scavengers of peroxynitrite, such as various flavonoids (e.g. ebselen, epicatechin and quercitin), urate, glutathione and other antioxidants [48]. As an antioxidant enzyme, PrxII was reported to metabolise peroxynitrite under non-stress conditions. The activity was inhibited by S-nitrosylation during the HR of *Arabidopsis* towards avirulent *P. syringae* causing an increase in protein nitration [57]. Hence, enzyme inhibition by NO facilitated accumulation of the NO-derivative peroxynitrite. Plants might have enzymes acting as denitrases, similarly to those known in animals [48]. One candidate denitrase is the methionine sulfoxide reductase PMSR2-1 of *Arabidopsis* which prevents nitration, oxidation and glycation of proteins in the night under non-stress conditions as detected by LC–MS/MS [58].

Conclusions

NO signalling in pathogen defence is probably complex. Although short signal cascades upstream and downstream of NO have been deciphered we are still quite far from understanding how the various NO-related second messengers interact to evoke a defence response. Moreover, new inducers as well as targets of NO are awaiting discovery in plants, including NO-modifications of signal compounds like fatty acids or nucleotide phosphates. Thus, in the future known signals must be integrated into signal networks and new NO-related messengers must be identified in plants in order to get a complete picture of pathogen defence signalling by NO.

Acknowledgements

References and recommended reading
Papers of particular interest, published within the period of review, have been highlighted as:

- • of special interest
- •• of outstanding interest

1. Leitner M, Vandelle E, Gaupels F, Bellin D, Delledonne M: **NO signals in the haze: nitric oxide signalling in plant defence**. *Curr Opin Plant Biol* 2009, **12**:451-458.

2. Moreau M, Lindermayr C, Durner J, Klessig DF: **NO synthesis and signaling in plants — where do we stand?** *Physiol Plant* 2009, **138**:372-383.

3. Gupta KJ, Fernie AR, Kaiser WM, van Dongen JT: **On the origins of nitric oxide**. *Trends Plant Sci* 2010, **16**:160-168.

4. Tanaka K, Gilroy S, Jones AM, Stacey G: **Extracellular ATP signaling in plants**. *Trends Cell Biol* 2010, **20**:601-608.

5. Ma W, Berkowitz GA: **Ca²⁺ conduction by plant cyclic nucleotide gated channels and associated signaling components in pathogen defense signal transduction cascades**. *New Phytol* 2011, **190**:566-572.

6. Foresi N, Correa-Aragunde N, Parisi G, Calo G, Salerno G,
• Lamattina L: **Characterization of a nitric oxide synthase from the plant kingdom: NO generation from the green alga *Ostreococcus tauri* is light irradiance and growth phase dependent**. *Plant Cell* 2010, **22**:3816-3830.
The authors reported identification and characterisation of the first NOS known in the plant kingdom. The NOS of the alga *Ostreococcus tauri* is 45% similar to human NOS but has no homologues in higher plants.

7. de Montaigu A, Sanz-Luque E, Galvan A, Fernandez E: **A soluble
•• guanylate cyclase mediates negative signaling by ammonium on expression of nitrate reductase in Chlamydomonas**. *Plant Cell* 2010, **22**:1532-1548.
A soluble GC of *Chlamydomonas reinhardtii* is involved in regulation of nitrate assimilation. Ammonium accumulation induced the NO-dependent sGCs CYG56. The subsequent increase in cGMP levels repressed transcription of NIA1 coding for NR. It remains to be demonstrated if so far unidentified sGC in higher plants have similar functions in NO-related signal cascades.

8. Rosales EP, Iannone MF, Groppa MD, Benavides MP: **Nitric oxide inhibits nitrate reductase activity in wheat leaves**. *Plant Physiol Biochem* 2010, **49**:124-130.

9. Wimalasekera R, Villar C, Begum T, Scherer GF: **COPPER AMINE OXIDASE1 (CuAO1) of *Arabidopsis thaliana* contributes to abscisic acid- and polyamine-induced nitric oxide biosynthesis and abscisic acid signal transduction**. *Mol Plant* 2011 doi: 10.1093/mp/ssr023.

10. Besson-Bard A, Pugin A, Wendehenne D: **New insights into nitric oxide signaling in plants**. *Annu Rev Plant Biol* 2008, **59**:21-39.

11. Chivasa S, Murphy AM, Hamilton JM, Lindsey K, Carr JP, Slabas AR: **Extracellular ATP is a regulator of pathogen defence in plants**. *Plant J* 2009, **60**:436-448.

12. Sueldo DJ, Foresi NP, Casalongue CA, Lamattina L, Laxalt AM:
• **Phosphatidic acid formation is required for extracellular ATP-mediated nitric oxide production in suspension-cultured tomato cells**. *New Phytol* 2010, **185**:909-916.
The membrane-derived signal molecule PA participates in eATP-induced NO production in suspension-cultured tomato cells. Phospholipids like PA are known as an important class of signal molecules in animals. This paper demonstrates for the first time a role for phospholipids in signalling upstream of NO-biosynthesis in plant cells.

13. Zhang Y, Zhu H, Zhang Q, Li M, Yan M, Wang R, Wang L, Welti R, Zhang W, Wang X: **Phospholipase Dα1 and phosphatidic acid regulate NADPH oxidase activity and production of reactive oxygen species in ABA-mediated stomatal closure in Arabidopsis**. *Plant Cell* 2009, **21**:2357-2377.

14. Qi Z, Verma R, Gehring C, Yamaguchi Y, Zhao YC, Ryan CA, Berkowitz GA: **Ca²⁺ signaling by plant *Arabidopsis thaliana* Pep peptides depends on AtPepR1, a receptor with guanylyl cyclase activity, and cGMP-activated Ca²⁺ channels**. *Proc Natl Acad Sci U S A* 2010, **107**:21193-21198.

15. Ma W, Qi Z, Smigel A, Walker RK, Verma R, Berkowitz GA: **Ca²⁺,**
•• **cAMP, and transduction of non-self perception during**
plant immune responses. *Proc Natl Acad Sci U S A* 2009,
106:20995-21000.
This paper convincingly described the interplay between the second
messengers cAMP, calcium, NO and ROS in the HR. cAMP was shown
to activate the calcium channel CNGC2. The CNGC2-mediated calcium
transient was necessary for induction of NO and ROS bursts and HR cell
death.

16. Asai S, Ohta K, Yoshioka H: **MAPK signaling regulates nitric**
oxide and NADPH oxidase-dependent oxidative bursts in
Nicotiana benthamiana. *Plant Cell* 2008, **20**:1390-1406.

17. Asai S, Mase K, Yoshioka H: **A key enzyme for flavin synthesis is**
required for nitric oxide and reactive oxygen species
production in disease resistance. *Plant J* 2010,
62:911-924.

18. Isner JC, Maathuis FJM: **Measurement of cellular cGMP in plant**
cells and tissues using the endogenous fluorescent reporter
FlincG. *Plant J* 2011, **65**:329-334.

19. Laxalt AM, Raho N, Have AT, Lamattina L: **Nitric oxide is critical**
for inducing phosphatidic acid accumulation in xylanase-
elicited tomato cells. *J Biol Chem* 2007, **282**:21160-21168.

20. Raho N, Ramirez L, Lanteri ML, Gonorazky G, Lamattina L, ten
Have A, Laxalt AM: **Phosphatidic acid production in chitosan-**
elicited tomato cells, via both phospholipase D and
phospholipase C/diacylglycerol kinase, requires nitric oxide. *J*
Plant Physiol 2011, **168**:534-539.

21. Aboul-Soud MA, Aboul-Enein AM, Loake GJ: **Nitric oxide triggers**
specific and dose-dependent cytosolic calcium transients in
Arabidopsis. *Plant Signal Behav* 2009, **4**:191-196.

22. Wawer I, Bucholc M, Astier J, Anielska-Mazur A, Dahan J, Kulik A,
Wyslouch-Cieszynska A, Zareba-Koziol M, Krzywinska E,
Dadlez M *et al.*: **Regulation of *Nicotiana tabacum* osmotic**
stress-activated protein kinase and its cellular partner GAPDH
by nitric oxide in response to salinity. *Biochem J* 2010,
429:73-83.

23. Lindermayr C, Saalbach G, Durner J: **Proteomic identification of**
S-nitrosylated proteins in Arabidopsis. *Plant Physiol* 2005,
137:921-930.

24. Romero-Puertas MC, Campostrini N, Matte A, Righetti PG,
Perazzolli M, Zolla L, Roepstorff P, Delledonne M: **Proteomic**
analysis of S-nitrosylated proteins in *Arabidopsis thaliana*
undergoing hypersensitive response. *Proteomics* 2008,
8:1459-1469.

25. Palmieri MC, Lindermayr C, Bauwe H, Steinhauser C, Durner J:
Regulation of plant glycine decarboxylase by S-nitrosylation
and glutathionylation. *Plant Physiol* 2010, **152**:1514-1528.

26. Mou Z, Fan W, Dong X: **Inducers of plant systemic acquired**
resistance regulate NPR1 function through redox changes.
Cell 2003, **113**:935-944.

27. Tada Y, Spoel SH, Pajerowska-Mukhtar K, Mou Z, Song J,
Wang C, Zuo J, Dong X: **Plant immunity requires conformational**
charges of NPR1 via S-nitrosylation and thioredoxins. *Science*
2008, **321**:952-956.

28. Lindermayr C, Sell S, Muller B, Leister D, Durner J: **Redox**
•• **regulation of the NPR1-TGA1 system of *Arabidopsis thaliana***
by nitric oxide. *Plant Cell* 2010 doi: 10.1105/tpc.109.066464.
NO is reported to regulate NPR1 and TGA1, key redox-controlled reg-
ulators of systemic acquired resistance in plants. Specific cysteine
residues of TGA1 were prone to S-nitrosylation. S-nitrosylation of
TGA1 increased its DNA binding activity and provided protection from
oxygen-mediated modifications. NO also promoted the nuclear localisa-
tion of NPR1. Thus, NO plays a key role in regulating NPR1/TGA1 system,
crucial in plant defence response.

29. Despres C, Chubak C, Rochon A, Clark R, Bethune T, Desveaux D,
Fobert PR: **The Arabidopsis NPR1 disease resistance protein is**
a novel cofactor that confers redox regulation of DNA binding
activity to the basic domain/leucine zipper transcription factor
TGA1. *Plant Cell* 2003, **15**:2181-2191.

30. Wang YQ, Feechan A, Yun BW, Shafiei R, Hofmann A, Taylor P,
• Xue P, Yang FQ, Xie JA, Pallas ZS *et al.*: **S-nitrosylation of**

AtSABP3 antagonizes the expression of plant immunity. *J Biol*
Chem 2009, **284**:2131-2137.
Pathogen-induced S-nitrosylation of SABP3 inhibited its SA-binding
and carbonic anhydrase activities that are required for successful plant
defence. Thus, NO through S-nitrosylation of SABP3 is reported to
antagonise plant defence response. It is speculated to represent an
active virulence strategy of the invading pathogen in the battle for
survival.

31. Chen R, Sun S, Wang C, Li Y, Liang Y, An F, Li C, Dong H, Yang X,
Zhang J *et al.*: **The Arabidopsis PARAQUAT RESISTANT2 gene**
encodes an S-nitrosoglutathione reductase that is a key
regulator of cell death. *Cell Res* 2009, **19**:1377-1387.

32. Feechan A, Kwon E, Yun BW, Wang Y, Pallas JA, Loake GJ: **A**
central role for S-nitrosothiols in plant disease resistance.
Proc Natl Acad Sci U S A 2005, **102**:8054-8059.

33. Rusterucci C, Espunya MC, Diaz M, Chabannes M, Martinez MC:
S-nitrosoglutathione reductase affords protection against
pathogens in Arabidopsis, both locally and systemically. *Plant*
Physiol 2007, **143**:1282-1292.

34. Holzmeister C, Frohlich A, Sarioglu H, Bauer N, Durner J,
Lindermayr C: **Proteomic analysis of defense response of**
wildtype *Arabidopsis thaliana* and plants with impaired NO-
homeostasis. *Proteomics* 2011, **11**:1664-1683.

35. Stamler JS, Hess DT: **Nascent nitrosylases**. *Nat Cell Biol* 2010,
12:1024-1026.

36. Tristan C, Shahani N, Sedlak TW, Sawa A: **The diverse functions**
of GAPDH: views from different subcellular compartments.
Cell Signal 2011, **23**:317-323.

37. Brandes N, Schmitt S, Jakob U: **Thiol-based redox switches in**
eukaryotic proteins. *Antioxid Redox Signal* 2009, **11**:997-1014.

38. Holtgrefe S, Gohlke J, Starmann J, Druce S, Klocke S, Altmann B,
Wojtera J, Lindermayr C, Scheibe R: **Regulation of plant**
cytosolic glyceraldehyde 3-phosphate dehydrogenase
isoforms by thiol modifications. *Physiol Plant* 2008,
133:211-228.

39. Lozano-Juste J, Colom-Moreno R, Leon J: **In vivo protein**
• **tyrosine nitration in *Arabidopsis thaliana***. *J Exp Bot* 2011,
62:3501-3517.
This report and [54•] are good examples of applying proteomic techni-
ques for efficient identification of nitrated plant proteins. Nitrated proteins
from untreated *Arabidopsis* plants were isolated by immunoprecipitation
with anti-nitrotyrosine antibodies and identified by LC–MS/MS. There
were 127 candidate nitro-proteins identified using this technique. How-
ever, due to the LC–MS/MS conditions used, no *in vivo* nitration sites
could be defined.

40. Sen N, Hara MR, Kornberg MD, Cascio MB, Bae BI, Shahani N,
Thomas B, Dawson TM, Dawson VL, Snyder SH *et al.*: **Nitric**
oxide-induced nuclear GAPDH activates p300/CBP and
mediates apoptosis. *Nat Cell Biol* 2008, **10**:866-873.

41. Kornberg MD, Sen N, Hara MR, Juluri KR, Nguyen JV,
•• Snowman AM, Law L, Hester LD, Snyder SH: **GAPDH mediates**
nitrosylation of nuclear proteins. *Nat Cell Biol* 2010,
12:1094-1100.
In this study, it was discovered that S-nitrosylation of nuclear proteins is a
selective process mediated by S-nitrosylated GAPDH. After S-nitrosyla-
tion cytosolic GAPDH binds nuclear-targeted Siah1 and translocates into
the nucleus where it selectively nitrosylates nuclear proteins. This is the
first report of an enzyme acting as nitrosylase.

42. Sweetlove LJ, Heazlewood JL, Herald V, Holtzapffel R, Day DA,
Leaver CJ, Millar AH: **The impact of oxidative stress on**
Arabidopsis mitochondria. *Plant J* 2002, **32**:891-904.

43. Graham JW, Williams TC, Morgan M, Fernie AR, Ratcliffe RG,
Sweetlove LJ: **Glycolytic enzymes associate dynamically with**
mitochondria in response to respiratory demand and support
substrate channeling. *Plant Cell* 2007, **19**:3723-3738.

44. Rius SP, Casati P, Iglesias AA, Gomez-Casati DF:
Characterization of Arabidopsis lines deficient in GAPC-1, a
cytosolic NAD-dependent glyceraldehyde-3-phosphate
dehydrogenase. *Plant Physiol* 2008, **148**:1655-1667.

45. Baek D, Jin Y, Jeong JC, Lee HJ, Moon H, Lee J, Shin D, Kang CH,
Kim DH, Nam J *et al.*: **Suppression of reactive oxygen species**

by glyceraldehyde-3-phosphate dehydrogenase. *Phytochemistry* 2008, **69**:333-338.

46. Chakravarti R, Aulak KS, Fox PL, Stuehr DJ: **GAPDH regulates cellular heme insertion into inducible nitric oxide synthase**. *Proc Natl Acad Sci U S A* 2010, **107**:18004-18009.

47. Abello N, Kerstjens HA, Postma DS, Bischoff R: **Protein tyrosine nitration: selectivity, physicochemical and biological consequences, denitration, and proteomics methods for the identification of tyrosine-nitrated proteins**. *J Proteome Res* 2009, **8**:3222-3238.

48. Arasimowicz-Jelonek M, Floryszak-Wieczorek J: **Understanding the fate of peroxynitrite in plant cells — from physiology to pathophysiology**. *Phytochemistry* 2011, **72**:681-688.

49. Ferrer-Sueta G, Radi R: **Chemical biology of peroxynitrite: kinetics, diffusion, and radicals**. *ACS Chem Biol* 2009, **4**:161-177.

50. Hill BG, Dranka BP, Bailey SM, Lancaster JR Jr, Darley-Usmar VM: **What part of NO don't you understand? Some answers to the cardinal questions in nitric oxide biology**. *J Biol Chem* 2010, **285**:19699-19704.

51. Gaupels F, Spiazzi-Vandelle E, Yang D, Delledonne M: **Detection of peroxynitrite accumulation in *Arabidopsis thaliana* during the hypersensitive defense response**. *Nitric Oxide-Biol Chem* 2011 doi: 10.1016/j.niox.2011.01.009.

52. Saito S, Yamamoto-Katou A, Yoshioka H, Doke N, Kawakita K: **Peroxynitrite generation and tyrosine nitration in defense responses in tobacco BY-2 cells**. *Plant Cell Physiol* 2006, **47**:689-697.

53. Cecconi D, Orzetti S, Vandelle E, Rinalducci S, Zolla L, Delledonne M: **Protein nitration during defense response in *Arabidopsis thaliana***. *Electrophoresis* 2009, **30**:2460-2468.

54. Galetskiy D, Lohscheider JN, Kononikhin AS, Popov IA,
• Nikolaev EN, Adamska I: **Mass spectrometric characterization of photooxidative protein modifications in *Arabidopsis thaliana* thylakoid membranes**. *Rapid Commun Mass Spectrom* 2011, **25**:184-190.
As for [39•], a proteomic approach was used for identification of nitrated plant proteins. Tyrosine and tryptophan-nitrated and oxidised proteins were identified in chloroplast extracts from *Arabidopsis* leaves. It was found that nitration of PSII proteins increased under high light stress. Improved experimental conditions during the LC–MS/MS allowed detection of nitrated tryptophan and tyrosine residues.

55. Chaki M, Valderrama R, Fernandez-Ocana AM, Carreras A, Lopez-Jaramillo J, Luque F, Palma JM, Pedrajas JR, Begara-Morales JC, Sanchez-Calvo B *et al*.: **Protein targets of tyrosine nitration in sunflower (*Helianthus annuus* L.) hypocotyls**. *J Exp Bot* 2009, **60**:4221-4234.

56. Alvarez C, Lozano-Juste J, Romero LC, Garcia I, Gotor C, Leon J: **Inhibition of Arabidopsis O-acetylserine(thiol)lyase A1 by tyrosine nitration**. *J Biol Chem* 2011, **286**:578-586.

57. Romero-Puertas MC, Laxa M, Matte A, Zaninotto F, Finkemeier I, Jones AM, Perazzolli M, Vandelle E, Dietz KJ, Delledonne M: **S-nitrosylation of peroxiredoxin II E promotes peroxynitrite-mediated tyrosine nitration**. *Plant Cell* 2007, **19**:4120-4130.

58. Bechtold U, Rabbani N, Mullineaux PM, Thornalley PJ: **Quantitative measurement of specific biomarkers for protein oxidation, nitration and glycation in Arabidopsis leaves**. *Plant J* 2009, **59**:661-671.

Detection of peroxynitrite accumulation in *Arabidopsis thaliana* during the hypersensitive defense response

Frank Gaupels [a,1,2], Elodie Spiazzi-Vandelle [a,1], Dan Yang [b], Massimo Delledonne [a,*]

[a] *Dipartimento di Biotecnologie, Università degli Studi di Verona, Strada Le Grazie, 15, 37 134 Verona, Italy*
[b] *Department of Chemistry and Morningside Laboratory for Chemical Biology, The University of Hong Kong, Pokfulam Road, Hong Kong, PR China*

ARTICLE INFO

ABSTRACT

Nitric oxide (NO) is synthesized in plants in response to stress, and its role in signaling is well-documented. In contrast, very little is known about the physiological role of its derivate peroxynitrite (ONOO⁻), which forms when NO reacts with O_2^- and induces protein modification by tyrosine nitration. Infection with an avirulent pathogen triggers the simultaneous production of NO and reactive oxygen species, as well as an increase in tyrosine nitration, so peroxynitrite could be physiologically relevant during this process. To gain insight into the role of peroxynitrite in plants, we measured its accumulation during the hypersensitive response in *Arabidopsis thaliana* using the specific peroxynitrite-sensitive fluorescent dye HKGreen-2 in a leaf disc assay. The avirulent pathogen *Pseudomonas syringae* pv. *tomato*, carrying the *AvrB* gene (Pst AvrB), induced a strong increase in fluorescence 3–4 h post-infiltration (hpi) which peaked 7–8 hpi. The increase in HKGreen-2 fluorescence was inhibited by co-injecting the peroxynitrite-scavenger urate together with the pathogen, and was almost completely eliminated by co-infiltrating urate with HKGreen-2, confirming that HKGreen-2 fluorescence *in planta* is induced specifically by peroxynitrite. This establishes a link between peroxynitrite synthesis and tyrosine nitration, and we therefore propose that peroxynitrite transduces the NO signal by modifying protein functions.

© 2011 Elsevier Inc. All rights reserved.

Introduction

Nitric oxide (NO) is a gaseous signaling molecule that has multiple roles during plant development and stress adaptation [1–3], particularly in the hypersensitive response (HR) against pathogens [4,5]. The HR is triggered when plants recognize a pathogen, and is therefore typical of plant–pathogen interactions that follow the "gene-for-gene" model, in which an avirulent pathogen carrying an avirulence (*Avr*) gene induces defense mechanisms in a resistant plant carrying the corresponding resistance (*R*) gene. One of the main features of the HR is the formation of necrotic lesions at the infection site [6], a process that is precisely controlled by the synergistic action of NO and peroxide (H_2O_2) produced simultaneously at the onset of the HR [7,8].

NO signaling cascades ultimately trigger downstream effects in the cell by modifying target proteins at the post-translational level, i.e. NO reacts with particular amino acid side chains leading to a change in protein conformation and activity. The best-characterized protein modification mediated by NO in plants is *S*-nitrosylation, in which NO binds to the sulfhydryl groups of cysteine residues in target proteins [9]. Several targets of *S*-nitrosylation have been identified, in particular during the HR [10,11]. Of particular interest, *S*-nitrosylation inhibits the activity of peroxiredoxin IIE (Prx IIE), which can detoxify both H_2O_2 and peroxynitrite (ONOO⁻) [12,13]. Peroxynitrite is a highly reactive molecule formed by the diffusion-limited reaction between NO and O_2^-. It has therefore been proposed that NO, via the inhibition of Prx IIE, could contribute to the accumulation of its own derivative [13].

Although peroxynitrite is highly reactive and toxic in animals, it is not involved in NO-mediated cell death in plants [8] and its physiological functions have yet to be determined. Peroxynitrite could play a role in NO signaling by mediating specific post-translational modifications, namely the nitration of tyrosine residues by the addition of a nitro group to the tyrosine aromatic ring [14]. Although the potential signaling role of peroxynitrite has not been investigated in detail, Tyr-nitrated proteins have been detected in various plant

species including nitrite reductase-deficient transgenic tobacco [15], pea plants exposed to abiotic stress [16] and, of particular interest, Arabidopsis thaliana plants infected with an avirulent pathogen [13,17]. Tyr-nitrated proteins are considered to be markers of nitrosative stress and indicators of peroxynitrite accumulation. However, peroxynitrite is not the only cellular nitrating agent, e.g. Tyr-nitration can be achieved in animals using a mechanism based on heme peroxidase–NO_2–H_2O_2 [14,18], and three A. thaliana hemoglobins with peroxidase activity have been shown to mediate nitrite-dependent Tyr-nitration [19]. Because protein Tyr-nitration can occur in the absence of peroxynitrite, it is therefore necessary to measure peroxynitrite levels in plants under various physiological and pathological conditions to determine its potential role in NO signaling.

Thus far, only one study has established a direct link between peroxynitrite levels and Tyr-nitration in plants, following the treatment of tobacco cell suspensions with the pathogen-derived elicitor INF1 [20]. However, the authors detected peroxynitrite using the fluorescent dye aminophenyl fluorescein (APF), which is also known to detect reactive oxygen species (ROS) such as the hydroxyl radical [21]. Recently, a new fluorescent dye named HKGreen-1 was developed for the specific detection and imaging of peroxynitrite [22]. HKGreen-1 has a much higher reactivity for peroxynitrite than NO and ROS (including the hydroxyl radical) so has a greater specificity than APF, and a more sensitive version (HKGreen-2) allowed the detection of peroxynitrite in living animal cells [23]. Here, using a leaf disc assay, we show that HKGreen-2 can also be used for the specific detection of peroxynitrite in plant tissues, and we describe for the first time the accumulation of peroxynitrite in plants undergoing the HR.

Materials and methods

Biological material

A. thaliana ecotype Columbia 0 plants were grown in soil culture at 60% relative humidity, with a 10-h photoperiod (light intensity 100 μmol m^{-2} s^{-1}) and a day/night temperature of 24/22 °C. The avirulent Pseudomonas syringae pv. tomato (Pst) strain DC3000, carrying the AvrB avirulence gene, was grown overnight at 28 °C in King's B medium (2% w/v Proteose Peptone, 6.1 mM $MgSO_4$, 8.6 mM K_2HPO_4 and 1% v/v glycerol, pH 7.2) supplemented with 50 mg/ml kanamycin and 50 mg/ml rifampicin. The bacterial suspension was infiltrated at OD_{600} = 0.1 in water into the abaxial surface of A. thaliana leaves using a hypodermic syringe without a needle. As a control, leaves were infiltrated with water. After infection, plants were returned to the growth chamber until the start of the photometric measurements. A. thaliana leaves were then collected from plants 0, 2, 4 and 6 h post-infiltration (hpi) and processed for peroxynitrite analysis.

Photometric measurements of peroxynitrite in vitro

Peroxynitrite was detected using the fluorescent dyes APF (A36003, Invitrogen, Gaithersburg, MD, USA) and HKGreen-2 [23]. Both dyes were assessed using the peroxynitrite donor SIN-1 (3-(4-morpholinyl) sydnonimine hydrochloride; M5793, Sigma–Aldrich, St. Louis) prepared in 0.1 M phosphate buffer (pH 7.2). The fluorescence intensity of APF and HKGreen-2 was measured at room temperature on a Victor™ plate reader (Perkin–Elmer) at excitation/emission wavelengths of 485/535 nm.

Photometric measurements of peroxynitrite in planta

Peroxynitrite was detected in 5-mm leaf discs punched from infiltrated leaves and vacuum-infiltrated with 20 μM HKGreen-2

[23] for 3 min with continuous agitation. We also prepared a 1 mM solution of urate, a peroxynitrite scavenger, in 3.36 mM NaOH and this was either co-injected into leaves with the pathogen or co-infiltrated into leaf discs with HKGreen-2. Leaf discs were incubated in darkness for 1 h, washed carefully with water and individual discs were transferred to wells containing 100 μl of water in a flat-bottomed 96-well plate. HKGreen-2 fluorescence was measured at room temperature on a Victor™ plate reader at excitation/emission wavelengths of 485/535 nm. Fluorescence intensity was also measured in control leaf discs that were infected but not treated with HKGreen-2. The plate was shaken before each reading. Eight replicates (leaf discs) were prepared for each time point and condition.

Results

Comparison of APF and HKGreen-2 for the detection of peroxynitrite

In an initial set of experiments we carried out a comparative analysis of APF and HKGreen-2 under the same in vitro conditions to determine whether HKGreen-2 would be suitable for the specific measurement of peroxynitrite levels in planta. Fluorescence was measured in the presence of 1 mM SIN-1, a peroxynitrite donor that produces equal amounts of NO and O_2^- which then react rapidly to form peroxynitrite. The optimal dye concentration was 10 μM for both APF and HKGreen-2 (data not shown). Real-time monitoring of fluorescence emission for 2 h showed that the fluorescence readings reached a plateau after approximately 80 min for both dyes (Fig. 1). We then added different amounts of SIN-1 to fixed concentrations (10 μM) of APF and HKGreen-2 to investigate dose-dependency. Real-time monitoring of fluorescence emission for 2 h showed that the fluorescence readings increased linearly at the lowest SIN-1 concentrations but reached a plateau after ∼80 min for the highest SIN-1 concentrations (Fig. 2). The slow increase in fluorescence observed with SIN-1 (Figs. 1 and 2) reflected the slow generation of peroxynitrite by the donor. In contrast, the addition of commercial peroxynitrite triggered a peak in fluorescence within a few seconds (data not shown). The sensitivity of each dye was then evaluated by determining fluorescence values after the 80-min period of linear intensification that occurred with all the test concentrations of SIN-1. As shown in Fig. 3, both dyes appeared equally sensitive becoming saturated at 0.6 mM SIN-1 (Fig. 3A and B). In both cases, fluorescence intensity increased in a linear manner from 0 to ∼0.1 mM SIN-1 (Fig. 3, inset panels). We concluded from the above data that HKGreen-2 was a suitable probe for peroxynitrite detection in planta, providing sensitivity in the same range as that reported for APF in plant cell suspensions [20] but greater peroxynitrite specificity [21–23].

Detection of endogenous peroxynitrite in A. thaliana leaves during the HR

Although HKGreen-2 is sensitive enough to allow the detection of peroxynitrite in murine macrophages in response to various stimuli [23], it does not provide a sufficient signal-to-noise ratio for the detection of peroxynitrite in A. thaliana leaves by microscopy. We therefore developed a photometric assay using leaf discs. Leaves of the A. thaliana ecotype Col0, which contains the RPM1 resistance gene, were infiltrated with an avirulent strain of P. syringae pv. tomato (Pst) carrying the AvrB avirulence gene (hereafter Pst AvrB), in order to induce the HR. Control leaves were infiltrated with water. For the analysis of peroxynitrite levels, leaf discs from infected and control plants were vacuum-infiltrated with HKGreen-2 at different time points post-infiltration, incubated in darkness for 1 h and then monitored for fluorescence emission
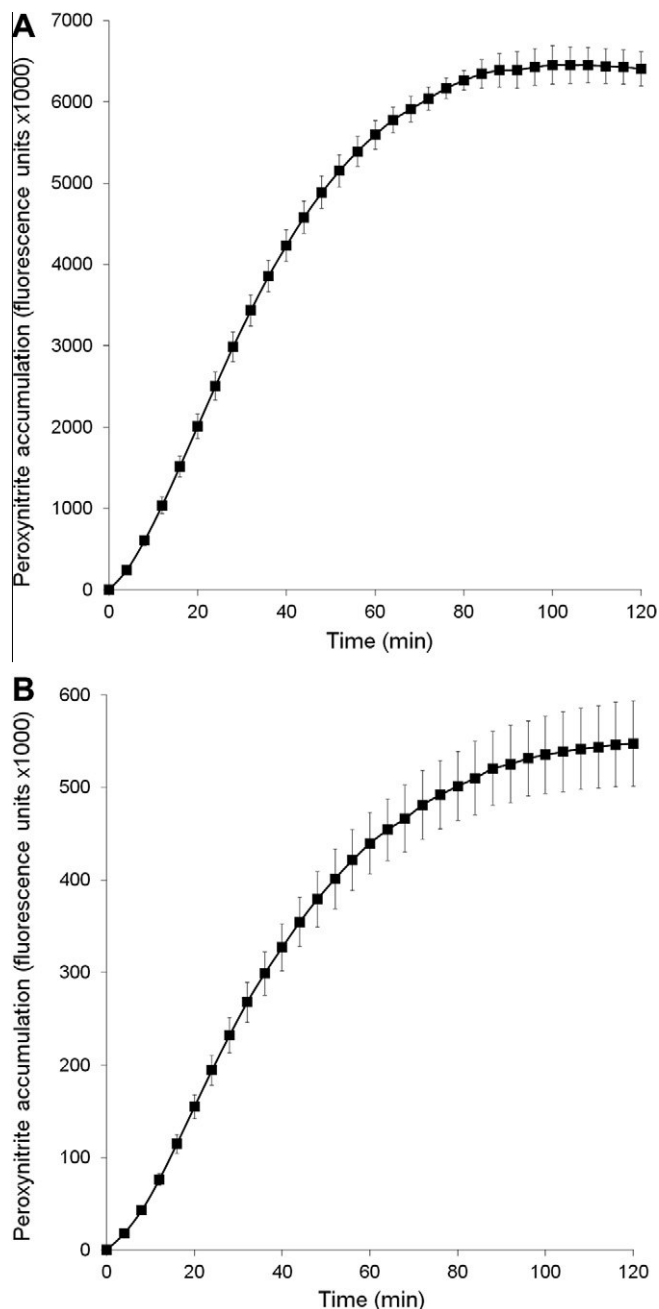
Fig. 1. Comparison of real-time detection of peroxynitrite by APF and HKGreen-2. Time course experiment for peroxynitrite detection by APF (A) and HKGreen-2 (B). Dye fluorescence emission was monitored in real-time using a plate reader photometer at room temperature for 2 h following the addition of APF or HKGreen-2, each prepared as a 10 μM solution, to 1 mM SIN-1 in 0.1 M phosphate buffer (pH 7.2). Values shown are means of four replicates ± SD. Fluorescence values have been divided by 1000 for clarity.

Fig. 2. SIN-1-dose dependency of APF and HKGreen-2 fluorescence intensity. APF or HKGreen-2, each prepared as a 10 μM solution, was added to different concentrations of SIN-1 (0.02–1 mM) prepared in 0.1 M phosphate buffer (pH 7.2). Fluorescence emission was measured for 2 h at room temperature in a plate reader photometer. Values shown are means of four replicates ± SD from a representative experiment (out of three). ctrl: Control (phosphate buffer). Fluorescence values have been divided by 1000 for clarity.

for 1 h. The evaluation of dye stability showed that HKGreen-2 is stable in cell extracts and that the 1-h incubation period appears to be necessary for the optimal detection of peroxynitrite because higher levels of fluorescence are observed in samples incubated for 1 h with the dye (data not shown). We found that dye-treated leaf discs from plants infiltrated with Pst AvrB were indistinguishable from controls 1–2 hpi, but thereafter displayed more intense fluorescence, indicating that peroxynitrite accumulation was induced by the avirulent pathogen (Fig. 4A). The increase in fluorescence induced by Pst AvrB is significantly higher in leaf discs treated with HKGreen-2 than in the absen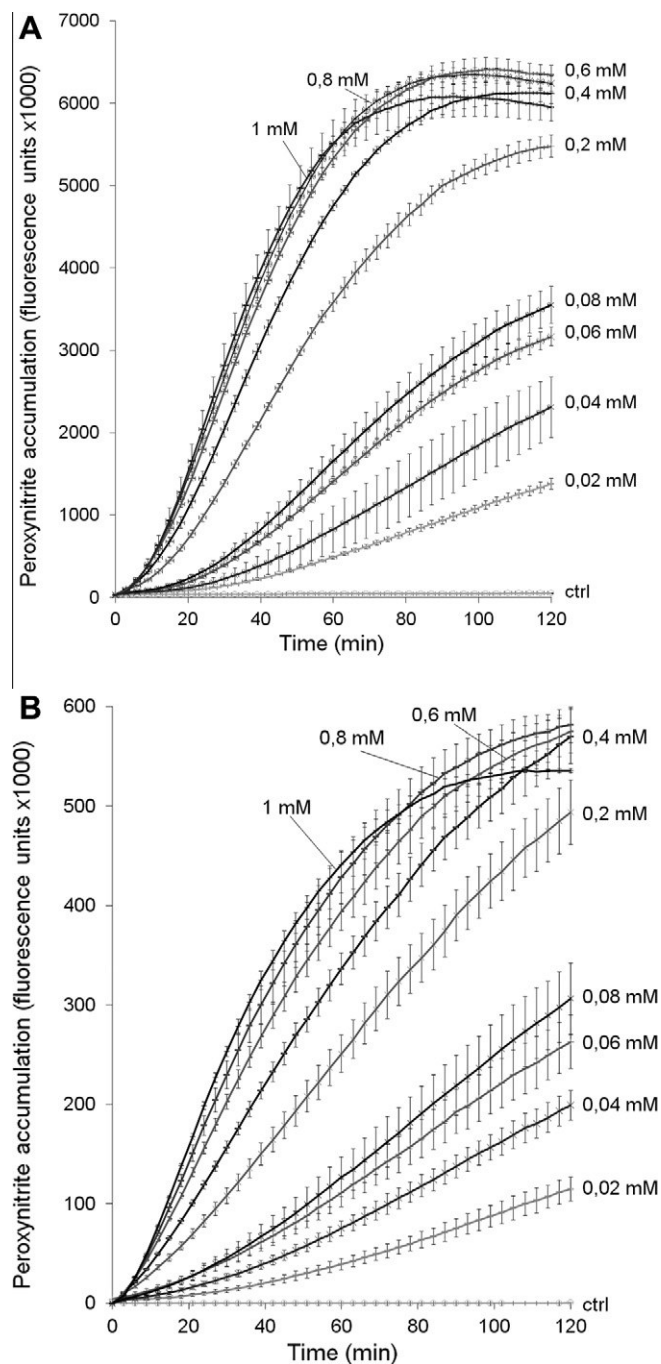ce of the dye, demonstrating that the increase in fluorescence observed during the HR is induced by peroxynitrite and is not caused by autofluorescence. It is noteworthy that the fluorescence intensity at the start of the monitoring period (1 h after infiltration with the dye) was already significantly higher in the Pst AvrB-infected discs compared to controls by 3 hpi, which shows there is a higher peroxynitrite content in infected leaves. Moreover, the fluorescence intensity increased during the HR, reaching a peak by 8 hpi, indicating that peroxynitrite continues to accumulate during this process (Fig. 4B). Accordingly, the
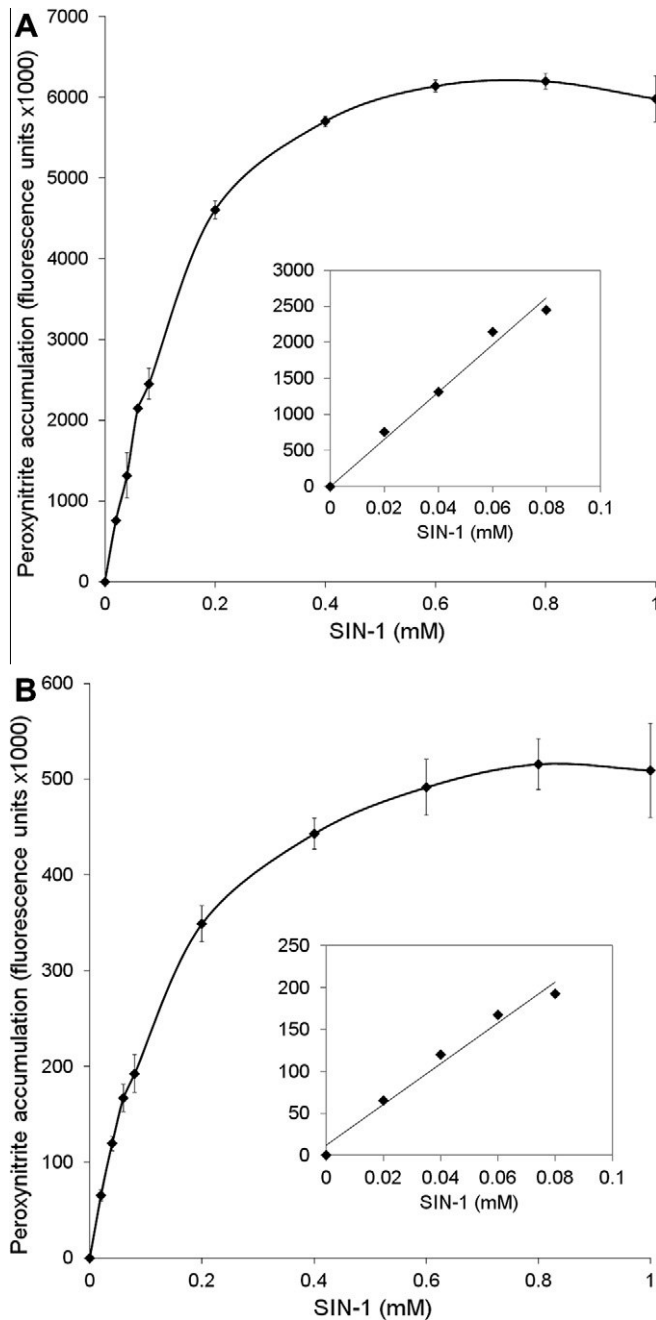
Fig. 3. Standard curve of peroxynitrite detected with APF or HKGreen-2. APF (A) or HKGreen-2 (B), each prepared as a 10 μM solution, was added to different concentrations of SIN-1 (0.02–1 mM) prepared in 0.1 M phosphate buffer (pH 7.2). Fluorescence emission was measured after 1 h in a plate reader photometer at room temperature. The inserts show fluorescence emission for the lowest concentrations of SIN1 (0.02–0.1 mM) in order to highlight the linear increase in fluorescence intensity within this range of peroxynitrite concentrations. Values shown are means of four replicates ± SD from a representative experiment (out of three). Fluorescence values have been divided by 1000 for clarity.

difference in fluorescence intensity observed during the monitoring period, corresponding to the real-time accumulation of peroxynitrite in response to infection, indicates that the rate of peroxynitrite production increases from 3 to 6 hpi and then remains stable until 8 hpi (Fig. 4C). In contrast, the fluorescence intensity increased much more slowly in control discs (Fig. 4A–C), the underlying accumulation of peroxynitrite presumably reflecting stress caused by vacuum infiltration of the dye. The comparison of infected and control samples leads to the conclusion that

most of the fluorescence detected in the infected samples is due to peroxynitrite accumulation induced by the avirulent pathogen.

Effect of urate on HKGreen-2 fluorescence

In order to confirm that the observed increase in HKGreen-2 fluorescence was due to the presence of peroxynitrite, we introduced a peroxynitrite scavenger into the *in vitro* and *in planta* systems. Fig. 5A shows that, *in vitro*, 1 mM urate completely eliminated the increase in fluorescence normally induced by 1 mM SIN-1. Complete inhibition was also observed with 1 mM epicatechin (another peroxynitrite scavenger) and 500 μM carboxy-2-phenyl-4,4,5,5-tetramethylimidazoline-3-oxide-1-oxyl (cPTIO, a scavenger of NO). This confirmed that the observed fluorescence signal was induced specifically by the release of peroxynitrite from SIN-1. Transferring this principle to the *in planta* system, we investigated two approaches, first introducing urate at the same time as the pathogen by co-injecting Pst AvrB and urate into intact leaves from which discs were later prepared, and second introducing urate at a later stage, by co-infiltrating leaf discs with urate and HKGreen-2. Fig. 5B shows that urate reduced HKGreen-2 fluorescence by ~25% when co-infiltrated with Pst AvrB at the beginning of the infection and by almost 80% when co-infiltrated with the dye 6 hpi, with both values monitored at 8 hpi. This difference could reflect the degradation of urate in plant cells in the 8 h that elapsed between infiltration and monitoring, so the effective concentration was lower by the time the dye was introduced into leaf discs. Notwithstanding the above, these data show clearly that HKGreen-2 fluorescence detected specifically during the HR is due to the accumulation of peroxynitrite.

Discussion

Peroxynitrite is a highly-reactive derivative of NO which is produced in plants under stress and causes specific post-translational modifications in proteins, namely tyrosine nitration. Little is known about the synthesis and potential physiological and pathological functions of peroxynitrite in plants, partly because the molecule has a short half life and is difficult to study directly. Its abundance is usually determined indirectly by the detection of reaction products such as nitrated lipids, amino acids and proteins using techniques such as chromatography, immunodetection and mass spectrometry [14,18,24].

Studies in animals have shown that Tyr-nitration is a widespread post-translational protein modification mediated by peroxynitrite [14], but only a few comparable investigations have been carried out in plants. These include reports showing that Tyr-nitrated proteins become more abundant in pea plants exposed to light and temperature stress, in elicitor-treated tobacco cell suspensions and in *A. thaliana* plants infected with the avirulent pathogen Pst AvrB [16,17,20]. The measurement of Tyr-nitration is difficult because only one in every 10,000 residues is modified, and its usefulness is debatable because although Tyr-nitration can be used as an indirect marker of peroxynitrite accumulation [25,26], the same modification can be caused by other mechanisms, e.g. peroxidase activity in the presence of reactive oxygen and nitrogen species (ROS/RNS) [19,25]. In order to gain insight into the precise function of peroxynitrite it plants, it is therefore necessary to establish assays that detect the molecule directly using fluorescent dyes that allow real-time monitoring of peroxynitrite levels. Current hypotheses dealing with the function of peroxynitrite rely on correlations between the production of NO and ROS and increases in Tyr-nitration, e.g. during the HR, and therefore lack conclusive data showing the production of peroxynitrite over time.
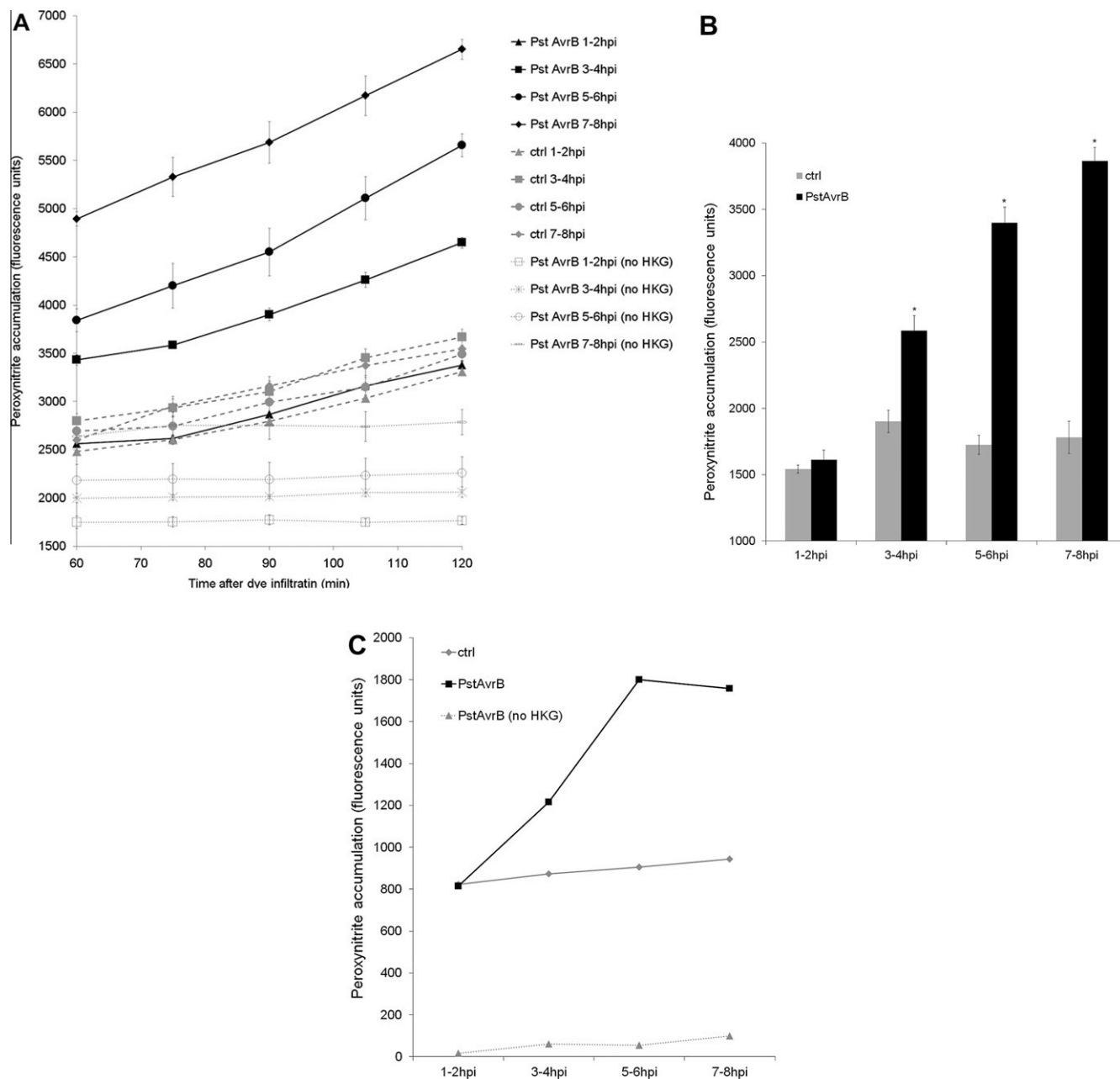
Fig. 4. Peroxynitrite formation in *A. thaliana* during the hypersensitive response. Peroxynitrite levels were estimated with HKGreen-2 (10 μM) by measuring fluorescence intensity. Fluorescence was monitored in real-time (A) or estimated at single time points (B) during the HR. Leaves were infected with an avirulent strain of *Pseudomonas syringae* pv. *tomato* carrying the *AvrB* gene (OD_{600} = 0.1) or with water (control). At different time points, leaf discs were vacuum-infiltrated with 20 μM HKGreen-2 and incubated with the dye for 1 h in darkness. Fluorescence emission was monitored in a plate reader photometer for 1 h (2 h total after dye infiltration) at room temperature. The values shown in B were obtained by subtracting leaf disc autofluorescence values (from discs that were not treated with the dye) from the fluorescence signal in leaf discs infiltrated with HKGreen-2. The rate of peroxynitrite accumulation in real-time (C) in uninfected leaf discs and leaf discs infected with the pathogen was obtained by calculating the difference between fluorescence signal at the beginning and end of the monitoring period. As a control, the increase in fluorescence increase was measured in infected leaf discs that were not treated with the dye. Values shown are means of 6–8 biological replicates ± SE. ctrl, Control (H_2O); *, $p < 0.05$ vs. control.

Addressing the challenges listed above, we established a photometric leaf disc assay using the novel boron-dipyrromethene (BODIPY) dye HKGreen-2, which is highly specific for peroxynitrite. HKGreen-2 reacts only weakly with other ROS/RNS [23] and is therefore preferable to aminophenyl fluorescein (APF), which detects peroxynitrite but is also highly sensitive to hydroxyl radicals [21]. We carried out a comparative analysis of HKGreen-2 and APF using the peroxynitrite donor SIN-1, and found that both dyes displayed the same sensitivity towards peroxynitrite with the intensity of fluorescence increasing linearly with both dyes up to a SIN-1 concentration of 0.1 mM.

The main aim of the investigation was to study peroxynitrite accumulation during the HR in *A. thaliana* plants infected with Pst AvrB, as this pathogen has previously been shown to trigger protein Tyr-nitration when infiltrated at OD_{600} = 0.1 [17]. Leaf discs were punched from the infiltrated leaves 0, 2, 4 and 6 hpi and infiltrated with HKGreen-2 to detect peroxynitrite. There was no significant difference between infected plants and controls at 1–2 hpi, but a weak increase in fluorescence was observed in both cases, presumably reflecting the production of small amounts of peroxynitrite in response to the stress of wounding and vacuum infiltration. Fluorescence increased significantly at 3–4 hpi
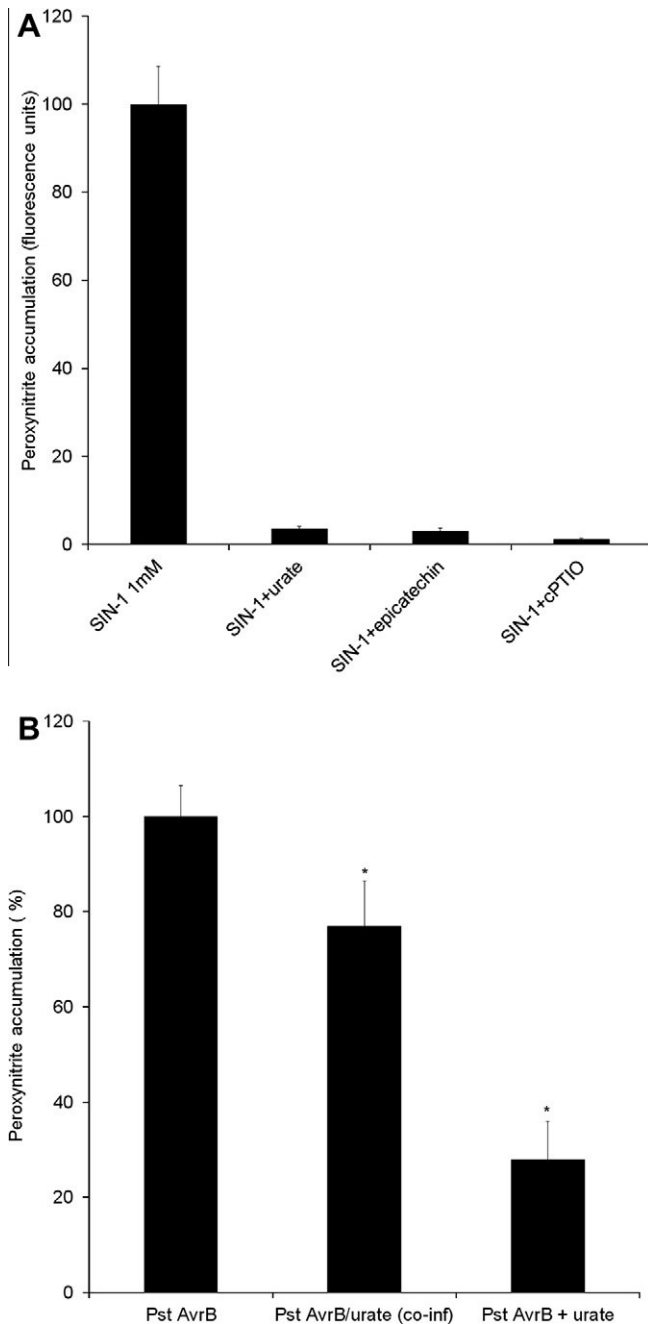
Fig. 5. Effect of urate on peroxynitrite accumulation in *A. thaliana* during the hypersensitive response. (A) Fluorescence emission of HKGreen-2 in the presence of SIN-1 (1 mM) ± urate (1 mM), epicatechin (1 mM), cPTIO (500 µM). A concentrated stock solution of urate was prepared in 1 M NaOH, whereas epicatechin and cPTIO were dissolved in water. The different scavengers were then added in a solution containing 1 mM SIN-1 prepared in 0.1 M phosphate buffer (pH 7.2). Fluorescence was measured after 80 min in a plate reader photometer at room temperature. (B) Urate (1 mM) was co-injected with the avirulent *Pseudomonas syringae* pv. *tomato* AvrB ($OD_{600} = 0.1$) or co-infiltrated with HKGreen-2 (10 µM). Fluorescence was measured in a plate reader photometer at room temperature after 2 h incubation with the dye, corresponding to 8 h after infection with the pathogen. Values shown are means of 6–8 biological replicates ± SE. ∗, $p < 0.05$ vs. Pst AvrB; co-inf, co-infiltration of Pst AvrB and urate.

specifically in the infected leaves, indicating that peroxynitrite was accumulating in response to the pathogen, and the intensity peaked at 7–8 hpi.

In order to determine that the increased HKGreen-2 fluorescence was specifically due to peroxynitrite and not other ROS/RNS, we introduced 1 mM urate into the system as a peroxynitrite scavenger. This resulted in complete suppression of HKGreen-2 fluorescence *in vitro* (confirmed with the additional scavengers epicatechin and cPTIO) and partial suppression *in planta*, specifically a ∼25% reduction when urate was introduced into leaves along with the pathogen and an 80% reduction when urate was introduced into the leaf discs along with the HKGreen-2. These data indicated that the observed increases in HKGreen-2 fluorescence in infected leaf discs were predominantly, if not entirely, dependent on increasing peroxynitrite levels. The difference in the impact of urate in each experiment is likely to reflect the degradation of urate introduced into plant tissue several hours before fluorescence measurement, which would reduce its effective concentration.

In agreement with our data, the treatment of tobacco BY-2 cells with the fungal elicitor INF1 induced maximum peroxynitrite production (estimated using APF) and protein Tyr-nitration 6–12 h after elicitation, but no difference between treated cells and controls was apparent up to 2.5 hpi [20]. *A. thaliana* leaves infected with Pst AvrB therefore behave with remarkable similarity to suspension cells exposed to the HR-inducing elicitor INF1. It is likely that the dense population of bacteria in the intercellular spaces within the leaf following infiltration ensures that most plant cells are in contact with the avirulent pathogen, leading to the induction of a highly synchronized and uniform HR as seen in cell suspensions. However, INF1-induced APF fluorescence in tobacco cell suspensions could be almost completely suppressed by urate, whereas in our system HKGreen-2 fluorescence was suppressed by only 25%. This discrepancy indicates that urate may be less efficient in the complex environment of the leaf than in suspension cells, especially over an 8-h treatment period, perhaps because of degradation in plant, limited diffusion or a combination of the two.

Urate reduced fluorescence levels not only in the infected leaf discs but also in controls (data not shown), suggesting that HKGreen-2 is able to detect peroxynitrite induced both by pathogen/HR stress and wounding stress. This confirms the sensitivity of the assay *in planta*, and suggests HKGreen-2 could be useful for the detection of peroxynitrite in the context of many different forms of stress. The HKGreen-2 assay allowed us to show definitively that peroxynitrite accumulates during the HR in *A. thaliana* following infection with an avirulent Pst strain, beginning within 4 hpi and peaking 7–8 hpi. The profile of peroxynitrite accumulation reported here correlates well with the *S*-nitrosylation and inhibition of Prx IIE (which breaks down peroxynitrite) [13] and the accumulation of Tyr-nitrated proteins [17]. This suggests that the inhibition of Prx IIE by NO effectively contributes to peroxynitrite accumulation, which would in turn promote Tyr-nitration, further suggesting that peroxynitrite has an integral role in mediating NO signaling via protein Tyr-nitration. In two recent studies, a total of 21 Tyr-nitrated proteins were identified in untreated sunflower plants [27] and 12 nitro-proteins were identified in *A. thaliana* plants infected with Pst AvrB [17]. However, the physiological significance of peroxynitrite-mediated Tyr-nitration in plants remains unknown because none of the identified nitro-proteins has been characterized. These proteins must be identified and their functions must be established in order to fully elucidate the regulatory role of peroxynitrite in plant cell signaling.

References

[1] M. Moreau, C. Lindermayr, J. Durner, D.F. Klessig, NO synthesis and signaling in plants – where do we stand?, Physiol Plant. 138 (2010) 372–383.

[2] A. Besson-Bard, A. Pugin, D. Wendehenne, New insights into nitric oxide signaling in plants, Annu. Rev. Plant Biol. 59 (2008) 21–39.

[3] S. Neill, R. Barros, J. Bright, R. Desikan, J. Hancock, J. Harrison, P. Morris, D. Ribeiro, I. Wilson, Nitric oxide, stomatal closure, and abiotic stress, J. Exp. Bot. 59 (2008) 165–176.

[4] M. Leitner, E. Vandelle, F. Gaupels, D. Bellin, M. Delledonne, NO signals in the haze: nitric oxide signaling in plant defense, Curr. Opin. Plant Biol. 12 (2009) 451–458.

[5] J.K. Hong, B.W. Yun, J.G. Kang, M.U. Raja, E. Kwon, K. Sorhagen, C. Chu, Y. Wang, G.J. Loake, Nitric oxide function and signaling in plant disease resistance, J. Exp. Bot. 59 (2008) 147–154.

[6] C. Lamb, R.A. Dixon, The oxidative burst in plant disease resistance, Annu. Rev. Plant Physiol. Plant Mol. Biol. 48 (1997) 251–275.

[7] M. Delledonne, J. Zeier, A. Marocco, C. Lamb, Signal interactions between nitric oxide and reactive oxygen intermediates in the plant hypersensitive disease resistance response, Proc. Natl. Acad. Sci. USA 98 (2001) 13454–13459.

[8] M. Delledonne, Y. Xia, R.A. Dixon RA, C. Lamb, Nitric oxide functions as a signal in plant disease resistance, Nature 394 (1998) 585–588.

[9] J.S. Stamler, D.I. Simon, J.A. Osborne, M.E. Mullins, O. Jaraki, T. Michel, D.J. Singel, J. Loscalzo, S-nitrosylation of proteins with nitric oxide: synthesis and characterization of biologically active compounds, Proc. Natl. Acad. Sci. USA 89 (1992) 444–448.

[10] M.C. Romero-Puertas, N. Campostrini, A. Mattè, P.G. Righetti, M. Perazzolli, L. Zolla, P. Roepstorff, M. Delledonne, Proteomic analysis of S-nitrosylated proteins in *Arabidopsis thaliana* undergoing hypersensitive response, Proteomics 8 (2008) 1459–1469.

[11] C. Lindermayr, S. Sell, B. Müller, D. Leister, J. Durner, Redox regulation of the NPR1-TGA1 system of *Arabidopsis thaliana* by nitric oxide, Plant Cell 22 (2010) 2894–2907.

[12] K.J. Dietz, S. Jacob, M.L. Oelze, M. Laxa, V. Tognetti, S. Marina, N. de Miranda, M. Baier, I. Finkemeier, The function of peroxiredoxins in plant organelle redox metabolism, J. Exp. Bot. 57 (2006) 1697–1709.

[13] M.C. Romero-Puertas, M. Laxa, A. Mattè, F. Zaninotto, I. Finkemeier, A.M. Jones, M. Perazzolli, E. Vandelle, K.J. Dietz, M. Delledonne, S-nitrosylation of peroxiredoxin II E promotes peroxynitrite-mediated tyrosine nitration, Plant Cell 19 (2007) 4120–4130.

[14] R. Radi, Nitric oxide, oxidants, and protein tyrosine nitration, Proc. Natl. Acad. Sci. USA 101 (2004) 4003–4008.

[15] Y. Morot-Gaudry-Talarmain, P. Rockel, T. Moureaux, I. Quilleré, M.T. Leydecker, W.M. Kaiser, J.F. Morot-Gaudry, Nitrite accumulation and nitric oxide emission in relation to cellular signaling in nitrite reductase antisense tobacco, Planta 215 (2002) 708–715.

[16] F.J. Corpas, M. Chaki, A. Fernández-Ocaña, R. Valderrama, J.M. Palma, A. Carreras, J.C. Begara-Morales, M. Airaki, L.A. del Río, J.B. Barroso, Metabolism of reactive nitrogen species in pea plants under abiotic stress conditions, Plant Cell Physiol. 49 (2008) 1711–1722.

[17] D. Cecconi, S. Orzetti, E. Vandelle, S. Rinalducci, L. Zolla, M. Delledonne, Protein nitration during defense response in *Arabidopsis thaliana*, Electrophoresis 30 (2009) 2460–2468.

[18] N. Abello, H.A. Kerstjens, D.S. Postma, R. Bischoff, Protein tyrosine nitration: selectivity, physicochemical and biological consequences, denitration, and proteomics methods for the identification of tyrosine-nitrated proteins, J. Proteome Res. 8 (2009) 3222–3238.

[19] A. Sakamoto, S.H. Sakurao, K. Fukunaga, T. Matsubara, M. Ueda-Hashimoto, S. Tsukamoto, M. Takahashi, H. Morikawa, Three distinct Arabidopsis hemoglobins exhibit peroxidase-like activity and differentially mediate nitrite-dependent protein nitration, FEBS Lett. 572 (2004) 27–32.

[20] S. Saito, A. Yamamoto-Katou, H. Yoshioka, N. Doke, K. Kawakita, Peroxynitrite generation and tyrosine nitration in defense responses in tobacco BY-2 cells, Plant Cell Physiol. 47 (2006) 689–697.

[21] K. Setsukinai, Y. Urano, K. Kakinuma, H.J. Majima, T. Nagano, Development of novel fluorescence probes that can reliably detect reactive oxygen species and distinguish specific species, J. Biol. Chem. 278 (2003) 3170–3175.

[22] D. Yang, H.L. Wang, Z.N. Sun, N.W. Chung, J. G Shen, A highly selective fluorescent probe for the detection and imaging of peroxynitrite in living cells, J. Am. Chem. Soc. 128 (2006) 6004–6005.

[23] Z.N. Sun, H.L. Wang, F.Q. Liu, Y. Chen, P.K. Tam, D. Yang, BODIPY-based fluorescent probe for peroxynitrite detection and imaging in living cells, Org. Lett. 11 (2009) 1887–1890.

[24] U. Bechtold, N. Rabbani, P.M. Mullineaux, P.J. Thornalley, Quantitative measurement of specific biomarkers for protein oxidation, nitration and glycation in Arabidopsis leaves, Plant J. 59 (2009) 661–671.

[25] S.A. Greenacre, H. Ischiropoulos, Tyrosine nitration: localisation, quantification, consequences for protein function and signal transduction, Free Radic. Res. 34 (2001) 541–581.

[26] C. Quijano, N. Romero, R. Radi, Tyrosine nitration by superoxide and nitric oxide fluxes in biological systems: modeling the impact of superoxide dismutase and nitric oxide diffusion, Free Radic. Biol. Med. 39 (2005) 728–741.

[27] M. Chaki, R. Valderrama, A. Fernández-Ocaña, A. Carreras, J. López-Jaramillo, F. Luque, J.M. Palma, J.R. Pedrajas, J.C. Begara-Morales, B. Sánchez-Calvo, M.V. Gómez-Rodríguez, F.J. Corpas, J.B. Barroso, Protein targets of tyrosine nitration in sunflower (*Helianthus annuus* L.) hypocotyls, J. Exp. Bot. 60 (2009) 4221–4234.

Journal of
Experimental
Botany
www.jxb.oxfordjournals.org

RESEARCH PAPER

Differential inhibition of *Arabidopsis* superoxide dismutases by peroxynitrite-mediated tyrosine nitration

Christian Holzmeister[1,*], Frank Gaupels[1,*], Arie Geerlof[2], Hakan Sarioglu[3], Michael Sattler[2,4], Jörg Durner[1,5] and Christian Lindermayr[1,†]

[1] Institute of Biochemical Plant Pathology, Helmholtz Zentrum München–German Research Center for Environmental Health, 85764 München/Neuherberg, Germany

[2] Institute of Structural Biology, Helmholtz Zentrum München–German Research Center for Environmental Health, 85764 München/Neuherberg, Germany

[3] Department of Protein Science, Helmholtz Zentrum München-German Research Center for Environmental Health, 85764 München/Neuherberg, Germany

[4] Munich Center for Integrated Protein Science at Chair of Biomolecular NMR, Department Chemie, Technische Universität München, 85747 Garching, Germany

[5] Chair of Biochemical Plant Pathology, Technische Universität München, 85354 Freising, Germany

* These authors contributed equally to this manuscript.
† To whom correspondence should be addressed. E-mail: Lindermayr@helmholtz-muenchen.de

Abstract

Despite the importance of superoxide dismutases (SODs) in the plant antioxidant defence system little is known about their regulation by post-translational modifications. Here, we investigated the *in vitro* effects of nitric oxide derivatives on the seven SOD isoforms of *Arabidopsis thaliana*. *S*-nitrosoglutathione, which causes *S*-nitrosylation of cysteine residues, did not influence SOD activities. By contrast, peroxynitrite inhibited the mitochondrial manganese SOD1 (MSD1), peroxisomal copper/zinc SOD3 (CSD3), and chloroplastic iron SOD3 (FSD3), but no other SODs. MSD1 was inhibited by up to 90% but CSD3 and FSD3 only by a maximum of 30%. Down-regulation of these SOD isoforms correlated with tyrosine (Tyr) nitration and both could be prevented by the peroxynitrite scavenger urate. Site-directed mutagenesis revealed that—amongst the 10 Tyr residues present in MSD1—Tyr63 was the main target responsible for nitration and inactivation of the enzyme. Tyr63 is located nearby the active centre at a distance of only 5.26 Å indicating that nitration could affect accessibility of the substrate binding pocket. The corresponding Tyr34 of human manganese SOD is also nitrated, suggesting that this might be an evolutionarily conserved mechanism for regulation of manganese SODs.

Key words: Antioxidant system, nitric oxide, nitrosative stress, post-translational modification, superoxide dismutase, tyrosine nitration.

Introduction

In plant cells the reactive oxygen species (ROS) superoxide (O_2^-) arises as a potentially harmful by-product of photosynthetic and respiratory electron transport chains. It can also be enzymatically produced by various oxidases to serve as a signal or intermediate in general metabolism, development, and stress responses (Mittler *et al.*, 2011). Independent of origin and function, O_2^- levels are carefully controlled by the antioxidant system (Foyer and Noctor, 2009). O_2^- is either scavenged by antioxidants such as reduced ascorbate and glutathione or is efficiently converted to hydrogen peroxide (H_2O_2) by superoxide dismutase (SOD; $O_2^- + 2\,H^+ \rightarrow H_2O_2 + O_2$). H_2O_2 in turn is subsequently degraded to water by catalase and peroxidases. Thus, by controlling O_2^- (and indirectly H_2O_2) levels SODs are important regulators of cellular redox homeostasis and signalling.

Plant SODs are commonly classified according to their active site cofactors into manganese SOD (MnSOD), iron SOD (FeSOD), and copper/zinc SOD (CuZnSOD). *Arabidopsis* possesses 7 SOD isoforms namely one MnSOD (MSD1), three FeSODs (FSD1–3), and three CuZnSODs (CSD1–3) (Kliebenstein *et al.*, 1998). Whereas MSD1 has a mitochondrial targeting sequence, FSD2, FSD3, and CSD2 are localized in chloroplasts, CSD1 and FSD1 in the cytosol, and CSD3 in peroxisomes (Huang *et al.*, 2012; Kliebenstein *et al.*, 1998; Myouga *et al.*, 2008). Gene expression of the SOD isoforms is differentially regulated in response to stress treatments known to promote the accumulation of ROS. For instance, ozone fumigation strongly induced CSD1 but repressed CSD3 and FSD1 expression (Kliebenstein *et al.*, 1998). These results suggest that the different SOD isoforms have specific functions under stress conditions. Moreover, SOD transcript levels did not always correlate with protein abundance and enzyme activity indicating that SODs are controlled on multiple levels including post-transcriptional and post-translational mechanisms (Kliebenstein *et al.*, 1998; Madamanchi *et al.*, 1994). In this context it is interesting that recent publications hint at a role of nitric oxide (NO) dependent protein modifications in the regulation of mammalian SODs (Radi, 2013).

NO is an important messenger in many physiological processes (Gaupels *et al.*, 2011a; Leitner *et al.*, 2009; Mur *et al.*, 2013; Yun *et al.*, 2011). During stress responses NO often interacts with ROS and antioxidants thereby forming reactive nitrogen species (RNS) (Gross *et al.*, 2013; Hill *et al.*, 2010; Scheler *et al.*, 2013). Such NO derivatives can cause post-translational modifications of proteins by *S*-nitrosylation (⋅NO adduct) of cysteine (Cys) residues and metal groups or nitration (-NO adduct) of tyrosine (Tyr) and tryptophan residues (Arasimowicz-Jelonek and Floryszak-Wieczorek, 2011; Astier and Lindermayr, 2012; Gaupels *et al.*, 2011a; Hill *et al.*, 2010; Kovacs and Lindermayr, 2013). *S*-nitrosoglutathione (GSNO), nitrosonium ion (NO^+), and dinitrogentrioxide (N_2O_3) represent major RNS promoting *S*-nitrosylation, whereas peroxynitrite ($ONOO^-$) and nitrogen dioxide (NO_2) mediate protein nitration (Hill *et al.*, 2010). NO-dependent protein modifications have an effect on the activity of antioxidant enzymes. One prominent example is mammalian MnSOD, which can be Tyr nitrated (MacMillan-Crow *et al.*, 1996; Radi, 2013). *In vitro* and *in vivo* under inflammatory conditions MnSOD was site-specifically nitrated at Tyr34, which caused inhibition of SOD activity and consequently disturbance of mitochondrial redox homeostasis (Radi, 2013; Yamakura *et al.*, 1998). Less is known about regulation of plant SODs by NO. Occasionally, SODs of various plant species were listed amongst candidate *S*-nitrosylated and Tyr nitrated proteins (Lin *et al.*, 2012; Sehrawat *et al.*, 2013; Tanou *et al.*, 2009). However, NO-modifications were not confirmed *in vitro* nor was the effect of RNS on SOD activity investigated in any detail.

Here, we report the differential inhibition of *Arabidopsis* SODs by Tyr nitration. We observed that overall SOD activity was decreased in leaf extracts from GSNO-/NO-accumulating GSNO reductase-deficient mutants as compared with WT although the expression of SOD-coding genes was nearly unchanged. From these results we concluded that SOD isoforms might be inhibited by NO-dependent post-translational modifications. This prompted us to undertake a systematic candidate approach for defining the role of RNS in regulation of all seven *Arabidopsis* SOD isoforms. *In vitro* tests demonstrated that SOD activities were not altered upon GSNO treatment but MSD1, FSD3, and CSD3 were inhibited to different degrees by $ONOO^-$. Inhibition of the enzymes correlated with increased Tyr nitration. Site-directed mutagenesis revealed that nitration of Tyr63 caused most of the almost complete inactivation of MSD1 by $ONOO^-$. In sum, nitration of MSD1 is a good model for post-translational regulation of plant enzymes as a whole and SOD isoforms in particular. Putative physiological effects of SOD inhibition by nitration under stress conditions are discussed.

Materials and methods

Plant material

Arabidopsis thaliana seeds (ecotype Col-0) were sown on soil:sand mixture (4:1). After vernalization for 2 days (4 °C dark), plants were cultivated in a climate chamber at 60% relative humidity under long-day conditions (16 h light/8 h dark cycle, 20 °C day/18 °C night regime, 70 µmol m^{-2} s^{-1} photon flux density).

Cloning and heterologous expression of Arabidopsis *SODs*

For cloning the cDNAs of the different SOD isoforms the lambda phage-based site-specific recombination (Stratagene) was used (Landy, 1989). The isolation of the cDNAs of the different SODs was achieved by RT-PCR using gene-specific oligonucleotides (Supplementary Table S1). Briefly, total RNA extractions were performed from 100 mg leaf tissue using the TRIzol reagent according to the supplier's instructions (Invitrogen). QuantiTect Reverse Transcription Kit (Qiagen) was used to synthesize cDNA according to the protocol of the supplier. The introduction of the DNA recombination sequence (att) at the 5'- and 3'-end of the coding sequence of each isoform was achieved by PCR using the isoform-specific att-primers (Supplementary Table S1) and the amplified cDNAs as template. The resulting PCR products were introduced into pDONR221 by recombination using BP Clonase enzyme mixture according to the instructions of the manufacturer. After verifying the sequences of the different SODs they were transferred into the expression vectors pDEST17 and pDEST42 by recombination using LP Clonase enzyme mixture. pDEST17 and pDEST42 allows production of N-terminal or C-terminal His_6-tag fusion proteins, respectively. For optimal production different bacterial expression strains were tested (BL21 DE3, Rosetta DE3, and Rosetta DE3 pLysS) and the most productive strain for each SOD was selected.

E. coli strains harbouring the different plasmids for production of recombinant SODs were grown in 50 ml Luria-Bertani medium at 37 °C overnight. These cultures were used to inoculate 2 l autoinduction medium (Studier, 2005). The bacteria were grown overnight at 37 °C until an OD_{600nm} of 2 was reached. Afterwards bacterial cells were harvested by centrifugation.

Extraction, purification, and treatments of SODs with GSNO and peroxynitrite

For protein extraction the cells were resuspended in 160 ml lysis buffer (50 mM Tris-HCl, pH 8.0, 300 mM NaCl, 20 mM imidazole, 10 mM $MgCl_2$, 1 mM protease-inhibitor AEBSF, 0.02% 1-thioglycerol, 0.2 µg ml^{-1} DNaseI, 1 mg ml^{-1} lysozyme) and disrupted by high pressure homogenization and sonication. Cellular debris was removed by centrifugation (25 000 g, 1 h, 4 °C). The recombinant proteins were purified by affinity chromatography using 1.0 ml Ni–NTA

agarose in Econo-Pac columns (Biorad, Munich, Germany). The protein extracts were applied onto the columns twice, and washed with 30 ml of washing buffer (50 mM Tris-HCl, pH 8.0, 300 mM NaCl, 20 mM imidazole, 0.02% glycerol). Adsorbed proteins were eluted from the matrix in three 5 ml fractions with 300 mM imidazole in washing buffer. Eluates were frozen in liquid nitrogen and stored at –20 °C until analysis.

The purified enzymes were re-buffered in potassium phosphate buffer (pH 8.0) using Zeba spin columns (Thermo Scientific, Rockford, USA). Afterwards, the enzymes were treated with 250 µM and 500 µM GSNO for 20 min (RT, in dark). Control treatment was done with 500 µM GSNO in presence of 5 mM DTT. Alternatively, purified SODs were treated for 20 min with different concentrations of ONOO⁻ (RT, in dark). ONOO⁻ was purchased from Calbiochem (Darmstadt, Germany) in 4.7% NaOH at 160–200 mM. The exact concentration was determined according to the manufacturer′s instructions. Control treatment was done with 500 µM ONOO⁻ in presence of 100 µM urate. Excess GSNO, DTT, ONOO⁻, and urate were removed with Zeba spin columns before determination of SOD activities.

The activity of the purified, recombinant SODs was determined using the nitroblue tetrazolium (NBT)–formazan method (McCord and Fridovich, 1969) or the cytochrome *c*-based assay (McCord, 2001).

Detection of SOD nitration by anti-nitrotyrosine western blot

Proteins were separated by SDS-PAGE on 12% polyacrylamide gels (Laemmli, 1970), transferred onto PVDF membranes, and blocked with 1% non-fat milk powder and 1% bovine serum albumin. The blots were incubated with goat anti-nitrotyrosine antibody (1:2000) at 4 °C overnight, followed by incubation with rabbit anti-goat IgG conjugated with horseradish peroxidase (1:3000) (Invitrogen, Darmstadt, Germany) for 1 h at RT. Cross-reacting protein bands were visualized via chemiluminescence using the West Pico Chemiluminescence Detection Kit (Thermo Scientific, Rockford, USA).

Site-directed mutagenesis

The modification of single nucleotide residues was performed as previously described (Lindermayr *et al.*, 2003). Briefly, for mutation, a pair of oligonucleotides was synthesized harbouring the desired alterations (Supplementary Table S1). For amplification, 60 ng plasmid DNA was used in a total volume of 10 µl, including 1 µM each primer, 200 µM dNTPs, and 1 U of iProof DNA polymerase. After denaturation (1 min at 98 °C) 20 cycles were conducted, consisting of 25 s at 98 °C, 55 s at 55 °C, and 6 min at 72 °C, followed by a final extension step at 72 °C for 10 min. Subsequently, the parental and hemi-parental template DNA was digested with *Dpn*I and the amplified plasmids were transformed into *E. coli* DH5α. The mutation was verified by sequencing.

Modelling of the 3D structure of MSD1

Amino acid sequences were aligned and modelled using SWISS-Model (www.expasy.ch). The crystal structure of *Caenorhabditis elegans* MnSOD (PDBcode: PDB 3DC6) was used as template for the prediction of the putative conformation of *Arabidopsis* MSD1. Pymol software (DeLano Scientific, Portland, USA) was used for model visualization.

Nano-HPLC-MS²/³ and data analysis

For mass spectrometric analyses proteins were digested with trypsin at 37 °C for 16 h in 50 mM NH₄HCO₃, pH 8.0. The used trypsin/protein ratio was 1/20. All nano-HPLC-MS²/³-experiments were performed on an Ultimate 3000 HPLC nanoflow system (Dionex) connected to a linear ion trap-Fourier transform mass spectrometer (LTQ-Orbitrap, Thermo Fisher Scientific, San Jose, CA, USA). For LTQ-Orbitrap mass spectrometry, the digested peptides were first separated by reversed-phase chromatography (PepMap, 15cm_75 mm id, 3 mm/100 Å pore size, LC Packings) operated on a nano-HPLC (Ultimate 3000, Dionex) with a nonlinear 170 min gradient using 2% ACN in 0.1% formic acid in water (A) and 0.1% formic acid in 98% ACN (B) as eluents with a flow rate of 250 nl min⁻¹. The nano-LC was connected to a linear quadrupole ion trap-Orbitrap (LTQ Orbitrap XL) mass spectrometer (Thermo-Fisher, Bremen, Germany) equipped with a nano-ESI source. The mass spectrometer was operated in the data-dependent mode to automatically switch between Orbitrap-MS and LTQ-MS/MS acquisition. Survey full scan MS spectra (from *m/z* 300–1500) were acquired in the Orbitrap with resolution R560 000 at *m/z* 400 (after accumulation to a target value of 1 000 000 charges in the LTQ). The method used allowed sequential isolation of the most intense ions, up to ten, depending on signal intensity, for fragmentation on the linear ion trap using collisionally induced dissociation at a target value of 100 000 ions. High-resolution MS scans in the orbitrap and MS/MS scans in the linear ion trap were performed in parallel. Target peptides already selected for MS/MS were dynamically excluded for 30 s. General conditions were as follows: electrospray voltage, 1.25–1.4 kV; no sheath and auxiliary gas flow. The following modifications were set to be variable: nitration of Tyr residues.

Results

Cloning, heterologous expression, and purification of *Arabidopsis* SODs

SODs are important enzymes of the antioxidant system and several enzyme activities of this system are affected by NO. Mammalian MnSOD, for instance, is a target for Tyr nitration (MacMillan-Crow *et al.*, 1996; Radi, 2013). Under inflammatory conditions human MnSOD is site-specifically nitrated at Tyr34, which results in inhibition of SOD activity and consequently disturbance of mitochondrial redox homeostasis (Radi, 2013; Yamakura *et al.*, 1998). Less is known about regulation of plant SODs by NO, although SODs of various plant species were identified as candidates for *S*-nitrosylation and Tyr nitration (Lin *et al.*, 2012; Sehrawat *et al.*, 2013; Tanou *et al.*, 2009), NO-dependent modifications were not confirmed until now. In *Arabidopsis* seven different SODs are described, including one MSD, three FSDs, and three CSDs. The deduced amino acid sequences of the different isoenzymes show very different homology among each other (44–46% within the FSDs, 45–57% within the CSDs) (Table 1). Moreover, the identity of the amino acid sequences between MSD1 and FSDs is higher (29–31%) than the identity between MSD1 and CSDs (18–21%), suggesting that MSD1 is closer related to FSDs (Table 1). The corresponding amino acid sequence alignments are provided in the Supplementary data (Figs S1–S4).

We heterologously produced and purified all seven *Arabidopsis* SOD proteins for *in vitro* analyses of their regulation by *S*-nitrosylation of cysteine residues or nitration of Tyr residues. First, we isolated the coding sequence of all seven *Arabidopsis* SOD proteins. The isolation of the cDNAs of the different SODs was achieved by RT-PCR using gene-specific oligonucleotides and the amplified coding sequences were expressed in *Escherichia coli* as fusion proteins containing either N-terminal or C-terminal His₆-tags. For optimal production different bacterial expression strains were tested

(BL21 DE3, Rosetta DE3, and Rosetta DE3 pLysS) and the most productive strain for each SOD was selected. After affinity chromatography on Ni–NTA–agarose, the seven proteins showed the expected relative molecular masses in SDS-polyacrylamide gels and on the immunoblot (Fig. 1).

The activity of the purified, recombinant SODs was determined using the nitroblue tetrazolium (NBT)–formazan

Table 1. *Amino acid sequence identity and similarity between the different Arabidopsis SOD isoforms*

	AA sequence identity (%)	AA sequence similarity (%)
FSD1–FSD2	46	57
FSD1–FSD3	44	58
FSD2–FSD3	45	59
CSD1–CSD2	47	53
CSD1–CSD3	57	67
CSD2–CSD3	45	54
MSD1–FSD1	47	53
MSD1–FSD2	57	67
MSD1–FSD3	45	54
MSD1–CSD1	19	28
MSD1–CSD2	21	30
MSD1–CSD3	18	31

method (Fig. 2). In this assay, O_2^- ions are generated from the conversion of xanthine and O_2 to uric acid and H_2O_2 by xanthine oxidase. The O_2^- anion then converts a NBT into a formazan dye. Addition of SOD to this reaction reduces O_2^- ion levels, thereby lowering the rate of formazan dye formation. SOD activity is monitored at a wavelength of 570 nm and determined as the percent inhibition of the rate of formazan dye formation. The different types of SODs were verified using specific inhibitors (H_2O_2 for FSDs and NaCN for CSDs). MSD1 is insensitive to both inhibitors (Fig. 2).

MSD1, FSD3, and CSD3 are inhibited by $ONOO^-$

The total SOD activity in *atgsnor* plants is lower than in WT plants (Supplementary Fig. S5), which is probably related to the higher levels of NO-derivatives in the mutant (Feechan *et al.*, 2005). As the decreased SOD activity in *atgsnor* cannot be explained by transcriptional regulation (Supplementary Fig. S6), we hypothesized that it is regulated on the protein level. The two most important NO-dependent post-translational modifications are *S*-nitrosylation of Cys residues and nitration of Tyr residues. Assuming that SOD activity might be inhibited by *S*-nitrosylation of critical Cys residues, MSD1, FSD3, and all three CSDs, were treated with the *S*-nitrosylating agent GSNO, as these isoform have at least one cysteine residue. However, none of these
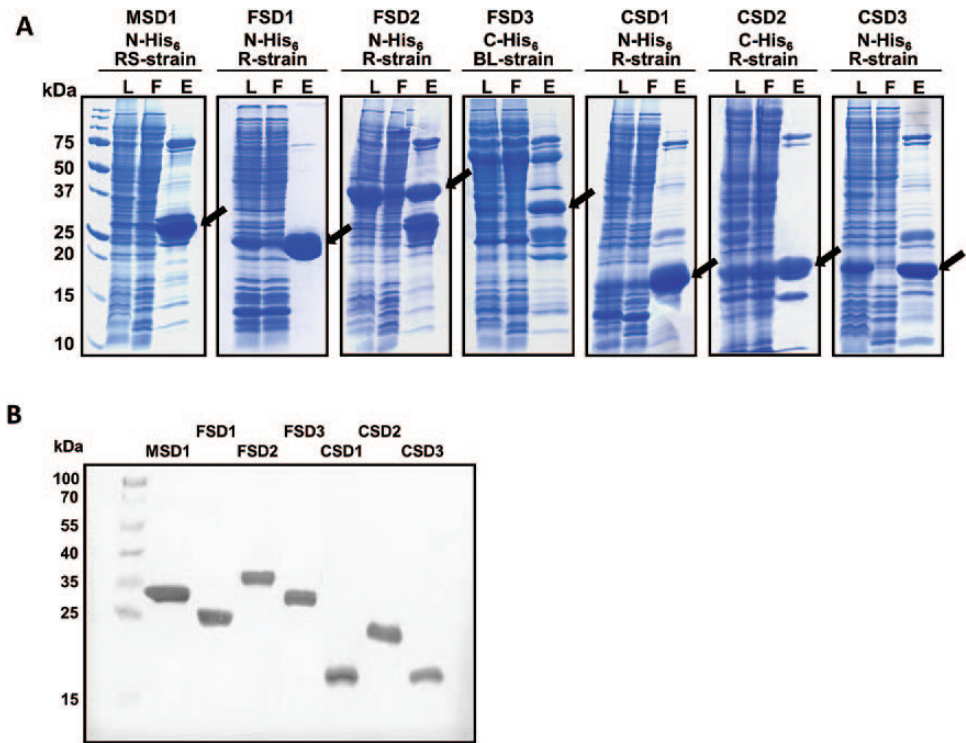

Fig. 1. Production, purification, and detection of recombinant *Arabidopsis* SODs. (A) The coding sequences of the different *Arabidopsis* SODs were cloned into pDEST17 (N-terminal His6) or pDEST42 (C-terminal His6) using the Gateway Technology. Three different bacteria production strains (RS-strain=Rosetta DE3 pLysS; R-strain=Rosetta DE3; BL-strain=BL21 DE3) were tested and the most productive one for each isoform was used. His-tagged SODs were purified by Ni–NTA affinity chromatography. Crude bacterial lysate (L), flow-through (F), and eluate (E) were separated by SDS-PAGE and visualized by Coomassie Blue staining. Arrows indicate the produced SOD isoforms. The relative mass of protein standards are shown on the left. (B) Detection of purified, recombinant *Arabidopsis* SOD isoforms. Eluates containing recombinant SOD isoforms were separated by SDS-PAGE and blotted onto nitrocellulose membrane. Detection of His-tagged proteins was achieved using anti-His antibody. The relative mass of protein standards are given on the left. (This figure is available in colour at *JXB* online.)
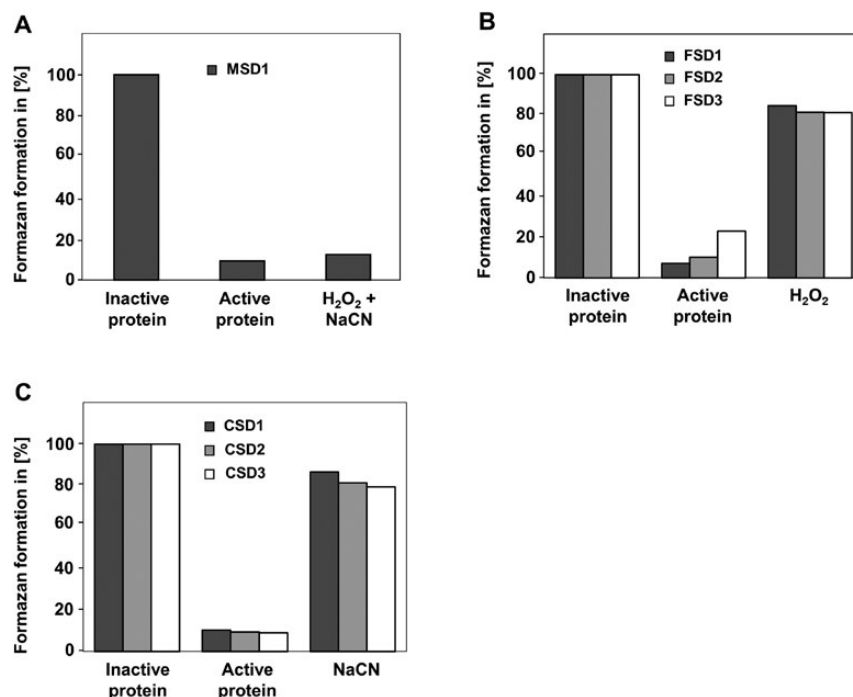
Fig. 2. Enzyme activities of purified, recombinant SODs. Shown is the inhibition of formazan formation by MSD1 (A), FSDs (B), and CSDs (C). Formazan formation with heat-inactivated protein extracts was set to 100%. To distinguish between the different SOD types specific inhibitors (H$_2$O$_2$ for FSDs and NaCN for CSDs) were used. MSD1 is insensitive to both inhibitors.

SODs was inhibited by GSNO (Fig. 3). Next, we tested the effect of ONOO$^-$ on SOD activity. To this end, all SODs, which have at least one Tyr residue (MSD1, all three FSDs, and CSD3) were treated with different concentrations of ONOO$^-$. A concentration-dependent inhibition of MSD1, FSD3, and CSD3 could be observed, whereas the activity of the other two tested FSD isoforms was not affected by this treatment (Fig. 4). Especially MSD1 seems to be very sensitive to this treatment. Its activity decreased to about 10% with 500 µM ONOO$^-$, whereas the activity of FSD3 and CSD3 was reduced to 65%. However, it has to be mentioned that the observed differences in the efficiency of ONOO$^-$-dependent inhibition of the different SODs could be caused by different ratio of applied protein and ONOO$^-$. For a better comparison we calculated the ratio of applied protein per nmol ONOO$^-$ for the highest ONOO$^-$ concentration used (500 µM) (Fig. 4).

Inhibition of enzyme activity by ONOO$^-$ correlated with increased protein nitration as detected by immunoblot analyses using an anti-nitrotyrosine antibody (Fig. 5). Notably, western blot signals were stronger for MSD1 than FSD3 and CSD3. Because of the high sensitivity of MSD1 to ONOO$^-$ this isoform has been analysed in more detail.

Mass spectrometric identification of nitrated Tyr residues in MSD1

To identify the modified Tyr residues in MSD1, peroxynitrite-treated MSD1 was analysed by mass spectrometry. In total, MSD1 has ten Tyr residues. Modelling of the three-dimensional structure of MSD11 revealed that especially Tyr63, Tyr198, and Tyr209 were located close to an active

site manganese ion at a distance lower than 10 Å (5.3 Å, 9.1 Å, 9.3 Å, respectively) (Fig. 6). MSD1 was treated with 500 µM peroxynitrite and digested with trypsin. This protease generated analysable peptides containing the different Tyr residues mentioned above. For each nitrated Tyr residue an increase in mass by 45 Da was expected. All identified nitrated Tyr residues are summarized in Table 2. Tyr residues 209, 221, and 226 are not accessible to nitration, as they were only found in their unmodified form. Especially nitration of Tyr63, which is closest to the active site manganese, could be of special importance for the inhibitory effect of peroxynitrite on MSD1, as it corresponds to Tyr34 in human MnSOD.

Nitration of Tyr63 is responsible for inhibition of MSD1 activity

To test if nitration of Tyr63 inhibits MSD1 activity this residue was changed by site-directed mutagenesis to phenylalanine. This amino acid is structurally related to Tyr but cannot be nitrated. Wild-type and mutated MSD1 (MSD1/Y63F) were treated with different concentrations of ONOO$^-$ and their activities were determined. Both wild type and modified MSD1 showed similar specific activity upon addition of decomposed ONOO$^-$ (control). However, treatment with 100 and 250 µM ONOO$^-$ resulted in no inhibition and 500 µM ONOO$^-$ in only 30% inhibition of MSD1/Y63F, whereas wild-type MSD1 was inhibited by about 30, 50, and 90%, respectively (Fig. 7A and B). Immunoblot analyses with anti-nitrotyrosine antibodies demonstrated that overall Tyr nitration of MSD1/Y63F was much lower than that of wild-type MSD1 (Fig. 7C).
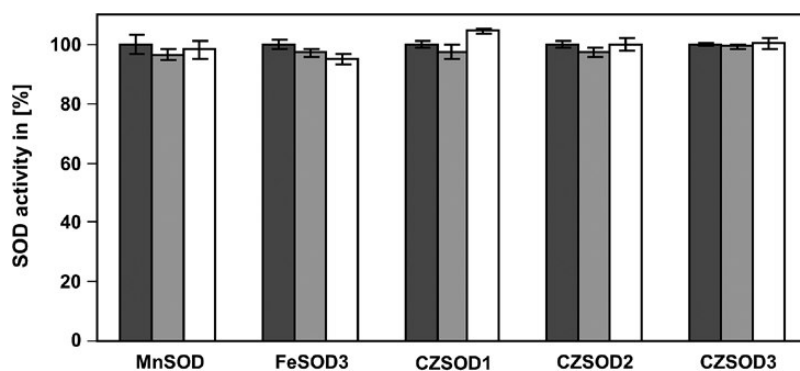
Fig. 3. Effect of GSNO on enzyme activity of cysteine containing SODs. Recombinant MnSOD, FeSOD3, Cu/ZnSOD1, Cu/ZnSOD2, and Cu/ZnSOD3 were treated with 250 μM (light grey) and 500 μM (white) GSNO for 20 min (RT, in dark). Control treatment was done with 500 μM GSNO in presence of 5 mM DTT (dark grey). Afterwards the activity was determined. Treatment with light-inactivated GSNO was used as control. These activities were set to 100%. Values represent means±SD of three independent experiments.
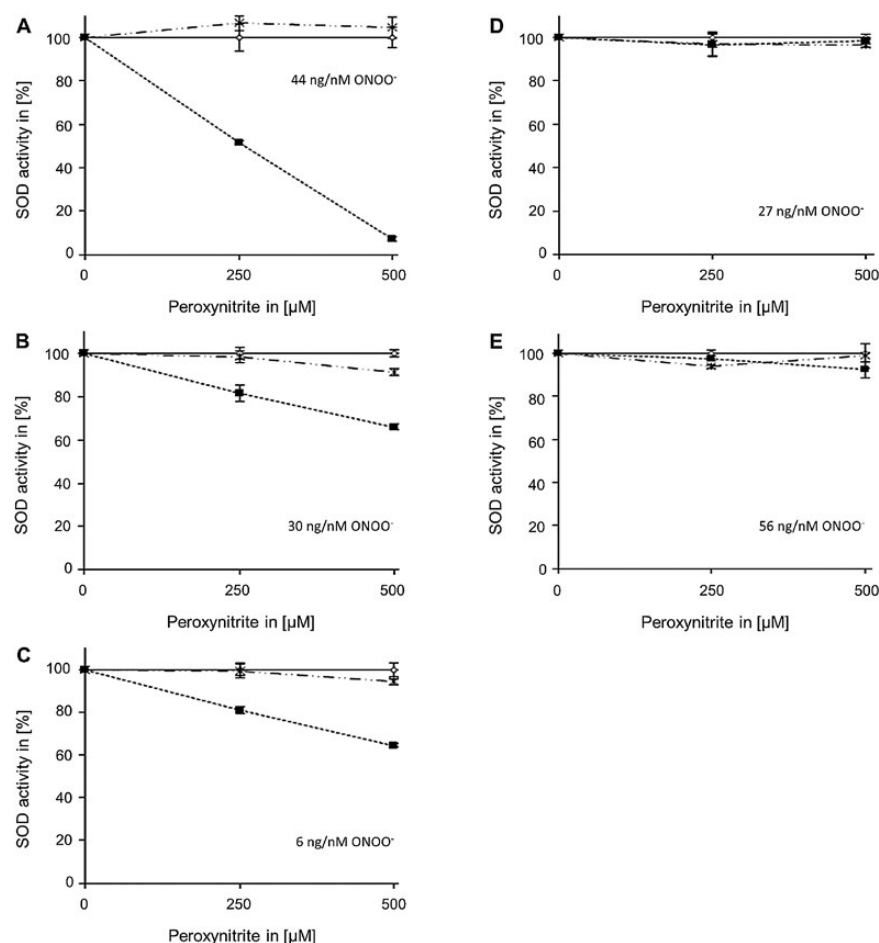

Fig. 4. Effect of peroxynitrite on enzyme activity of Tyr-containing SODs. Recombinant MSD1 (A, 22 μg), FSD3 (B, 15 μg), Cu/ZnSOD3 (C, 3 μg), FSD1 (D, 13 μg), and FSD2 (E, 28 μg) were treated with peroxynitrite for 20 min (RT, in dark). Afterwards the activity was determined by monitoring reduction of cytochrome *c*. The given values indicate the ratio of applied protein per nmol ONOO⁻ calculated for the highest ONOO⁻ used (500 μM). Filled squares: peroxynitrite treatment; open squares: peroxynitrite treatment in presence of 100 μM urate; crosses: treatment with decomposed peroxynitrite. The activities of urate-treated samples were set to 100%. Values represent means±SD of three independent experiments.

Discussion

ROS are produced in unstressed and stressed cells as a by-product of aerobic metabolism. Plants have a well-developed antioxidant defence, involving both limiting the formation of

ROS as well as instituting their removal. SODs are enzymes that catalyse the dismutation of O_2^- into oxygen and H_2O_2. In *Arabidopsis* seven different SODs are described, which differ in their metal-cofactor and subcellular location. Here we present MSD1, FSD3, and CSD3 as new candidates for

NO-dependent post-translational regulation. GSNO, which can *S*-nitrosylate Cys residues, did not affect activity of MSD1, FSD3, and CSD3. However, incubation with the Tyr nitrating agent ONOO⁻ significantly reduced the activity of all three enzymes with MSD1 being the most sensitive isoform. Because of the variable purification efficiency of the five tested SOD isoforms we had to use different amounts of total protein. This could affect the inhibition efficiency of ONOO⁻. Therefore, we calculated the ratio of applied protein per nmol ONOO⁻ for the highest ONOO⁻ concentration used (500 µM). The highest protein amount was used in the FSD2 and MSD1 inhibition assays. As 500 µM ONOO⁻ resulted in nearly total loss of MSD1 activity this enzyme seems to be the most ONOO⁻-sensitive SOD isoform. FSD2 activity is only slightly affected by ONOO⁻ (10% with 500 µM ONOO⁻), but a stronger inhibition cannot be excluded, if lower protein amounts are used.
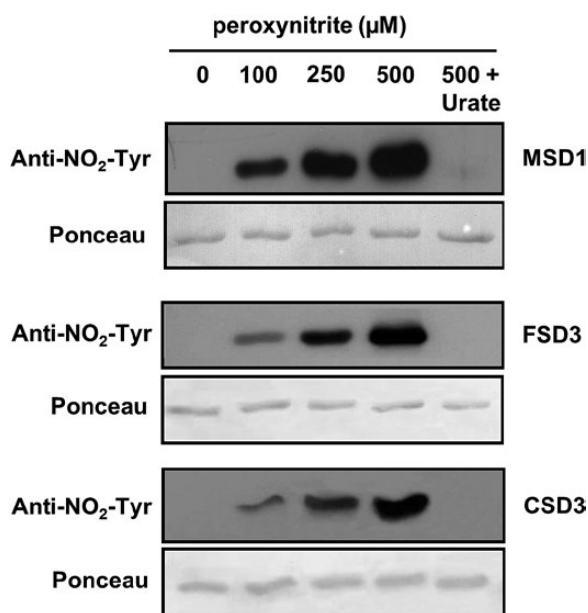
Similar to the plant MSD1, human and bacterial MnSODs are also very sensitive to ONOO⁻ (MacMillan-Crow *et al.*, 1998; Surmeli *et al.*, 2010). An inhibition of 30% with 100 µM ONOO⁻ might occur under physiological conditions assuming that ONOO⁻ levels in plants are similar to that in the animal system. Here the rate of ONOO⁻ production can reach 50–100 µM min⁻¹ in certain cellular compartments including mitochondria (Szabo *et al.*, 2007). However, as NO production in plants is lower than in the animal system, ONOO⁻ levels might be also lower. The concentration-dependent inhibition of MSD1 positively correlated with the level of Tyr nitration (Figs 4 and 5). Inhibition of activity as well as protein nitration was prevented by the ONOO⁻ scavenger urate.

Primarily nitration of Tyr63 was responsible for the ONOO⁻ sensitivity of MSD1, as inferred by the finding
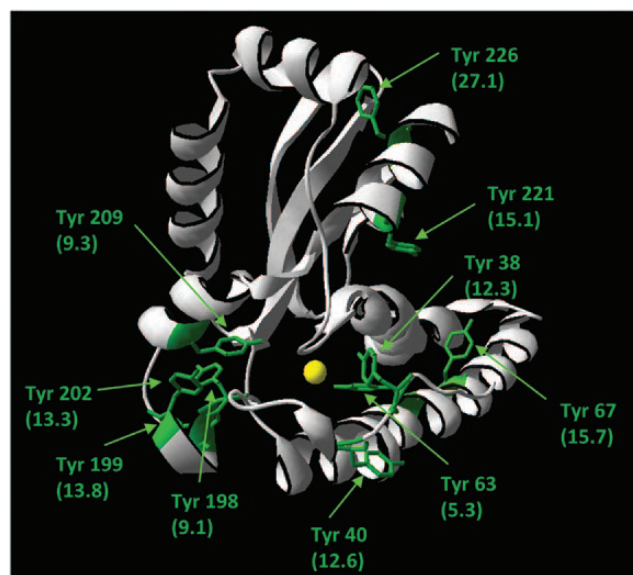
Fig. 5. Detection of nitrated Tyr residues. Purified, recombinant MSD1, FSD3, and Cu/ZnSOD3 were treated with different concentrations of peroxynitrite, separated by SDS-PAGE, and blotted onto nitrocellulose membrane. Detection of nitrated Tyr residues was achieved using anti-NO₂–Tyr antibody. Treatment with 500 µM peroxynitrite in presence of 100 µM urate was used as control.

Fig. 6. Structural model of *Arabidopsis* MSD1. The structural model of *Arabidopsis* MSD1 was generated using SWISS-MODEL with the crystal structure of *Caenorhabditis elegans* MnSOD as template (PDBcode: PDB 3DC6). The Tyr residues are marked in green. The distances between Tyr side chains and the active side manganese ion (yellow) is given in Ångström in brackets.
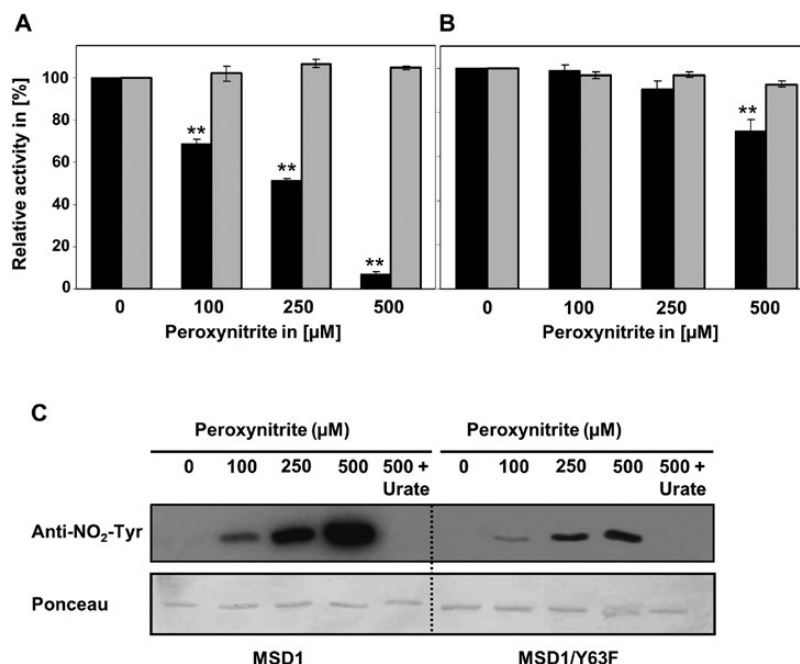
Table 2. *Determination of Tyr nitration of MSD1 by mass spectrometry*

Purified, reduced, recombinant MSD1 was incubated with 500 µM peroxynitrite and digested with trypsin. Peptides containing at least one Tyr residue were analysed by mass spectrometry to determine Tyr nitration. Expected (single charged) and observed (multiple charged) *m/z* values for the different peptides are shown.

Identified peptide	Mascot Score	m/z (expected)	m/z (observed)	charge	modification
KHHQAYVTNY⁶⁷NNALEQLDQAVNKG	76	1.307	1.308	2	Nitro (+45)
KHHQAY⁶³VTNYNNALEQLDQAVNKGDASTVVKL	70	0.843	0.844	4	Nitro (+45)
KGGSLVPLVGIDVWEHAY¹⁹⁸YLQYKN	46	1.276	1.277	2	Nitro (+45)
KGGSLVPLVGIDVWEHAYY¹⁹⁹LQYKN	45	1.276	1.277	2	Nitro (+45)
KGGSLVPLVGIDVWEHAYYLQY²⁰²KN	42	1.276	1.277	2	Nitro (+45)
RGIQTFTLPDLPYDY⁴⁰GALEPAISGEIMQIHHQKH	39	1.209	1.210	3	Nitro (+45)
RGIQTFTLPDLPY³⁸DYGALEPAISGEIMQIHHQKH	36	0.907	0.908	4	Nitro (+45)

Fig. 7. Effect of peroxynitrite on enzyme activity of MSD1/WT and MSD1/Y63F. Recombinant MSD1/WT (A) and MSD1/Y63F (B) were treated with different concentrations of peroxynitrite in the presence (grey bars) and absence (black bars) of 100 µM urate for 20 min (RT, in dark). Afterwards the activity was determined. Activities without peroxynitrite were set to 100%. Values represent means±SD of three independent experiments. Asterisks (**) indicate significant differences treatment with and without urate (t-test, *P*≤0.01). Tyr nitration was detected by immunoblot analysis (C). Purified, recombinant MSD1 and MSD1/Y63 protein were separated by SDS-PAGE and blotted onto nitrocellulose membrane. Detection of nitrated Tyr residues was achieved using anti-NO$_2$–Tyr antibody.

that the ONOO$^-$-dependent inhibition was strongly reduced in a MSD1 mutant with Tyr63 replaced by phenylalanine, which cannot be nitrated. Tyr63 is located very close to the active centre of the enzyme (5.26 Å distance) in an amino acid sequence, which is also conserved in human MnSOD (Fig. 8A). Accordingly, the corresponding Tyr34 of human MnSOD is nitrated by ONOO$^-$ resulting in down-regulation of the enzymatic activity (MacMillan-Crow *et al.*, 1998; Yamakura *et al.*, 1998). It was proposed that a -NO$_2$ group at ortho-position of the aromatic ring further reduces the distance to the manganese-ion in the active centre (Fig. 8B), thereby affecting access and ligation of O$_2^-$ to the substrate binding pocket. Moreover, crystal structure analyses of human MnSOD revealed a network of hydrogen bonds in the direct environment of the active centre (Perry *et al.*, 2010). Tyr34 is part of this network that probably promotes the proton transfer onto a bond O$_2^-$ anion. Nitration of the Tyr residue followed by a decrease of its pKa-value would probably deprotonate the phenol ring system causing a decrease or disruption of the hydrogen bond network. Other possible consequences of Tyr34 nitration include electrostatic interference between the nitro group and the negatively charged substrate O$_2^-$ and a shift in the redox potential of the enzyme (Edwards *et al.*, 2001). The observed inactivation of *Arabidopsis* MSD1 by ONOO$^-$-mediated nitration of Tyr63 is probably based on a similar mechanism as described above for Tyr34 nitration of human MnSOD. However, it has to be mentioned that the activity of the MSD1 mutant (MSD1/Y63F) is still slightly inhibited by ONOO$^-$ (Fig. 7B), suggesting that probably also nitration of other tyrosine residues

affect MSD1 activity, although to a much smaller extent than nitration of Tyr63.

Previously, MnSODs of rice and potato were identified as targets for phosphorylation and oxidation, but an effect on the enzyme activity was not analysed (Bykova *et al.*, 2003; Kristensen *et al.*, 2004). It will be interesting to investigate whether Tyr nitration interferes with phosphorylation or oxidation events.

In comparison to MnSODs much less is known about the regulation of CSDs and FSDs by ONOO$^-$. *Arabidopsis* FSD3 shares 45% identity and 54% similarity in the amino acid sequence with MSD1 (Table 1). The structure is also similar between both SODs (Fig. 9). Moreover, Tyr82 of FSD3 is in the same conserved amino acid sequence as Tyr63 of MSD1 and Tyr34 of human MnSOD (Fig. 8A), all of which are located in a distance of only 5.25–5.40 Å from their active centre ion (Fig. 9). According to these sequence comparisons Tyr82 would be a good candidate regulatory site for inhibition of FSD3 by nitration. However, FSD1 and FSD2 possess the same conserved Tyr residue (Fig. 9) without being ONOO$^-$ sensitive. Small variations in sequence and/or protein conformation might explain the differences in ONOO$^-$ sensitivity amongst FSD isoforms as well as between FSD3 and MSD1. Alternatively, Tyr nitration of FSD3 correlates with but is not the cause of enzyme inhibition. CSDs are different from MSD1 and FSDs both in sequence as well as structure (Table 1 and Fig. 9). Amongst the three CSD isoforms of *Arabidopsis* only CSD3 has a Tyr residue. Our data demonstrate that Tyr115 is nitrated by ONOO$^-$ concomitant with a reduced enzyme activity. Notably, human recombinant CuZnSOD was shown to be inhibited by tryptophan rather than Tyr nitration (Yamakura

A

| hMnSOD | 30 | DLPYDYGALEPHINAQIMQLHHSKHHAAYVNNLNVTEEKYQ----EALAKGDVTAQIAL | 84 |
MSD1	35	DLPYDYGALEPAISGEIMQIHHQKHHQAYVTNYNNALEQLD----QAVNKGDASTVVKL	89
FSD1	15	PPPFALDALEPHMSKQTLEFHWGKHHRAYVDNLKKQVLGTE-LEGKPLEHIIHSTYNNG	72
FSD2	57	PPPYPLDALEPHMSRETLDYHWGKHHKTYVENLNKQILGTD-LDALSLEEVVLLSYNKG	114
FSD3	54	TPPYPLDALEPYMSRRTLEVHWGKHHRGYVDNLNKQLGKDDRLYGYTMEELIKATYNNG	112

B
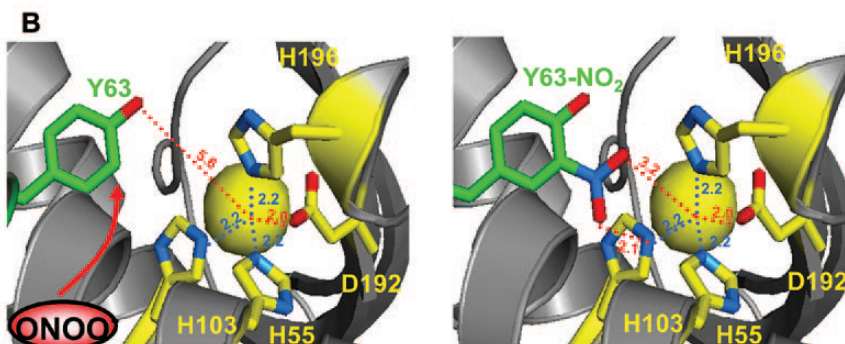
Fig. 8. Structural illustration of nitration of conserved Tyr63 of MSD1. (A) Alignment of amino acid sequences of *Arabidopsis* FSD isoforms, MSD1, and human MnSOD (Genbank accession number: CAA32502). Dashes: Introduced gaps to maximize sequence similarity. Tyr63 of MSD1 and the corresponding Tyr in FSD1 (Tyr43), FSD2 (Tyr85), FSD3 (Tyr82), and human MnSOD (Tyr34) are highlighted in red. (B) Part of the structural model of AtMSD1 showing the substrate binding pocket. The structural model of *Arabidopsis* MSD1 was generated using SWISS-MODEL with the crystal structure of *Caenorhabditis elegans* MnSOD as template (PDB code: 3DC6). Left: the substrate binding pocket is modelled with unmodified Tyr63 (left). The position where peroxynitrite attacks the aromatic ring system of Tyr63 is indicated with a red arrow. Right: the modelled substrate binding site is shown with nitrated Tyr63. Histidine and aspartate side chains are shown in yellow; the side chain of Tyr63 is marked in green. The distance of each side chain to the manganese ion within the active site is given.
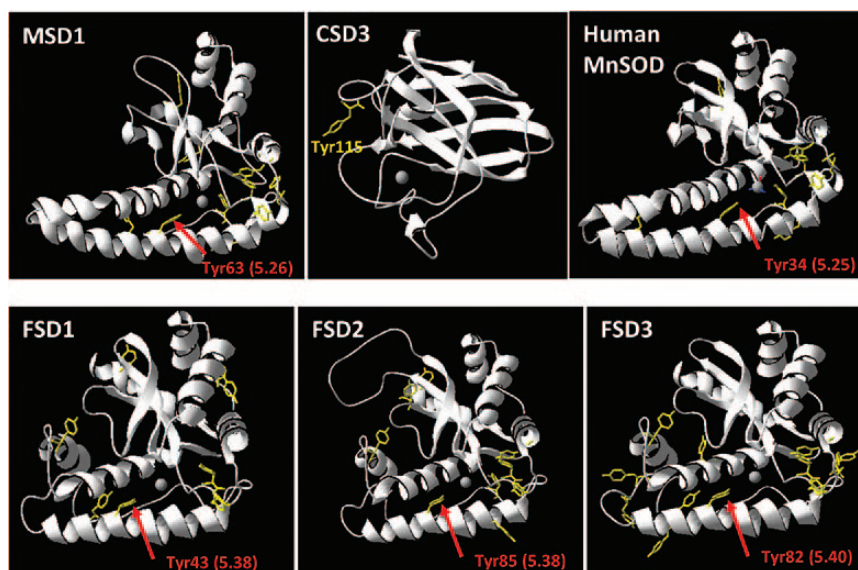

Fig. 9. Structural model of MSD1, CSD3, human MnSOD, FSD1, FSD2, and FSD3. The structural model of *Arabidopsis* SODs was generated using SWISS-MODEL with the crystal structure of *Caenorhabditis elegans* MnSOD as template (PDBcode: PDB 3DC6). The active site ion is shown in grey. All Tyr residues are highlighted in yellow. Tyr63 of MSD1 and the corresponding tyrosine residues in FSD1 (Tyr43), FSD2 (Tyr85), FSD3 (Tyr82), and human MnSOD (Tyr34) are marked with a red arrow. The distance to the active site ion is given in brackets. Tyr115 of CSD3 is indicated in yellow.

et al., 2001). The exact mechanism of differential inhibition of FSD3 and CSD3 but no other FSDs and CSDs remains to be deciphered in future studies using site-directed mutagenesis and structural analyses.

Our data imply that MSD1, CSD3, and FSD3 would be partially inhibited by Tyr nitration under stress conditions, which promote the formation of ONOO⁻. Studies with *Arabidopsis* lines altered in the expression of SOD isoforms

provide some hints on possible consequences of SOD inhibition. A detailed functional investigation of *Arabidopsis* FSDs revealed that chloroplastic FSD2 and FSD3 collaborate in ROS scavenging and chloroplast development (Myouga *et al.*, 2008). *fsd2-1 fsd3-1* double mutants showed an albino phenotype and were hypersensitive to oxidative stress induced by methyl viologen (Myouga *et al.*, 2008). By comparison, antisense lines of MSD1 displayed a disturbed redox homeostasis

primarily in the mitochondria but to some extent also in the cytosol (Morgan *et al.*, 2008). Importantly, the mitochondrial tricarboxylic acid cycle (TCA) was interrupted through inhibition of aconitase and isocitrate dehydrogenase activity. The transgenic lines were able to adapt and did not show a decrease in downstream respiratory CO_2 output (Morgan *et al.*, 2008). However, during short-term responses to stress, down-regulation of MSD1 might have transient but severe effects on mitochondrial TCA cycle, energy metabolism and redox homeostasis. For human kidney cells it was demonstrated that MnSOD inhibition by Tyr nitration induced irreversible oxidative injury of mitochondria during chronic rejection of human renal allografts (MacMillan-Crow *et al.*, 1996; MacMillan-Crow *et al.*, 1998).

In addition to their role in the antioxidant system SODs have relatively under-investigated functions in regulating the RNS composition and signalling. Interactions of free radicals such as O_2^- and NO are important under stress conditions (Gross *et al.*, 2013). Excessive levels of O_2^- during oxidative stress cause a limitation in NO bioavailability through formation of $ONOO^-$. SOD in turn competes with NO for O_2^- thereby preventing the formation of $ONOO^-$ while favouring the accumulation of NO. Peroxiredoxin II E (PrxIIE) is another emerging player in RNS homeostasis. This hydroperoxidase reduces peroxides to H_2O and the corresponding alcohol using reducing equivalents from glutaredoxin or thioredoxin (Dietz, 2003). Recently it was found that PrxIIE degrades $ONOO^-$ under normal growth conditions. However, after infection by an avirulent strain of *Pseudomonas syringae* PrxIIE was inhibited by *S*-nitrosylation of Cys121 resulting in $ONOO^-$ accumulation and increased Tyr nitration during the hypersensitive defence response (Gaupels *et al.*, 2011*b*; Romero-Puertas *et al.*, 2007). Combining the above pieces of information would suggest that elevated levels of NO in stressed WT *Arabidopsis* cause an inhibition of PrxIIE, accumulation of $ONOO^-$, and subsequently nitration-mediated inhibition of MSD1, CSD3, and FSD3. Down-regulation of the SODs would then lead to accumulation of O_2^-, which would further react with NO giving rise to even more $ONOO^-$ in the course of a self-amplification loop. On the other side elevated levels of NO might also result in *S*-nitrosylation of NADPH oxidase (Yun *et al.*, 2011), inhibiting its activity and blunting the production of O_2^-. In this way the self-amplification loop would be slowed down. It is noteworthy, that MSD1, FSD3, and CSD3 are localized in mitochondria, chloroplasts, and peroxisomes, respectively, which represent major sites of ROS and NO synthesis during stress responses (Gross *et al.*, 2013). In sum, the results of our *in vitro* study provide a biochemical framework for future research aimed at deciphering how the differential regulation of SODs is involved in stress signalling, defence, or cytotoxicity.

Supplementary data

Supplementary data are available at *JXB* online

References

Arasimowicz-Jelonek M, Floryszak-Wieczorek J. 2011. Understanding the fate of peroxynitrite in plant cells—from physiology to pathophysiology. *Phytochemistry* **72,** 681–688.

Astier J, Lindermayr C. 2012. Nitric oxide-dependent posttranslational modification in plants: an update. *International journal of molecular sciences* **13,** 15193–15208.

Bykova NV, Egsgaard H, Moller IM. 2003. Identification of 14 new phosphoproteins involved in important plant mitochondrial processes. *FEBS Letters* **540,** 141–146.

Dietz KJ. 2003. Plant peroxiredoxins. *Annual Review of Plant Biology* **54,** 93–107.

Edwards RA, Whittaker MM, Whittaker JW, Baker EN, Jameson GB. 2001. Outer sphere mutations perturb metal reactivity in manganese superoxide dismutase. *Biochemistry* **40,** 15–27.

Feechan A, Kwon E, Yun BW, Wang Y, Pallas JA, Loake GJ. 2005. A central role for *S*-nitrosothiols in plant disease resistance. *Proceedings of the National Academy of Sciences, USA* **102,** 8054–8059.

Foyer CH, Noctor G. 2009. Redox regulation in photosynthetic organisms: signaling, acclimation, and practical implications. *Antioxidants and Redox Signaling* **11,** 861–905.

Gaupels F, Kuruthukulangarakoola GT, Durner J. 2011a. Upstream and downstream signals of nitric oxide in pathogen defence. *Current Opinion in Plant Biology* **14,** 707–714.

Gaupels F, Spiazzi-Vandelle E, Yang D, Delledonne M. 2011b. Detection of peroxynitrite accumulation in *Arabidopsis* thaliana during the hypersensitive defense response. *Nitric Oxide* **25,** 222–228.

Gross F, Durner J, Gaupels F. 2013. Nitric oxide, antioxidants and prooxidants in plant defence responses. *Frontiers in Plant Science* **4,** 419.

Hill BG, Dranka BP, Bailey SM, Lancaster JR, Jr., Darley-Usmar VM. 2010. What part of NO don't you understand? Some answers to the cardinal questions in nitric oxide biology. *The Journal of Biological Chemistry* **285,** 19699–19704.

Huang CH, Kuo WY, Weiss C, Jinn TL. 2012. Copper chaperone-dependent and -independent activation of three copper-zinc superoxide dismutase homologs localized in different cellular compartments in *Arabidopsis*. *Plant Physiology* **158,** 737–746.

Kliebenstein DJ, Monde RA, Last RL. 1998. Superoxide dismutase in *Arabidopsis*: an eclectic enzyme family with disparate regulation and protein localization. *Plant Physiology* **118,** 637–650.

Kovacs I, Lindermayr C. 2013. Nitric oxide-based protein modification: formation and site-specificity of protein *S*-nitrosylation. *Frontiers in Plant Science* **4,** 137.

Kristensen BK, Askerlund P, Bykova NV, Egsgaard H, Moller IM. 2004. Identification of oxidised proteins in the matrix of rice leaf mitochondria by immunoprecipitation and two-dimensional liquid chromatography-tandem mass spectrometry. *Phytochemistry* **65,** 1839–1851.

Laemmli UK. 1970. Cleavage of structural proteins during the assembly of the head of bacteriophage T4. *Nature* **227,** 680–685.

Landy A. 1989. Dynamic, structural, and regulatory aspects of lambda site-specific recombination. *Annual Review of Biochemistry* **58,** 913–949.

Leitner M, Vandelle E, Gaupels F, Bellin D, Delledonne M. 2009. NO signals in the haze: nitric oxide signalling in plant defence. *Current Opinion of Plant Biology* **12,** 451–458.

Lin A, Wang Y, Tang J, Xue P, Li C, Liu L, Hu B, Yang F, Loake GJ, Chu C. 2012. Nitric oxide and protein *S*-nitrosylation are integral to hydrogen peroxide-induced leaf cell death in rice. *Plant Physiology* **158,** 451–464.

Lindermayr C, Fliegmann J, Ebel J. 2003. Deletion of a single amino acid residue from different 4-coumarate:CoA ligases from soybean results in the generation of new substrate specificities. *Journal of Biological Chemistry* **278,** 2781–2786.

MacMillan-Crow LA, Crow JP, Kerby JD, Beckman JS, Thompson JA. 1996. Nitration and inactivation of manganese superoxide dismutase in chronic rejection of human renal allografts. *Proceedings of the National Academy of Sciences, USA* **93,** 11853–11858.

MacMillan-Crow LA, Crow JP, Thompson JA. 1998. Peroxynitrite-mediated inactivation of manganese superoxide dismutase involves nitration and oxidation of critical tyrosine residues. *Biochemistry* **37,** 1613–1622.

Madamanchi NR, Donahue JL, Cramer CL, Alscher RG, Pedersen K. 1994. Differential response of Cu,Zn superoxide dismutases in two pea cultivars during a short-term exposure to sulfur dioxide. *Plant Molecular Biology* **26,** 95–103.

McCord JM. 2001. Analysis of superoxide dismutase activity. *Current Protocols in Toxicology* doi: 10.1002/0471140856.tx0703s00

McCord JM, Fridovich I. 1969. Superoxide dismutase. An enzymic function for erythrocuprein (hemocuprein). *Journal of Biological Chemistry* **244,** 6049–6055.

Mittler R, Vanderauwera S, Suzuki N, Miller G, Tognetti VB, Vandepoele K, Gollery M, Shulaev V, Van Breusegem F. 2011. ROS signaling: the new wave? *Trends in Plant Science* **16,** 300–309.

Morgan MJ, Lehmann M, Schwarzlander M *et al.* 2008. Decrease in manganese superoxide dismutase leads to reduced root growth and affects tricarboxylic acid cycle flux and mitochondrial redox homeostasis. *Plant Physiology* **147,** 101–114.

Mur LA, Mandon J, Persijn S, Cristescu SM, Moshkov IE, Novikova GV, Hall MA, Harren FJ, Hebelstrup KH, Gupta KJ. 2013. Nitric oxide in plants: an assessment of the current state of knowledge. *AoB plants* **5,** pls052.

Myouga F, Hosoda C, Umezawa T, Iizumi H, Kuromori T, Motohashi R, Shono Y, Nagata N, Ikeuchi M, Shinozaki K. 2008. A heterocomplex of iron superoxide dismutases defends chloroplast nucleoids against oxidative stress and is essential for chloroplast development in *Arabidopsis*. *The Plant Cell* **20,** 3148–3162.

Perry JJ, Shin DS, Getzoff ED, Tainer JA. 2010. The structural biochemistry of the superoxide dismutases. *Biochimica et Biophysica Acta* **1804,** 245–262.

Radi R. 2013. Protein tyrosine nitration: biochemical mechanisms and structural basis of functional effects. *Accounts of Chemical Research* **46,** 550–559.

Romero-Puertas MC, Laxa M, Matte A, Zaninotto F, Finkemeier I, Jones AM, Perazzolli M, Vandelle E, Dietz KJ, Delledonne M. 2007. *S*-nitrosylation of peroxiredoxin II E promotes peroxynitrite-mediated tyrosine nitration. *The Plant Cell* **19,** 4120–4130.

Scheler C, Durner J, Astier J. 2013. Nitric oxide and reactive oxygen species in plant biotic interactions. *Current Opinion in Plant Biology* **16,** 534–539.

Sehrawat A, Abat JK, Deswal R. 2013. RuBisCO depletion improved proteome coverage of cold responsive *S*-nitrosylated targets in Brassica juncea. *Frontiers in Plant Science* **4,** 342.

Studier FW. 2005. Protein production by auto-induction in high density shaking cultures. *Protein Expression and Purification* **41,** 207–234.

Surmeli NB, Litterman NK, Miller AF, Groves JT. 2010. Peroxynitrite mediates active site tyrosine nitration in manganese superoxide dismutase. Evidence of a role for the carbonate radical anion. *Journal of the American Chemical Society* **132,** 17174–17185.

Szabo C, Ischiropoulos H, Radi R. 2007. Peroxynitrite: biochemistry, pathophysiology and development of therapeutics. *Nature Reviews Drug Discovery* **6,** 662–680.

Tanou G, Job C, Rajjou L, Arc E, Belghazi M, Diamantidis G, Molassiotis A, Job D. 2009. Proteomics reveals the overlapping roles of hydrogen peroxide and nitric oxide in the acclimation of citrus plants to salinity. *The Plant Journal* **60,** 795–804.

Yamakura F, Matsumoto T, Fujimura T, Taka H, Murayama K, Imai T, Uchida K. 2001. Modification of a single tryptophan residue in human Cu,Zn-superoxide dismutase by peroxynitrite in the presence of bicarbonate. *Biochimica and Biophysica Acta* **1548,** 38–46.

Yamakura F, Taka H, Fujimura T, Murayama K. 1998. Inactivation of human manganese-superoxide dismutase by peroxynitrite is caused by exclusive nitration of tyrosine 34 to 3-nitrotyrosine. *Journal of Biological Chemistry* **273,** 14085–14089.

Yun BW, Feechan A, Yin M, Saidi NB, Le Bihan T, Yu M, Moore JW, Kang JG, Kwon E, Spoel SH, Pallas JA, Loake GJ. 2011. *S*-nitrosylation of NADPH oxidase regulates cell death in plant immunity. *Nature* **478,** 264–268.

Nitric oxide, antioxidants and prooxidants in plant defence responses

*Felicitas Groß , Jörg Durner and Frank Gaupels **

German Research Center for Environmental Health, Institute of Biochemical Plant Pathology, Helmholtz-Zentrum München, Munich, Germany

In plant cells the free radical nitric oxide (NO) interacts both with anti- as well as prooxidants. This review provides a short survey of the central roles of ascorbate and glutathione—the latter alone or in conjunction with S-nitrosoglutathione reductase—in controlling NO bioavailability. Other major topics include the regulation of antioxidant enzymes by NO and the interplay between NO and reactive oxygen species (ROS). Under stress conditions NO regulates antioxidant enzymes at the level of activity and gene expression, which can cause either enhancement or reduction of the cellular redox status. For instance chronic NO production during salt stress induced the antioxidant system thereby increasing salt tolerance in various plants. In contrast, rapid NO accumulation in response to strong stress stimuli was occasionally linked to inhibition of antioxidant enzymes and a subsequent rise in hydrogen peroxide levels. Moreover, during incompatible *Arabidopsis thaliana-Pseudomonas syringae* interactions ROS burst and cell death progression were shown to be terminated by S-nitrosylation-triggered inhibition of NADPH oxidases, further highlighting the multiple roles of NO during redox-signaling. In chemical reactions between NO and ROS reactive nitrogen species (RNS) arise with characteristics different from their precursors. Recently, peroxynitrite formed by the reaction of NO with superoxide has attracted much attention. We will describe putative functions of this molecule and other NO derivatives in plant cells. Non-symbiotic hemoglobins (nsHb) were proposed to act in NO degradation. Additionally, like other oxidases nsHb is also capable of catalyzing protein nitration through a nitrite- and hydrogen peroxide-dependent process. The physiological significance of the described findings under abiotic and biotic stress conditions will be discussed with a special emphasis on pathogen-induced programmed cell death (PCD).

Keywords: nitric oxide, reactive oxygen species, signaling, peroxynitrite, glutathione, ascorbate, antioxidant system, programmed cell death

INTRODUCTION

Exposure of plants to abiotic and biotic stress can cause a deregulation, over-flow or even disruption of electron transport chains (ETC) in mitochondria and chloroplasts. Under these conditions molecular oxygen (O_2) acts as an electron acceptor giving rise to the accumulation of reactive oxygen species (ROS). Singlet oxygen ($^1O_2$), the hydroxyl radical (OH), the superoxide radical (O_2^-) and hydrogen peroxide (H_2O_2) are all strongly oxidizing compounds and therefore potentially harmful for cell integrity. Among them, H_2O_2 is the most stable ROS being formed in the reaction of $^1O_2$ with O_2^- and as a product of spontaneous dismutation of O_2^- (Foyer and Noctor, 2009).

During evolution, land plants have developed sophisticated measures for controlling ROS levels amongst others by the antioxidant system or—as named after their discoverers—Foyer-Halliwell-Asada cycle (**Figure 1**) (Buchanan et al., 2002; Foyer and Noctor, 2009). Central elements of the system are the two redox couples ascorbate (AsA)/dehydroascorbate (DHA) and glutathione (GSH)/glutathione disulfide (GSSG). In the detoxification part of the antioxidant system superoxide dismutase (SOD) converts O_2^- to O_2 and H_2O_2. The latter then can be degraded by catalase (CAT), ascorbate peroxidase (APX) and several other enzymes (**Figure 1**). In the course of H_2O_2 degradation by APX AsA is oxidized to monodehydroascorbate (MDHA) and DHA. AsA and GSH can also directly be oxidized by ROS, although with slower kinetics. In the regeneration pathway MDHA reductase (MDHAR), DHA reductase (DHAR) and glutathione reductase (GR) recycle the antioxidants from their oxidized back to the reduced form. MDHAR and GR use NADPH as a reducing equivalent whereas DHAR uses GSH (**Figure 1**).

However, apart from being toxic by-products of energy metabolism, ROS have also essential functions in primary and secondary metabolism, development, and stress responses. For instance, H_2O_2 acts as a signal in the regulation of stomatal closure and serves as a substrate of peroxidases during cell wall synthesis and fortification (Neill et al., 2008; O'brien et al., 2012). To date, O_2^- and H_2O_2 are the best studied ROS, mainly because of well-established detection techniques. During signaling processes, ROS arises from the ETC but are also enzymatically produced by various peroxidases and oxidases (Foyer and Noctor, 2009; Mittler et al., 2011). Here, we will assign the term prooxidants for ROS and ROS-producing enzymes and the term antioxidants
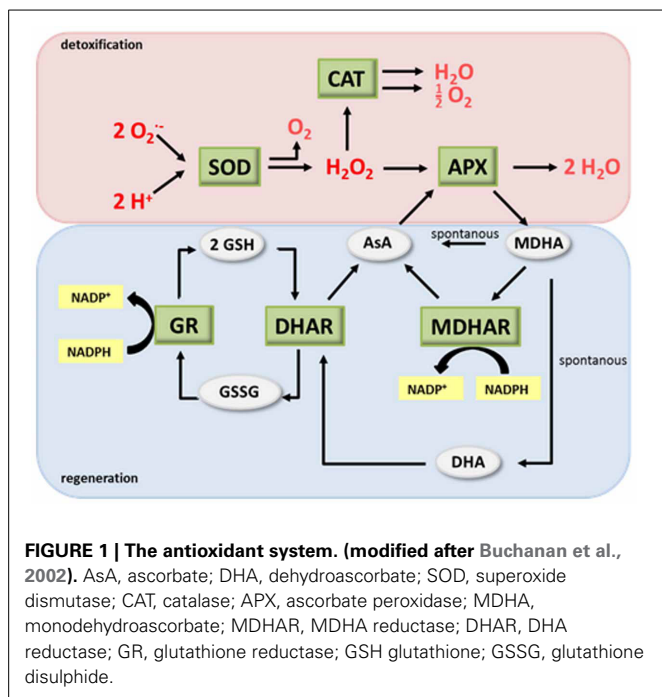
FIGURE 1 | The antioxidant system. (modified after Buchanan et al.,
2002). AsA, ascorbate; DHA, dehydroascorbate; SOD, superoxide
dismutase; CAT, catalase; APX, ascorbate peroxidase; MDHA,
monodehydroascorbate; MDHAR, MDHA reductase; DHAR, DHA
reductase; GR, glutathione reductase; GSH glutathione; GSSG, glutathione
disulphide.

for elements of the antioxidant system. During stress signaling, the redox homeostasis of plant cells is tightly controlled. Antioxidants modulate timing and extent of ROS accumulation and additionally function as signals by their own rights. ROS levels increase either by up-regulation of prooxidant enzyme activity, (de−) regulation of electron flow or down-regulation of the antioxidant system. Redox signals are probably transduced by oxidation of proteins such as ROS-activated transcription factors and kinases (Foyer and Noctor, 2009; Mittler et al., 2011). Also other molecules including lipids and fatty acids are modified by ROS with implications for their signaling functions (Farmer and Mueller, 2013).

Similar to ROS, NO is a small redox signal with versatile chemistry. It is a relatively stable radical but rapidly reacts with other radicals including ROS (Hill et al., 2010). Products of these reactions are reactive nitrogen species (RNS) such as the nitrosonium cation (NO^+), the nitroxyl anion (NO^-) and higher oxides of NO including $ONOO^-$, NO_2, and N_2O_3. RNS have chemical properties different from their precursors and may trigger specific physiological responses. Like ROS, NO is an important messenger in many physiological processes. It is a stress signal involved in plant responses to high salt, excess light, cold, heat, ozone, UV-B and various pathogens (Leitner et al., 2009; Gaupels et al., 2011a; Mur et al., 2013). Despite the ever-growing importance of NO in plant research, only little is known about enzymatic sources and molecular receptors of NO. Best characterized is the role of NO in stomatal closure and pathogen defence (Mur et al., 2013). In both processes, NO interacts with H_2O_2 without exact molecular mechanisms deciphered.

The aim of this review is to summarize current knowledge on the interaction of NO with ROS and the antioxidant system in plant stress responses. We will explore how NO can

chemically react with pro- and antioxidants and how NO might regulate activity and expression of pro- and antioxidant enzymes. Additionally, functions of non-symbiotic hemoglobins, SOD, GSNOR and peroxiredoxins in regulating RNS homeostasis will be discussed. The last section of this review will detail the roles of individual NO and redox messengers in signaling during stress-induced programmed cell death (PCD).

MANIPULATION OF THE NO LEVEL HAS AN IMPACT ON THE ANTIOXIDANT SYSTEM

The relevance of NO in stress-induced redox signaling was repeatedly investigated by treatment of plants with NO donors before or during exposure to abiotic stress conditions (Hasanuzzaman et al., 2010; Saxena and Shekhawat, 2013). **Table 1** summarizes selected literature reporting the impact of NO donor treatment on H_2O_2 level, antioxidants and activity of antioxidant enzymes in stressed plants. The authors studied 14 different plant species, 11 stressors, and 6 different NO donors providing a comprehensive overview of the current literature on this topic. A common effect of all stress treatments was the accumulation of H_2O_2 often accompanied by an increase in malondialdehyde (MDA) levels pointing to ROS-dependent oxidation of lipids. In 19 of the 23 studies activities of all or at least some of the analyzed antioxidant enzymes were up-regulated. These data suggest that stress causes accumulation of ROS, which may then trigger enhancement of the antioxidant defence system.

Most of the published studies demonstrated accumulation of NO under stress conditions (Hasanuzzaman et al., 2010; Saxena and Shekhawat, 2013). However, results given in **Table 1** as well as other data imply that NO cannot be considered to be a general stress signal. For instance, comparing the effect of 25 μM arsenic between two studies, NO production was induced in *Festuca arundinaceae* but decreased in *Oryza sativa* (**Table 1**) (Singh et al., 2009; Jin et al., 2010). During plant responses to cadmium stress, NO was increased or decreased acting as inducer or inhibitor of stress tolerance, depending on plant species and experimental setup (Arasimowicz-Jelonek et al., 2011a). Moreover, iron deficiency triggered NO signaling in *Arabidopsis thaliana* (Chen et al., 2010) but repressed basal NO synthesis in *Zea mays* (**Table 1**) (Kumar et al., 2010). In this context it is interesting that recent studies revealed NO being a modulator rather than an essential signal in the adaptation of *A. thaliana* to iron deficiency (Meiser et al., 2011). Together, these findings demonstrate that the link between stress perception and NO signaling is seemingly rather indirect whereas stress can directly cause ROS accumulation by disturbing the mitochondrial and plastidic ETC. Further studies are needed for investigating the biological background of the observed species-specific differences in NO regulation under stress conditions. In sum, the above findings support the notion that endogenous NO is often but not always involved in stress tolerance.

Exogenous NO always improved abiotic stress tolerance concomitant with a decrease in H_2O_2 and MDA levels (**Table 1**). This held true, even when endogenous NO was down-regulated, implying that the tested NO donors do not necessarily mimic functions of NO under natural conditions. In the displayed 23 studies, NO treatments either reversed the stress-induced decline

Table 1 | NO donors induce stress tolerance by effecting on the antioxidant properties of plant tissues.

Stress[a]	NO donor	Plant species	Stress effect[c]			Impact of NO donor treatment on abiotic stress-induced changes in antioxidant properties[d]										References
			H2O2	NO	Antiox. enz.	H2O2	MDA	Glutathione	Ascorbate	SOD	CAT	APX	DHAR	MDHAR	GR	
50 mM NaCl	0.05 mM SNP	*Hordeum vulgare*	+		+	↓	↓			↑	↑	↑				Li et al., 2008
150, 300 mM NaCl	1 mM SNP	*Triticum aestivum*	+		=	↓	↓	↑			↑	↔	↑	↑	↑	Hasanuzzaman et al., 2011
150 mM NaCl	0.2 mM SNP	*Brassica juncea*	+		+	↓	↓			↓	↓	↓			↑	Khan et al., 2012
150 mM NaCl	0.01 mM DETA/NO	*Zea mays*	+	+	+	↓	↓	↑	↑			↑	↑		↑	Keyster et al., 2012
100 mM NaCl	0.2 mM SNP	*Cicer arietinum*			+		↓			↓	↑	↑	↔		↓	Sheokand et al., 2008
Drought (less water)	0.05–0.15 mM SNP	*Oryza sativa*	+		−	↓	↓			↑	↑	↑				Farooq et al., 2009
Drought (10% PEG)	0.1 mM SNP	*Zea mays*	+		+	↓				↑[e]		↑			↑	Sang et al., 2007
Drought (15% PEG)	0.2 mM SNP	*Triticum aestivum*	+		+	↓	↓			↑	↔					Tian and Lei, 2006
0.25, 0.5 mM arsenic	0.25 mM SNP	*Triticum aestivum*	+		±	↓	↑	↑	↑		↑	↔	↑	↑	↑	Hasanuzzaman and Fujita, 2013
0.025 mM arsenic	0.1 mM SNP	*Festuca arundinacea*	+	+	+	↓	↓			↑	↑	↑				Jin et al., 2010
0.025, 0.05 mM arsenic	0.05 mM SNP	*Oryza sativa*	+	−	+	↓	↓			↓	↓	↓				Singh et al., 2009
0.050 mM copper	0.1 mM SNP	*Panax ginseng*	+	+	−	↓	↓	↑	↔	↑	↑	↑			↑	Tewari et al., 2008
0.025 mM cadmium	5 mM SNP	*Brassica juncea*	+	+	+		↓	↓		↓	↓	↓				Verma et al., 2013
5 mM cadmium	0.1 mM SNP	*Oryza sativa*	+		+	↓	↓	↑	↑	↓	↓	↓			↓	Hsu and Kao, 2007
0.5 mM cadmium	0.1 mM SNP	*Helianthus annuus*			±	↓	↑	↓		↓	↓				↓	Laspina et al., 2005
0.01 mM Fe-EDTA	0.01, 0.1 mM SNP	*Zea mays*	+	−	−	↓	↑	↓		↓	↑	↑				Kumar et al., 2010
0.025 mM paraquat	SIN-1, Asc/NaNO2[b]	*Oryza sativa*			+		↓			↑	↑				↑	Hung et al., 2002
0.8–4 mg L^{-1} diquat	0.1 mM SNP	*Solanum tuberosum*	+		±	↓	↓			↔	↑					Beligni and Lamattina, 2002
15 μmol m^{-2} s^{-1} UV-B	0.1 mM SNP	*Phaseolus vulgaris*	+		+	↓		↑		↑	↑	↑				Shi et al., 2005
0.6 W m^{-2} s^{-1} UV-B	1 mM SNP	*Spirulina platensis*		+	+		↓			↑	↑					Xue et al., 2007
High light	0.1 mM SNP	*Festuca arundinacea*	+		+	↓	↓			↑	↑	↑			↑	Xu et al., 2010
Desiccation of seeds	100 ppm NO gas	*Antiaris toxicaria*	+		+	↓						↑	↑	↑	↑	Bai et al., 2011
Chilling of seeds	0.03 mM NOC-18	*Baccaurea ramiflora*	+		+	↓			↑			↑	↑	↑	↑	Bai et al., 2012

[a] *Drought stress was induced either by reduced watering or treatment with polyethylene glycol (PEG). 0.01 mM Fe-EDTA causes iron deficiency. Paraquat and diquat are herbicides.*

[b] *0.1 mM SIN-1 or 0.1mM ascorbate (Asc)/0.2 mM NaNO$_2$ was used as NO donors.*

[c] *Stress-induced changes in H$_2$O$_2$ and NO levels as well as antioxidant enzyme activities (general tendency).*

[d] *Comparison of combined stress and NO treatment with stress alone treatment. Metabolites are high-lighted. All other parameters represent enzyme activities.*

[e] *Regulation of chloroplastic SOD activity; cytosolic SOD was not influenced by NO donor treatment.*

Arrows indicate up-, down- or no regulation. $+, -, \pm$ *and* $=$ *indicate up-, down-, differential- or no regulation.*

or even further amplified up-regulation of the antioxidant system. NO donors never caused a down-regulation of antioxidant enzymes as compared to untreated control plants. For instance, salt stress stimulated SOD, CAT, and APX activities, and this effect was enhanced by SNP co-treatment, whereas copper uptake repressed the same enzymes in *Panax ginseng*, which was prevented by SNP (**Table 1**) (Li et al., 2008; Tewari et al., 2008). Again the same enzyme activities were enhanced after arsenic poisoning of *O. sativa* but SNP application prevented this stress effect (**Table 1**) (Singh et al., 2009). These findings were explained by NO acting either (I) as a direct scavenger of ROS or (II) inducer of the antioxidant system. In the first case NO would take over functions of the antioxidant system and thereby prevent its activation, like e.g. in arsenic-exposed rice as described above. In the second case NO would trigger antioxidant gene expression or activate antioxidant enzymes e.g., by posttranslational modifications. Previously, NO donors were reported to repress antioxidant enzyme activities. Particularly, SNP inhibited APX and CAT, decreased GSH/GSSG ratio and induced PCD in Arabidopsis suspension cultured cells (Murgia et al., 2004a). However, the research summarized in **Table 1** was focussed on investigating mechanisms of NO-mediated stress tolerance. Therefore, NO donors were probably applied in such a way as to prevent any severe stress or damage to the plants although sometimes up to 5 mM SNP was used. We will discuss later in this review the dose dependent effects of NO on the antioxidant system and cell death initiation.

A direct chemical interaction of NO with ROS is only possible if cells or plant parts are being loaded with active NO donor solution from start of the stress treatment until sampling as was the case for *Spirulina platensis* cells exposed to UV-B and SNP and *Brassica junceae* leaf discs incubated in salt and DETA/NO donors (**Table 1**) (Xue et al., 2007; Khan et al., 2012). In other studies, however, measurements were done after NO donors were exhausted suggesting that NO released from the donor did not have a direct influence on ROS levels but might be rather involved in the induction of signaling events controlling the cellular redox status. Farooq et al. (2010) reported that imbibition of seeds in SNP solution rendered adult rice plants more tolerant to drought stress. Hence, NO pre-treatment could induce a primed state, which prepares plants to respond more efficiently to future stress episodes (Conrath, 2011). Alternatively, NO treatment itself could impose stress to the plants acting as the priming stimulus. Exogenous NO might also induce synthesis of endogenous NO, which then can exert signaling or scavenger functions even long after the NO donor is exhausted.

NO donors can have undesired side-effects on the plant's physiology. Therefore, NO accumulating transgenic and mutant plant lines were used for assessing the involvement of NO in development and stress signaling. Transgenic *Nicotiana tabacum* and *A. thaliana* expressing the rat neuronal nitric oxide synthase (NOS) behind a 35S promoter accumulated high levels of NO concomitant with developmental defects and altered stress resistance (Chun et al., 2012; Shi et al., 2012). 35S::nNOS lines of Arabidopsis constitutively expressed pathogenesis related (PR) genes, which correlated with enhanced pathogen resistance toward virulent *Pseudomonas syringae DC3000* (Shi et al., 2012).
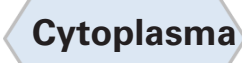
These plants also had improved salt and drought tolerance due to reduced stomatal aperture, and were delayed in flowering. The H_2O_2 content was not determined, but MDA levels were found to be lowered. By comparison, nNOS-expressing tobacco showed growth retardation and constitutive inhibition of CAT, which caused an increase in H_2O_2 levels (Chun et al., 2012). Probably as a consequence of high NO and H_2O_2 levels, these plants developed spontaneous lesions, strongly elevated salicylic acid (SA) levels and PR gene expression. Reduced growth, increased oxidative stress and spontaneous lesions was not observed in nNOS expressing *A. thaliana* plants indicating that they either were less sensitive to NO or accumulated lower levels of NO than the corresponding tobacco transgenic lines.

Collectively, the discussed research argues for ROS being a general stress signal whereas NO signaling depends on the plant species and stress conditions investigated. It can be speculated that NO or the interaction between ROS and NO adds some degree of specificity to the stress signaling by ROS alone. Treatment of plants with NO donors caused a decrease in stress-induced ROS levels and a concomitant enhancement of abiotic stress tolerance. In this process NO might act as a scavenger of ROS or as a signal stimulating the antioxidant potential and/or a primed state of stress defence. Interpretation of the data is complicated by the fact that most of the studies are rather descriptive without exploring the underlying signaling cascades. Moreover, the biological significance of some observed weak effects of NO on ROS and the antioxidant system is ambiguous because slight changes in the cellular redox status could be just a stress marker.

SOURCES AND CELLULAR LOCALIZATION OF NO AND ROS PRODUCTION

NO and certain ROS cooperate in stress signaling, which is partly independent of their respective production sites because both molecules are supposed to be mobile intra- as well as intercellularly (Foyer and Noctor, 2009; Frohlich and Durner, 2011). Therefore, apoplastic sources can contribute to NO and ROS signal transduction within the cell (**Table 2**). Important ROS producing enzymes are the members of the NADPH oxidase family (NOX or Respiratory burst oxidase homolog, RBOH). These plasma membrane-associated enzymes synthesize O_2^- in the apoplast through transfer of electrons from NADPH to molecular oxygen (Mittler et al., 2011). A rapid ROS burst, frequently observed during plant responses to pathogen infection, is usually mediated by the NOX isoforms D and F (Torres et al., 2002). Further oxidases and cell wall-associated peroxidases are present in the apoplast but their roles in stress responses are less well-defined. In comparison to ROS only little is known about NO formation in the extracellular space (**Table 2**). At the acidic pH of the apoplast exogenous NO_2^- was non-enzymatically reduced to NO, which was accelerated by AsA and phenolics (Bethke et al., 2004). The pathway has been investigated in the barley aleuron layer but might occur also in other tissues. A stress-induced NO burst derived from this spontaneous reaction seems only feasible if NO_2^- levels could be rapidly up-regulated, which has not been observed so far. NO_2^- could also be reduced to NO by a membrane-associated nitrite:NO reductase (NiNOR) as described for tobacco (Stöhr et al., 2001). However, NiNOR

Table 2 | Localization of NO and ROS sources in plant cells.

	NO sources	ROS sources
Chloroplast	Nitric oxide synthase–like activity Photosynthetic ETC dependent nitrite reduction	Photosynthetic ETC –ROS production at photosystem I & II $^1O_2$ production by triplet state chlorophyll
Peroxisome	Nitric oxide synthase–like activity *Nitrite reduction by xanthine oxidoreductase*	Photorespiration Fatty acid β-oxidation Xanthine oxidase Flavin oxidase
Mitochondria	Respiratory ETC dependent nitrite reduction *Nitric oxide synthase–like activity*	Respiratory ETC –ROS production at complexI, II & III
Cytoplasma	Nitrite reduction by nitrate reductase	Plasma membrane associated quinone oxidase
Apoplast	Spontanous nitrite reduction at acidic pH Plasma-membrane bound nitrite reductase (root specific–NO release to apoplast) *Polyamineoxidase*	Plasma membrane associated NADPH oxidase (ROS release into apolast) Cell wall associated peroxidase Amine oxidase Oxalate oxidase

ETC, electron transport chain. NO sources under debate are given in italics.

cannot be considered a major player in NO signaling because it is exclusively present in roots functioning in the regulation of NO_3^- uptake. Copper amine oxidase 1 (CuAO1) is another candidate enzyme involved in NO synthesis (Wimalasekera et al., 2011). The *A. thaliana* cuao1 mutant is impaired in polyamine- and abscisic acid-induced NO production. The molecular background underlying this interesting phenotype is still unknown.

Cellular compartments simultaneously producing NO and ROS might be focal points of stress signaling (**Table 2**). While chloroplasts and mitochondria are major sources of ROS from photosynthetic and respiratory ETC these organelles are also capable of NO synthesis, one proposed mechanism being the transfer of electrons from the ETCs to NO_2^- by a nitrite: NO-reductase activity. Such ETC-dependent NO formation was observed in isolated choroplasts from tobacco supplied with 25–100 μM NO_2^- and in mitochondria of tobacco suspension cells under anoxia (Planchet et al., 2005; Jasid et al., 2006). More work is needed for investigating if this pathway is active also in stress responses under normoxic conditions. Mammalian NOS oxidizes arginine to citrulline and NO. Although NOS-like activity is considered the most important source of NO accumulation in plant reactions to various stresses the corresponding plant NOS still awaits identification (Leitner et al., 2009; Mur et al., 2013). Recent publications reported on the detection of a NOS-like activity in chloroplasts (Jasid et al., 2006; Tewari et al., 2013). In *A. thaliana* and *Brassica napus* protoplasts NO generation was highest immediately after the isolation procedure and decreased during culture. Experiments with a NOS activity assay

and specific enzyme inhibitors suggested that NO originated from a NOS-like source. Moreover, simultaneous accumulation of NO and ROS resulted in the formation of $ONOO^-$ as detected by the fluorescent dye aminophenyl fluorescein (APF) (Tewari et al., 2013). In line with this, treatment with the fungal elicitor cryptogein also triggered rapid accumulation of both NO and ROS in tobacco epidermal cells (Foissner et al., 2000). The above data imply that stress induces the accumulation of ROS and RNS in the chloroplast, which could then locally effect on photosynthesis or diffuse out of the chloroplast to other cellular compartments.

To date, there is no convincing proof of NOS-like activity in mitochondria (**Table 2**; Gupta et al., 2011). In contrast, peroxisomes are a source of NO both during salt stress as well as developmental processes such as lateral root growth (Corpas et al., 2009; Schlicht et al., 2013). In *A. thaliana* transgenic lines expressing GFP linked to peroxisomal targeting signal 1 (PTS1) fluorescence of the NO-specific dye diaminorhodamine co-localized with GFP fluorescence in the peroxisomes. Isolated peroxisomes displayed NOS-like activity, which was calcium dependent and could be inhibited by NOS inhibitors (**Table 2**). 100 mM NaCl stimulated NO synthesis in peroxisomes, which spread into the cytosol, where it probably contributed to $ONOO^-$ formation and protein tyrosine nitration (Corpas et al., 2009). Peroxisomes are active sites of ROS scavenging as well as formation. The main function of peroxisomes is the removal of ROS originating from photosynthetic and mitochondrial ETCs. For this purpose, peroxisomes contain large amounts of CAT but also APX and other antioxidant enzymes. However, after a stress stimulus antioxidant

enzymes can be down-regulated possibly by S-nitrosylation or nitration rendering peroxisomes a ROS source rather than a sink (Sandalio et al., 2013). Peroxisomes are often closely associated with mitochondria and/or chloroplasts. Such functional units are essential for efficient ROS scavenging but it can be speculated that they also represent "reaction vessels" for enhancing ROS/RNS signal interaction.

In the past, microscopic studies with NO-specific dyes suggested higher stress-induced NO accumulation in chloroplasts and peroxisomes than in the cytoplasm (e.g., Foissner et al., 2000; Gaupels et al., 2008; Corpas et al., 2009). One possible explanation for this finding would be that the cytoplasm has a rather low capacity of NO synthesis. While NOS-like activity was not detected, nitrate reductase (NR) is the only confirmed NO source in the cytoplasm (**Table 2**). However, under normal growth conditions NR preferably reduces NO_3^- to NO_2^-, which is then further reduced by nitrite reductase to NH_4^+. Only under special conditions such as anoxia when NO_2^- reaches high levels NR reduces NO_2^- to NO at considerable rates (Gupta et al., 2011; Mur et al., 2013). For this reason, it seems unlikely that NR significantly contributes to rapid stress signaling by NO. Overall, chloroplasts and peroxisomes are probably the most important sources of NO and ROS during stress responses. Available data indicate that both signal molecules are produced simultaneously giving rise to the formation of RNS such as $ONOO^-$. ROS mainly originated from NADPH oxidases and ETCs. The NO burst was driven by a yet unidentified NOS-like activity in chloroplasts and peroxisomes. Nitrite reduction to NO either non-enzymatically or by various reductases is thought to contribute comparably less to the NO burst.

INTERACTIONS BETWEEN NO AND ROS

Chemical interactions between NO and ROS influence concentration, composition and signaling functions of both reaction partners. For instance, H_2O_2 was proposed to react with NO yielding $^1O_2$ and NO^- *in vitro* (Noronha-Dutra et al., 1993). If this chemical pathway occurs *in vivo* is still ambiguous since NO is a rather stable radical, which does not easily bind nonradical species such as H_2O_2. Physiologically more significant is the fusion of NO with O_2^- to give $ONOO^-$ (**Table 3**) (Hill et al., 2010). This radical-radical reaction has a high rate constant and is favored instead of O_2^- dismutation to H_2O_2. As a result, highly cytotoxic and long-lived ROS are replaced by $ONOO^-$, which is short-lived in the cellular environment (Pryor et al., 2006). The exact pathway of $ONOO^-$ and ONOOH (peroxynitrous acid) decay to NO_2^- and NO_3^- at neutral pH is still debated (**Table 3**). It was suggested that ONOOH isomerises to NO_3^- and H^+ either directly or indirectly via the radical intermediates NO_2 and OH (Goldstein and Merenyi, 2008; Koppenol et al., 2012). The peroxynitrite anion on the other hand yields the RNS NO_2, NO, and N_2O_3 during its degradation to NO_2^- (Goldstein and Merenyi, 2008). At neutral pH $ONOO^-$ and ONOOH are both present in cells and together form peroxynitrate (O_2NOO^-/O_2NOOH), which decays to NO_2^- and O_2 as well as $^1O_2$ and NO^- (Khan et al., 2000; Jourd'heuil et al., 2001; Gupta et al., 2009; Miyamoto et al., 2009). Meanwhile it is widely accepted that CO_2 is an important modulator of $ONOO^-$ chemistry in cells. The atmospheric gas

Table 3 | Reaction stoichiometry between ROS and RNS.

ROS	RNS
Hydrogen peroxide: H_2O_2	Nitric oxide: NO
Superoxide: O_2^-	Peroxynitrite: $ONOO^-$
Singlet oxygen: $^1O_2$	Peroxynitrous acid: ONOOH
Hydroxyl radical: OH	Peroxynitrate: O_2NOO^-
Oxygen: O_2	Peroxynitric acid: O_2NOOH
	Nitrosonium cation: NO^+
	Nitroxyl anion: NO^-
	Nitrogen dioxide: NO_2
	Dinitrogentrioxide: N_2O_3
	Nitrosoglutathione: GSNO

REACTION STOICHIOMETRY	References
$NO_2^- + 2\,H^+ \leftrightarrow NO + H_2O$	Pryor et al., 2006
$NO^+ + H_2O_2 \rightarrow ONOO^- + 2\,H^+$	Beligni and Lamattina, 2002
$NO + O_2^- \rightarrow ONOO^-$	Miyamoto et al., 2009
$2\,NO + O_2 \rightarrow 2\,NO_2$	Moller et al., 2007
$NO_2 + NO \leftrightarrow N_2O_3$	Moller et al., 2007
$N_2O_3 + H_2O \rightarrow 2\,NO_2^- + 2\,H^+$	Moller et al., 2007
$ONOOH \rightarrow ONOO^- + H^+$ (Ionisation)	Koppenol et al., 2012
$ONOOH \rightarrow NO_3^- + H^+$ (Isomerisation)	Koppenol et al., 2012
$ONOOH \rightarrow NO_2 + HO$ (Homolysis)	Koppenol et al., 2012
$ONOO^- \rightarrow NO + O_2^-$ (Homolysis)	Koppenol et al., 2012
$O_2NOO^- \leftrightarrow NO_2 + O_2^-$ (Homolysis)	Gupta et al., 2009
$ONOOH + ONOO^- \rightarrow O_2NOO^- + NO_2^- + H^+$	Gupta et al., 2009
$CO_2 + ONOO^- \rightarrow CO_3^- + NO_2$	Pryor et al., 2006

rapidly reacts with $ONOO^-$ resulting in NO_3^- and the radicals NO_2 and CO_3^- (carbonate anion radical Bonini et al., 1999; Pryor et al., 2006).

High levels of NO can react with O_2 giving rise to the NO_2 radical (**Table 3**). This pathway is slow in the cytosol but might be efficient in membrane-rich cellular compartments such as chloroplasts and mitochondria owing to the lipophilic nature of NO and O_2 (Liu et al., 1998; Pryor et al., 2006). Under continuous NO production NO_2 will further react to N_2O_3 (Pryor et al., 2006; Moller et al., 2007). All reactive nitrogen oxides decompose to the stable derivatives NO_2^- and NO_3^- within cells. However, as described in the previous section, under acidic conditions e.g., in macrophages and in the plant apoplast N_2O_3, NO, and NO^+ can also originate from NO_2^- upon enzymatic or non-enzymatic reduction (**Table 3**) (Pryor et al., 2006; Combet et al., 2010; Frohlich and Durner, 2011). Hence, dependent on the prevailing cellular environment NO and ROS can interact resulting in the formation of intermediates with distinct molecular properties. For instance, NO, NO^-, NO^+, and N_2O_3 bind to nucleophilic residues of proteins causing nitrosation (covalently bound nitroso/-NO adduct) and cysteine- as well as metal S-nitrosylation (coordinate nitrosyl/··NO adduct) (Hill et al., 2010; Fukuto and Carrington, 2011). In contrast, $ONOO^-$ and the NO_2 radical are involved in oxidation and nitration (covalently bound nitro/-NO_2 adduct) of proteins the best studied modifications being 3-nitro-tyrosine residues (Arasimowicz-Jelonek and Floryszak-Wieczorek, 2011; Gaupels et al., 2011a;

Radi, 2013). NO_2 has less nitrating power than $ONOO^-$ except with protein radicals, which result from the reaction of proteins with ROS or CO_3^- radicals (Bonini et al., 1999; Pryor et al., 2006). To date, the CO_3^- catalyzed binding of NO_2 to tyrosyl residues is thought to be the major route of protein nitration.

NO-dependent protein modifications are reversible, which is important for efficient recovery of NO receptors during stress signaling. In mammalian cells, thioredoxins (TRX) denitrosylate proteins (Tada et al., 2008; Benhar et al., 2009). Recently, the central redox switch NPR1 was suggested to be denitrosylated by TRX-h-3 and -5 during incompatible *A. thaliana/P. syringae* interactions, which caused its monomerisation from oligomers, transfer into the nucleus and subsequent induction of PR genes (Tada et al., 2008). However, the exact mechanism of NPR1 regulation by S-nitrosylation and TRX is still debated (Lindermayr et al., 2010). Denitration of proteins in *A. thaliana* is probably mediated by peptide methionine sulfoxide reductase (PMSR) under normal growth conditions since *pmsr2-1* mutants displayed elevated protein nitration in the night (Bechtold et al., 2009). This enzyme reduces oxidized protein methionine residues using TRX as a co-substrate but how it can function as a denitratase is not yet resolved. Future research will uncover if additional reductases, peroxiredoxin oxidases and peroxidases such as TRX peroxidase are involved in stress signaling by NO-dependent protein modifications.

Apart from proteins many other molecules can be nitrated including lipids, fatty acids, amino acids and nucleotides (Arasimowicz-Jelonek and Floryszak-Wieczorek, 2011). Recently, 8-nitro-cGMP was uncovered as a down-stream signal of ABA, NO, and ROS in inducing stomatal closure at daytime, whereas cGMP regulated stomatal opening at night (Joudoi et al., 2013). 8-nitro-cGMP is now a prime example of how NO, ROS, and cGMP can be integrated in one signaling cascade triggering a physical response.

NO AND ROS INFLUENCE EACH OTHER'S BIOSYNTHESIS AND DEGRADATION

ROS are well-known inducers of NO synthesis in various plant species, plant parts and tissues. For example, treatment with 100 μM H_2O_2 triggered NO synthesis in roots of *A. thaliana*, which was used in a screen for identification of mutants defective in NO accumulation. This way, the prohibitin PHB3 was uncovered as a regulatory element of ABA- and auxin-induced NO signaling (Wang et al., 2010). Moreover, H_2O_2 elicited a rapid NO burst in guard cells of mung bean leaves (*Phaseolus aureus*) (Lum et al., 2002) as well as NOS activity along with PCD in tobacco BY-2 cells (De Pinto et al., 2006). The interplay between ROS, NO and the antioxidant system will be discussed in more detail in the last section of this review. Exposure to ozone (O_3) led to high ROS levels and rapid NO production in the leaves of *A. thaliana* plants (Ahlfors et al., 2009). During the O_3 response NO acted as a signal in the onset of the hypersensitive response (HR) and in the regulation of defence-related genes thereby interacting with jasmonic acid (JA), ethylene and SA. In the phloem of *Vicia faba* NO accumulation upon treatment with 10 and 100 μM H_2O_2 was dependent on Ca^{2+} and NOS-like enzyme activity (Gaupels et al., 2008). Although induction of NO biosynthesis through H_2O_2 and

Ca^{2+} is widely accepted, exact signaling cascades and enzymatic sources of NO are still not well-understood. Effects of H_2O_2 on NO scavenging enzymes such as GSNOR and hemoglobins were not yet investigated.

NO is not just a down-stream signal of H_2O_2 but was also reported to influence ROS production and degradation, which hints at complex feed-back regulation between both signal molecules. NO limits ROS accumulation for instance by inhibition of the ROS producing enzyme NADPH oxidase (Yun et al., 2011). After infection of *A. thaliana* with avirulent pathogens the elevated SNO content inhibited the NADPH oxidase isoform AtRBOHD by S-nitrosylation at Cys 890. According to the author's hypothesis this regulatory process constrains ROS accumulation and subsequent cell death progression (Yun et al., 2011). A means of enhancing antioxidant enzyme activities is the induction of the corresponding genes by NO. Accordingly, 2D-electrophoresis and Western blot analyses revealed that pretreatment with the NO donor SNAP further increased the Al^{3+}-induced protein levels and activities of APX, SOD, and GR, whereas NOS inhibitor and cPTIO suppressed both the Al^{3+} and the SNAP effect (Yang et al., 2013). Alternatively, NO could directly modify protein functions. In *Antiaris toxicaria* NO fumigation improved desiccation tolerance of recalcitrant seeds, which correlated with a decrease in H_2O_2 levels. The authors proposed that S-nitrosylation enhanced the activities of the antioxidant enzymes GR, APX, and DHAR by preventing their oxidation/carbonylation during desiccation (Bai et al., 2011). Moreover, in salt stressed *B. juncea* S-nitrosylation of a Fe-SOD caused an increase in its enzyme activity (Sehrawat et al., 2013).

More commonly, however, NO was associated with inhibition rather than activation of antioxidant enzymes. *In vitro*, tobacco APX and CAT were reversibly inhibited by GSNO, SNAP, and NOC-9 but irreversibly inactivated by SIN-1 (Clark et al., 2000). Inhibition of APX and CAT by NO donors was confirmed in isolated pea mitochondria, leaves of *Pelargonium peltatum* and suspension cultured cells of *A. thaliana* and *N. tabacum* (Murgia et al., 2004a; Arasimowicz-Jelonek et al., 2011b; Marti et al., 2013). SNP and SNAP were the most effective NO donors, whereas GSNO produced variable results. The chemical properties of the donors is an important issue because SNP releases NO^+ and SIN-1 simultaneously O_2^- and NO whereas most other donors deliver NO. Thus, dependent on the NO donor used and the prevailing redox conditions antioxidant enzyme activity could be affected due to oxidation, S-nitrosylation, nitrosation or nitration. Unfortunately, NO- and ROS-dependent protein modifications were not investigated in the above studies.

Any of the enzymes APX, SOD, MDHAR, DHAR, GR, and CAT was proposed to be S-nitrosylated and/or tyrosine nitrated *in vivo* in unstressed *A. thaliana*, salt-stressed citrus (*Citrus aurantium*), GSNO-treated potato or rice injected with H_2O_2 for eliciting cell death (Tanou et al., 2009, 2010; Fares et al., 2011; Kato et al., 2012; Lin et al., 2012). S-nitrosylation, however, was only confirmed for APX from GSNO-treated potato leaves (Kato et al., 2012). In the same study DHAR was demonstrated to be S-nitrosylated and inhibited by NO. A possible target Cys essential for enzymatic function was revealed by point mutation of candidate Cys residues. Human manganese SOD is

a mitochondrial protein that undergoes site-specific nitration at Tyr34 during inflammation. Inactivation of Mn-SOD by nitration provokes oxidative stress and ultimately dysfunction of mitochondria (Radi, 2013). It would be interesting to elucidate if plant SODs are targets of nitrating species with possible roles e.g., in PCD. Collectively, the discussed data suggest that APX, CAT, and DHAR are good candidates for NO-regulated antioxidant enzymes in plants. A systematic approach is needed for deciphering, which antioxidant enzymes are controlled by NO under stress conditions, and what are the underlying molecular mechanisms.

We mentioned before that NO bioactivity has been implicated both in increased as well as decreased antioxidant enzyme activities and ROS levels. One way of explaining the contradictory findings is based on the hypothesis that NO has a dose-dependent effect on the cellular redox status (**Figure 2**) (Thomas et al., 2008). At low concentrations NO might stimulate the antioxidant system and promote cell survival while high concentrations of NO cause severe cell damage and even death. In this model trace NO would preferably react with nucleophiles such as lipids, DNA and metal centered proteins but also with oxygen species forming oxidizing and nitrating species including $ONOO^-$ and NO_2. Little damage and NO-induced signaling will be perceived by the cell triggering antioxidant defence and repair mechanisms. Profound NO production, on the other hand, would promote secondary reactions of NO_2 and $ONOO^-$ with NO and consequently the accumulation of N_2O_3. This would shift conditions in the cell from weak oxidative stress toward heavy nitrosative stress, which—according to the hypothesis of Thomas et al. (2008)—inflicts severe damage ultimately leading to cell death. For some biological effects the duration of NO production is decisive because certain target molecules bind NO very slowly or need sequential NO and

FIGURE 2 | Hypothetical model on the dynamic interaction between NO, ROS and the antioxidant system under stress conditions. Weak stress triggers a moderate elevation of ROS (reactive oxygen species) and NO levels. ROS act as signals inducing NO synthesis and activation of the antioxidant system for improved metabolic adaptation. If ROS is produced at a somewhat higher rate than NO there would be mainly formation of oxidizing and nitrating RNS (reactive nitrogen species) imposing a weak oxidative stress to the cell. Heavy stress leads to a strong ROS and RNS burst. High NO levels promote formation of N_2O_3 from NO_2 and NO and consequently nitrosative stress. Under these conditions ROS and RNS inhibit the antioxidant system causing damage and ultimately death of plant cells.

ROS modifications (Thomas et al., 2008). Thus, in addition to the chemical environment of the cell, which defines the RNS/ROS composition, the extent of NO production is critical in shaping stress signaling by NO.

INTERACTIONS BETWEEN NO AND ANTIOXIDANTS

The versatility of signaling by RNS and ROS is further extended by their interaction with antioxidants. Reduced ascorbate does not react with NO but with nitrosating species NO^+, N_2O_3 and with S-nitrosothiols (Scorza et al., 1997; Kytzia et al., 2006). Consequently, NO is released and AsA is converted to DHA (Combet et al., 2010). DHA spontaneously decays to the ascorbyl radical, which can combine with NO to give O-nitrosoascorbate. The latter finally undergoes hydrolysis to ascorbate and NO_2^- (Kytzia et al., 2006). AsA can also scavenge $ONOO^-$ with rather slow kinetics at neutral pH but rapid kinetics at pH 5.8 yielding NO_2^- and NO_3^- via unknown intermediates (Kurz et al., 2003). Likewise, GSH affects $ONOO^-$ levels either by reduction to NO_2^- or by radical-radical interactions of NO_2 with the glutathiyl radical resulting in the formation of nitroglutathione $GSNO_2$, which in turn can release NO (Balazy et al., 1998). Moreover, GSH effectively prevents $ONOO^-$ mediated tyrosine nitration by re-reducing tyrosyl radicals and catalysing the formation of non-nitrating O_2NOO^- from NO_2 and O_2^- (Kirsch et al., 2001). The biological significance of the above proposed pathways of $ONOO^-$ degradation remains to be investigated. However, the high concentrations of GSH and AsA in plant cells could contribute to maintaining low levels of NO derivatives under non-stress conditions.

Other known plant scavengers of $ONOO^-$ include gamma-tocopherol (vitamin E; Desel et al., 2007), carotenoids and the flavonoids ebselen, epicatechin and quercetin (Haenen et al., 1997). Some of the above compounds are not specific for $ONOO^-$ but scavenge NO and ROS, too. Recently, cytokinins were demonstrated to be involved in controlling NO levels in *A. thaliana* (Liu et al., 2013). Continuous root-uptake of $120\,\mu M$ SNP severely inhibited growth of *A. thaliana* WT plants whereas the mutant line cnu-1/amp1 was resistant to the same NO treatment. Further characterization of the mutant revealed a correlation between NO resistance and elevated cytokinin levels. Accordingly, WT plants infiltrated with the cytokinin zeatin displayed improved growth on SNP-loaded agar medium. *In vitro*, zeatin was nitrated by peroxynitrite, which produced 8-nitro-zeatin. *In vivo*, SNP caused strong accumulation of 8-nitro-zeatin in cnu-1 as compared to WT. From these results, the authors concluded that cytokinins regulate NO levels by binding the NO derivative $ONOO^-$ (Liu et al., 2013).

NO interacts with glutathione in various ways. At the transcriptional level SNP and GSNO stimulated genes involved in GSH synthesis causing elevated levels of total glutathione in *Medicago truncatula* roots (Innocenti et al., 2007). Accordingly, NO donor treatment triggered an increase in total glutathione in 8 of 10 studies summarized in **Table 1**. In contrast, SNP had no strong effect on GSH concentrations in tobacco BY-2 cells (De Pinto et al., 2002). At the level of chemical interactions GSH binds NO by S-nitrosylation. GSNO is formed either after (1) ROS-induced accumulation of glutathiyl radicals, which bind NO with
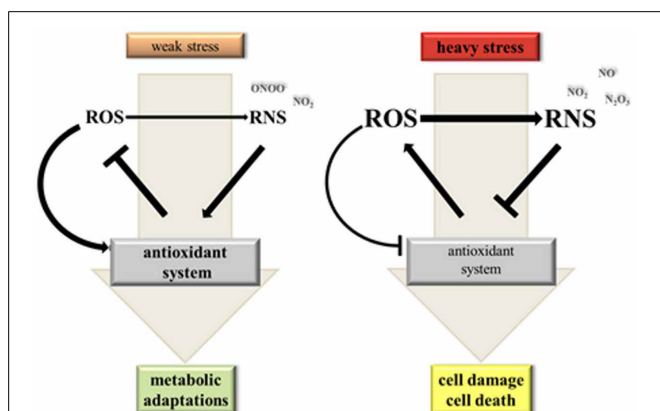
rate constants near the diffusion-controlled limit (Madej et al., 2008) or after (2) S-nitrosylation of GSH by nitrogen oxides such as NO^+ and N_2O_3 (Broniowska et al., 2013). GSNO then functions as storage and transport form of NO. It is regarded as an endogenous NO donor, which releases free NO (2 GSNO → 2 NO + GSSG) or S-nitrosylates proteins by transferring the nitroso adduct (Broniowska et al., 2013; Mur et al., 2013).

ENZYMATIC REGULATION OF NO HOMEOSTASIS BY GSNOR, HEMOGLOBIN AND PRO- AS WELL AS ANTIOXIDANT ENZYMES

Levels of the S-nitrosylated tripeptide GSNO are tightly controlled by the enzyme GSNOR. This GSH-dependent formaldehyde dehydrogenase catalyzes the transformation of GSNO to GSSG and hydroxylamine (NH_2NO) in the presence of GSH and NADH as the reducing species (**Figure 3**) (Liu et al., 2001; Sakamoto et al., 2002). In *A. thaliana* silencing or mutation of *GSNOR1* caused accumulation of S-nitrosothiols, NO and NO_3^- indicating that the corresponding enzyme is a major player in NO homeostasis (Sakamoto et al., 2002). *GSNOR1* deficient plants were severely affected in growth and development (Kwon et al., 2012). They also showed increased resistance to the herbicide paraquat and altered responses toward heat stress and pathogen infection (Diaz et al., 2003; Feechan et al., 2005; Rusterucci et al., 2007; Lee et al., 2008; Chen et al., 2009; Holzmeister et al., 2011). In addition to control of NO levels, GSNOR is also indirectly involved in protein denitrosylation because GSNO and S-nitrosylated proteins are in equilibrium (Benhar et al., 2009; Malik et al., 2011). For more information on GSNOR functions refer to recent reviews (Leitner et al., 2009; Gaupels et al., 2011a; Mur et al., 2013). In mammalian/human cells CuZn-SOD and GPX (glutathione peroxidase) were proposed to use GSNO as a substrate and might act in protein denitrosylation without physiological functions being well-established yet (Benhar et al., 2009).

Another upcoming topic is the modulation of NO homeostasis by plant hemoglobins. Class-1 Hb1 catalyse the turnover

of NO to NO_3^- thereby influencing growth, development and stress responses (**Figure 3**) (Hill et al., 2010; Hebelstrup et al., 2012). Particularly, the role of alfalfa and *A. thaliana* Hb1 in hypoxia has been studied in more detail (Dordas et al., 2003; Perazzolli et al., 2004; Hebelstrup et al., 2012). It was shown that hypoxia triggered expression of the Hb1-coding gene in roots, probably for confining the stress-induced accumulation of NO. Reduced expression of *Hb1* in transgenic and mutant lines caused an increase in NO levels concomitant with decreased plant growth whereas *Hb1* over-expression improved plant fitness during hypoxia. By scavenging NO the plant might suppress a costly defence response for saving energy and valuable nitrogen under limited oxygen availability (Hebelstrup et al., 2012). Recently, Hb1 was found to be involved in pathogen resistance. *A. thaliana* mutants defective in the Hb1-coding gene *GLB1* were more resistant to the hemibiotrophic *P. syringae* and the necrotrophic fungus *Botrytis cinerea* (Mur et al., 2012). The mutant phenotype was reversed by over-expression of *GLB1* under control of the 35S promoter. The enhanced resistance in the *glb1* mutant correlated with accumulation of SA, JA, and ET. *GLB1* was down-regulated in WT plants during infection, which probably facilitated the induction of defence responses by NO accumulation.

Notably, human hemoglobin degrades $ONOO^-$ to NO_3^- *in vitro* further extending possible functions of hemoglobins in NO signaling (Romero et al., 2003). By comparison plants have evolved efficient mechanisms for enzymatic detoxification of $ONOO^-$ by thiol-dependent peroxidases. The *A. thaliana* peroxiredoxin IIE (PrxII E) and glutathione peroxidase 5 (Gpx5) of poplar both reduce $ONOO^-$ to NO_2^- (**Figure 3**) (Sakamoto et al., 2003; Romero-Puertas et al., 2008; Ferrer-Sueta and Radi, 2009). Both enzymes are then reactivated by thioredoxin in a NADPH-consuming manner. Hence, thioredoxin functions include ROS and $ONOO^-$ scavenging as well as protein denitrosylation illustrating again the essential roles of this enzyme in ROS and RNS control.

At neutral (but not acidic) pH NO_2^- is a rather stable decomposition product of NO and its derivatives. However, a number of plant enzymes can convert NO_2^- to RNS most prominent examples being nitrite reductase and nitrate reductase, which reduce NO_2^- to NO (Stöhr et al., 2001; Morot-Gaudry-Talarmain et al., 2002; Gupta et al., 2011). During severe hypoxia deoxygenated *A. thaliana* Hb1 might act as nitrite reductase although with rather slow kinetics (Tiso et al., 2012). Given the high concentrations of NO_2^- in hypoxic plant tissues Hb1 might still significantly contribute to NO accumulation (Sturms et al., 2011). A more widespread phenomenon could be the nitration-promoting activity of peroxidases. For instance, three *A. thaliana* hemoglobins and Hb1 of *Medicago sativa* were capable of mediating protein nitration via NO_2^- oxidation to NO_2 by a H_2O_2-dependent peroxidase activity (Sakamoto et al., 2004; Maassen and Hennig, 2011). Sakihama et al. (2003) demonstrated the enzymatic nitration of *p*-coumaric acid by action of horseradish peroxidase in the presence of NO_2^- and H_2O_2. All the above data on Hb1 acting as nitrite reductase and enzymatic nitration by peroxidases were obtained *in vitro* and it is difficult to draw any meaningful conclusions for the *in vivo* situation.

FIGURE 3 | Enzymatic regulation of NO homeostasis by (1) S-nitrosogutathione reductase (GSNOR), (2) hemoglobin (Hb), and (3) peroxiredoxin IIE (PrxIIE). PrxIIE is reduced by thioredoxin (Trx).

$$(1) \quad GSNO + GSH \xrightarrow{\text{GSNOR}} GSSG + NH_2OH$$

NADH → NAD$^+$

NADPH → NADP$^+$

Hb(Fe^{2+}) → Hb(Fe^{3+})

$$(2) \quad NO + O_2 \longrightarrow NO_3^-$$

NADPH → NADP$^+$

Trx$_{red}$ → Trx$_{ox}$

PrxII$_{red}$ → PrxII$_{ox}$

$$(3) \quad ONOO^- \longrightarrow NO_2^- + H_2O$$
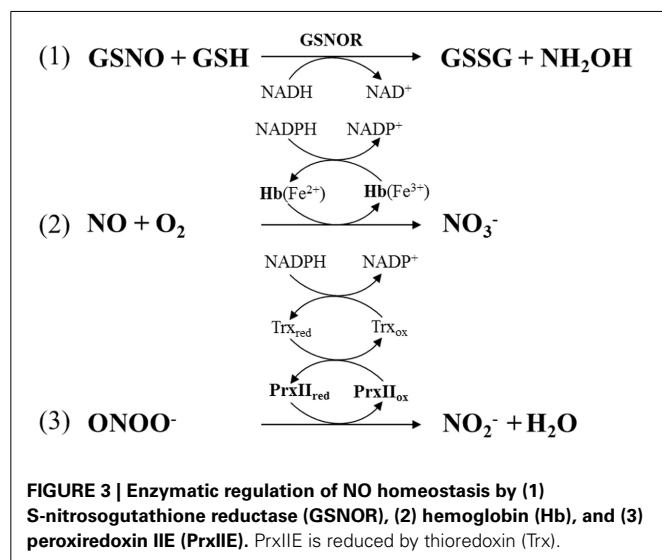
NO AND REDOX SIGNALING IN CELL DEATH

ROS and RNS are major players in plant stress signaling. In this section we will survey current knowledge on the roles of ROS, RNS and elements of the antioxidant system in cell death events induced by biotic and abiotic stressors. Plant PCD was described as a genetically controlled cell suicide exhibiting marked similarities but also considerable differences to apoptosis in animal/human cells (Mur et al., 2008; De Pinto et al., 2012). Plants attacked by an avirulent pathogen develop HR, which is a defence mechanism for restricting the spread of pathogens by cell wall reinforcement, production of defensive secondary metabolites and ultimately cell death (Mur et al., 2008).

Almost 20 years ago Chris Lamb and his co-workers discovered that soybean cells infected with avirulent *Pseudomonas syringae pv. glycinea* accumulated high levels of H_2O_2, which functioned as a cell death inducer during the HR (Levine et al., 1994). Suppression of the pathogen-induced H_2O_2 burst by the NADPH oxidase inhibitor diphenylene iodonium (DPI) prevented cell death whereas low millimolar concentrations of exogenous H_2O_2 triggered HR-PCD in a calcium-dependent manner (Levine et al., 1994, 1996). Later, researchers of the same group demonstrated that NO was another essential messenger in cell death execution (Delledonne et al., 1998). Application of a NO scavenger and a NOS activity inhibitor both reduced HR-PCD of soybean suspension cells infected with avirulent bacterial pathogens. Importantly, SNP triggered cell death most efficiently in conjunction with ROS but not in the presence of DPI or CAT. ROS donors in turn efficiently killed soybean cells only if applied together with SNP (Delledonne et al., 1998). Comparable results were obtained with tobacco BY-2 cells. Simultaneous application of SNP and the H_2O_2-generating donor system glucose/glucose oxidase but not each individual donor alone caused a drop in ascorbate and glutathione levels, inhibition of APX and consequently PCD of tobacco BY-2 cells (De Pinto et al., 2002). Therefore, it was postulated that NO and ROS cooperate in cell death signaling (**Figure 2**).

Recent studies have begun to unravel the underlying modes of interactions between NO, ROS and the antioxidant system during PCD. It was shown that $ONOO^-$ arose in *A. thaliana* plants challenged by avirulent *Pseudomonas syringae* (Gaupels et al., 2011b). The peak of $ONOO^-$ formation from NO and O_2^- coincided with the onset of the PCD. In unstressed plants $ONOO^-$ was continuously scavenged by PrxIIE, which was inhibited by S-nitrosylation in course of the HR (Romero-Puertas et al., 2007). The fact that $ONOO^-$ levels are controlled in a sophisticated manner would imply an important role of this RNS in the induction of cell death and pathogen resistance. However, contrary to mammalian cells this RNS does not kill plant cells (Delledonne et al., 2001). It was demonstrated that SOD, GR, CAT, and APX, which are all involved in ROS depletion, can be tyrosine nitrated by $ONOO^-$ (Chaki et al., 2009; Lozano-Juste et al., 2011). If this is a significant process *in vivo* remains to be proven.

H_2O_2 rather than O_2^- was proposed to be a pivotal signal in regulating PCD. This particular ROS acts as an inducer of NO synthesis in tobacco cells (De Pinto et al., 2006) and in mutant plants with disturbed redox homeostasis. For instance, rice knock-out mutants defective in a CAT-coding gene showed increased H_2O_2 levels, nitrate reductase-dependent accumulation of NO and spontaneous leaf cell death (Lin et al., 2012). Application of the NO scavenger PTIO mitigated the cell death phenotype. The importance of a down-regulation of ROS detoxifying enzymes during PCD was further corroborated by the finding that overexpression of thylakoidal APX led to a higher resistance against SNP induced cell death (Murgia et al., 2004b). In *A. thaliana* WT plants 5mM SNP triggered H_2O_2 accumulation and cell death, which was both reduced in the transgenic line probably because H_2O_2 was degraded by the elevated APX activity in these plants. The antioxidant enzymes CAT and APX control H_2O_2 levels under mild stress conditions. Severe cadmium stress triggered NO as well as H_2O_2 accumulation and senescence-like PCD of *A. thaliana* suspension cultured cells (De Michele et al., 2009). However, co-treatment with the NOS inhibitor L-NMMA prevented the NO-dependent inhibition of CAT and APX, which in turn reduced H_2O_2 levels and increased cell viability under cadmium stress.

Mechanical wounding provokes cell damage, which could serve as a point of entry into the plant e.g., for pathogenic bacteria. To avoid this, PCD is triggered in intact cells nearby the damaged cells for sealing the wound site. In wounded leaves of *Pelargonium peltatum* NO accumulation was restricted to the site of injury (Arasimowicz et al., 2009). Treatment with cPTIO confirmed that NO inhibited APX and CAT activity thereby temporarily enhancing the H_2O_2 content at the edge of the wound. Pre-treatment of leaves with NO donors before wounding prevented the H_2O_2 burst and reduced necrotic cell death in sweet potato (Lin et al., 2011). The exact mechanism of NO action was not determined but available data suggest that APX, GR, MDHAR and thioredoxin are S-nitrosylated during PCD, which could affect their activity (Murgia et al., 2004b; Lin et al., 2012). Inhibition of GR and MDHAR would also impact on the redox status of the glutathione and ascorbate pools. It should be considered that enzymatic activity can also be influenced by ROS-dependent modifications, which was proposed for oxidation-triggered inhibition of APX (**Figure 2**) (De Pinto et al., 2006). The latter enzyme was also suppressed in gene expression during PCD (De Pinto et al., 2006).

The role of NO in incompatible interactions between *A. thaliana* and avirulent *Pseudomonas syringae* was investigated using transgenic plant lines expressing a bacterial NO dioxygenase (NOD, flavohemoglobin) (Zeier et al., 2004). NOD expression attenuated the pathogen-induced NO accumulation. As a consequence the H_2O_2 burst was diminished and transgenic plants developed less HR-PCD and were delayed in SA-dependent *PR1* expression. These results support again the hypothesis that high levels of NO amplify redox signaling during PCD by inhibiting the plant antioxidant machinery (Zeier et al., 2004). NO and H_2O_2 might mutually enhance each other's accumulation by positive feed-back regulation. To this end, NO and ROS producing enzymes as well as elements of the antioxidant system must be regulated in a highly coordinate fashion for initiation of PCD. The exact signaling pathways remain to be deciphered in future studies.

However, the plant must also constrain stress signaling by NO, ROS and the antioxidant system for avoiding excessive damage by

runaway cell death. Therefore, it is worth mentioning that both ROS as well as NO were found to induce genes involved in cell protection such as a gene coding for glutathione S-transferase (Levine et al., 1994). Yun and colleagues (Yun et al., 2011) even demonstrated inhibition of the ROS-producing enzyme AtRBOHD by NO in *A. thaliana* challenged by avirulent bacteria. The authors proposed a model, in which the early burst of ROS and NO initiates HR-PCD but at later stages of the defence response the SNO levels exceed a certain threshold and subsequently the AtRBOHD is inactivated by S-nitrosylation at Cys 890, which terminates the HR. In contrast to R gene-mediated resistance against avirulent pathogens, bacterial lipopolysaccharides (LPS) elicit basal pathogen resistance without onset of HR-PCD. LPS-induced NO synthesis by an arginine-dependent enzymatic source even protected plant cells against oxidative stress and cell death by enhancing the activities of CAT, SOD, and POD. The changed cellular redox status contributed to the regulation of NPR1-dependent expression of defence genes (Sun et al., 2012). In sum, NO can either act as an inducer or suppressor of plant PCD dependent on its local cellular levels and its tightly controlled interaction with ROS and elements of the antioxidant system (**Figure 2**).

CONCLUDING REMARKS

ROS and NO are increasingly recognized signaling molecules in plant physiology. While research on ROS has a long history NO came into focus only 15 years ago. In the present paper we reviewed recent literature dealing with the interaction between ROS, NO and the antioxidant system during stress defence. As one interesting outcome we found that exposure of plants to unfavorable conditions inevitably induced ROS but not necessarily NO accumulation. ROS can arise as a toxic by-product of disturbed energy metabolism and/or can be produced for signaling purposes. In contrast, NO is rather a highly specialized second messenger, which modifies ROS signaling or acts independently of ROS. Significantly, ROS and NO bursts are often triggered simultaneously—sometimes even in the same cellular compartment. Particularly chloroplasts and peroxisomes are hotspots of NO-ROS interactions. NO, ROS and antioxidants chemically react resulting in the formation of RNS such as $ONOO^-$, NO_2, N_2O_3, and GSNO. More indirect interactions include induction of NO synthesis by H_2O_2 and accumulation of ROS due to inhibition of antioxidant enzymes by NO-dependent protein modifications. Uncontrolled self-amplification of ROS/RNS signaling might provoke nitrosative stress and ultimately PCD. Therefore, plants have developed efficient measures for controlling NO levels by GSNOR, hemoglobins and other RNS scavenging enzymes. This review was also aimed at investigating the extreme versatility of possible reactions between NO, ROS and the antioxidant system. Many of the discussed findings originate from *in vitro* systems or animal/human models. More basic research is urgently needed for defining chemical reactions and their products actually occurring *in planta*.

ACKNOWLEDGMENTS

REFERENCES

Ahlfors, R., Brosche, M., Kollist, H., and Kangasjarvi, J. (2009). Nitric oxide modulates ozone-induced cell death, hormone biosynthesis and gene expression in *Arabidopsis thaliana*. *Plant J.* 58, 1–12. doi: 10.1111/j.1365-313X.2008.03756.x

Arasimowicz-Jelonek, M., and Floryszak-Wieczorek, J. (2011). Understanding the fate of peroxynitrite in plant cells - from physiology to pathophysiology. *Phytochemistry* 72, 681–688. doi: 10.1016/j.phytochem.2011.02.025

Arasimowicz-Jelonek, M., Floryszak-Wieczorek, J., and Gwozdz, E. A. (2011a). The message of nitric oxide in cadmium challenged plants. *Plant Sci.* 181, 612–620. doi: 10.1016/j.plantsci.2011.03.019

Arasimowicz-Jelonek, M., Floryszak-Wieczorek, J., and Kosmala, A. (2011b). Are nitric oxide donors a valuable tool to study the functional role of nitric oxide in plant metabolism. *Plant Biol.* 13, 747–756. doi: 10.1111/j.1438-8677.2010.00430.x

Arasimowicz, M., Floryszak-Wieczorek, J., Milczarek, G., and Jelonek, T. (2009). Nitric oxide,

induced by wounding, mediates redox regulation in pelargonium leaves. *Plant Biol.* 11, 650–663. doi: 10.1111/j.1438-8677.2008.00164.x

Bai, X., Yang, L., Tian, M., Chen, J., Shi, J., Yang, Y., et al. (2011). Nitric oxide enhances desiccation tolerance of recalcitrant *Antiaris toxicaria* seeds via protein S-nitrosylation and carbonylation. *PLoS ONE* 6:e20714. doi: 10.1371/journal.pone.0020714

Bai, X.-G., Chen, J.-H., Kong, X.-X., Todd, C. D., Yang, Y.-P., Hu, X.-Y., et al. (2012). Carbon monoxide enhances the chilling tolerance of recalcitrant *Baccaurea ramiflora* seeds via nitric-oxide-mediated glutathione homeostasis. *Free Radic. Biol. Med.* 53, 710–720. doi: 10.1016/j.freeradbiomed.2012.05.042

Balazy, M., Kaminski, P. M., Mao, K., Tan, J., and Wolin, M. S. (1998). S-Nitroglutathione, a product of the reaction between peroxynitrite and glutathione that generates nitric oxide. *J. Biol. Chem.* 273, 32009–32015. doi: 10.1074/jbc.273.48.32009

Bechtold, U., Rabbani, N., Mullineaux, P. M., and Thornalley, P. J. (2009). Quantitative measurement of

specific biomarkers for protein oxidation, nitration and glycation in Arabidopsis leaves. *Plant J.* 59, 661–671. doi: 10.1111/j.1365-313X.2009.03898.x

Beligni, M. V., and Lamattina, L. (2002). Nitric oxide interferes with plant photo-oxidative stress by detoxifying reactive oxygen species. *Plant Cell Environ.* 25, 737–748. doi: 10.1046/j.1365-3040.2002.00857.x

Benhar, M., Forrester, M. T., and Stamler, J. S. (2009). Protein denitrosylation: enzymatic mechanisms and cellular functions. *Nat. Rev. Mol. Cell Biol.* 10, 721–732. doi: 10.1038/nrm2764

Bethke, P. C., Badger, M. R., and Jones, R. L. (2004). Apoplastic synthesis of nitric oxide by plant tissues. *Plant Cell* 16, 332–341. doi: 10.1105/tpc.017822

Bonini, M. G., Radi, R., Ferrer-Sueta, G., Ferreira, A. M., and Augusto, O. (1999). Direct EPR detection of the carbonate radical anion produced from peroxynitrite and carbon dioxide. *J. Biol. Chem.* 274, 10802–10806. doi: 10.1074/jbc.274.16.10802

Broniowska, K. A., Diers, A. R., and Hogg, N. (2013).

S-nitrosoglutathione. *Biochim. Biophys. Acta* 1830, 3173–3181. doi: 10.1016/j.bbagen.2013.02.004

Buchanan, B., Gruissem, W., and Jones, R. (2002). *Biochemistry and Molecular Biology of Plants*. Hoboken, NJ: John Wiley and Sons.

Chaki, M., Valderrama, R., Fernandez-Ocana, A. M., Carreras, A., Lopez-Jaramillo, J., Luque, F., et al. (2009). Protein targets of tyrosine nitration in sunflower (*Helianthus annuus* L.) hypocotyls. *J. Exp. Bot.* 60, 4221–4234. doi: 10.1093/jxb/erp263

Chen, R., Sun, S., Wang, C., Li, Y., Liang, Y., An, F., et al. (2009). The Arabidopsis PARAQUAT RESISTANT2 gene encodes an S-nitrosoglutathione reductase that is a key regulator of cell death. *Cell Res.* 19, 1377–1387. doi: 10.1038/cr.2009.117

Chen, W. W., Yang, J. L., Qin, C., Jin, C. W., Mo, J. H., Ye, T., et al. (2010). Nitric oxide acts downstream of auxin to trigger root ferric-chelate reductase activity in response to iron deficiency in Arabidopsis. *Plant Physiol.* 154, 810–819. doi: 10.1104/pp.110.161109

Chun, H. J., Park, H. C., Koo, S. C., Lee, J. H., Park, C. Y., Choi, M. S., et al.

(2012). Constitutive expression of mammalian nitric oxide synthase in tobacco plants triggers disease resistance to pathogens. *Mol. Cells* 34, 463–471. doi: 10.1007/s10059-012-0213-0

Clark, D., Durner, J., Navarre, D. A., and Klessig, D. F. (2000). Nitric oxide inhibition of tobacco catalase and ascorbate peroxidase. *Mol. Plant Microbe Interact.* 13, 1380–1384. doi: 10.1094/MPMI.2000.13.12.1380

Combet, E., El Mesmari, A., Preston, T., Crozier, A., and McColl, K. E. (2010). Dietary phenolic acids and ascorbic acid: influence on acid-catalyzed nitrosative chemistry in the presence and absence of lipids. *Free Radic. Biol. Med.* 48, 763–771. doi: 10.1016/j.freeradbiomed.2009.12.011

Conrath, U. (2011). Molecular aspects of defence priming. *Trends Plant Sci.* 16, 524–531. doi: 10.1016/j.tplants.2011.06.004

Corpas, F. J., Hayashi, M., Mano, S., Nishimura, M., and Barroso, J. B. (2009). Peroxisomes are required for *in vivo* nitric oxide accumulation in the cytosol following salinity stress of Arabidopsis plants. *Plant Physiol.* 151, 2083–2094. doi: 10.1104/pp.109.146100

De Michele, R., Vurro, E., Rigo, C., Costa, A., Elviri, L., Di Valentin, M., et al. (2009). Nitric oxide is involved in cadmium-induced programmed cell death in Arabidopsis suspension cultures. *Plant Physiol.* 150, 217–228. doi: 10.1104/pp.108.133397

De Pinto, M. C., Locato, V., and De Gara, L. (2012). Redox regulation in plant programmed cell death. *Plant Cell Environ.* 35, 234–244. doi: 10.1111/j.1365-3040.2011.02387.x

De Pinto, M. C., Paradiso, A., Leonetti, P., and De Gara, L. (2006). Hydrogen peroxide, nitric oxide and cytosolic ascorbate peroxidase at the crossroad between defence and cell death. *Plant J.* 48, 784–795. doi: 10.1111/j.1365-313X.2006.02919.x

De Pinto, M. C., Tommasi, F., and De Gara, L. (2002). Changes in the antioxidant systems as part of the signaling pathway responsible for the programmed cell death activated by nitric oxide and reactive oxygen species in tobacco Bright-Yellow 2 cells. *Plant Physiol.* 130, 698–708. doi: 10.1104/pp.005629

Delledonne, M., Xia, Y., Dixon, R. A., and Lamb, C. (1998). Nitric oxide functions as a signal in plant disease resistance. *Nature* 394, 585–588. doi: 10.1038/29087

Delledonne, M., Zeier, J., Marocco, A., and Lamb, C. (2001). Signal interactions between nitric oxide and reactive oxygen intermediates in the plant hypersensitive disease resistance response. *Proc. Natl. Acad. Sci. U.S.A.* 98, 13454–13459. doi: 10.1073/pnas.231178298

Desel, C., Hubbermann, E. M., Schwarz, K., and Krupinska, K. (2007). Nitration of gamma-tocopherol in plant tissues. *Planta* 226, 1311–1322. doi: 10.1007/s00425-007-0552-9

Diaz, M., Achkor, H., Titarenko, E., and Martinez, M. C. (2003). The gene encoding glutathione-dependent formaldehyde dehydrogenase/GSNO reductase is responsive to wounding, jasmonic acid and salicylic acid. *FEBS Lett.* 543, 136–139. doi: 10.1016/S0014-5793(03)00426-5

Dordas, C., Hasinoff, B. B., Igamberdiev, A. U., Manac'h, N., Rivoal, J., and Hill, R. D. (2003). Expression of a stress-induced hemoglobin affects NO levels produced by alfalfa root cultures under hypoxic stress. *Plant J.* 35, 763–770. doi: 10.1046/j.1365-313X.2003.01846.x

Fares, A., Rossignol, M., and Peltier, J. B. (2011). Proteomics investigation of endogenous S-nitrosylation in Arabidopsis. *Biochem. Biophys. Res. Commun.* 416, 331–336. doi: 10.1016/j.bbrc.2011.11.036

Farmer, E. E., and Mueller, M. J. (2013). ROS-mediated lipid peroxidation and RES-activated signaling. *Annu. Rev. Plant Biol.* 64, 429–450. doi: 10.1146/annurev-arplant-050312-120132

Farooq, M., Basra, S. M. A., Wahid, A., Ahmad, N., and Saleem, B. A. (2009). Improving the drought tolerance in rice (*Oryza sativa* L.) by exogenous application of salicylic acid. *J. Agron. Crop Sci.* 195, 237–246. doi: 10.1111/j.1439-037x.2009.00365.x

Farooq, M., Kobayashi, N., Ito, O., Wahid, A., and Serraj, R. (2010). Broader leaves result in better performance of indica rice under drought stress. *J. Plant Physiol.* 167, 1066–1075. doi: 10.1016/j.jplph.2010.03.003

Feechan, A., Kwon, E., Yun, B. W., Wang, Y., Pallas, J. A., and Loake, G. J. (2005). A central role for S-nitrosothiols in plant disease resistance. *Proc. Natl. Acad. Sci. U.S.A.* 102, 8054–8059. doi: 10.1073/pnas.0501456102

Ferrer-Sueta, G., and Radi, R. (2009). Chemical biology of peroxynitrite: kinetics, diffusion, and radicals. *ACS Chem. Biol.* 4, 161–177. doi: 10.1021/cb800279q

Foissner, I., Wendehenne, D., Langebartels, C., and Durner, J. (2000). *In vivo* imaging of an elicitor-induced nitric oxide burst in tobacco. *Plant J.* 23, 817–824. doi: 10.1046/j.1365-313X.2000.00835.x

Foyer, C. H., and Noctor, G. (2009). Redox regulation in photosynthetic organisms: signaling, acclimation, and practical implications. *Antioxid. Redox Signal.* 11, 861–905. doi: 10.1089/ars.2008.2177

Frohlich, A., and Durner, J. (2011). The hunt for plant nitric oxide synthase (NOS): is one really needed. *Plant Sci.* 181, 401–404. doi: 10.1016/j.plantsci.2011.07.014

Fukuto, J. M., and Carrington, S. J. (2011). HNO signaling mechanisms. *Antioxid. Redox Signal.* 14, 1649–1657. doi: 10.1089/ars.2010.3855

Gaupels, F., Furch, A. C., Will, T., Mur, L. A., Kogel, K. H., and Van Bel, A. J. (2008). Nitric oxide generation in Vicia faba phloem cells reveals them to be sensitive detectors as well as possible systemic transducers of stress signals. *New Phytol.* 178, 634–646. doi: 10.1111/j.1469-8137.2008.02388.x

Gaupels, F., Kuruthukulangarakoola, G. T., and Durner, J. (2011a). Upstream and downstream signals of nitric oxide in pathogen defence. *Curr. Opin. Plant Biol.* 14, 707–714. doi: 10.1016/j.pbi.2011.07.005

Gaupels, F., Spiazzi-Vandelle, E., Yang, D., and Delledonne, M. (2011b). Detection of peroxynitrite accumulation in *Arabidopsis thaliana* during the hypersensitive defense response. *Nitric Oxide* 25, 222–228. doi: 10.1016/j.niox.2011.01.009

Goldstein, S., and Merenyi, G. (2008). The chemistry of peroxynitrite: implications for biological activity. *Meth. Enzymol.* 436, 49–61. doi: 10.1016/S0076-6879(08)36004-2

Gupta, D., Harish, B., Kissner, R., and Koppenol, W. H. (2009). Peroxynitrate is formed rapidly during decomposition of peroxynitrite at neutral pH. *Dalton Trans.* 29, 5730–5736. doi: 10.1039/b905535e

Gupta, K. J., Fernie, A. R., Kaiser, W. M., and Van Dongen, J. T. (2011). On the origins of nitric oxide. *Trends Plant Sci.* 16, 160–168. doi: 10.1016/j.tplants.2010.11.007

Haenen, G. R., Paquay, J. B., Korthouwer, R. E., and Bast, A. (1997). Peroxynitrite scavenging by flavonoids. *Biochem. Biophys. Res. Commun.* 236, 591–593. doi: 10.1006/bbrc.1997.7016

Hasanuzzaman, M., and Fujita, M. (2013). Exogenous sodium nitroprusside alleviates arsenic-induced oxidative stress in wheat (*Triticum aestivum* L.) seedlings by enhancing antioxidant defense and glyoxalase system. *Ecotoxicology* 22, 584–596. doi: 10.1007/s10646-013-1050-4

Hasanuzzaman, M., Hossain, M. A., and Fujita, M. (2010). Physiological and biochemical mechanism of nitric oxide induced abiotic stress tolerance in plants. *Am. J. Plant Physiol.* 5, 295–324. doi: 10.3923/ajpp.2010.295.324

Hasanuzzaman, M., Hossain, M. A., and Fujita, M. (2011). Nitric oxide modulates antioxidant defense and the methylglyoxal detoxification system and reduces salinity-induced damage of wheat seedlings. *Plant Biotechnol. Rep.* 5, 353–365. doi: 10.1007/s11816-011-0189-9

Hebelstrup, K. H., Van Zanten, M., Mandon, J., Voesenek, L. A., Harren, F. J., Cristescu, S. M., et al. (2012). Haemoglobin modulates NO emission and hyponasty under hypoxia-related stress in *Arabidopsis thaliana*. *J. Exp. Bot.* 63, 5581–5591. doi: 10.1093/jxb/ers210

Hill, B. G., Dranka, B. P., Bailey, S. M., Lancaster, J. R. Jr., and Darley-Usmar, V. M. (2010). What part of NO don't you understand. Some answers to the cardinal questions in nitric oxide biology. *J. Biol. Chem.* 285, 19699–19704. doi: 10.1074/jbc.R110.101618

Holzmeister, C., Frohlich, A., Sarioglu, H., Bauer, N., Durner, J., and Lindermayr, C. (2011). Proteomic analysis of defense response of wildtype *Arabidopsis thaliana* and plants with impaired NO- homeostasis. *Proteomics* 11, 1664–1683. doi: 10.1002/pmic.201000652

Hsu, Y. T., and Kao, C. H. (2007). Toxicity in leaves of rice exposed to cadmium is due to hydrogen peroxide accumulation. *Plant Soil* 298, 231–241. doi: 10.1007/s11104-007-9357-7

Hung, K. T., Chang, C. J., and Kao, C. H. (2002). Paraquat toxicity is reduced by nitric oxide in rice leaves. *J. Plant Physiol.* 159, 159–166. doi: 10.1078/0176-1617-00692

Innocenti, G., Pucciariello, C., Le Gleuher, M., Hopkins, J., De Stefano, M., Delledonne, M., et al. (2007). Glutathione synthesis is regulated by nitric oxide in *Medicago truncatula* roots. *Planta* 225, 1597–1602. doi: 10.1007/s00425-006-0461-3

Jasid, S., Simontacchi, M., Bartoli, C. G., and Puntarulo, S. (2006).

Chloroplasts as a nitric oxide cellular source. Effect of reactive nitrogen species on chloroplastic lipids and proteins. *Plant Physiol.* 142, 1246–1255. doi: 10.1104/pp.106.086918

Jin, J.-W., Xu, Y.-F., and Huang, Y.-F. (2010). Protective effect of nitric oxide against arsenic-induced oxidative damage in tall fescue leaves. *Afr. J. Biotechnol.* 9, 1619–1627. ISSN: 1684-5315

Joudoi, T., Shichiri, Y., Kamizono, N., Akaike, T., Sawa, T., Yoshitake, J., et al. (2013). Nitrated cyclic GMP modulates guard cell signaling in Arabidopsis. *Plant Cell* 25, 558–571. doi: 10.1105/tpc.112.105049

Jourd'heuil, D., Jourd'heuil, F. L., Kutchukian, P. S., Musah, R. A., Wink, D. A., and Grisham, M. B. (2001). Reaction of superoxide and nitric oxide with peroxynitrite. Implications for peroxynitrite-mediated oxidation reactions *in vivo. J. Biol. Chem.* 276, 28799–28805. doi: 10.1074/jbc.M102341200

Kato, H., Takemoto, D., and Kawakita, K. (2012). Proteomic analysis of S-nitrosylated proteins in potato plant. *Physiol. Plantarum.* 148, 371–386. doi: 10.1111/j.1399-3054.2012.01684.x

Keyster, M., Klein, A., and Ludidi, N. (2012). Caspase-like enzymatic activity and the ascorbate-glutathione cycle participate in salt stress tolerance of maize conferred by exogenously applied nitric oxide. *Plant Signal. Behav.* 7, 349–360. doi: 10.4161/psb.18967

Khan, A. U., Kovacic, D., Kolbanovskiy, A., Desai, M., Frenkel, K., and Geacintov, N. E. (2000). The decomposition of peroxynitrite to nitroxyl anion (NO-) and singlet oxygen in aqueous solution. *Proc. Natl. Acad. Sci. U.S.A.* 97, 2984–2989. doi: 10.1073/pnas.97.7.2984

Khan, M. N., Siddiqui, M. H., Mohammad, F., and Naeem, M. (2012). Interactive role of nitric oxide and calcium chloride in enhancing tolerance to salt stress. *Nitric Oxide* 27, 210–218. doi: 10.1016/j.niox.2012.07.005

Kirsch, M., Lehnig, M., Korth, H. G., Sustmann, R., and De Groot, H. (2001). Inhibition of peroxynitrite-induced nitration of tyrosine by glutathione in the presence of carbon dioxide through both radical repair and peroxynitrate formation. *Chemistry* 7, 3313–3320. doi: 10.1002/1521-3765(20010803)7:15<3313::AID-CHEM3313>3.0.CO;2-7

Koppenol, W. H., Bounds, P. L., Nauser, T., Kissner, R., and Ruegger, H. (2012). Peroxynitrous acid: controversy and consensus surrounding an enigmatic oxidant. *Dalton Trans.* 41, 13779–13787. doi: 10.1039/c2dt31526b

Kumar, P., Tewari, R. K., and Sharma, P. N. (2010). Sodium nitroprusside-mediated alleviation of iron deficiency and modulation of antioxidant responses in maize plants. *AoB plants* 2010:plq002. doi: 10.1093/aobpla/plq002

Kurz, C. R., Kissner, R., Nauser, T., Perrin, D., and Koppenol, W. H. (2003). Rapid scavenging of peroxynitrous acid by monohydroascorbate. *Free Radic. Biol. Med.* 35, 1529–1537. doi: 10.1016/j.freeradbiomed.2003.08.012

Kwon, E., Feechan, A., Yun, B. W., Hwang, B. H., Pallas, J. A., Kang, J. G., et al. (2012). AtGSNOR1 function is required for multiple developmental programs in Arabidopsis. *Planta* 236, 887–900. doi: 10.1007/s00425-012-1697-8

Kytzia, A., Korth, H. G., Sustmann, R., De Groot, H., and Kirsch, M. (2006). On the mechanism of the ascorbic acid-induced release of nitric oxide from N-nitrosated tryptophan derivatives: scavenging of NO by ascorbyl radicals. *Chemistry* 12, 8786–8797. doi: 10.1002/chem.200600405

Laspina, N., Groppa, M., Tomaro, M., and Benavides, M. (2005). Nitric oxide protects sunflower leaves against Cd-induced oxidative stress. *Plant Sci.* 169, 323–330. doi: 10.1016/j.plantsci.2005.02.007

Lee, U., Wie, C., Fernandez, B. O., Feelisch, M., and Vierling, E. (2008). Modulation of nitrosative stress by S-nitrosoglutathione reductase is critical for thermotolerance and plant growth in *Arabidopsis. Plant Cell* 20, 786–802. doi: 10.1105/tpc.107.052647

Leitner, M., Vandelle, E., Gaupels, F., Bellin, D., and Delledonne, M. (2009). NO signals in the haze: nitric oxide signalling in plant defence. *Curr. Opin. Plant Biol.* 12, 451–458. doi: 10.1016/j.pbi.2009.05.012

Levine, A., Pennell, R. I., Alvarez, M. E., Palmer, R., and Lamb, C. (1996). Calcium-mediated apoptosis in a plant hypersensitive disease resistance response. *Curr. Biol.* 6, 427–437. doi: 10.1016/S0960-9822(02)00510-9

Levine, A., Tenhaken, R., Dixon, R., and Lamb, C. (1994). H_2O_2 from the oxidative burst orchestrates the plant hypersensitive disease resistance response. *Cell* 79, 583–595. doi: 10.1016/0092-8674(94)90544-4

Li, Q. Y., Niu, H. B., Yin, J., Wang, M. B., Shao, H. B., Deng, D. Z., et al. (2008). Protective role of exogenous nitric oxide against oxidative-stress induced by salt stress in barley (*Hordeum vulgare*). *Colloids Surf. B Biointerfaces* 65, 220–225. doi: 10.1016/j.colsurfb.2008.04.007

Lin, A., Wang, Y., Tang, J., Xue, P., Li, C., Liu, L., et al. (2012). Nitric oxide and protein S-nitrosylation are integral to hydrogen peroxide-induced leaf cell death in rice. *Plant Physiol.* 158, 451–464. doi: 10.1104/pp.111.184531

Lin, C. C., Jih, P. J., Lin, H. H., Lin, J. S., Chang, L. L., Shen, Y. H., et al. (2011). Nitric oxide activates superoxide dismutase and ascorbate peroxidase to repress the cell death induced by wounding. *Plant Mol. Biol.* 77, 235–249. doi: 10.1007/s11103-011-9805-x

Lindermayr, C., Sell, S., Muller, B., Leister, D., and Durner, J. (2010). Redox regulation of the NPR1-TGA1 system of *Arabidopsis thaliana* by nitric oxide. *Plant Cell* 22, 2894–2907. doi: 10.1105/tpc.109.066464

Liu, L., Hausladen, A., Zeng, M., Que, L., Heitman, J., and Stamler, J. S. (2001). A metabolic enzyme for S-nitrosothiol conserved from bacteria to humans. *Nature* 410, 490–494. doi: 10.1038/35068596

Liu, W. Z., Kong, D. D., Gu, X. X., Gao, H. B., Wang, J. Z., Xia, M., et al. (2013). Cytokinins can act as suppressors of nitric oxide in Arabidopsis. *Proc. Natl. Acad. Sci. U.S.A.* 110, 1548–1553. doi: 10.1073/pnas.1213235110

Liu, X., Miller, M. J., Joshi, M. S., Thomas, D. D., and Lancaster, J. R., Jr. (1998). Accelerated reaction of nitric oxide with O_2 within the hydrophobic interior of biological membranes. *Proc. Natl. Acad. Sci. U.S.A.* 95, 2175–2179. doi: 10.1073/pnas.95.5.2175

Lozano-Juste, J., Colom-Moreno, R., and Leon, J. (2011). *In vivo* protein tyrosine nitration in *Arabidopsis thaliana. J. Exp. Bot.* 62, 3501–3517. doi: 10.1093/jxb/err042

Lum, H. K., Butt, Y. K., and Lo, S. C. (2002). Hydrogen peroxide induces a rapid production of nitric oxide in mung bean (Phaseolus aureus). *Nitric Oxide* 6, 205–213. doi: 10.1006/niox.2001.0395

Maassen, A., and Hennig, J. (2011). Effect of *Medicago sativa* Mhb1gene expression on defense response of *Arabidopsis thaliana* plants. *Acta Biochim. Pol.* 58, 427–432.

Madej, E., Folkes, L. K., Wardman, P., Czapski, G., and Goldstein, S. (2008). Thiyl radicals react with nitric oxide to form S-nitrosothiols with rate constants near the diffusion-controlled limit. *Free Radic. Biol. Med.* 44, 2013–2018. doi: 10.1016/j.freeradbiomed.2008.02.015

Malik, S. I., Hussain, A., Yun, B. W., Spoel, S. H., and Loake, G. J. (2011). GSNOR-mediated de-nitrosylation in the plant defence response. *Plant Sci.* 181, 540–544. doi: 10.1016/j.plantsci.2011.04.004

Marti, M. C., Florez-Sarasa, I., Camejo, D., Pallol, B., Ortiz, A., Ribas-Carbo, M., et al. (2013). Response of mitochondrial antioxidant system and respiratory pathways to reactive nitrogen species in pea leaves. *Physiol. Plant.* 147, 194–206. doi: 10.1111/j.1399-3054.2012.01654.x

Meiser, J., Lingam, S., and Bauer, P. (2011). Posttranslational regulation of the iron deficiency basic helix-loop-helix transcription factor FIT is affected by iron and nitric oxide. *Plant Physiol.* 157, 2154–2166. doi: 10.1104/pp.111.183285

Mittler, R., Vanderauwera, S., Suzuki, N., Miller, G., Tognetti, V. B., Vandepoele, K., et al. (2011). ROS signaling: the new wave. *Trends Plant Sci.* 16, 300–309. doi: 10.1016/j.tplants.2011.03.007

Miyamoto, S., Ronsein, G. E., Correa, T. C., Martinez, G. R., Medeiros, M. H., and Di Mascio, P. (2009). Direct evidence of singlet molecular oxygen generation from peroxynitrate, a decomposition product of peroxynitrite. *Dalton Trans.* 29, 5720–5729. doi: 10.1039/b905560f

Moller, M. N., Li, Q., Lancaster, J. R. Jr., and Denicola, A. (2007). Acceleration of nitric oxide autoxidation and nitrosation by membranes. *IUBMB Life* 59, 243–248. doi: 10.1080/15216540701311147

Morot-Gaudry-Talarmain, Y., Rockel, P., Moureaux, T., Quillere, I., Leydecker, M. T., Kaiser, W. M., et al. (2002). Nitrite accumulation and nitric oxide emission in relation to cellular signaling in nitrite reductase antisense tobacco. *Planta* 215, 708–715. doi: 10.1007/s00425-002-0816-3

Mur, L. A., Kenton, P., Lloyd, A. J., Ougham, H., and Prats, E. (2008). The hypersensitive response; the centenary is upon us but how much do we know. *J. Exp. Bot.* 59, 501–520. doi: 10.1093/jxb/erm239

Mur, L. A., Mandon, J., Persijn, S., Cristescu, S. M., Moshkov, I. E.,

Novikova, G. V., et al. (2013). Nitric oxide in plants: an assessment of the current state of knowledge. *AoB Plants* 5:pls052. doi: 10.1093/aob-pla/pls052

Mur, L. A., Sivakumaran, A., Mandon, J., Cristescu, S. M., Harren, F. J., and Hebelstrup, K. H. (2012). Haemoglobin modulates salicylate and jasmonate/ethylene-mediated resistance mechanisms against pathogens. *J. Exp. Bot.* 63, 4375–4387. doi: 10.1093/jxb/ers116

Murgia, I., De Pinto, M. C., Delledonne, M., Soave, C., and De Gara, L. (2004a). Comparative effects of various nitric oxide donors on ferritin regulation, programmed cell death, and cell redox state in plant cells. *J. Plant Physiol.* 161, 777–783. doi: 10.1016/j.jplph.2003.12.004

Murgia, I., Tarantino, D., Vannini, C., Bracale, M., Carravieri, S., and Soave, C. (2004b). *Arabidopsis thaliana* plants overexpressing thylakoidal ascorbate peroxidase show increased resistance to Paraquat-induced photooxidative stress and to nitric oxide-induced cell death. *Plant J.* 38, 940–953. doi: 10.1111/j.1365-313x.2004.02092.x

Neill, S., Barros, R., Bright, J., Desikan, R., Hancock, J., Harrison, J., et al. (2008). Nitric oxide, stomatal closure, and abiotic stress. *J. Exp. Bot.* 59, 165–176. doi: 10.1093/jxb/erm293

Noronha-Dutra, A. A., Epperlein, M. M., and Woolf, N. (1993). Reaction of nitric oxide with hydrogen peroxide to produce potentially cytotoxic singlet oxygen as a model for nitric oxide-mediated killing. *FEBS Lett.* 321, 59–62. doi: 10.1016/0014-5793(93)80621-Z

O'brien, J. A., Daudi, A., Butt, V. S., and Bolwell, G. P. (2012). Reactive oxygen species and their role in plant defence and cell wall metabolism. *Planta* 236, 765–779. doi: 10.1007/s00425-012-1696-9

Perazzolli, M., Dominici, P., Romero-Puertas, M. C., Zago, E., Zeier, J., Sonoda, M., et al. (2004). Arabidopsis nonsymbiotic hemoglobin AHb1 modulates nitric oxide bioactivity. *Plant Cell* 16, 2785–2794. doi: 10.1105/tpc.104.025379

Planchet, E., Jagadis Gupta, K., Sonoda, M., and Kaiser, W. M. (2005). Nitric oxide emission from tobacco leaves and cell suspensions: rate limiting factors and evidence for the involvement of mitochondrial electron transport. *Plant J.* 41, 732–743. doi: 10.1111/j.1365-313X.2005.02335.x

Pryor, W. A., Houk, K. N., Foote, C. S., Fukuto, J. M., Ignarro, L. J., Squadrito, G. L., et al. (2006). Free radical biology and medicine: it's a gas, man! *American journal of physiology. Regul. Integr. Comp. Physiol.* 291, R491–R511. doi: 10.1152/ajpregu.00614.2005

Radi, R. (2013). Protein tyrosine nitration: biochemical mechanisms and structural basis of functional effects. *Acc. Chem. Res.* 46, 550–559. doi: 10.1021/ar300234c

Romero-Puertas, M. C., Campostrini, N., Matte, A., Righetti, P. G., Perazzolli, M., Zolla, L., et al. (2008). Proteomic analysis of S-nitrosylated proteins in *Arabidopsis thaliana* undergoing hypersensitive response. *Proteomics* 8, 1459–1469. doi: 10.1002/pmic.200700536

Romero-Puertas, M. C., Laxa, M., Matte, A., Zaninotto, F., Finkemeier, I., Jones, A. M., et al. (2007). S-nitrosylation of peroxiredoxin II E promotes peroxynitrite-mediated tyrosine nitration. *Plant Cell* 19, 4120–4130. doi: 10.1105/tpc.107.055061

Romero, N., Radi, R., Linares, E., Augusto, O., Detweiler, C. D., Mason, R. P., et al. (2003). Reaction of human hemoglobin with peroxynitrite. Isomerization to nitrate and secondary formation of protein radicals. *J. Biol. Chem.* 278, 44049–44057. doi: 10.1074/jbc.M305895200

Rusterucci, C., Espunya, M. C., Diaz, M., Chabannes, M., and Martinez, M. C. (2007). S-nitrosoglutathione reductase affords protection against pathogens in Arabidopsis, both locally and systemically. *Plant Physiol.* 143, 1282–1292. doi: 10.1104/pp.106.091686

Sakamoto, A., Sakurao, S. H., Fukunaga, K., Matsubara, T., Ueda-Hashimoto, M., Tsukamoto, S., et al. (2004). Three distinct Arabidopsis hemoglobins exhibit peroxidase-like activity and differentially mediate nitrite-dependent protein nitration. *FEBS Lett.* 572, 27–32. doi: 10.1016/j.febslet.2004.07.005

Sakamoto, A., Tsukamoto, S., Yamamoto, H., Ueda-Hashimoto, M., Takahashi, M., Suzuki, H., et al. (2003). Functional complementation in yeast reveals a protective role of chloroplast 2-Cys peroxiredoxin against reactive nitrogen species. *Plant J.* 33, 841–851. doi: 10.1046/j.1365-313X.2003.01669.x

Sakamoto, A., Ueda, M., and Morikawa, H. (2002). Arabidopsis glutathione-dependent formaldehyde dehydrogenase is an S-nitrosoglutathione reductase. *FEBS Lett.* 515, 20–24. doi: 10.1016/S0014-5793(02)02414-6

Sakihama, Y., Tamaki, R., Shimoji, H., Ichiba, T., Fukushi, Y., Tahara, S., et al. (2003). Enzymatic nitration of phytophenolics: evidence for peroxynitrite-independent nitration of plant secondary metabolites. *FEBS Lett.* 553, 377–380. doi: 10.1016/S0014-5793(03)01059-7

Sandalio, L. M., Rodriguez-Serrano, M., Romero-Puertas, M. C., and Del Rio, L. A. (2013). Role of peroxisomes as a source of reactive oxygen species (ROS) signaling molecules. *Subcell. Biochem.* 69, 231–255. doi: 10.1007/978-94-007-6889-5_13

Sang, J. R., Jiang, M. Y., Lin, F., Li, J., and Xu, S. C. (2007). Role of nitric oxide in abscisic acid-induced subcellular antioxidant defense of maize leaves. *Zhi Wu Sheng Li Yu Fen Zi Sheng Wu Xue Xue Bao* 33, 553–566.

Saxena, I., and Shekhawat, G. S. (2013). Nitric oxide (NO) in alleviation of heavy metal induced phytotoxicity and its role in protein nitration. *Nitric Oxide* 32, 13–20. doi: 10.1016/j.niox.2013.03.004

Schlicht, M., Ludwig-Muller, J., Burbach, C., Volkmann, D., and Baluska, F. (2013). Indole-3-butyric acid induces lateral root formation via peroxisome-derived indole-3-acetic acid and nitric oxide. *New Phytol.* 200, 473–482. doi: 10.1111/nph.12377

Scorza, G., Pietraforte, D., and Minetti, M. (1997). Role of ascorbate and protein thiols in the release of nitric oxide from S-nitroso-albumin and S-nitroso-glutathione in human plasma. *Free Radic. Biol. Med.* 22, 633–642. doi: 10.1016/S0891-5849(96)00378-4

Sehrawat, A., Abat, J. K., and Deswal, R. (2013). RuBisCO depletion improved proteome coverage of cold responsive S-nitrosylated targets in Brassica juncea. *Front. Plant Sci.* 4:342. doi: 10.3389/fpls.2013.00342

Sheokand, S., Kumari, A., and Sawhney, V. (2008). Effect of nitric oxide and putrescine on antioxidative responses under NaCl stress in chickpea plants. *Physiol. Mol. Biol. Plants* 14, 355–362. doi: 10.1007/s12298-008-0034-y

Shi, H. T., Li, R. J., Cai, W., Liu, W., Wang, C. L., and Lu, Y. T. (2012). Increasing nitric oxide content in *Arabidopsis thaliana* by expressing rat neuronal nitric oxide synthase resulted in enhanced stress tolerance. *Plant Cell Physiol.* 53, 344–357. doi: 10.1093/pcp/pcr181

Shi, S., Wang, G., Wang, Y., Zhang, L., and Zhang, L. (2005). Protective effect of nitric oxide against oxidative stress under ultraviolet-B radiation. *Nitric Oxide* 13, 1–9. doi: 10.1016/j.niox.2005.04.006

Singh, H. P., Kaur, S., Batish, D. R., Sharma, V. P., Sharma, N., and Kohli, R. K. (2009). Nitric oxide alleviates arsenic toxicity by reducing oxidative damage in the roots of *Oryza sativa* (rice). *Nitric Oxide* 20, 289–297. doi: 10.1016/j.niox.2009.02.004

Stöhr, C., Strube, F., Marx, G., Ullrich, W. R., and Rockel, P. (2001). A plasma membrane-bound enzyme of tobacco roots catalyses the formation of nitric oxide from nitrite. *Planta* 212, 835–841. doi: 10.1007/s004250000447

Sturms, R., Dispirito, A. A., and Hargrove, M. S. (2011). Plant and cyanobacterial hemoglobins reduce nitrite to nitric oxide under anoxic conditions. *Biochemistry* 50, 3873–3878. doi: 10.1021/bi2004312

Sun, X., Li, Y., Cai, H., Bai, X., Ji, W., Ding, X., et al. (2012). The Arabidopsis AtbZIP1 transcription factor is a positive regulator of plant tolerance to salt, osmotic and drought stresses. *J. Plant Res.* 125, 429–438. doi: 10.1007/s10265-011-0448-4

Tada, Y., Spoel, S. H., Pajerowska-Mukhtar, K., Mou, Z., Song, J., Wang, C., et al. (2008). Plant immunity requires conformational charges of NPR1 via S-nitrosylation and thioredoxins. *Science* 321, 952–956. doi: 10.1126/science.1156970

Tanou, G., Job, C., Belghazi, M., Molassiotis, A., Diamantidis, G., and Job, D. (2010). Proteomic signatures uncover hydrogen peroxide and nitric oxide cross-talk signaling network in citrus plants. *J. Proteome Res.* 9, 5994–6006. doi: 10.1021/pr100782h

Tanou, G., Job, C., Rajjou, L., Arc, E., Belghazi, M., Diamantidis, G., et al. (2009). Proteomics reveals the overlapping roles of hydrogen peroxide and nitric oxide in the acclimation of citrus plants to salinity. *Plant J.* 60, 795–804. doi: 10.1111/j.1365-313X.2009.04000.x

Tewari, R. K., Hahn, E. J., and Paek, K. Y. (2008). Function of nitric oxide and superoxide anion in the adventitious root development and antioxidant defence in Panax ginseng. *Plant Cell Rep.* 27, 563–573. doi: 10.1007/s00299-007-0448-y

Tewari, R. K., Prommer, J., and Watanabe, M. (2013). Endogenous nitric oxide generation in protoplast

chloroplasts. *Plant Cell Rep.* 32, 31–44. doi: 10.1007/s00299-012-1338-5

Thomas, D. D., Ridnour, L. A., Isenberg, J. S., Flores-Santana, W., Switzer, C. H., Donzelli, S., et al. (2008). The chemical biology of nitric oxide: implications in cellular signaling. *Free Radic. Biol. Med.* 45, 18–31. doi: 10.1016/j.freeradbiomed.2008.03.020

Tian, X., and Lei, Y. (2006). Nitric oxide treatment alleviates drought stress in wheat seedlings. *Biol. Plant.* 50, 775–778. doi: 10.1007/s10535-006-0129-7

Tiso, M., Tejero, J., Kenney, C., Frizzell, S., and Gladwin, M. T. (2012). Nitrite reductase activity of non-symbiotic hemoglobins from *Arabidopsis thaliana. Biochemistry* 51, 5285–5292. doi: 10.1021/bi300570v

Torres, M. A., Dangl, J. L., and Jones, J. D. (2002). Arabidopsis gp91phox homologues AtrbohD and AtrbohF are required for accumulation of reactive oxygen intermediates in the plant defense response. *Proc. Natl. Acad. Sci. U.S.A.* 99, 517–522. doi: 10.1073/pnas.012452499

Verma, K., Mehta, S., and Shekhawat, G. (2013). Nitric oxide (NO) counteracts cadmium induced cytotoxic processes mediated by reactive oxygen species (ROS) in *Brassica juncea*: cross-talk between ROS, NO and antioxidant responses. *Biometals* 26, 255–269. doi: 10.1007/s10534-013-9608-4

Wang, Y., Ries, A., Wu, K., Yang, A., and Crawford, N. M. (2010). The arabidopsis prohibitin gene PHB3 functions in nitric oxide-mediated responses and in hydrogen peroxide-induced nitric oxide accumulation. *Plant Cell* 22, 249–259. doi: 10.1105/tpc.109.072066

Wimalasekera, R., Villar, C., Begum, T., and Scherer, G. F. (2011). COPPER AMINE OXIDASE1 (CuAO1) of *Arabidopsis thaliana* contributes to abscisic acid- and polyamine-induced nitric oxide biosynthesis and abscisic acid signal transduction. *Molecular Plant* 4, 663–678. doi: 10.1093/mp/ssr023

Xu, Y., Sun, X., Jin, J., and Zhou, H. (2010). Protective effect of nitric oxide on light-induced oxidative damage in leaves of tall fescue.

J. Plant Physiol. 167, 512–518. doi: 10.1016/j.jplph.2009.10.010

Xue, L., Li, S., Sheng, H., Feng, H., Xu, S., and An, L. (2007). Nitric oxide alleviates oxidative damage induced by enhanced ultraviolet-B radiation in cyanobacterium. *Curr. Microbiol.* 55, 294–301. doi: 10.1007/s00284-006-0621-5

Yang, L., Tian, D., Todd, C. D., Luo, Y., and Hu, X. (2013). Comparative proteome analyses reveal that nitric oxide is an important signal molecule in the response of rice to aluminum toxicity. *J. Proteome Res.* 12, 1316–1330. doi: 10.1021/pr300971n

Yun, B. W., Feechan, A., Yin, M., Saidi, N. B., Le Bihan, T., Yu, M., et al. (2011). S-nitrosylation of NADPH oxidase regulates cell death in plant immunity. *Nature* 478, 264–268. doi: 10.1038/nature10427

Zeier, J., Delledonne, M., Mishina, T., Severi, E., Sonoda, M., and Lamb, C. (2004). Genetic elucidation of nitric oxide signaling in incompatible plant-pathogen interactions. *Plant Physiol.* 136, 2875–2886. doi: 10.1104/pp.104.042499

Publications – Part 2. Local and systemic defence responses of the phloem

Gaupels, F., Knauer, T. and van Bel, A.J. 2008. A combinatory approach for analysis of protein sets in barley sieve-tube samples using EDTA-facilitated exudation and aphid stylectomy. J Plant Physiol, 165(1): 95-103.

Gaupels, F., Buhtz, A., Knauer, T., Deshmukh, S., Waller, F., van Bel, A.J., Kogel, K.H. and Kehr, J. 2008. Adaptation of aphid stylectomy for analyses of proteins and mRNAs in barley phloem sap. J Exp Bot, 59(12): 3297-306.

Gaupels, F., Furch, A.C., Will, T., Mur, L.A., Kogel, K.H. and van Bel, A.J. 2008. Nitric oxide generation in Vicia faba phloem cells reveals them to be sensitive detectors as well as possible systemic transducers of stress signals. New Phytol, 178(3): 634-46.

Fröhlich, A., Gaupels, F., Sarioglu, H., Holzmeister, C., Spannagl, M., Durner, J. and Lindermayr, C. 2012. Looking deep inside: detection of low-abundance proteins in leaf extracts of Arabidopsis and phloem exudates of pumpkin. Plant Physiol, 159(3): 902-14.

Gaupels, F., Sarioglu, H., Beckmann, M., Hause, B., Spannagl, M., Draper, J., Lindermayr, C. and Durner, J. 2012. Deciphering systemic wound responses of the pumpkin extrafascicular phloem by metabolomics and stable isotope-coded protein labeling. Plant Physiol, 160(4): 2285-99.

Gaupels, F. and Ghirardo, A. 2013. The extrafascicular phloem is made for fighting. Front Plant Sci, 4: 187.

Available online at www.sciencedirect.com

ScienceDirect

JOURNAL OF PLANT PHYSIOLOGY

www.elsevier.de/jplph

A combinatory approach for analysis of protein sets in barley sieve-tube samples using EDTA-facilitated exudation and aphid stylectomy

Frank Gaupels[a,b,1,2], Torsten Knauer[a,2], Aart J.E. van Bel[a,*]

[a]*Plant Cell Biology Research Group, Institute of General Botany, Justus-Liebig University, Senckenbergstrasse 17, D-35390 Giessen, Germany*
[b]*Institute of Phytopathology and Applied Zoology, IFZ, Heinrich-Buff-Ring 26-32, Justus-Liebig University, D-35392 Giessen, Germany*

Summary

This study investigated advantages and drawbacks of two sieve-tube sap sampling methods for comparison of phloem proteins in powdery mildew-infested vs. non-infested *Hordeum vulgare* plants. In one approach, sieve tube sap was collected by stylectomy. Aphid stylets were cut and immediately covered with silicon oil to prevent any contamination or modification of exudates. In this way, a maximum of 1 μL pure phloem sap could be obtained per hour. Interestingly, after pathogen infection exudation from microcauterized stylets was reduced to less than 40% of control plants, suggesting that powdery mildew induced sieve tube-occlusion mechanisms. In contrast to the laborious stylectomy, facilitated exudation using EDTA to prevent calcium-mediated callose formation is quick and easy with a large volume yield. After two-dimensional (2D) electrophoresis, a digital overlay of the protein sets extracted from EDTA solutions and stylet exudates showed that some major spots were the same with both sampling techniques. However, EDTA exudates also contained large amounts of contaminative proteins of unknown origin. A combinatory approach may be most favourable for studies in which the protein composition of phloem sap is compared between control and pathogen-infected plants. Facilitated exudation may be applied for subtractive identification of differentially expressed proteins by 2D/mass spectrometry, which requires large amounts of protein. A reference gel loaded with pure phloem sap from stylectomy

may be useful for confirmation of phloem origin of candidate spots by digital overlay. The method provides a novel opportunity to study differential expression of phloem proteins in monocotyledonous plant species.

Introduction

Systemic signalling in plants

Systemic signalling encompasses signal generation at the signal-triggering or challenge sites (e.g. Jones and Dangl, 2006; Hückelhoven, 2007), propagation along the pathway and signal implementation at the induction sites (e.g. Scheer and Ryan, 2002; Harman et al., 2004). These long-distance messages enable a concerted whole-plant reaction to phytopathogenic infestation (Durrant and Dong, 2004; Kogel and Langen, 2005), chewing (Kessler and Baldwin, 2002) or phloem-feeding insects (Thompson and Goggin, 2006), and herbivores (Walling, 2000).

At either end of the systemic pathway, local cellular signal cascades have been disclosed (Scheer and Ryan, 2002; Harman et al., 2004; Jones and Dangl, 2006; Hückelhoven, 2007). By contrast, processing and nature of the systemic signals along the long-distance pathway largely is a mystery despite the identification of some compounds involved. As for phytohormones, it is evident that xylem (abscisic acid, Sauter et al., 2001; Hartung et al., 2002) and phloem (jasmonic acid (JA); Li et al., 2002; Stratmann, 2003) are both involved in systemic signalling. Similarly, protein-processing cascades seem to operate both along the phloem (Walz et al., 2004; Giavalisco et al., 2006) and xylem (Buhtz et al., 2004; Kehr et al., 2005) pathway.

There is a variety of other candidates for systemic signalling in the phloem (e.g. van Bel and Gaupels, 2004), but they may have variable and specialized functions, even within plant families. For instance, systemin, an established wound-induced systemic signal in solanaceous plants (Narvaez-Vasquez et al., 1995; Lee and Howe, 2003), does not occur in other families (Ryan and Pearce, 2003). To add to the complexity, the production of systemic compounds may be distributed between various cell types along the phloem pathway. Systemin, a peptide of 18 amino acids is cleaved from the protein prosystemin in the phloem parenchyma cells (Narvaez-Vasquez and Ryan, 2004). Systemin is supposed to be involved in a self-amplified propagation wave along the phloem, in which JA plays a prominent role. Recently, JA was uncovered as an essential systemic wound signal and its interaction with systemin along the transport route was suggested (Li et al., 2002). Thus, the systemic wound signalling by JA and systemin provides a good example for the complexity of signal production and propagation in the phloem.

It has been suggested that various webs of systemic signalling operate in parallel at different time scales in the same plant species (e.g. Gilbertson et al., 2005; van Bel and Ehlers, 2005). In the absence of clear-cut information on the nature of systemic signals, broad-spectrum analyses of sieve-tube compounds after induction of systemic signalling events may assist to unravel systemic networks. Direct probing of phloem sap may be a timely effort given the fact that the success of molecular approaches, such as mutant screenings, in identifying systemic signals has been limited thus far.

Collection of phloem-sap samples for detection of systemic signals

A variety of compounds has been postulated to be systemically active (van Bel and Gaupels, 2004) without any conclusive experimental support. Candidates for systemic signalling range from small molecules such as calcium, NO, ROS up to macromolecules such as proteins and mRNA (van Bel and Gaupels, 2004), with profound consequences for the way of separation and identification. The time-consuming procedure urges one to focus on likely candidates on the risk of missing the actual signals. We chose proteins as the first targets, since they occur in larger amounts in the phloem sap (Hayashi et al., 2000), are translocated over long distances (Fisher et al., 1992; Golecki et al., 1998) and are therefore suspected to operate in long-distance signalling (Gilbertson et al., 2005). For instance, the putative lipid transport protein DIR1 is essential for induction of an SAR (Maldonado et al., 2002). It was shown to be synthesized in CCs and translocated in the phloem probably carrying a lipid-derived systemic signal (e.g. van Bel and Gaupels, 2004; Durrant and Dong, 2004).

Expectedly, the quantities of systemic compounds may be extremely low. Moreover, phloem sampling itself may induce local changes in the composition of phloem sap. Exudates may be fraught with artefacts, since sieve tubes are reputed for their sensitivity to wounding (Behnke and Sjolund, 1990). Upon injury, sieve tubes show all sorts of stress and occlusion reactions ranging from the production of callose (King and Zeevaart, 1974; Nakashima et al., 2003) to the deposition of various protein complexes (Cronshaw and Sabnis, 1990; Knoblauch and van Bel, 1998; Furch et al., 2007). Therefore, the choice of an appropriate sampling method is crucial.

Persistent phloem bleeding in cucurbits (Walz et al., 2002, 2004), *Brassica napus* (Giavalisco et al., 2006) and *Ricinus communis* (Doering-Saad et al., 2002, 2006; Barnes et al., 2004) was employed as a tool for proteome or transcriptome research on sieve-tube components. As spontaneous phloem bleeding does not occur in *Hordeum vulgare*, we adopted other methods of phloem-sap collection here. Phloem sap was either collected by facilitated exudation into solutions with the calcium-chelator ethylenediaminetetraacetic acid disodium salt dehydrate (EDTA), which precludes sieve-tube occlusion (King and Zeevaart, 1974), or via cut aphid stylets (Doering-Saad et al., 2002). The latter method provides a less invasive alternative to phloem-sap collection via cut surfaces. Both methods have their advantages and drawbacks and it was the goal of this study to assess their utility for comparison of phloem protein composition between powdery mildew-infected and control barley plants. The results of our study indicate that a combination of facilitated exudation and aphid stylectomy provides a promising option for future studies.

Materials and methods

Plant and aphid cultivation

H. vulgare cv. Pallas plants were grown in pots placed in controlled environment chambers illuminated by artificial light sources (Philips SON-T Agro 400, HRI-BT 400, Radium Lampenwerk, Wipperfürth, Germany; light intensity $180\,\mu mol\,m^{-2}\,s^{-1}$) under a 16 h day–21 °C/8 h night–18 °C regime at a relative humidity of 70%. The plants were used for phloem-sap collection 8–12 days after germination.

Rhopalosiphum padi aphids were cultivated on 14-day-old *H. vulgare* plants enclosed in perspex boxes (ca. 50 cm × 50 cm × 60 cm) covered with a gauze cloth for better air circulation. Under continuous light ($60\,\mu mol\,m^{-2}\,s^{-1}$, HRI-BT 400, Radium Lampenwerk,

Wipperfürth, Germany), at room temperature and a relative humidity of 60%, apterous aphid colonies developed.

Collection of EDTA-mediated exudates for protein separation

The essentials of the EDTA (Sigma, St. Louis, USA) technique have been described extensively elsewhere (King and Zeevaart, 1974). Barley plants were cut just above the stem/root junction, and immediately re-cut, being submersed in 2.5 mM Na$_2$EDTA, pH 7.0/KOH with a fresh razor blade. The cuttings were incubated in 2.5 mM Na$_2$EDTA, pH 7.0/KOH solution, for 1 h at room temperature. Groups of five plants were transferred with their cut ends into 2 mL Eppendorf cups filled with 1.5 mL 2.5 mM Na$_2$EDTA dissolved in a 1.0 mM MES/KOH buffer (pH 7.0) for one-dimensional (1D) protein separation (Figure 1A). The buffer was omitted in exudation media used for two-dimensional (2D) protein separation. Exudation took place in a water vapour-saturated atmosphere under light ($40\,\mu mol/ms$). The exudates were collected after 8 h and the samples were concentrated by centrifugation (Eppendorf, 5810R, Hamburg, Germany) at 4 °C in 2 mL Vivaspin 2 tubes (Sartorius, Göttingen, Germany) to an end volume of 20 μL.

Collection of stylet exudates for protein separation

The aphids were collected after gently shaking the colonized plants, resulting in the downfall of mainly adults into a plastic box. Adult aphids were placed into cages manufactured from propylene tubes that are glued (solvent-free glue, Pattex) onto the upper surface of barley leaves (Figure 1B,C) and left there overnight for settling and feeding. After cutting the aphid stylets with a microcautery device (Figure 1D) (HF-microcautery unit CF-50, Syntech, Hilversum, the Netherlands) according Fisher and Frame (1984), the cages were flooded with water-saturated silicon oil (Sigma-Aldrich, St. Louis, USA) to prevent contamination or evaporation of the exudates; Figure 1E). The exudates were collected using a borosilicate microcapillary with a tip diameter of 0.1 mm that was connected to a 10 mL syringe (Braun Melsungen, Germany) via a silicone tube with a side valve (Figure 1F). Within the first 6 h, about 6 μL of sieve-tube exudate was collected from nine plants and pooled. About 10 μL sieve-tube exudate was collected during the following 16 h overnight. During overnight collection, the aphid cages were covered with a coverslip to prevent leakage of silicon oil.

One-dimensional and two-dimensional protein separation

Stylet exudates (6 μL) or EDTA-mediated exudates collected from five plants (and concentrated to 20 μL) were separated by SDS-PAGE in one direction. For 2D separation by IEF/SDS PAGE, 20 μL of stylet exudate or 20 μL of EDTA-mediated exudate (after concentration of
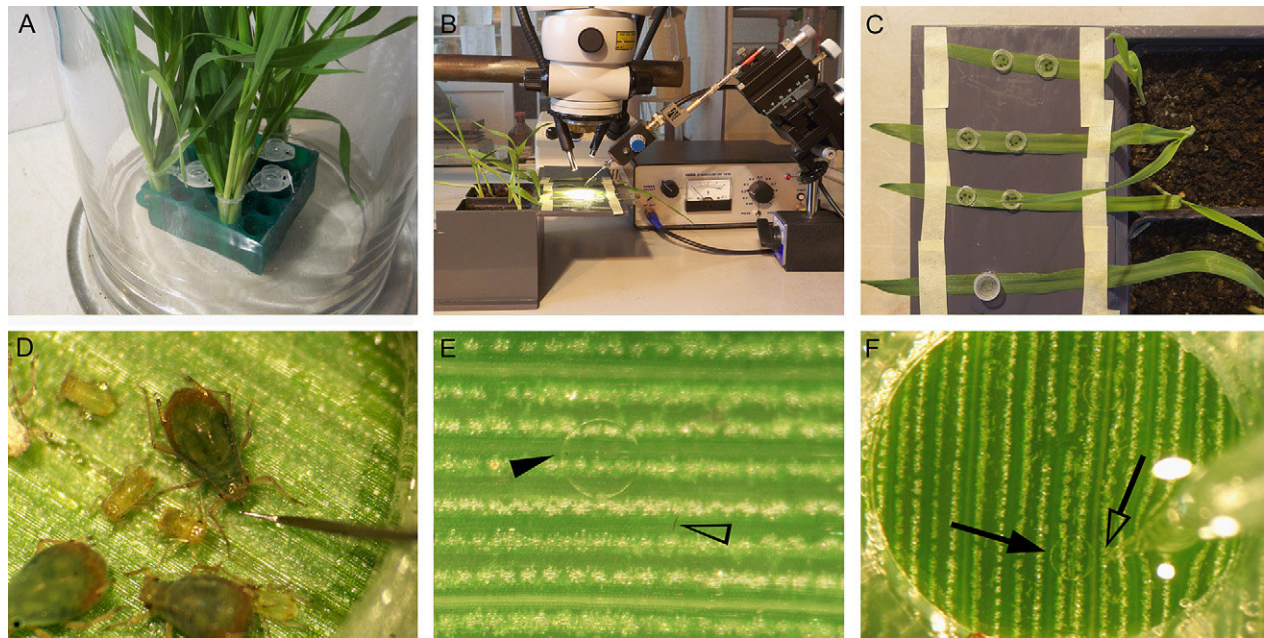
Figure 1. Phloem exudation techniques. (A) EDTA-mediated phloem exudation from excised *Hordeum vulgare* shoots. (B) Working bench with binocular, movable platform and microcautery device for stylectomy. (C) Encaged aphids on *Hordeum vulgare* leaves in lidless cages to display the inside arrangement. Closing off the cages (lowest leaf) prevents the escape of aphids overnight. (D) Microcautery of an aphid (*Rhopalosiphum padi*) by means of a hot tungsten needle. (E) Two cut stylets, one exuding a drop of phloem sap (closed arrow head) and the other non-exuding (open arrow head) inside a cage filled with silicon oil. The white stripes are the main and intermediate parallel veins of the *Hordeum vulgare* leaf. (F) Removal of a phloem sap stylet exudate drop (solid arrow) by means of a glass microelectrode tip (open arrow).

exudate from 20 plants) was applied. 1D separation was performed on 10–16% gradient SDS-PA gels (Laemmli, 1970) in 1D Mini Protean®3 systems (Biorad, Hercules, CA, USA). Proteins including the marker standards (Marker Biorad Precision Plus Protein Standard) were visualized using a combination of silver staining procedures (Switzer et al., 1979; Schoenle et al., 1984). The gels were gently shaken in a fixative containing 50% (v/v) ethanol, 12%(v/v) acetic acid and 0.018% (v/v) formaldehyde, washed in 50% (v/v) ethanol for 3×20 min, immersed in $0.2\,g\,L^{-1}$ sodium thiosulphate for 1 min, rinsed in Millipore water during 3×20 s, submersed in a solution containing $2\,g\,L^{-1}$ silver nitrate in 0.007% (v/v) formaldehyde for 25 min, washed in Millipore water for 2×20 s and fixed in a solution with $60\,g\,L^{-1}$ sodium carbonate, $4\,mg\,L^{-1}$ sodium thiosulphate pentahydrate and 0.005% (v/v) formaldehyde until a good contrast had been reached. The reaction was stopped by 10% (v/v) acetic acid. Molecular weights were calculated with the aid of GelDoc™XR and Quantity One™ (Biorad, München, Germany) and gel images were edited by PD Quest™Basic (Biorad, München, Germany).

For 2D separation, untreated $20\,\mu L$ phloem samples were suspended in $110\,\mu L$ first-dimension buffer (8 M urea, 50 mM DTT, 4% CHAPS and 0.2% carrier ampholytes). The first-step separation was performed in an IEF chamber (Biorad Protean IEF Cell, Biorad, München, Germany) on 7 cm long pH 5–8 IPGstrips (Biorad,

München, Germany) at end voltages of 4000 V and 12,000 V h, respectively. The strips were gently shaken in an equilibration buffer with 2% DTT for 10 min and then for 10 min in an equilibration buffer with 2.5% iodoacetamide. The equilibration buffer was composed of 6 M urea, 2% SDS, 0.05% Tris–HCl, pH 8.8, and 30% glycerol. Separation in the second dimension was performed on 12% SDS-PA gel. Proteins were stained by silver nitrate as mentioned above. Gel images were edited by use of PDQuest™Basic (Biorad); overlay of the edited images was executed by Adobe Photoshop CS2.

Results and discussion

Collection of phloem sap via microcauterized stylets

The essence of so-called stylectomy is that an aphid stylet is cut once the aphid is ingesting phloem sap. As a result, pure and unaltered sieve-tube sap is presumed to exude from the microcauterized stylet stump. A phenomenon seldom appreciated is the transpiration from exuding drops, which leads to a gross overestimation of the solute concentration. Fisher (e.g. Fisher and

Cash-Clarke, 2000) recognized water evaporation as a serious problem. Therefore, we consistently covered the exuding drops with silicon oil in our study (Figure 1E). Use of silicon oil also limited effects of air oxygen on exudate compounds. Oxygen seems to play an important role in the clogging of sieve-element proteins as part of the defence strategies against damage. Drops of cucurbit phloem sap that exude spontaneously from cut sieve tubes show heavy gelling after several minutes probably due to coagulation of redox-sensitive proteins (Alosi et al., 1988). The low oxygen concentration in the phloem would explain why sieve-element proteins do not coagulate under *in situ* conditions (van Dongen et al., 2003). Further, covering of cut stylets with oil also prevents airborne contaminations (Doering-Saad et al., 2002).

At first sight, stylet exudation looks ideal for the collection of pure phloem sap. However, there are some practical problems associated with this method:

(a) The minuscule volume of the exuding drops, which are mainly in the nanolitre range, demands long-lasting routines of exudate sampling. In a typical experiment, 50 "cages" containing the aphids were glued onto *Hordeum* leaves the day before stylet exudate collection. Next day, 45 stylet cauterizations (40%) of about 125 attempts were successful. As about 30% of the cauterized stylets were functional, only 15 stylets were actually exuding. A well-exuding stylet produces 400 nL of sieve-tube sap during 6 h (Figure 1E). Thus, about 1 day is required for the collection of 6 μL of stylet exudates, which is needed for a 1D SDS-PAGE run. Three working days must be invested to collect 20 μL of exudates required for one 2D IEF/SDS-PAGE run. In order to increase yield of phloem sap we tested the delivery of stylet exudate overnight. With well-exuding stylets (production 6 μL in 6 h), exudation was hardly affected during the next 16 h (10.0 μL in 16 h) and the composition remained virtually unaltered during the night (Figure 2).

(b) That aphids trigger defence reactions in plants may induce shifts in the components of the sieve-element sap. Some of the compounds identified in phloem sap may have been triggered by stylet insertion (Thompson and Goggin, 2006; Klingler et al., 2007). However, contamination of stylet exudate by saliva proteins is unlikely given the immense amounts of aphids (several thousands, Will et al., 2007) needed for one usable SDS-PAGE separation of
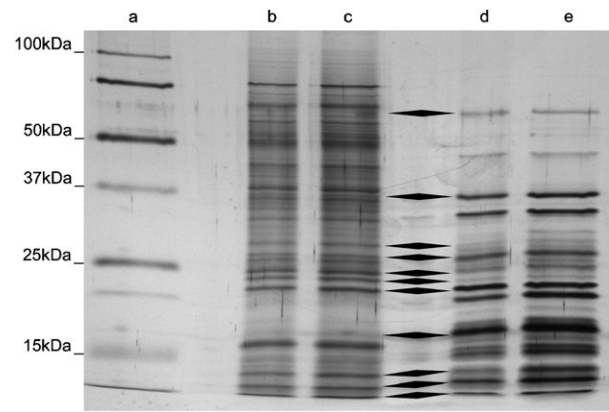

Figure 2. Silver-stained 1D SDS-PAGE (10–16% polyacrylamide) of EDTA-mediated phloem exudates (8 h of exudation time) and phloem sap stylet exudates from *Hordeum vulgare*. (a) Marker lane; (b, c) EDTA-mediated exudates of 6 and 12 μL, respectively; (d, e) exudates sequentially collected from the same group of stylets during the daytime (0–6 h, (d)) and overnight (6–22 h (e)). Common major bands are marked with an arrow.

aphid saliva. Aphid-induced artefacts may not be serious as long as only phloem-sap samples of pathogen-infected and control plants are compared for analysis of differentially expressed proteins.

(c) As soon as the stylet is cut, the supply of watery saliva to the food channel is disrupted suddenly, which has major consequences for the exudation rates. Proteins in the watery saliva of aphids not only sabotage the occlusion of sieve plates by binding free Ca^{2+} in the sieve elements (Will et al., 2007) but also prevent clogging of sieve-element proteins ingested into the food channel (Tjallingii, 2006). In the absence of saliva protein supply after microcautery, sieve-element proteins in the exudate start clogging in the stylet stump. It appears that occlusion mechanisms are generally more elaborate in dicotyledons than in monocotyledons (van Bel, 2006; Will and van Bel, 2006) since dicotyledons allow only a few minutes of exudate collection, producing drops in the picolitre range (van Bel and Biehl, unpublished results). Therefore, use of stylectomy is mainly restricted to monocotyledons, of which larger amounts of phloem sap exuding can be collected for several hours (Hayashi et al., 2000).

An interesting feature is the reduced stylet exudation in infested plants. *H. vulgare* plants infected by *Blumeria graminis* show not only a lower number of exuding stylets (Figure 3A), but also a clearly decreased exudation rate (Figure 3B). As shown in a typical experiment, the amount of
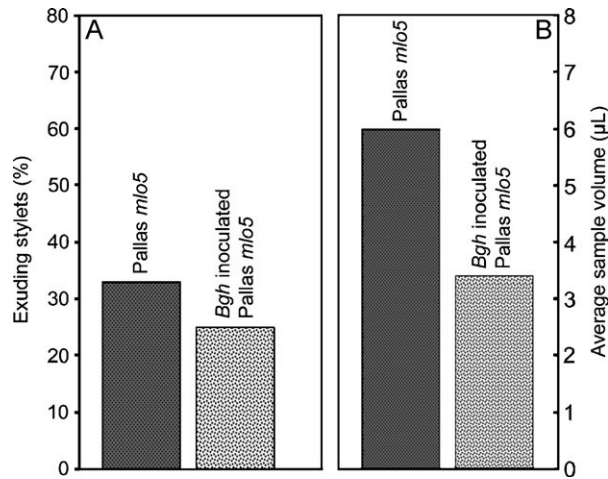
Figure 3. Effect of *Blumeria graminis* (*Bgh*) infection on stylet exudation from *Hordeum vulgare* cv. Pallas *mlo5* leaves. (A) Reductive impact on the success rate of microcauterization expressed as the percentage of exuding stylets. (B) Reductive impact on the average sample volume expressed in microlitres.

exuding stylets was always higher for control than for infected plants (33% vs. 25%, Figure 3A). Infection also induced a reduction to 55% (3.4 vs. 6.0 μL, Figure 3B) in the volume of the exudate drops. Together, this means a reduction to 42% of the exudate volume.

The reason for the lower exudation is unclear. Most likely, depositions in the sieve tubes, induced by the infection, narrow the sieve-tube path (Donofrio and Delaney, 2001) and present obstacles to mass flow. Or pathogens may induce aggregation of water-soluble sieve-element proteins, which may retard mass flow as a result of a higher viscosity. Just as well, the presence of phytopathogens may reduce the rate of phloem loading and, by doing so, decline mass flow through sieve tubes. It was previously shown that both fungal pathogens and aphids induce JA- and salicylic acid-dependent defence pathways (Moran and Thompson, 2001). Down-regulation of phloem transport could be a so far unknown pathogen-triggered defence mechanism, which also has effects on sucking insects.

Collection of phloem sap by use of EDTA-facilitated exudation

A major technical problem associated with collection of phloem sap pertains to the sensitivity of sieve tubes to wounding. Release of wound calcium as the result of cutting the vascular bundles induces the production of protein plugs (Will and

van Bel, 2006) and/or callose constrictions that cause occlusion of the sieve plates (Furch et al., 2007). Therefore, stems or petioles are cut, submersed in solutions with calcium-binding compounds and phloem sap exudation is maintained by adding calcium chelators (e.g. EDTA) to the collection medium (King and Zeevaart, 1974).

Facilitated exudation is a quick and easy method for collection of phloem exudates, but three principal drawbacks have been identified:

(a) The amount of phloem sap released into the exudation medium is unknown, which makes it virtually impossible to calculate protein concentrations in the phloem sap.

(b) It is uncertain to which extent cutting or wounding triggers release of artefactual substances from the cutting surface into the exudation medium.

(c) Most importantly, EDTA is suspected to damage plasma membranes and, hence, to be responsible for an artefactual composition of phloem exudates. At least for amino acids, contamination of exudates seems to be more limited (Weibull et al., 1990, J. Pritchard, personal communication) than reported elsewhere (Girousse et al., 1991). Comparison between amino acid samples acquired by EDTA-mediated exudation and by stylet exudation show negligible qualitative differences for *Avena* (Weibull et al., 1990), *Hordeum* (Weibull et al., 1990) and *Arabidopsis* (J. Pritchard, personal communication) phloem sap. For sugars, too, the effect of EDTA on sugar composition appears to be limited when the exudation is restricted to a few hours (Groussol et al., 1986; Olesinski et al., 1996; Almon et al., 1997; van Bel and Hess, personal communication).

Use of EDTA-facilitated exudation has seldom been applied for analysis of sieve-tube protein composition (Marentes and Grusak, 1998; Hoffmann-Benning et al., 2002), since potential artefacts and the impossibility to quantify sieve-tube contents deemed this method to be unsuitable for conclusive phloem-sap analyses. However, EDTA-mediated exudation may be better than its reputation for our purposes. It is useful when compounds in the phloem sap of pathogen-inoculated and control plants are compared. Under these conditions, EDTA-induced artefacts occurring in both samples are subtracted after digital overlay of the gel images. Importantly, as detailed below, further careful controls of phloem origin of differentially expressed proteins are required.

Protein composition of phloem sap collected using EDTA or cut aphid stylets

To explore the suitability of both methods for the collection of representative phloem-sap samples, the protein composition was compared between the exudates. As previously reported (Fisher, 2000), separation by SDS-PAGE evidenced differences in protein patterns. For samples collected by facilitated exudation, the number of bands (Figure 2, lanes b,c) exceeded that in stylet exudates (Figure 2, lanes d,e) particularly in the higher molecular weight range. Accordingly, 2D IEF/SDS-PAGE also showed a larger variety of proteins in the samples acquired with EDTA (Figure 4A,C). However, major bands in stylectomy samples also showed up in EDTA-facilitated exudates (cf. Figure 4A,C).

Image editing of the 2D gel pictures (Figure 4B,D) yields an appreciable larger number of proteins in the stylet exudate than those readily visible on the crude image (Figure 4A,C). An overlay of the edited 2D pictures (Figure 5) displays only a partial overlap of proteins in stylet and EDTA-mediated exudates. In this respect, the results deviate from those obtained for amino acid composition in barley, rye

and *Arabisopsis* (Weibull et al., 1990; J. Pritchard, personal communication) but are in agreement with the findings of Girousse et al. (1991). The latter authors report on variations in sugar and amino acid content in phloem exudates of *Medicago sativa* depending on the sampling method used.
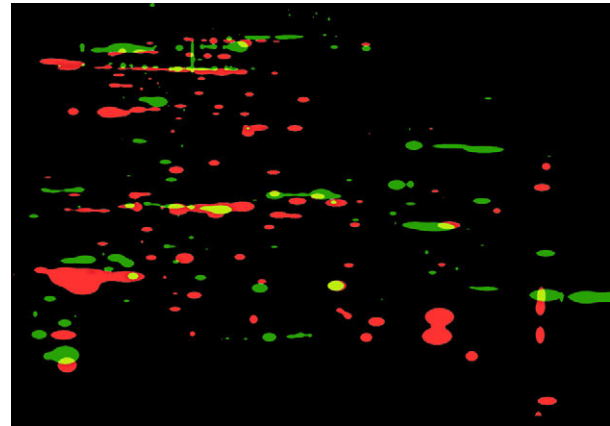

Figure 5. Projection of the two image-edited 2D gels (Figure 4B, D) processed by Adobe Photoshop. The protein spots from the EDTA exudate are false-coloured in red, those from the stylet exudate in green. Overlaying proteins stand out by a yellow colour.
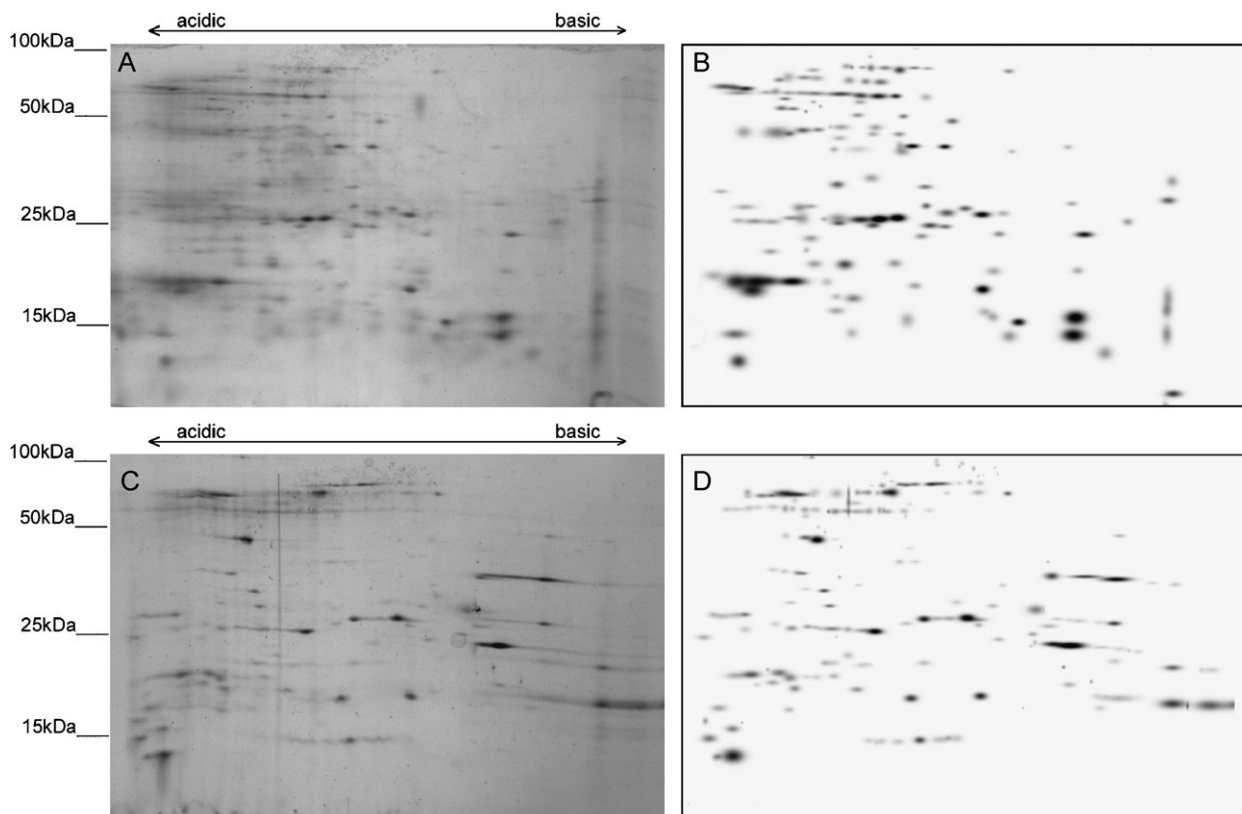

Figure 4. Comparison of silver-stained 2D gels from an EDTA-mediated phloem exudate (A, B) and a stylet exudate (C, D) from *Hordeum vulgare* before (A, C) and after (B, D) image editing by spot detection.

As a first interpretation, solely the overlapping spots represent actual sieve-element proteins in EDTA-exudation samples. It appears that EDTA-facilitated exudation provoked the release of more proteins than those occurring in pure phloem sap sampled by stylectomy (Figures 2 and 5). Many of these proteins are probably contaminations caused by cutting and EDTA effects.

In summary, facilitated exudation is quick and easy but samples contain artefacts, whereas stylectomy is laborious yielding only small amounts of pure phloem sap. Most promising for the purposes of our future work seems to be a combined approach. The EDTA technique may be used for a rough but rapid identification of the changes in the phloem sap in response to powdery mildew infection using 2D electrophoresis, Coomassie staining and mass spectrometry. Spots on 2D gels representing candidates for differentially transported phloem proteins should correspond to a spot on a reference gel loaded with stylectomy samples. A further gel with protein extracts from stem tissue might serve as a negative control.

Acknowledgement

References

Almon E, Horowitz M, Wang H-L, Lucas WJ, Zamski E, Wolf S. Phloem-specific expression of the tobacco mosaic virus movement protein alters carbon metabolism and partitioning in transgenic plants. Plant Physiol 1997;115:1599–607.

Alosi MC, Melroy DI, Park RB. The regulation of gelation of exudates from *Cucurbita* by dilution, glutathione and glutathione reductase. Plant Physiol 1988;86:1089–94.

Barnes A, Bale J, Constantinidou C, Ashton P, Jones A, Pritchard J. Determining protein identity from sieve element sap in *Ricinus communis* L. by quadrupole time of flight (Q-TOF) mass spectrometry. J Exp Bot 2004;55:1473–81.

Behnke H-D, Sjolund RD. Sieve elements. Comparative structure, induction and development. Berlin: Springer; 1990.

Buhtz A, Kolasa A, Arlt K, Walz C, Kehr J. Xylem sap protein composition is conserved among different plant species. Planta 2004;219:610–8.

Cronshaw J, Sabnis DD. Phloem proteins. In: Behnke H-D, Sjolund R, editors. Sieve elements. Comparative structure, induction and development. Berlin: Springer; 1990. p. 257–83.

Doering-Saad C, Newbury HJ, Bale JS, Pritchard J. Use of aphid stylectomy and RT-PCR for the detection of transporter mRNAs in sieve elements. J Exp Bot 2002;53:631–7.

Doering-Saad C, Newbury HJ, Couldridge CE, Bale JS, Pritchard J. A phloem enriched cDNA library from *Ricinus*: insight into phloem function. J Exp Bot 2006; 57:3183–93.

Donofrio NM, Delaney TP. Abnormal callose response phenotype and hypersusceptibility to *Peronospora parasitica* in defense-compromised *Arabidopsis* nim 1-1 and salicylate-expressing plants. Mol Plant Microbe Interact 2001;14:439–50.

Durrant WE, Dong X. Systemic acquired resistance. Annu Rev Phytopathol 2004;42:185–209.

Fisher DB. Long-distance transport. In: Buchanan BB, Gruissem W, Jones RL, editors. Biochemistry and molecular biology of plants. Rockville, MD, USA: American Society of Plant Physiologists; 2000. p. 730–84.

Fisher DB, Cash-Clarke C. Gradients in water potential and turgor pressure along the translocation pathway during grain filling in normally watered and water-stressed wheat plants. Plant Physiol 2000;123: 139–48.

Fisher DB, Frame JM. A guide to the use of the exuding-stylet technique in phloem physiology. Planta 1984; 161:385–93.

Fisher DB, Wu Y, Ku M. Turnover of soluble proteins in the wheat sieve tube. Plant Physiol 1992;100:1433–41.

Furch ACU, Hafke JB, Schulz A, van Bel AJE. Ca^{2+}-mediated remote control of reversible sieve-tube occlusion in *Vicia faba*. J Exp Bot 2007;58:2827–38.

Giavalisco P, Kapitza K, Kolasa A, Buhtz A, Kehr J. Towards the proteome of *Brassica napus* phloem sap. Proteomics 2006;6:896–909.

Gilbertson RL, Rojas MR, Lucas WJ. Plasmodesmata and the phloem: conduits for local and long-distance signalling. In: Oparka K, editor. Plasmodesmata. Oxford: Blackwell Publishing; 2005. p. 162–87.

Girousse C, Bonnemain J-L, Delrot S, Bournoville R. Sugar and amino acid composition of phloem sap of *Medicago sativa*: a comparative study of two collecting methods. Plant Physiol Biochem 1991;29:41–8.

Golecki B, Schulz A, Carstens-Behrens U, Kollmann R. Evidence for graft transmission of structural phloem proteins and their precursors in heterografts of Cucurbitaceae. Planta 1998;206:630–40.

Groussol J, Delrot S, Caruhel P, Bonnemain J-L. Design of an improved exudation method for phloem sap collection and its use for the study of the mobility of pesticides. Physiol Végét 1986;24:123–33.

Harman GE, Howell CR, Viterbo A, Chet I, Lorito M. *Trichoderma* species – opportunistic, avirulent plant symbionts. Nat Rev Microbiol 2004;2:43–56.

Hartung W, Sauter A, Hose E. Abscisic acid in the xylem: where does it come from – where does it go to? J Exp Bot 2002;53:27–32.

Hayashi H, Fukuda A, Suzui N, Fujimaki S. Proteins in the sieve-element companion cell complexes: their detection, localization and possible functions. Aust J Plant Physiol 2000;27:489–96.

Hoffmann-Benning S, Gage DA, McIntosh L, Kende H, Zeevaart JAD. Comparison of peptides in the phloem sap of flowering and non-flowering *Perilla* and lupine plants using microbore HPLC followed by matrix-assisted laser desorption/ionization time-of-flight mass spectrometry. Planta 2002;216:140–7.

Hückelhoven R. Cell-wall associated mechanisms of disease resistance and susceptibility. Annu Rev Phytopathol 2007;45.

Jones JDG, Dangl JL. The plant immune system. Nature 2006;444:323–9.

Kehr J, Buhtz A, Giavalisco P. Analysis of xylem sap proteins from *Brassica napus*. BMC Plant Biology 2005;5:11.

Kessler A, Baldwin IT. Plant responses to insect herbivory. Annu Rev Plant Biol 2002;53:299–328.

King RW, Zeevaart JAD. Enhancement of phloem exudation from cut petioles by chelating agents. Plant Physiol 1974;53:96–103.

Klingler JP, Edwards OR, Singh KB. Independent action and contrasting phenotypes of resistance genes against spotted alfafa aphid and bluegreen aphid in *Medicago trunculata*. New Phytol 2007;173:630–40.

Knoblauch M, van Bel AJE. Sieve tubes in action. Plant Cell 1998;10:35–50.

Kogel K-H, Langen G. Induced disease resistance and gene expression in cereals. Cell Microbiol 2005;7:1555–64.

Laemmli UK. Cleavage of structural proteins during the assembly of the head of the bacteriophage T4. Nature 1970;227:680–5.

Lee GI, Howe GA. The tomato mutant *spr1* is defective in systemin perception and the production of a systemic wound signal for defence gene expression. Plant J 2003;33:567–76.

Li L, Li C, Lee GI, Howe GA. Distinct roles for jasmonate synthesis in the systemic wound response of tomato. Proc Natl Acad Sci USA 2002;99:6416–21.

Maldonado AM, Doerner P, Dixon RA, Lamb CJ, Cameron RK. A putative lipid transfer protein involved in systemic resistance signalling in *Arabidopsis*. Nature 2002;419:399–403.

Marentes E, Grusak MA. Mass determination of low-molecular-weight proteins in phloem sap using matrix-assisted laser desorption/ionization time-of-flight mass spectrometry. J Exp Bot 1998;195:903–11.

Moran PJ, Thompson GA. Molecular responses to aphid feeding in *Arabidopsis* in relation to plant defense pathways. Plant Physiol 2001;125:1074–85.

Nakashima J, Laosinchai W, Cui X, Brown RM. New insight into the mechanism of cellulose and callose biosynthesis; proteases may regulate biosynthesis upon wounding. Cellulose 2003;10:369–89.

Narvaez-Vasquez J, Ryan C. The cellular location of prosystemin: a functional role for phloem parenchyma in systemic wound signalling. Planta 2004;218:360–9.

Narvaez-Vasquez J, Pearce G, Orozco-Cardenas ML, Francheschi VR, Ryan CA. Autoradiographic and biochemical evidence for the systemic translocation of systemin in tomato plants. Planta 1995;195:593–600.

Olesinski AA, Almon E, Navot N, Perl A, Galun E, Lucas WJ, et al. Tissue-specific expression of the tobacco mosaic virus movement protein in transgenic potato plants alters plasmodesmal function and carbohydrate partitioning. Plant Physiol 1996;111:541–50.

Ryan CA, Pearce G. Systemins: a functionally defined family of peptide signals that regulate defensive genes in Solanceae. Proc Natl Acad Sci USA 2003;100: 14577–80.

Sauter A, Davies WJ, Hartung W. The long distance abscisic acid signal: the fate of the hormone on its way from root to shoot. J Exp Bot 2001;52:1991–7.

Scheer JM, Ryan CA. The systemin receptor SR 160 from *Lycopersicum peruvianum* is a member of the LRR receptor kinase family. Proc Natl Acad Sci USA 2002; 99:9585–90.

Schoenle EJ, Adams LD, Sammons DW. Insulin-induced rapid decrease of a major protein in fat cell plasma membranes. J Biol Chem 1984;19:12112–6.

Stratmann JW. Long distance run in the wound response – jasmonic acid is pulling ahead. Trends Plant Sci 2003; 8:247–50.

Switzer RC, Merril CR, Shifrin S. A highly sensitive silver stain for detecting proteins and peptides in polyacrylamide gels. Anal Biochem 1979;98:231–7.

Thompson GA, Goggin FL. Transcriptomics and functional genomics of plant defence induction by phloem-feeding insects. J Exp Bot 2006;57:755–66.

Tjallingii WF. Salivary secretions by aphids interacting with proteins of phloem wound responses. J Exp Bot 2006;57:739–45.

Van Bel AJE. Sieve-pore plugging mechanisms. In: Baluska F, Volkmann D, Barlow PW, editors. Cell–cell channels. Georgetown/New York: Springer Science/Landes Bioscience; 2006. p. 113–8.

Van Bel AJE, Ehlers K. Electrical signalling via plasmodesmata. In: Oparka KJ, editor. Plasmodesmata. Oxford: Blackwell Publishing; 2005. p. 261–78.

Van Bel AJE, Gaupels F. Pathogen-induced resistance and alarm signals in the phloem. Mol Plant Pathol 2004;5: 495–504.

Van Dongen JT, Schurr U, Pfister M, Geigenberger P. Phloem metabolism and function have to cope with low internal oxygen. Plant Physiol 2003;131:1529–43.

Walling LL. The myriad plant responses to herbivores. J Plant Growth Regul 2000;19:195–216.

Walz C, Juenger M, Schad M, Kehr J. Evidence for the presence and activity of a complete antioxidant defence system in mature sieve tubes. Plant J 2002; 31:189–97.

Walz C, Giavalisco P, Schad M, Juenger M, Klose J, Kehr J. Proteomics of cucurbit phloem exudate reveals a network of defence proteins. Phytochemistry 2004;65: 1795–804.

Weibull J, Ronquist F, Brishammer S. Free amino acid composition of leaf exudates and phloem sap. Plant Physiol 1990;92:222–6.

Will T, van Bel AJE. Physical and chemical interactions between aphids and plants. J Exp Bot 2006;47:729–37.

Will T, Tjallingii WF, Thönnessen A, van Bel AJE. Molecular sabotage of plant defense by aphids. Proc Natl Acad Sci USA 2007;104:10536–41.

RESEARCH PAPER

Adaptation of aphid stylectomy for analyses of proteins and mRNAs in barley phloem sap

Frank Gaupels[1,2,*], Anja Buhtz[3], Torsten Knauer[2], Sachin Deshmukh[1], Frank Waller[1], Aart J. E. van Bel[2], Karl-Heinz Kogel[1] and Julia Kehr[3,†]

[1] Institute of Phytopathology and Applied Zoology, IFZ, Heinrich-Buff-Ring 26–32, D-35392 Gießen, Germany

[2] Plant Cell Biology Research Group, Institute of General Botany, Senckenbergstrasse 17, D-35390 Gießen, Germany

[3] Max Planck Institute of Molecular Plant Physiology, Department Lothar Willmitzer, Am Mühlenberg 1, D-14424 Golm/Potsdam, Germany

Abstract

Sieve tubes are transport conduits not only for photo-assimilates but also for macromolecules and other compounds that are involved in sieve tube maintenance and systemic signalling. In order to gain sufficient amounts of pure phloem exudates from barley plants for analyses of the protein and mRNA composition, a previously described stylectomy set-up was optimized. Aphids were placed in sealed cages, which, immediately after microcauterization of the stylets, were flooded with water-saturated silicon oil. The exuding phloem sap was collected with a capillary connected to a pump. Using up to 30 plants and 600 aphids (*Rhopalosiphum padi*) in parallel, an average of 10 µl of phloem sap could be obtained within 6 h of sampling. In first analyses of the macromolecular content, eight so far unknown phloem mRNAs were identified by cDNA-amplified fragment length polymorphism. Transcripts in barley phloem exudates are related to metabolism, signalling, and pathogen defence, for example coding for a protein kinase and a pathogen- and insect-responsive WIR1A (wheat-induced resistance 1A)-like protein. Further, one-dimensional gel electrophoresis and subsequent partial sequencing by mass spectrometry led to the identification of seven major proteins with putative functions in stress responses and transport of mRNAs, proteins, and sugars. Two of the discovered proteins probably represent isoforms of a new phloem-mobile sucrose transporter. Notably, two-dimensional electrophoresis confirmed that there are >250 phloem proteins awaiting identification in future studies.

Key words: Aphid, barley, cDNA-AFLP, mRNA, phloem, protein, *Rhopalosiphum padi*, signalling, stylectomy, two-dimensional gel electrophoresis.

Introduction

The past few years have brought new insights into functions of the phloem in addition to the transport of assimilates from source leaves to sink organs. Meanwhile, systemic signalling is an issue of increasing importance. For instance, phloem translocation of auxin was shown to be essential for regulation of polar growth (Kramer and Bennett, 2006), while salicylic acid and jasmonic acid were detected in sieve tube exudates and suggested to be involved in systemic acquired pathogen resistance (Durrant and Dong, 2004) and the systemic wound reaction (Schilmiller and Howe, 2005).

Besides such small and highly mobile substances, macromolecules present in sieve tubes are being increasingly studied. The major reason is that mature sieve elements (SEs) lose their capability for transcription and translation during differentiation, and therefore any macromolecule in the phloem transport fluid is likely to be imported from the adjacent companion cells (CCs) and constitutes a potential signalling compound. Phloem-mobile

mRNAs were shown to be involved in the regulation of meristem differentiation and leaf development (Lough and Lucas, 2006; Kehr and Buhtz, 2008). By the use of grafting approaches, it was, for example, demonstrated that mRNAs of genes that were mutated in a *KNOTTED*-like transcription factor or the gene *GIBBERRELIC ACID INSENSITIVE* were systemically transported from mutant stocks via the phloem into scions, where they caused the mutant phenotype in differentiating young leaves (Kim *et al.*, 2001; Haywood *et al.*, 2005).

That proteins can also transfer information via the phloem was recently demonstrated in several published studies describing the phloem transport of the protein FLOWERING LOCUS T that leads to the induction of flowering in different plant species (Corbesier *et al.*, 2007; Jaeger and Wigge, 2007; Tamaki *et al.*, 2007; Aki *et al.*, 2008). Moreover, some proteins function in distal signalling as carriers for messenger molecules such as RNAs, proteins, and lipid-derived compounds (van Bel and Gaupels, 2004; Kehr, 2006). On the other hand, proteins also maintain efficiency and longevity of sieve tubes, by protecting SEs from biotic and abiotic stresses. For example, an antioxidant defence system and a set of protease inhibitors were detected in phloem exudates, and other proteins are involved in sugar metabolism (Hayashi *et al.*, 2000; Walz *et al.*, 2002, 2004; Giavalisco *et al.*, 2006).

There is meanwhile clear evidence that phloem macromolecules fulfil an important role in whole-plant integration of developmental processes and stress responses, and this underlines the need for a deeper knowledge about the macromolecular composition of the phloem transport fluid. Using the model plants *Ricinus communis*, *Brassica napus*, and various cucurbits, which allow easy sampling by incisions in stems and petioles, >100 proteins and hundreds of mRNAs were identified (Hayashi *et al.*, 2000; Barnes *et al.*, 2004; Walz *et al.*, 2004; Doering-Saad *et al.*, 2006; Giavalisco *et al.*, 2006; Kehr, 2006; Omid *et al.*, 2007; Ruiz-Medrano *et al.*, 2007). Vilaine *et al.* (2003) analysed the mRNA content of isolated celery (*Apium graveolens*) phloem strands by cDNA macroarray and construction of a cDNA library with subsequent sequencing of clones. However, with this approach it was not possible to distinguish between immobile CC- and mobile sieve tube-derived transcripts. Bearing in mind that the total number of both proteins and mRNAs is >1500 in pumpkin sieve tubes, as estimated by Lough and Lucas (2006), efficient sampling and screening techniques are urgently required.

To date, most comprehensive approaches are underway in dicots and only little progress was achieved in deciphering the macromolecular phloem composition of the economically highly important monocot species. In rice, 111 proteins could be identified (Ishiwatari *et al.*, 1995; Fukuda *et al.*, 2004*a*, *b*; Suzui *et al.*, 2006; Aki *et al.*, 2008), whereas no phloem proteins from other monocot species are as yet known. In addition, six mRNAs were found in barley and rice coding for thioredoxin h, actin, oryzacystatin-1, sucrose transporter 1, proton ATPase, and aquaporin (Sasaki *et al.*, 1998; Doering-Saad *et al.*, 2002).

While sieve tube exudates from incisions were shown to be contaminated by cell contents of injured tissues surrounding the phloem (Ruiz-Medrano *et al.*, 1999), stylectomy is regarded to yield pure phloem sap (Fisher *et al.*, 1992; Sasaki *et al.*, 1998; Doering-Saad *et al.*, 2002). In this report, the application of a high-throughput stylectomy set-up for identification of authentic barley phloem mRNAs and proteins is described.

Materials and methods

Plant material and aphids

Hordeum vulgare L. cv. Ingrid plants were grown in pots placed in controlled-environment chambers illuminated by artificial light sources (Philips SON-T Agro 400, HRI-BT 400, Radium Lamp-enwerk, Wipperfürth, Germany; light intensity 180 μmol m^{-2} s^{-1}) under a 16 h day–21 °C/8 h night–18 °C regime at a relative humidity of 70%. The plants were used for phloem sap collection 8–12 d after germination. *Rhopalosiphum padi* aphids were cultivated on 2- to 4-week-old barley plants enclosed in perspex boxes (~50 cm×50 cm×60 cm) covered with a gauze cloth, under continuous light (60 μmol m^{-2} s^{-1}, HRI-BT 400, Radium Lampenwerk, Wipperfürth, Germany), at room temperature and a relative humidity of 60%.

Aphid stylectomy

Between five and 10 aphids were placed into cages manufactured from propylene tubes, two of which were fixed onto the upper surface of each first barley leaf with a solvent-free glue (Fig. 1A). After the aphids had settled overnight, stylets were cut with a microcautery device (Fig. 1B, D) (HF-microcautery unit CF-50, Syntech, Hilversum, The Netherlands) according to Fisher and Frame (1984). Immediately after cutting off the stylets, cages were flooded with water-saturated silicon oil DC 200 (Sigma-Aldrich, St Louis, MO, USA) to prevent contamination or evaporation of the exudates (Fig. 1C), and leaves were transferred to a second platform. Every 30 min phloem exudates were collected using a borosilicate microcapillary with a tip diameter of 0.1 mm and backloaded with oil (Fig. 1C, E). The capillary was connected to a pump, and pressure could be fine-tuned with a valve. Exudates were collected for 6 h while keeping the pooled samples on ice, and the total volume was estimated with a microlitre-scaled capillary.

RNase test of phloem samples

RNA integrity/degradation was analysed by detecting the rRNA peaks of a barley leaf total RNA sample on an Agilent 2100 Bioanalyzer (Agilent Technologies, Palo Alto, CA, USA) following the Agilent RNA 6000 Nano assay reagent kit guide using the Eukaryote Total RNA Nano assay. A 200 ng aliquot of the RNA sample was incubated with serial dilutions of RNase A (20 mg ml^{-1}; Sigma), a barley total leaf extract, or with phloem sap samples in a 10 μl reaction volume for 30 min at 25 °C. A 1 μl aliquot of each of these reactions was separated on the Agilent 6000 chip.
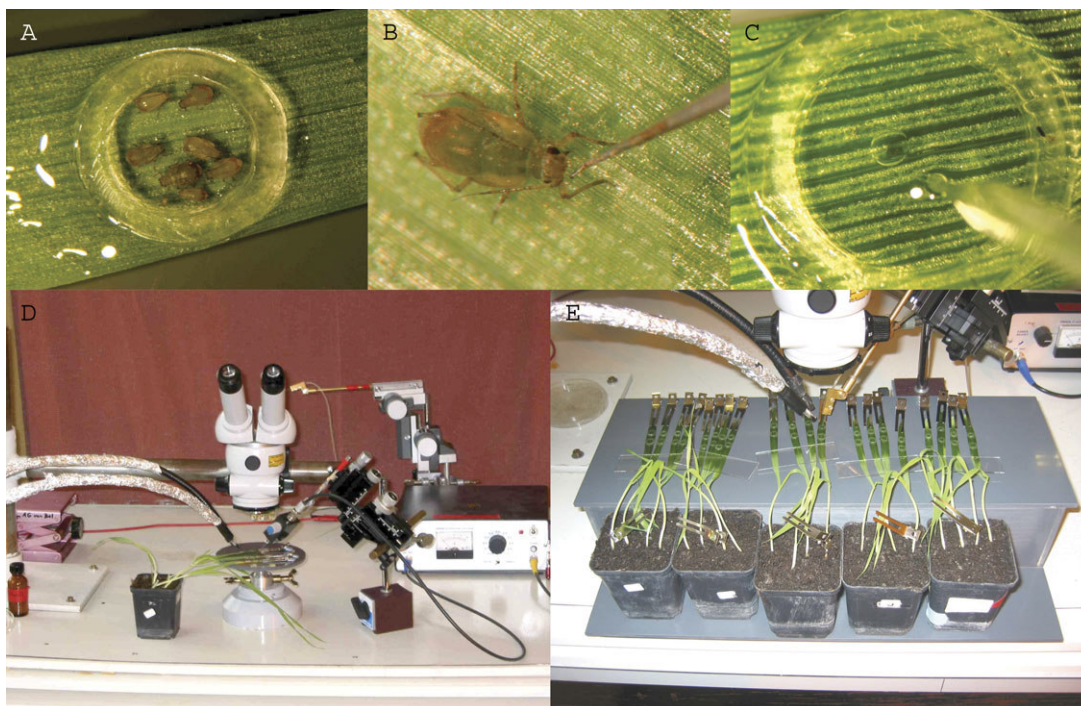
Fig. 1. Aphid stylectomy with barley. (A) Aphids (*Rhopalosiphum padi*) on a barley leaf. The cage was fixed and sealed with glue. (B) Cutting off the stylet of the aphids with a hot tungsten needle. (C) The cage flooded with silicon oil. Collection of exuding phloem sap with a capillary. (D) Work bench with binocular platform which can be raised and lowered, and turned, microcautery unit, and capillary (background). (E) Barley leaves with flooded cages placed on a platform for collection of phloem exudates.

cDNA-AFLP

Poly(A)$^+$ RNA was isolated from 5 μl of barley phloem sap using a Dynabeads Oligo (dT)$_{25}$ mRNA Purification Kit (Dynal, Hamburg, Germany) according to the manufacturer's instructions, and cDNA synthesis was performed with SUPERSCRIPT II RNase H$^-$ Reverse Transcriptase (Gibco-BRL, Karlsruhe, Germany). cDNA-amplified fragment length polymorphism (AFLP) was carried out following a protocol of R Bruggmann, University of Zürich, Switzerland. The method was originally published by Bachem *et al.* (1996) and applied to barley plants by Eckey *et al.* (2004).

cDNA from phloem mRNA was digested with the restriction enzymes *Sau*3AI and *Nco*I, and the following adaptors were ligated to the cut ends: *Sau*3AI adaptor top strand 5′-AGCGAT-GAGTCCTGAG; *Sau*3AI adaptor bottom strand 5′-TACTCAG-GACTCCTAG; *Nco*I adaptor top strand 5′-CCTGTAGACT-GCGTACAC; and *Nco*I adaptor bottom strand 5′-CATCTGACG-CATGTGGTAC. Primers against the adaptor sequences were used for pre-amplification of the cDNA pool: *Sau*3AI pre-amplification primer (S+0 primer) 5′-ATGAGTCCTGAGGATC; and *Nco*I pre-amplification primer (N+0 primer) 5′-AGACTGCGTACAC-CATGG. For selective amplification of a subset of the total cDNA pool, the unspecific N+0 primer was [γ-^{33}P]dATP end-labelled and combined with one of seven selective *Sau*3AI (S-) primers, which consisted of the nucleotides 5′-ATGAGTCCTGAGGATC+NN-3′, with NN representing +AG (S1 primer), +AC (S2), +TA (S3), +TT (S4), +TG (S5), +TC (S6), and +GG (S7). Conditions for pre-amplification PCR were 30 s at 94 °C, 1 min at 60 °C, 2 min at 72 °C (30 cycles). Selective touch-down settings were 30 s at 94 °C, 30 s at 65 °C (–1 °C cycle^{-1}) and 2 min at 72 °C (nine cycles), 30 s at 94 °C, 30 s at 57 °C, and 2 min at 72 °C (25 cycles). After separation of amplification products on an 8% polyacrylamide gel, the gel was dried onto 3MM Whatman paper (Whatman,

Maidstone, UK) and exposed to Kodak Biomax MR film for 24 h. Bands were cut from the gel and cDNA was reamplified with the N+0 and S+0 primers. Subsequently, cDNAs were subcloned and sequenced. Sequences of transcript-derived fragments were compared with the entries of NCBI (National Center for Biotechnology Information, Bethesda, MD, USA) and TIGR (The Institute for Genomic Research, Rockville, MD, USA) databases employing the BLAST (Basic Local Alignment Search Tool) algorithm tool (Altschul *et al.*, 1997).

Protein determination, gel electrophoresis, and mass spectrometry

The protein concentration of 1 μl of barley phloem sap in a 500 μl sample volume was determined with the Bradford assay (Bradford 1976). Preparative one-dimensional electrophoresis of phloem proteins was done as described previously (Walz *et al.*, 2002) and proteins were stained overnight using the Novex Colloidal Blue Staining Kit (Invitrogen, San Diego, CA, USA). Bands were cut, gel pieces destained, and proteins digested with trypsin. After extraction from the gel and desalting, peptides were analysed with an ESI-Q-TOF (electrospray ionization-quadrupole time-of-flight) mass spectrometer (Micromass, Altrincham, UK) as described in Walz *et al.* (2002).

SDS–PAGE and silver staining have been described previously in Gaupels *et al.* (2008). Two-dimensional electrophoresis with a phloem sap volume equivalent to 5 μg of protein was carried out in the Bioanalytics group, Institute of Molecular Biotechnology, RWTH Aachen, Germany, using the Protean IEF in combination with the Mini-Protean gel electrophoresis system (Bio-Rad, München, Germany). Proteins were visualized with silver stain. Further details can be found at www.molbiotech.rwth-aachen.de.

Results and Discussion

Limitations in conducting phloem research with monocots are mostly caused by difficulties with phloem sampling. In contrast to various dicot species such as cucurbits, rice, yucca, lupin, or oilseed rape that allow the comparably easy collection of phloem sap exuding spontaneously from small incisions (Ziegler, 1975; Kehr and Rep, 2006), there seems to be only one monocot species, *Triticum aestivum*, showing spontaneous phloem exudation from grain pedicles in sufficient amounts for subsequent analyses (Fisher and Gifford, 1986; Fisher *et al.*, 1992). EDTA exudation and insect stylectomy offer two alternative ways of obtaining phloem samples from monocots, since they are mostly independent from the experimental plant species.

Facilitated exudation using the chelator EDTA to prevent calcium-dependent sieve tube occlusion by proteins and callose (King and Zeevaart, 1974) is a quick and easy method, but can lead to a significant amount of contamination. EDTA renders cell membranes permeable, causing contamination of the phloem sap by cell contents from surrounding tissues and, in addition, apoplastic contents can reach the exudates (Girousse *et al.*, 1991; van Bel and Gaupels, 2004). In contrast, insect stylectomy, where stylets of phloem-feeding insects are excised to collect the exuding phloem contents (Kennedy and Mittler, 1953; Fisher *et al.*, 1992), is regarded as a method that provides pure phloem samples from monocots (Fisher *et al.*, 1992; Sasaki *et al.*, 1998; Doering-Saad *et al.*, 2002). Gaupels *et al.* (2008) concluded from their studies with barley that stylectomy is the reference method for identification of phloem macromolecules from monocots. The purity of phloem exudates is particularly important for avoiding artefacts in mRNA analysis, since the copy number of phloem transcripts is probably very low (Doering-Saad *et al.*, 2002). Facilitated exudation may, however, be a useful tool for functional analyses of known phloem compounds in subsequent studies.

The main drawback of stylectomy is that it is time consuming and yields only small sample volumes in the nanolitre scale (Gaupels *et al.*, 2008). In order to circumvent this restriction, a set-up was developed for aphid stylectomy that allows the use of many plants and cut aphid stylets in parallel. The resultant barley exudates were analysed by cDNA-AFLP, one-dimensional SDS–PAGE followed by mass spectrometry, and two-dimensional electrophoresis. Eight transcripts previously unknown to be present in sieve tubes and seven proteins (two unknowns) could be identified, and their putative functions in the phloem are discussed.

Improved insect stylectomy

To carry out broad-spectrum analyses of the macromolecular content in barley phloem sap it was necessary to increase the efficiency of the previously described style-

ctomy method (Gaupels *et al.*, 2008). In the improved experimental set-up, small plastic rings were fixed on the leaves and sealed with solvent-free glue, serving as cages for 5–10 aphids (Fig. 1A). The cages restrict aphids to a certain place on the leaf and at the same time allow easy access for cutting off the stylets. Modified cages can be easily attached to various plant organs including stems and petioles (not shown). Aphids were allowed to settle overnight and stylets were cut the next morning using a microcautery unit and a platform which could be raised and lowered, and turned (Fig. 1B, C). About five well-exposed stylets were cut per cage and immediately covered with water-saturated silicon oil to avoid evaporation and contaminations (Doering-Saad *et al.*, 2002). In water-saturated silicon oil DC 200, phloem exudates form spherical droplets on the inert chitin stylet stump (Fig. 1C). The exudate does not come into contact with air or the surface of the leaf. In this way, contamination or modifications (e.g. oxidation) of mRNAs and proteins can be reliably prevented. Leaves were then transferred to another platform for collection of exuding phloem sap using a microcapillary filled with silicon oil and connected to a pump (Fig. 1E).

Exposure to room temperature during the experiment did not seem to affect sample quality, probably because there is no mRNase activity in pure phloem exudates (Sasaki *et al.*, 1998; Doering-Saad *et al.*, 2002), and the presence of various protease inhibitors protects proteins from degradation (Kehr, 2006). Accordingly, no change in protein patterns or evidence for protein degradation could be detected even after 16 h of exudation under oil (Gaupels *et al.*, 2008).

From an average of 46 exuding stylets, $\sim$10 µl of phloem sap could be obtained within 6 h of sampling (Table 1). The exudate volume per stylet was 0.22 µl and the estimated exudation rate was $\sim$0.05 µl h^{-1} stylet^{-1} (Table 1). This corresponds well to the 0.06–0.12 µl h^{-1} stylet^{-1} reported in an earlier study with barley (Doering-Saad *et al.* 2002). A protein concentration of 0.4 µg µl^{-1} (Table 1) was measured, which is somewhat higher than the reported 0.1 µg µl^{-1} and 0.2 µg µl^{-1} in wheat and rice phloem exudates, respectively (Schobert *et al.*, 1998). However, the exudation rate and protein concentration of

Table 1. *Sampling of barley phloem sap by aphid stylectomy—facts and numbers*

Number of leaves per experiment	20–30
Cages/leaf	2
Aphids/cage	10
Exuding stylets/experiment	46$\pm$10 (n=9)
Exudation volume/experiment	10$\pm$3 µl ($n = 9$)
Exudation volume/stylet	0.22 µl
Exudation volume h^{-1} stylet^{-1}	$\sim$0.05 µl
Protein concentration of exudates	0.40$\pm$0.16 µg µl^{-1} (n=7)

phloem sap depend on the developmental stage and growth conditions of the plants, as shown for *R. communis* (Sakuth *et al.*, 1993). Moreover, abiotic and biotic stress such as pathogen infection can have a significant impact on the yield of phloem samples (Gaupels *et al.*, 2008; F Gaupels, unpublished observation).

In the present study, using up to 30 plants and 600 aphids in parallel, an average of 10 µl of pure phloem sap could be obtained within 6 h of sampling. Altogether, it was possible to collect and analyse >150 µl of barley phloem sap.

Quality control of phloem samples collected by aphid stylectomy

Previously, the purity of phloem samples was assessed by determination of the RNase activity (Sasaki *et al.*, 1998; Doering-Saad *et al.*, 2002). Addition of 40, 8, and as little as 1.6 ng ml^{-1} RNase A to a barley leaf RNA sample caused significant degradation of the RNA (Fig. 2), which could be visualized in an Agilent Bioanalyzer 2100. The RNase content in leaf extracts (0.5 g ml^{-1}) corresponded to the 40 ng ml^{-1} RNase A standard, while no RNase activity was detectable in phloem sap (Fig. 2). Similarly, RNases were absent in stylectomy samples from rice and barley (Sasaki *et al.*, 1998; Doering-Saad *et al.*, 2002). As
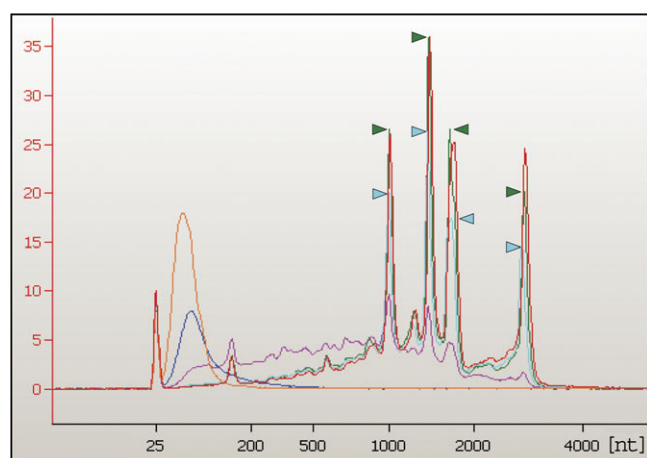

Fig. 2. Determination of RNase activity in stylectomy exudate of barley plants. RNase activity was tested with barley leaf total RNA. Samples were separated and visualized using an Agilent Bioanalyzer 2100. Phloem sap (green), leaf extract (blue), water (red), or 1.6 ng ml^{-1} (light blue), 8 ng ml^{-1} (pink), or 40 ng ml^{-1} (orange) RNase A standards were added to total RNA. RNase activity caused a decrease in the amount of high molecular weight rRNA—visible as four peaks between 1000 and 3600 nucleotides (nt)—and an accumulation of low molecular weight RNA fragments between 25 and 900 nt. Note that the peak maxima for the 1.6 ng ml^{-1} RNase A standard (light blue arrowheads) are consistently lower than the peak maxima for the phloem sample (green arrowheads) and the water control (red curve), whereas the light blue curve runs on top of the red and green (less pronounced) curves in the low molecular weight range. RNA concentration is depicted in arbitrary units and plotted versus the molecular weight in nucleotides determined by an internal RNA size marker.

a second quality control, phloem samples were analysed by RT-PCR with primers against the coding sequence for Rubisco small subunit (rbcS), because SEs are not photosynthetically active and should therefore not contain this protein (Ruiz-Medrano *et al.*, 1999; Giavalisco *et al.*, 2006). No specific rbcS product could be detected with 0.5 or 2 µl of barley phloem sap after 30, or even after 60 cycles of RT-PCR, while 30 cycles were sufficient to produce visible rbcS bands when using leaf extracts as template (results not shown).

Taken together, the results of both approaches indicate that the obtained samples are of high purity and not contaminated by the contents of leaf cells.

Identification of mRNAs in phloem exudates of barley by cDNA-AFLP

The first endogenous plant mRNA that was reliably found inside SEs and the plasmodesmata connecting SEs to CCs by immunolocalization was mRNA of the sucrose transporter 1 (SUT1) in *Solanaceae* (Kühn *et al.*, 1997). Since then, mRNAs for thioredoxin h, cystatin, and actin have been detected by RT-PCR in the phloem from rice and *Brassica* (Sasaki *et al.*, 1998; Giavalisco *et al.*, 2006). Other approaches resulted in the collection of several functionally unrelated mRNAs from *Cucurbita maxima* exudate (Ruiz-Medrano *et al.*, 1999) and a phloem-enriched cDNA library from *Ricinus* (Doering-Saad *et al.*, 2006). There have been only two studies published regarding monocot species that found several transcripts, including SUT1, aquaporin, and a proton ATPase, in phloem sap of barley (Doering-Saad *et al.*, 2002), and actin, cystatin, and thioredoxin from rice (Sasaki *et al.*, 1998), by RT-PCR using gene-specific primers.

With small amounts such as samples from aphid stylectomy, RT-PCR has so far been the only option available to evaluate the presence of specific transcripts inside the phloem (Sasaki *et al.*, 1998; Doering-Saad *et al.*, 2002). To ensure that the phloem collection method is suitable for transcript analysis from barely phloem samples, the differential display technique cDNA-AFLP was applied, since this strategy, in contrast to RT-PCR with specific primers, represents an unbiased approach for transcript analysis. cDNA-AFLP allows both sensitive detection and identification of transcripts as well as analysis of gene expression upon treatment (e.g. infection) of plants (Bachem *et al.*, 1996; Eckey *et al.*, 2004). After extraction of poly(A)$^+$ RNA, reverse transcription, and amplification, cDNA was digested, yielding theoretically one adaptor-ligated cDNA fragment for each poly(A)$^+$ RNA species present in the original sample. Using primers against the adaptor sequence with a two base overhang specific for the fragment sequence, it was possible to divide the total cDNA pool into subsets of ^{33}P-labelled amplification products that were then

separated on polyacrylamide gels. Subsequently, fragment cDNAs were extracted from the gel, sequenced, and mRNAs were identified by database searches.

The method used 5 µl of barley phloem sap with a combination of an unspecific N+0 primer and seven (out of 16) specific S-primers. Application of the N+0 primer led to unspecific detection of fragments with more than one primer combination [Table 2, see imidazoleglycerol-phosphate synthase (IGPS), carbonic anhydrase, and protein kinase]. An increase in the amount of sample and use of specific N-primers should prevent this problem in future experiments. A total of 23 bands were extracted from polyacrylamide gels. cDNAs were reamplified and yielded 15 sequences of good quality. Database searches with the 10 non-redundant sequences allowed identification of eight phloem mRNAs, whereas two sequences yielded no database hits (see Supplementary data available at *JXB* online).

None of these transcripts was described previously in the phloem of other plant species, and the translation product of only one mRNA (ferredoxin, electron transfer) has also been detected as a phloem protein in *B. napus* (G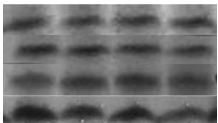iavalisco *et al.*, 2006). However, transcripts from the same functional categories (metabolism, defence, signalling) have been found in earlier studies (Doering-Saad *et al.*, 2006; Omid *et al.*, 2007; Ruiz-Medrano *et al.*, 2007). For instance, IGPS is an enzyme of the histidine biosynthesis pathway, while elongin C is involved in protein processing by the ubiquitin system, which is a major functional category also found among *R. communis* and melon phloem mRNAs (Doering-Saad *et al.*, 2006; Omid *et al.*, 2007). Glycosyl transferases modify secondary metabolites, thereby regulating their storage and functions, for example in pathogen and herbivore defence (Gachon *et al.*, 2005).

Particularly interesting with respect to a putative role as phloem-translocated signals are the transcripts coding for a protein kinase, carbonic anhydrase, and a protein homologous to both WIR1A and a planthopper-inducible protein. These proteins are involved in signalling and defence reactions to pathogens and phloem-sucking insects (Bull *et al.*, 1992; Slaymaker *et al.*, 2002; Yuan *et al.*, 2004). Interestingly, after infection of pumpkin plants with cucumber mosaic virus, Ruiz-Medrano *et al.*, (2007) detected phloem mRNAs coding for the pathogen defence proteins PR1, a glucanase, and an F-box protein.

Table 2.   *cDNA-AFLP with phloem sap of barley*
For fragment sequences, see Supplementary Table S1 at JXB online.

At, *Arabidopsis thaliana*; Hv, *Hordeum vulgare*; Os, *Oryza sativa*.

Code[a]	cDNA-AFLP[b] bands 1 2 3 4	Length(bp)	Database search with BLASTN[c]: expected value, identities	Database search with BLASTX[c]: expected value, identities
S1-02 S5-14 S4-18 S7-23		92	BE213945 (*Hv*): $3e^{-44}$, 100%	Imidazoleglycerol-phosphate synthase subunit H-like: NP568922 (*At*) $1e^{-04}$, 70%
S2-03		134	BE421279 (*Hv*): $5e^{-62}$, 97%	Putative ferredoxin: AC087851 (*At*) $3e^{-14}$, 79%
S2-04		77	CD054184 (*Hv*): $4e^{-30}$, 97%	Hom.[d]: WIR1A protein, planthopper-inducible protein-like
S2-05		97	CD056186 (*Hv*): $7e^{-45}$, 97%	Putative regulatory protein: AA037940 (*Os*) $2e^{-10}$, 100%
S2-07 S1-15		172	CD057212 (*Hv*): $4e^{-51}$, 93%	Hom.: carbonic anhydrase
S3-09 S6-20		99	AV936683 (*Hv*): $1e^{-34}$, 97%	Protein kinase family: NP17196 (*At*) $7e^{-13}$, 100%
S5-13		82	AV939559 (*Hv*): $2e^{-23}$, 90%	Hom.: putative glycosyl transferase
S6-19		88	CA024028 (*Hv*): $5e^{-36}$, 96%	Hom.: elongin C

[a] Spezific S-primer (combined with unspecific N+0 primer)—serial number of the band.
[b] Four independent phloem samples.
[c] Homology search with BLASTN in EST- and with BLASTX in protein databases of NCBI and TIGR.
[d] Sequence of EST used for homology search with BLAST.

Such stress- and signalling-related mRNAs could be translated into proteins or could induce gene expression within the phloem or in distant target tissues. However, to date, it is completely unknown if these RNAs are localized in the phloem by accident or if they fulfil a specific function as signalling molecules.

SEs lack nuclei and a functional transcription and translation machinery. The SE–CC complexes are symplastically isolated, with only a few plasmodesmata connecting them to surrounding tissue. Hence, mRNAs in sieve tube sap most probably originate from CCs. The RNAs thus either could represent accidental RNA outflow from CCs to SEs, could fulfil unknown local duties, or could function in systemic signal transduction, as has been demonstrated for specific mRNAs. Phloem transport of a *CmNACP* mRNA from pumpkin could be directly demonstrated by heterograft experiments between pumpkin and cucumber plants, in which *CmNACP* transcripts from a pumpkin stock moved to cucumber scion tissues (Ruiz-Medrano *et al.*, 1999). Also movement of the transcript of a *KNOTTED1*-like homeobox gene has been demonstrated in tomato (Kim *et al.*, 2001), and a *BEL1*-like transcription factor was graft-transmissible in potato (Banerjee *et al.*, 2006). The same was observed for another gene, *GIBBERELLIC ACID INSENSITIVE* (GAI), in *Cucurbita maxima* and *Arabidopsis* gain-of-function mutants (Haywood *et al.*, 2005). In all these cases, the transport of mRNA led to observable phenotypic alterations, which indicates a physiological function for mRNA transport.

Future studies will be needed to establish functions for the growing set of as yet unknown mRNAs found in the phloem in the present and in previous studies.

Identification of barley phloem proteins by mass spectrometry after SDS–PAGE

One-dimensional electrophoresis was used to separate the proteins prior to trypsin digestion and identification by mass spectrometry. Despite the low amounts of protein loaded and the weak Coomassie staining (Fig. 3A), proteins could be assigned in seven protein bands (Table 3). Silver staining confirmed that the analysed bands represent major phloem proteins (Fig. 3B). Among the identified proteins were ubiquitin, thioredoxin h, cyclophilin, and a glycine-rich RNA-binding protein that were also found at detectable levels in phloem samples from other plant species (Barnes *et al.*, 2004; Giavalisco *et al.*, 2006; Aki *et al.*, 2008).

Thioredoxin h is thought to be part of the antioxidant defence machinery inside sieve tubes that is probably important to keep SE components intact over their complete, usually long, lifetime (Walz *et al.*, 2002). Cyclophilins have chaperone-like activity and are therefore likely to be involved in protein folding for import into and transport through SEs (Balachandran *et al.*, 1997). Also ubiquitin could be involved in protein sorting rather than in degradation (Giavalisco *et al.*, 2006). One of the most interesting protein classes are probably the various kinds of RNA-binding proteins also present in different species examined. Like CmPP16, the lectin PP2, or the small RNA-binding protein CmPSRP1, the glycine-rich RNA-binding protein present in barley phloem exudates might bind RNAs in order to facilitate their trafficking through plasmodesmata (Xoconostle-Cazares *et al.*, 1999; Barnes *et al.*, 2004; Gomez and Pallas, 2004; Yoo *et al.*, 2004; Giavalisco *et al.*, 2006; Aki *et al.*, 2008).
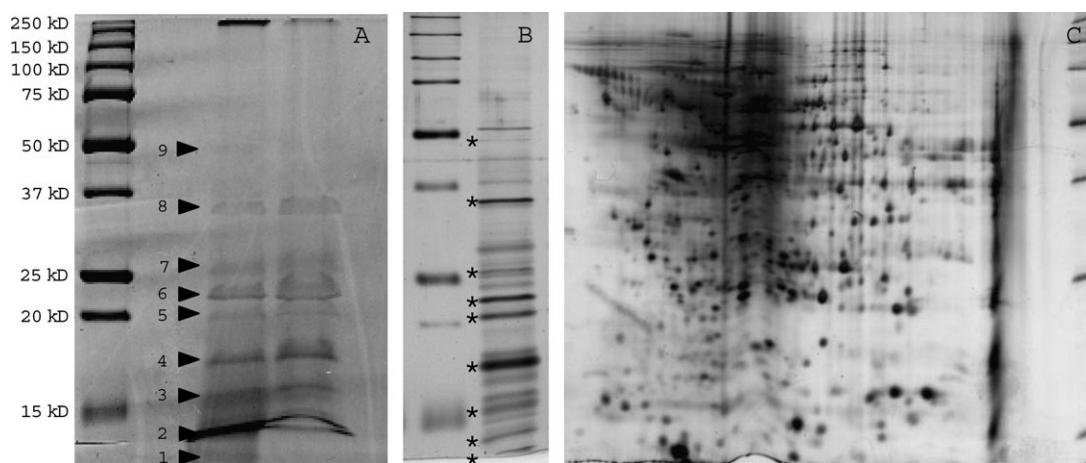

Fig. 3. Analysis of proteins in barley phloem exudates. (A) Preparative gel electrophoresis with 20 μl (left) and 30 μl (right) of barley phloem sap sampled by aphid stylectomy. The indicated Coomassie-stained bands were cut and analysed by mass spectrometry. (B) About 30 phloem proteins were visualized by SDS–PAGE and silver staining (5 μl of phloem sap). Major bands corresponding to the nine Coomassie-stained proteins in A are marked with asterisks. (C) More than 250 silver-stained phloem proteins can be distinguished after two-dimensional electrophoresis and silver staining.

Table 3. *Proteins in barley phloem sap*

Hv, *Hordeum vulgare*; M_{ox}, oxidized methionine; Mw_{ob} obtained mass in one-dimensional electrophoresis; Mw_{th}, theoretical mass; *Os*, *Oryza sativa*; *Ta*, *Triticum aestivum*. For band number, see Fig. 3A. Bold letters indicate amino acids that are identical to the respective database sequence.

Band no.	m/z	Sequence	Accession number	Plant	Annotation	Mw_{th} (Mw_{ob}) in kDa
1	–	No peptides detected				
2	534	**ESTLHLVLR**	gi|60499796	*Os*	Polyubiquitin	8.9 (~12)
2	882	**TITLEVESSDTIDNVK**	gi|60499796	*Os*		
2	596	**IM**$_{ox}$**APVFADLAK**	gi|32186042	*Hv*	Thioredoxin h isoform 2	13.2 (~12)
2	629	**VVGAIKEELTAK**	gi|32186042	*Hv*		
2	967	**VEAMPTFLFM**$_{ox}$**K**	gi|32186042	*Hv*		
3	1053	**GGGGGYGGGGGYG GQGGGYGGQGGGG YGGQGGGGYGGQR**	gi|728594	*Hv*	Glycine-rich/RNA-binding protein	16.8 (~16)
3	775	**GFVTFGSEESMR**	gi|728594	*Hv*		
3	783	**GFGFVTFGSEESM**$_{ox}$**R**	gi|728594	*Hv*		
4	712	**VFFDMTVGGAPAGR**	gi|13925737	*Ta*	Cyclophilin A-3	18.4 (~18)
4	720	**VFFDM**$_{ox}$**TVGGAPAGR**	gi|13925737	*Ta*		
4	822	**HVVFGEVVEGMDVVK**	gi|13925737	*Ta*		
5	454	**VVLAPANPK**	gi|66277464	*Ta*	Stress-responsive protein	22.2 (~20)
5	569	**ANPNYAM**$_{ox}$**SVR**	gi|66277464	*Ta*		
6	554	**DINAQTFVDNLKER**	gi|112821176	*Hv*	Hypothetical protein	23.0 (~22)
6	617	**SGVFGTPISEK**	gi|112821176	*Hv*		
6	625	**TNIGEGSTMNAR**	gi|112821176	*Hv*		
6	633	**TNIGEGSTM**$_{ox}$**NAR**	gi|112821176	*Hv*		
6	689	**DINAQTFVDNLK**	gi|112821176	*Hv*		
6	717	**NAQTFVDNLKER**	gi|112821176	*Hv*		
6	805	**LIYNATGATLSLAK**	gi|112821176	*Hv*		
6	839	**TVIATGEYKEPITQK**	gi|112821176	*Hv*		
6	995	**LANSDLNSTDKNYGYVSK**	gi|112821176	*Hv*		
7	839	**TVIATGEYKEPITQK**	gi|112821176	*Hv*	Hypothetical protein	23.0 (~26)
7	617	**GGLLDEK**	gi|112821176	*Hv*		
7	995	**LANSDLNSTDKNYGYVSK**	gi|112821176	*Hv*		
8	–	No peptides detected				
9	–	No peptides detected				

In addition to these known proteins, it was possible to identify two proteins formerly not found in phloem sap: a stress-responsive protein known from *T. aestivum* and a hypothetical protein from *H. vulgare* (Table 3). The stress-responsive protein is induced by abiotic stress and thus probably adds to the large family of stress- and defence-related phloem sap proteins already described (Giavalisco *et al.*, 2006; Kehr, 2006). The hypothetical protein is an interesting new candidate, because this protein has been shown to localize to scutellum and vascular bundles of barley seedlings and is induced by sugars, especially glucose and sucrose (Kidou *et al.*, 2006). Therefore, this protein has been associated with sugar mobilization and eventually sugar translocation from the seed into growing tissues, although its precise physiological function has as yet not been established (Kidou *et al.*, 2006). So far, sucrose transporters that mediate phloem sugar loading are known to occur in the plasma membrane of SEs in apoplastic loaders like barley (Kühn *et al.*, 1999). In addition, several enzymes from the glycolytic pathway have been found (Giavalisco *et al.*, 2006). Further analysis of this new sugar mobilization protein might allow new insights into sugar transport and metabolism inside the phloem tubes.

In the future, broad-spectrum analysis of proteins in barley phloem exudates will have to be performed. In these first experiments, silver-stained two-dimensional gels loaded with 5 µg of barley phloem proteins displayed >250 well separated spots (Fig. 3C). Very recently, Aki *et al.* (2008) applied nano-flow liquid chromatography/ mass spectrometry for the identification of 107 phloem proteins in rice phloem samples collected by stylectomy. Combined approaches utilizing the improved sampling techniques as described in the present report, and highly sensitive analysis methods would allow a comprehensive identification of phloem proteins from different monocots in the future.

Conclusions

A major barrier for molecular profiling of phloem sap from important monocot crop species is the small amount of phloem samples that can be obtained by insect stylectomy. The present experimental set-up overcomes this problem by allowing the collection of relatively large amounts of pure phloem sap from many barley plants in parallel. It is demonstrated that the obtained samples are

suitable for transcript and protein analysis by cDNA-AFLP and gel electrophoresis coupled to mass spectrometric protein identification.

Supplementary data

Supplementary data are available at *JXB* online.

Table S1. Sequences of transcript-derived fragments.

Acknowledgements

References

Aki T, Shigyo M, Nakano R, Yoneyama T, Yanagisawa S. 2008. Nano scale proteomics revealed the presence of regulatory proteins including three FT-like proteins in phloem and xylem saps from rice. *Plant and Cell Physiology* **49,** 767–790.

Altschul SF, Madden TL, Schäffer AA, Zhang J, Zhang Z, Miller W, Lipman DJ. 1997. Gapped BLAST and PSI-BLAST: a new generation of protein database search programs. *Nucleic Acids Research* **25,** 3389–3402.

Bachem CW, van der Hoeven RS, de Bruijn SM, Vreugdenhil D, Zabeau M, Visser RG. 1996. Visualisation of differential gene expression using a novel method of RNA fingerprinting based on AFLP: analysis of gene expression during potato tuber development. *The Plant Journal* **9,** 745–753.

Balachandran S, Xiang Y, Schobert C, Thompson GA, Lucas WJ. 1997. Phloem sap proteins from *Cucurbita maxima* and *Ricinus communis* have the capacity to traffic cell to cell through plasmodesmata. *Proceedings of the National Academy of Sciences, USA* **94,** 14150–14155.

Banerjee AK, Chatterjee M, Yu Y, Suh S-G, Miller WA, Hannapel DJ. 2006. Dynamics of a mobile RNA of potato involved in a long-distance signaling pathway. *The Plant Cell* **18,** 3443–3457.

Barnes A, Bale J, Constantinidou C, Ashton P, Jones A, Pritchard J. 2004. Determining protein identity from sieve element sap in *Ricinus communis* L. by quadrupole time of flight (Q-TOF) mass spectrometry. *Journal of Experimental Botany* **55,** 1473–1481.

Bradford MM. 1976. A rapid and sensitive method for the quantitation of microgram quantities of protein utilizing the principle of protein–dye binding. *Analytical Biochemistry* **72,** 248–254.

Bull J, Mauch F, Hertig C, Rebmann G, Dudler R. 1992. Sequence and expression of a wheat gene that encodes a novel protein associated with pathogen defense. *Molecular Plant-Microbe Interactions* **5,** 516–519.

Corbesier L, Vincent C, Jang S, Fornara F, Fan Q, Searle I, Giakountis A, Farrona S, Gissot L, Turnbull C, Coupland G. 2007. FT protein movement contributes to long-distance signaling in floral induction of *Arabidopsis*. *Science* **316,** 1030–1033.

Doering-Saad C, Newbury HJ, Bale JS, Pritchard J. 2002. Use of aphid stylectomy and RT-PCR for the detection of transporter mRNAs in sieve elements. *Journal of Experimental Botany* **53,** 631–637.

Doering-Saad C, Newbury HJ, Couldridge CE, Bale JS, Pritchard J. 2006. A phloem-enriched cDNA library from Ricinus: insights into phloem function. *Journal of Experimental Botany* **57,** 3183–3193.

Durrant WE, Dong X. 2004. Systemic acquired resistance. *Annual Review of Phytopathology* **42,** 185–209.

Eckey C, Korrell M, Leib K, Biedenkopf D, Jansen C, Langen G, Kogel KH. 2004. Identification of powdery mildew-induced barley genes by cDNA-AFLP: functional assessment of an early expressed MAP kinase. *Plant Molecular Biology* **55,** 1–15.

Fisher DB, Frame JM. 1984. A guide to the use of the exuding stylet technique in phloem physiology. *Planta* **161,** 385–393.

Fisher DB, Gifford RM. 1986. Accumulation and conversion of sugars by developing wheat grains. *Plant Physiology* **82,** 1024–1030.

Fisher DB, Wu Y, Ku MSB. 1992. Turnover of soluble proteins in the wheat sieve tube. *Plant Physiology* **100,** 1433–1441.

Fukuda A, Okada Y, Suzui N, Fujiwara T, Yoneyama T, Hayashi H. 2004*a*. Cloning and characterization of the gene for a phloem-specific glutathione S-transferase from rice leaves. *Physiologia Plantarum* **120,** 595–602.

Fukuda A, Okada Y, Suzui N, Fujiwara T, Yoneyama T, Hayashi H. 2004*b*. Cloning of the phloem-specific small heat-shock protein from leaves of rice plants. *Soil Science and Plant Nutrition* **50,** 1255–1262.

Gachon CMM, Langlois-Meurinne M, Saindrenan P. 2005. Plant secondary metabolism glycosyltransferases: the emerging functional analysis. *Trends in Plant Science* **10,** 542–549.

Gaupels F, Knauer T, van Bel AJE. 2008. A combinatory approach for analysis of protein sets in barley sieve tube samples using EDTA-facilitated exudation and aphid stylectomy. *Journal of Plant Physiology* **165,** 95–103.

Giavalisco P, Kapitza K, Kolasa A, Buhtz A, Kehr J. 2006. Towards the proteome of *Brassica napus* phloem sap. *Proteomics* **6,** 896–909.

Girousse C, Bonnemain J-L, Delrot S, Bournoville R. 1991. Sugar and amino acid composition of phloem sap of Medicago sativa: a comparative study of two collecting methods. *Plant Physiology and Biochemistry* **29,** 41–48.

Gomez G, Pallas V. 2004. A long-distance translocatable phloem protein from cucumber forms a ribonucleoprotein complex *in vivo* with Hop stunt viroid RNA. *Journal of Virology* **78,** 10104–10110.

Hayashi H, Fukuda A, Suzui N, Fujimaki S. 2000. Proteins in the sieve element–companion cell complexes: their detection, localization and possible functions. *Australian Journal of Plant Physiology* **27,** 489–496.

Haywood V, Yu T-S, Huang N-C, Lucas WJ. 2005. Phloem long-distance trafficking of *GIBBERELLIC ACID-INSENSITIVE* RNA regulates leaf development. *The Plant Journal* **42,** 49–68.

Ishiwatari Y, Honda C, Kawashima I, Nakamura S, Hirano H, Mori S, Fujiwara T, Hayashi H, Chino M. 1995. Thioredoxin h is one of the major proteins in rice phloem sap. *Planta* **195,** 456–463.

Jaeger KE, Wigge PA. 2007. FT protein acts as a long-range signal in *Arabidopsis*. *Current Biology* **17,** 1050–1054.

Kehr J. 2006. Phloem sap proteins: their identities and potential roles in the interaction between plants and phloem-feeding insects. *Journal of Experimental Botany* **57,** 767–774.

Kehr J, Buhtz A. 2008. Long distance transport and movement of RNA through the phloem. *Journal of Experimental Botany* **59,** 85–92.

Kehr J, Rep M. 2006. Protein extraction from xylem and phloem sap. In: Thiellement H, ed. *Methods in Molecular Biology*. Totowa, NJ: Humana Press, 27–35.

Kennedy JS, Mittler TE. 1953. A method of obtaining phloem sap via the mouth parts of aphids. *Nature* **171,** 528.

Kidou S, Oikawa A, Sasaki N, Yasuda H, Yamashita T, Koiwa H, Kato K, Ejiri S. 2006. Identification of a 23 kDa protein (P23k) related to the sugar supply in germinating barley seeds. *Plant Biotechnology* **23,** 357–364.

Kim M, Canio W, Kessler S, Sinha N. 2001. Developmental changes due to long-distance movement of a homeobox fusion transcript in tomato. *Science* **293,** 287–289.

King RW, Zeevaart JAD. 1974. Enhancement of phloem exudation from cut petioles by chelating agents. *Plant Physiology* **53,** 96–103.

Kramer EM, Bennett MJ. 2006. Auxin transport: a field in flux. *Trends in Plant Science* **11,** 382–386.

Kühn C, Barker L, Bürkle L, Frommer WB. 1999. Update on sucrose transport in higher plants. *Journal of Experimental Botany* **50,** 935–953.

Kühn C, Franceschi VR, Alexander Schulz, Lemoine R, Frommer WB. 1997. Macromolecular trafficking indicated by localization and turnover of sucrose transporters in enucleate sieve elements. *Science* **275,** 1298–1300.

Lough TJ, Lucas WJ. 2006. Integrative plant biology: role of phloem long-distance macromolecular trafficking. *Annual Review of Plant Biology* **57,** 203–232.

Omid A, Keilin T, Glass A, Leshkowitz D, Wolf S. 2007. Characterization of phloem-sap transcription profile in melon plants. *Journal of Experimental Botany* **58,** 3645–3656.

Ruiz-Medrano R, Moya JH, Xoconostle-Cazares B, Lucas WJ. 2007. Influence of cucumber mosaic virus infection on the mRNA population present in the phloem translocation stream of pumpkin plants. *Functional Plant Biology* **34,** 292–301.

Ruiz-Medrano R, Xoconostle-Cázares B, Lucas WJ. 1999. Phloem long-distance transport of *CmNACP* mRNA: implications for supracellular regulation in plants. *Development* **126,** 4405–4419.

Sakuth T, Schobert C, Pecsvaradi A, Eichholz A, Komor E, Orlich G. 1993. Specific proteins in the sieve-tube exudate of *Ricinus communis* L. seedlings: separation, characterization and in-vivo labelling. *Planta* **191,** 207–213.

Sasaki T, Chino M, Hayashi H, Fujiwara T. 1998. Detection of several mRNA species in rice phloem sap. *Plant and Cell Physiology* **39,** 895–897.

Schilmiller AL, Howe GA. 2005. Systemic signaling in the wound response. *Current Opinion in Plant Biology* **8,** 369–377.

Schobert C, Baker L, Szederkenyi J, Großmann P, Komor E, Hayashi H. 1998. Identification of immunologically related proteins in sieve-tube exudate collected from monocotyledonous and dicotyledonous plants. *Planta* **206,** 245–252.

Slaymaker DH, Navarre DA, Clark D, del Pozo O, Martin GB, Klessig DF. 2002. The tobacco salicylic acid-binding protein 3 (SABP3) is the chloroplast carbonic anhydrase, which exhibits antioxidant activity and plays a role in the hypersensitive defense response. *Proceedings of the National Academy of Sciences, USA* **99,** 11640–11645.

Suzui N, Nakamura S-i, Fujiwara T, Hayashi H, Yoneyama T. 2006. A putative acyl-CoA-binding protein is a major phloem sap protein in rice (*Oryza sativa* L.). *Journal of Experimental Botany* **57,** 2571–2576.

Tamaki S, Matsuo S, Wong HL, Yokoi S, Shimamoto K. 2007. Hd3a protein is a mobile flowering signal in rice. *Science* **316,** 1033–1036.

van Bel AJE, Gaupels F. 2004. Pathogen-induced resistance and alarm signals in the phloem. *Molecualr Plant Pathology* **5,** 495–504.

Vilaine F, Palauqui J-C, Amselem J, Kusiak C, Lemoine R, Dinant S. 2003. Towards deciphering phloem: a transcriptome analysis of the phloem of *Apium graveolens*. *The Plant Journal* **36,** 67–81.

Walz C, Giavalisco P, Schad M, Juenger M, Klose J, Kehr J. 2004. Proteomics of curcurbit phloem exudate reveals a network of defence proteins. *Phytochemistry* **65,** 1795–1804.

Walz C, Juenger M, Schad M, Kehr J. 2002. Evidence for the presence and activity of a complete antioxidant defence system in mature sieve tubes. *The Plant Journal* **31,** 189–197.

Xoconostle-Cazares B, Xiang Y, Ruiz-Medrano R, Wang H-L, Monzer J, Yoo B-C, McFarland KC, Franceschi VR, Lucas WJ. 1999. Plant paralog to viral movement protein that potentiates transport of mRNA into the phloem. *Science* **283,** 94–98.

Yoo B-C, Kragler F, Varkonyi-Gasic E, Haywood V, Archer-Evans S, Lee YM, Lough TJ, Lucas WJ. 2004. A systemic small RNA signaling system in plants. *The Plant Cell* **16,** 1979–2000.

Yuan H, Chen X, Zhu L, He G. 2004. Isolation and characterization of a novel rice gene encoding a putative insect-inducible protein homologous to the wheat Wir1. *Journal of Plant Physiology* **161,** 79–85.

Ziegler H. 1975. Nature of transported substances. In: Zimmermann MH, Milburn JA, eds. *Transport in Plants. I. Phloem Transport. Encyclopedia of Plant Physiology*. Berlin: Springer Verlag, 59–100.

Nitric oxide generation in *Vicia faba* phloem cells reveals them to be sensitive detectors as well as possible systemic transducers of stress signals

Frank Gaupels[1,2,4], Alexandra C. U. Furch[2], Torsten Will[2], Luis A. J. Mur[3], Karl-Heinz Kogel[1] and Aart J. E. van Bel[2]

[1]Institute of Phytopathology and Applied Zoology, IFZ, Heinrich-Buff-Ring 26-32, D-35392 Gießen and [2]Plant Cell Biology Research Group, Institute of General Botany, Senckenbergstrasse 17, D-35390 Gießen, Justus-Liebig-University, Gießen, Germany; [3]Institute of Biological Sciences, University of Wales Aberystwyth, Aberystwyth, Ceredigion SY23 2DA, UK; [4]Dipartimento Scientifico e Tecnologico, Università degli Studi di Verona, Strada le Grazie 15, I-37134 Verona, Italy

Summary

• Vascular tissue was recently shown to be capable of producing nitric oxide (NO), but the production sites and sources were not precisely determined. Here, NO synthesis was analysed in the phloem of *Vicia faba* in response to stress- and pathogen defence-related compounds.

• The chemical stimuli were added to shallow paradermal cortical cuts in the main veins of leaves attached to intact plants. NO production in the bare-lying phloem area was visualized by real-time confocal laser scanning microscopy using the NO-specific fluorochrome 4,5-diaminofluorescein diacetate (DAF-2 DA).

• Abundant NO generation in companion cells was induced by 500 μM salicylic acid (SA) and 10 μM hydrogen peroxide (H_2O_2), but the fungal elicitor chitooctaose was much less effective. Phloem NO production was found to be dependent on Ca^{2+} and mitochondrial electron transport and pharmacological approaches found evidence for activity of a plant NO synthase but not a nitrate reductase. DAF fluorescence increased most strongly in companion cells and was occasionally observed in phloem parenchyma cells. Significantly, accumulation of NO in sieve elements could be demonstrated.

• These findings suggest that the phloem perceives and produces stress-related signals and that one mechanism of distal signalling involves the production and transport of NO in the phloem.

Key words: hydrogen peroxide (H_2O_2), nitric oxide (NO), nitric oxide synthase, pathogen resistance, phloem, salicylic acid, stress, systemic signalling.

Introduction

Plant responses to abiotic and biotic stress involve the early generation of chemical cues, which can have discrete but also overlapping roles in conferring plant stress tolerance. One common stress response is the generation of partially reduced oxygen species ($O_2^- + 2H \rightarrow H_2O_2 \rightarrow 2 \cdot OH$). Elevated oxidative stress is a feature of the hypersensitive response (HR), a localized programmed cell death associated with resistance to pathogens (Levine *et al.*, 1994), wounding (Orozco-Càrdenas *et al.*, 2001), anoxia (Baxter-Burrell *et al.*, 2003), chilling (Prasad *et al.*, 1994) and thermotolerance (Dat *et al.*, 1998). Other stress signals have been thought to exhibit greater specificity in their production. Salicylic acid (SA) has

been associated with local resistance mechanisms to biotrophic pathogens based on the HR, and with systemic acquired resistance (SAR; Ryals *et al.*, 1996). However, subsequent investigations have shown much wider roles in plant stress biology with, for example, SA being involved in abiotic stress signalling (Clarke *et al.*, 2004; Scott *et al.*, 2004).

Nitric oxide (NO) is a gaseous signal molecule involved in plant reactions to various stresses (for recent reviews, see Neill *et al.*, 2003; del Río *et al.*, 2004; Crawford & Guo, 2005). For instance, heat, salt and hyperosmotic stress induce NO production in tobacco (*Nicotiana tabacum*) cell suspensions (Gould *et al.*, 2003). Moreover, NO accumulation upon wounding was detected in Arabidopsis and sweet potato (*Ipomoea batatas*; Jih *et al.*, 2003; Huang *et al.*, 2004). The production of NO during plant defence against pathogens is also well documented, with roles during the HR (reviewed by Mur *et al.*, 2006) and also in papilla formation in barley/powdery mildew (*Hordeum vulgare/Blumeria graminis*) interactions (Prats *et al.*, 2005). Detailed analyses revealed a tight interaction of NO and hydrogen peroxide (H_2O_2) in the HR induced by phytopathogens or pathogen-derived elicitors (Delledonne *et al.*, 1998, 2001; de Pinto *et al.*, 2002). Furthermore, NO is a potent regulator of defence-related gene expression (Delledonne *et al.*, 1998; Durner *et al.*, 1998; Zeidler *et al.*, 2004; Zeier *et al.*, 2004), enzyme activity (Clark *et al.*, 2000; Navarre *et al.*, 2000; Igamberdiev *et al.*, 2006) and phytoalexin production (Modolo *et al.*, 2002; Xu *et al.*, 2005). NO is likely to be a major modulator of other defence signals with, for example, the initiation of SA and jasmonic acid biosynthesis being influenced by NO (Durner *et al.*, 1998; Xu *et al.*, 2005).

Use of NO synthase (NOS) inhibitors showed that an NOS-like enzyme was activated in plant stress reactions (Foissner *et al.*, 2000; Xu *et al.*, 2005). Recently, a gene for a plant NOS was identified in *Arabidopsis thaliana* (Guo *et al.*, 2003). *AtNOS1* is involved in induction of defence gene expression by lipopolysaccharides (Zeidler *et al.*, 2004). However, NOS activity of AtNOS1 could not be confirmed (and AtNOS1 has since been re-designated AtNOA1 – nitric oxide associated); thus, the identity of the plant NOS remains obscure (Zemojtel *et al.*, 2006). Other workers have suggested that nitrite is a source of NO in plants, derived either nonenzymatically at high pH or via nitrate reductase (NR) activity (Neill *et al.*, 2003; del Río *et al.*, 2004).

The mobilization of signals from one plant organ to another is a major theme of plant physiology. In view of its high mobility, NO has been suggested to be a systemic stress signal (Durner & Klessig, 1999; Foissner *et al.*, 2000; Neill *et al.*, 2003; van Bel & Gaupels, 2004). In support of this suggestion, injection of NO donors into tobacco leaves reduced the size of lesions caused by tobacco mosaic virus on treated and systemic nontreated leaves (Song & Goodman, 2001). Also, local treatment with NOS inhibitors or an NO scavenger attenuated SAR in distal leaves (Song & Goodman, 2001).

Grafting and girdling experiments provided evidence that translocation of distal signalling takes place in the sieve tubes (Durrant & Dong, 2004; van Bel & Gaupels, 2004). Using the specific NO-sensing fluorochrome 4,5-diaminofluorescein diacetate (DAF-2 DA), NO was detected in vascular bundles and was suggested to have functions in senescense, cell wall lignification and the salt stress response (Corpas *et al.*, 2004; Gabaldon *et al.*, 2005; Valderrama *et al.*, 2007). In pepper (*Capsicum annuum*) plants, infection with *Phytophtora capsici* induced NO production more abundantly in vascular bundles as compared with other tissues (Requena *et al.*, 2005). Significantly, Rusterucci *et al.* (2007) recently showed that antisense lines of the S-nitrosoglutathione (GSNO) catabolizing S-nitrosoglutathione reductase (GSNOR) displayed elevated resistance and constitutive SAR. These workers also observed that GSNOR was primarily located in companion cells and proposed that inhibition of GSNOR, leading to the accumulation of GSNO, may be an important factor in the generation of SAR. Despite these hints at a possible role of NO in systemic signalling, to date detailed reports on inducible NO synthesis or transport in phloem tissue are lacking.

Our goal was to investigate whether phloem tissue is able to synthesize and/or transport NO as a distal signal. We tested the ability of the stress signals H_2O_2 and SA as well as the fungal elicitor chitooctaose to induce NO production in intact phloem tissue. Confocal laser scanning microscopy (CLSM) with DAF-2 DA revealed rapid and strong NO synthesis primarily in companion cells (CCs) which was dependent on calcium and could be suppressed by NOS inhibitors. Our results further provide indirect evidence for a role of NO in systemic signalling through sieve tubes.

Materials and Methods

Plant material

Potted plants of *Vicia faba* L. cv. Witkiem major and *Cucurbita maxima* Duchesne ex Lam. cv. Gele Centenaar (pumpkin) were grown in a 3 : 3 : 1 mixture of compost, peat and sand in a glasshouse at 60–70% relative humidity, a minimum day temperature of 22°C and a minimum light period of 14 h. Minimum irradiance of 250 μmol m^{-2} s^{-1} at plant level was maintained with daylight plus additional lamp light (model SONT Agro 400 W; Philips, Eindhoven, the Netherlands). Plants 3–5-wk old were used for the experiments.

Chemicals

All chemicals for microscopy were dissolved in loading buffer (2 mM KCl, 1 mM MgCl$_2$, 1 mM CaCl$_2$ and 2.5 mM morpholine ethanesulfonic acid (MES), adjusted to pH 5.7 with NaOH). DAF-2 DA (dissolved as a 5 mM stock solution in dimethyl sulphoxide (DMSO)), N^G-nitro-L-arginine-methyl ester (L-NAME), N^G-nitro-D-arginine-methyl ester (D-NAME),

2-(4-carboxyphenyl)-4,4,5,5-tetramethylimidazoline-1-oxyl-3-oxide (cPTIO) and the nitrotyrosine monoclonal antibody (mouse) were purchased from Axxora (Grünberg, Germany). All other chemicals including octa-N-acetylchitooctaose (ONA) were from Sigma-Aldrich (Taufkirchen, Germany). The SA solutions were adjusted to pH 5.7 with NaOH before application.

Tissue preparation for *in vivo* microscopy of the intact phloem

Tissue preparation was carried out as described by Knoblauch & van Bel (1998). A shallow paradermal incision was made using a razor blade, and a few cortical cell layers from the mid vein of a *V. faba* leaf, which stayed attached to the plant, were removed from the abaxial side, leaving the phloem intact. The cortical window allowed observation of undamaged phloem tissue through one or two cell layers. The leaf was fixed, the lower side upwards, on a microscope slide with double-sided adhesive tape and the window was covered with loading buffer.

Confocal laser scanning microscopy

The leaf was placed on the stage of a confocal laser scanning microscope. After 30 min of recovery time, the buffer on the cortical window was exchanged with 10 μм DAF-2 DA in loading buffer. The tissue was stained in the dark for 30 min and covered again with loading buffer, and control pictures were taken. All elicitors and modulators of NO synthesis were carefully supplied directly to the phloem tissue under continuous optical surveillance.

For *in vivo* observation of the phloem tissue, use was made of a Leica Microsystems (Bensheim, Germany) TCS SP2 confocal laser scanning microscope equipped with a 63× water immersion objective. DAF-2 DA was excited by the 488-nm line of an argon/krypton laser and emission was recorded using a 500–520-nm band-pass filter. Autofluorescence of chloroplasts was detected in the range of 600–700 nm. Pictures were processed with Leica Confocal Software and Adobe Photoshop 7.0.

Western blot analyses of pumpkin phloem exudates using nitrotyrosine antibodies

Pumpkin plants were watered with 10 mм H_2O_2 or water (control) and phloem samples were subsequently collected from cut petioles and stems after cleaning the cut surface with tissue paper. Phloem exudates treated for 30 min with 2 mм peroxynitrite (or KOH, control) served as positive controls. For western blot analyses, a 1-μl sample was mixed with 50 μl of reducing buffer (50 mм Tris/HCl, pH 7.8, and 0.1% 2-mercaptoethanol) and the samples were loaded onto a nitrocellulose membrane using a vacuum dot-blot device. Equal loading was checked by Ponceau staining of the blot

membrane before blocking with milk powder. The primary antibody against nitrotyrosine (of mouse origin) was diluted 1 : 1000 and the second antibody (anti-mouse/peroxidase conjugate) 1 : 20 000. After addition of the chemiluminescent peroxidase substrate, X-ray films were exposed to the blot membranes for 10–20 s and processed in a developer machine.

Results

Detection of inducible NO synthesis in the phloem of *Vicia faba*

Our group has pioneered *in planta* observation of phloem function through the dissection of a paradermal window in *V. faba* plants (Knoblauch & van Bel, 1998), which we here applied to the analysis of stress-initiated NO effects. H_2O_2 is regarded as a universal stress signal and acts with NO in a variety of defence and signalling processes (Neill *et al.*, 2002). We initially applied 10 mм H_2O_2 to the phloem window and visualized NO production using the membrane-permeant fluorochrome DAF-2 DA dye. The strong increase in DAF fluorescence in CCs in response to the supply of H_2O_2 was observed (green colour, Fig. 1a,b, Table 1). The specifity of this response was demonstrated when fluorescence was suppressed by the addition of the NO scavenger cPTIO (0.5 mм; Fig. 1c,d, Table 1).

Companion cells are the predominant sites of NO production

The phloem is comprised of phloem parenchyma (PP), CCs and sieve elements (SEs). The enucleate SEs, which form the assimilate-transporting sieve tubes, are dependent on supply of metabolites by the metabolically highly active CCs (e.g. van Bel, 2003).

CCs appeared to be the main site of NO generation (Figs 1, 2), although in all experiments a slow and weak increase in DAF fluorescence was observed in sieve tubes after H_2O_2 treatment (Fig. 1h, left sieve tube and Fig. 2b,c, right sieve tube). It was hypothesized that the weak NO-derived fluorescence in SEs is a result of permanent mass flow away from the production site. To test this hypothesis, the det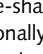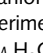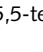ergent Triton X-100 (0.1%) was applied, which causes SE plugging by irreversible dispersal of forisomes (Knoblauch *et al.*, 2001; see below for details on forisome functions). When 1 mм H_2O_2 was subsequently added, strong DAF fluorescence emerged in SEs within 2 min (Fig. 1e–g), consistent with increased accumulation as a result of suspended mass flow. Occasionally, H_2O_2-induced fluorescence was observed in naturally occluded SEs (Fig. 1h, right sieve tube; Figs 1i, 2b,c, left sieve tube). It is not clear if staining of the SEs is caused by an influx of NO or fluorescent dye from CCs or if there is a source of NO in the SEs themselves. Figure 1i would argue for the latter, as the strongly fluorescent SE was accompanied by an only faintly

Table 1 Imaging of nitric oxide (NO) production in companion cells of *Vicia faba* (combined results of confocal laser scanning microscopy using the fluorescent dye 4,5-diaminofluorescein diacetate (DAF-2 DA) after treatment with various elicitors and modulators of NO synthesis)

Elicitor	Modulator	Forisome[1] (SE reaction)	Fluorescence[2]	CC reaction[3]
10 mM H_2O_2		⬡ (framed)	↑↑↑	8/8
10 mM H_2O_2	0.5 mM cPTIO	⬡ (framed)	=	5/5
0.5, 1 mM H_2O_2		⬡	↑↑↑	10/10
0.01, 0.1 mM H_2O_2		◆	↑↑	5/6
10 mM SA		◆ ⬡	↑↑	6/6
0.5, 1 mM SA		◆	↑↑	8/10
0.2 mM SA		◆	↑	2/5
0.025 mM chitooctaose		◆ ⬡	↑	7/21
250 mM NaCl		⬡	=	4/4
1, 10 mM H_2O_2	0.1 mM $LaCl_3$	◆	=	7/7
0.1% Triton X-100		⬡ (framed)	=	4/4
Triton X-100/H_2O_2[4]		⬡ (framed)	↑↑↑	3/3
1 mM H_2O_2	1 mM aminoguanidine	⬡	=	5/5
1 mM H_2O_2	0.2 mM AET	⬡	↑	4/4
0.2 mM spermine		⬡	↑↑	5/5
1 mM H_2O_2	0.1 mM tungstate	⬡	↑↑↑	3/3
1 mM $NaNO_2$		◆	=	4/4
1 mM H_2O_2	2.5 mM SHAM	⬡	=	4/5
1 mM H_2O_2	0.5 mM KCN	⬡	↑	6/6

[1]Configuration of forisomes in sieve elements (SEs): condensed (spindle-shaped), temporarily (round) or permanently dispersed (round with frame) – chitooctaose and 10 mM salicylic acid (SA) occasionally caused forisome dispersal.
[2]No (=), minor (↑), intermediate (↑↑) or strong (↑↑↑) increase in companion cell (CC) fluorescence.
[3]Experiments with indicated fluorescence increase/total number of experiments.
[4]Incubation in 0.1% Triton X-100 and subsequent treatment with 1 mM H_2O_2.
AET, 2-aminoethyl-2-thiopseudurea; cPTIO, 2-(4-carboxyphenyl)-4,4,5,5-tetramethylimidazoline-1-oxyl-3-oxide; KCN, potassium cyanide; SHAM, salicylhydroxamic acid.

fluorescing CC. No DAF fluorescence was noted within organelles or in any distinct cellular structure, which suggests that NO in SEs might arise from a cytosolic source.

Apart from the CCs, phloem parenchyma cells (PPCs) were sometimes stained (Fig. 2b,c). Nonphloem cells never showed a distinct increase in fluorescence in response to the treatments, which were sometimes harsh (Figs 1, 2). Taken together, these observations suggest that the phloem is a sensitive sensor-transducer of oxidative stress signals rather than only a transducer.

Induction of NO synthesis by H_2O_2, SA and chitooctaose and subcellular localization of the NO source

Because 10 mM H_2O_2 is probably a nonphysiological concentration, we tested lower concentrations for their ability to induce NO synthesis in the phloem. As little as 0.01 and 0.1 mM H_2O_2 resulted in an increase in DAF-2 DA fluorescence within 10 min (Table 1), while concentrations of 0.5 and 1 mM H_2O_2 elicited an NO burst within 1–2 min (Fig. 2a–c,
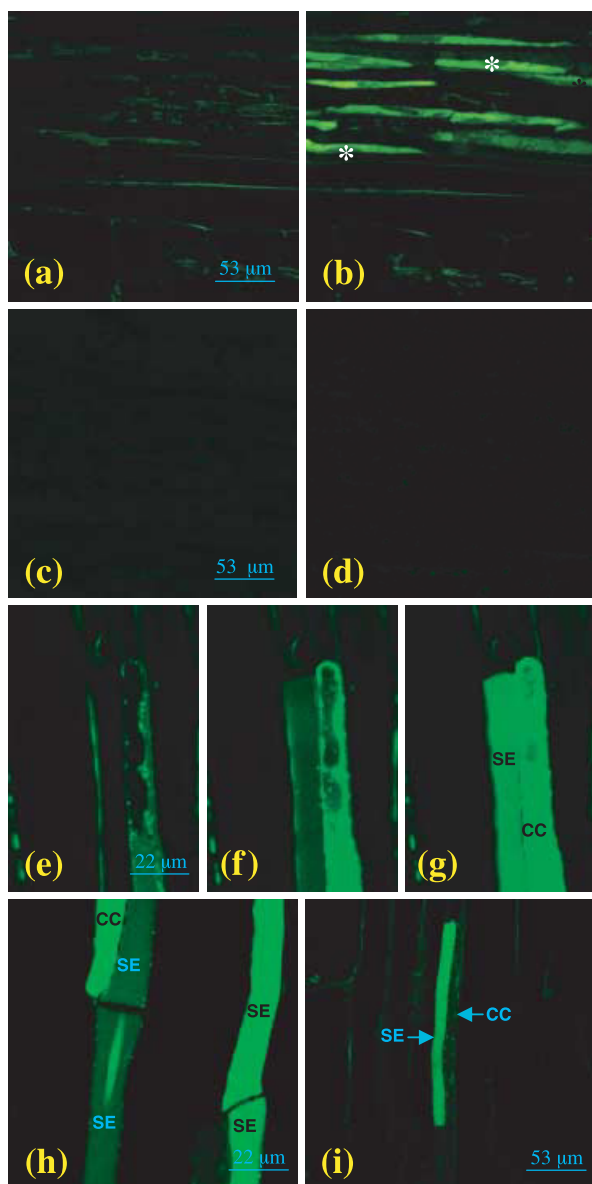
Fig. 1 Confocal laser scanning microscopy of hydrogen peroxide (H_2O_2)-induced 4,5-diaminofluorescein diacetate (DAF-2 DA) fluorescence in companion cells and sieve elements of intact phloem tissue of *Vicia faba*. (a) Control image of DAF-2 DA-stained tissue before treatment with 10 mM H_2O_2. (b) H_2O_2 elicits DAF-2 DA fluorescence (green colour) in companion cells (CCs) but not in nonphloem tissue. CCs are readily recognizable by the large, faintly stained nuclei (e.g. see asterisks). (c) Phloem tissue loaded with DAF-2 DA and the nitric oxide (NO) scavenger 2-(4-carboxyphenyl)-4,4,5,5-tetramethylimidazoline-1-oxyl-3-oxide (cPTIO) (0.5 mM) and (d) 10 min after addition of 10 mM H_2O_2/0.5 mM cPTIO. (e) Sieve element/companion cell complex after incubation in DAF-2 DA and 0.1% Triton X-100. (f, g) Increased fluorescence in the CC and the plugged sieve element (SE) 1 min (f) and 2 min (g) after subsequent application of 1 mM H_2O_2. (h) A transporting (left) and a nontransporting (right) sieve tube show different fluorescence intensities 10 min after application of 1 mM H_2O_2. (i) Strongly stained plugged SE. Note the weak DAF-2 DA fluorescence in the accompanying CC.

Table 1). Video recording confirmed that DAF fluorescence was visible already 20–40 s after treatment with H_2O_2 (Supplementary material Movie S1). Faint fluorescence in CCs of untreated phloem tissue (Fig. 2a) may be a response to the preparation of the paradermal window or the result of some constitutive NO production.

The elicitation of NO production in the phloem is likely to reflect the initiation of distal signalling mechanisms. Therefore, signals previously associated with systemic signalling were assessed for their ability to elicit NO generation. SA is an essential component of the SAR signal cascade (Ryals *et al.*, 1996; Durrant & Dong, 2004), and 0.5, 1 and 10 mM initiated high NO synthesis in 14 of 16 experiments, whereas 0.2 mM SA induced a faint increase in DAF fluorescence which could be visualized in two of five experiments. SA-induced DAF-2 DA fluorescence seemed to be localized to the CCs and appeared more slowly than that induced by H_2O_2, showing up between 10 and 30 min following application (Fig. 2e–g). These observations are consistent with SA initiating NO production in the phloem and possibly contributing to systemic signal dispersal.

Some fungal elicitors are known to be potent inducers of NO production in leaf tissues and cultured cells (Foissner *et al.*, 2000; Modolo *et al.*, 2002; Lamotte *et al.*, 2004; Xu *et al.*, 2005); we therefore tested the NO-eliciting properties of the oligomeric chitin elicitor chitooctaose when applied to the phloem tissue. In previous studies, chitosans evoked a rapid alkalinization of the barley leaf apoplast (Felle *et al.*, 2004; Hanstein & Felle, 2004), oxidative burst and Ca^{2+}-mediated programmed cell death (Zuppini *et al.*, 2003). However, chtitooctaose proved to be a relatively poor elicitor of NO production. In only seven of 21 experiments, 25 μM chitooctaose induced a slight increase in DAF staining between 20 and 60 min following application (Table 1). In 14 experiments, weak NO production might have escaped detection.

The strong DAF fluorescence in CCs upon treatment with 1 mM H_2O_2 allowed identification of sites of subcellular NO generation. Three putative NO-producing compartments could be distinguished, namely the cytosol, several dot-like structures and the chloroplasts (Fig. 2h).

Forisomes as indicators for stress-induced calcium fluxes

A special feature of fabacean phloem is the presence of spindle-shaped protein bodies, the so-called forisomes, one in each sieve element (Knoblauch & van Bel, 1998). In reaction to turgor loss and corresponding Ca^{2+} influx, forisomes disperse rapidly and occlude the sieve tubes (Knoblauch & van Bel, 1998; Knoblauch *et al.*, 2001). In this study, forisomes served as a sensor for Ca^{2+} influx into SEs in response to stress reactions in the phloem. In all of our experiments we used only phloem preparations with condensed forisomes as indicators of an unstressed state of the phloem tissue.
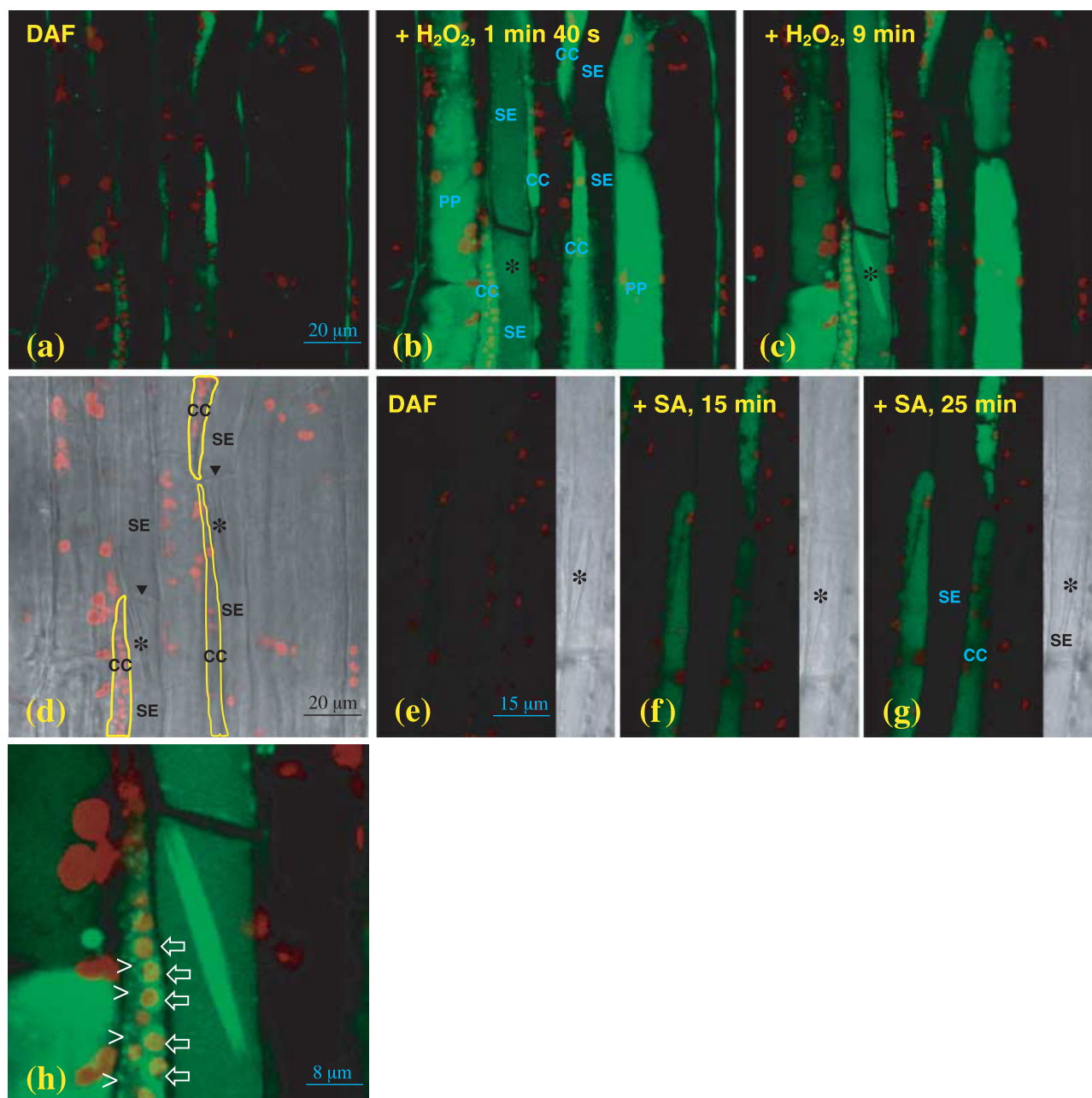
Fig. 2 Nitric oxide (NO) production in the phloem of *Vicia faba* in response to hydrogen peroxide (H_2O_2) and salicylic acid (SA) treatments visualized with the fluorescent dye 4,5-diaminofluorescein diacetate (DAF-2 DA) using confocal laser scanning microscopy (CLSM). (a–c, e–h) Digital overlay of DAF fluorescence (green) and autofluorescence of chloroplasts (red); (d) overlay of transmission image and autofluorescence of chloroplasts. Condensed Ca^{2+}-sensitive forisomes (asterisks) and sieve plates (black arrow heads) are indicated. Companion cell (CC) borders are delineated by yellow lines. (a, d) Control images (DAF fluorescence vs transmission) before treatment with H_2O_2. (b) Emergence of DAF fluorescence 1 min 40 s and (c) 9 min after treatment with 1 mM H_2O_2. The forisomes disperse (b) and recondense (c) in response to H_2O_2 treatment. (c) Sensitivity of photomultipliers downregulated. (b, c) Note appearance of DAF fluorescence in the left sieve tube while only weak staining is visible in the right sieve tube. (e) Control image before treatment with SA. (f, g) Emergence of DAF fluorescence, 15 and 25 min after incubation of the tissue in 1 mM SA. (h) Detail of Fig. 2(c). After treatment with 1 mM H_2O_2, fluorescence shows up in unidentified dot-like structures (arrow heads) and in chloroplasts (arrows) of CCs. CC, companion cell; PP, phloem parenchyma cell; SE, sieve element.

Dispersal of the forisomes upon treatment with cPTIO/ H_2O_2 suggested a reaction of the sieve tubes to H_2O_2 even when the DAF-2 DA fluorescence was unchanged as a result of suppression of NO accumulation (Table 1). Similarly,

treatment of the phloem with abiotic stressors such as 250 mM NaCl or 0.1% Triton X-100 led to forisome dispersal, while no or only faint NO production was detectable (Table 1). Forisomes recondensed under salt stress, but not after

application of the detergent. Thus, by observing the forisome configuration it was possible to assess the contribution of Ca^{2+}-dependent effects on the diverse treatments used in this study, irrespective of changes in DAF-2 DA fluorescence.

Detailed analyses revealed that the forisome reaction to H_2O_2 and SA was concentration dependent. Upon treatment with 10 mM H_2O_2, the dispersed forisomes did not recondense (Table 1) and the tissue turned brown and died. The inability of forisomes to recondense hints at severe damage of the phloem tissue inflicted by treatment with 10 mM H_2O_2 or with Triton X-100 (Table 1). By contrast, 1 mM H_2O_2 caused transient dispersal of the forisomes which recondensed after a few minutes even when H_2O_2 remained on the treated surface (Fig. 2a–d, Table 1). Application of neither 0.01 and 0.1 mM H_2O_2 (Table 1) nor 0.2, 0.5 and 1 mM SA (Fig. 2e–g, Table 1) induced forisome dispersal, suggesting that no strong stress reaction of the phloem had occurred. This correlated with rather low NO production in the phloem. However, 10 mM SA – which is probably a nonphysiological concentration – provoked occasional forisome dispersal but no stronger NO production than with 0.5 and 1 mM SA. Finally, forisomes only rarely dispersed upon chitooctaose treatment.

It was noted that Ca^{2+}-dependent dispersal of forisomes occurred simultaneously with the initiation of NO production (Fig. 2a–c). As interactions between NO and Ca^{2+} have been described in both mammalian and plant systems (Stuehr, 1999; Lamotte *et al.*, 2004) the effects of applying 1 and 10 mM H_2O_2 with the nonspecific Ca^{2+}-channel blocker $LaCl_3$ on NO production were examined. Addition of 0.1 mM $LaCl_3$ suppressed H_2O_2-elicited NO generation, indicating that production was Ca^{2+}-dependent (Fig. 3a,b, Table 1). Forisomes were dispersed when just 0.5 mM H_2O_2 was added but $LaCl_3$ blocked forisome dispersal even when up to 10 mM H_2O_2 was used (Fig. 3a,b, Table 1). The suppressed rise in DAF staining would also indicate that DAF-2 DA was not detecting H_2O_2, which was in agreement with previous studies that demonstrated NO specificity of DAF-2 DA (Kojima *et al.*, 1998; Foissner *et al.*, 2000).

To investigate whether Ca^{2+} influx alone is sufficient to induce NO production in the phloem, 0.1% Triton X-100 was applied, which renders the plasma membrane permeable to Ca^{2+}. The detergent caused dispersal of forisomes and release of chlorophyll from chloroplasts but did not induce cytosolic fluorescence and caused only weak fluorescence in dot-like structures (Fig. 3c). Only after treatment with 1 mM H_2O_2 did strong DAF fluorescence emerge, within 1 min (Fig. 3d). This shows that Ca^{2+} is an essential cofactor but is in itself insufficient to induce NO production in CCs.

Pharmacological investigations of NO sources in the phloem

Mammalian NOS may be Ca^{2+} responsive, and NOS-like activity has been reported in plant/pathogen interactions and
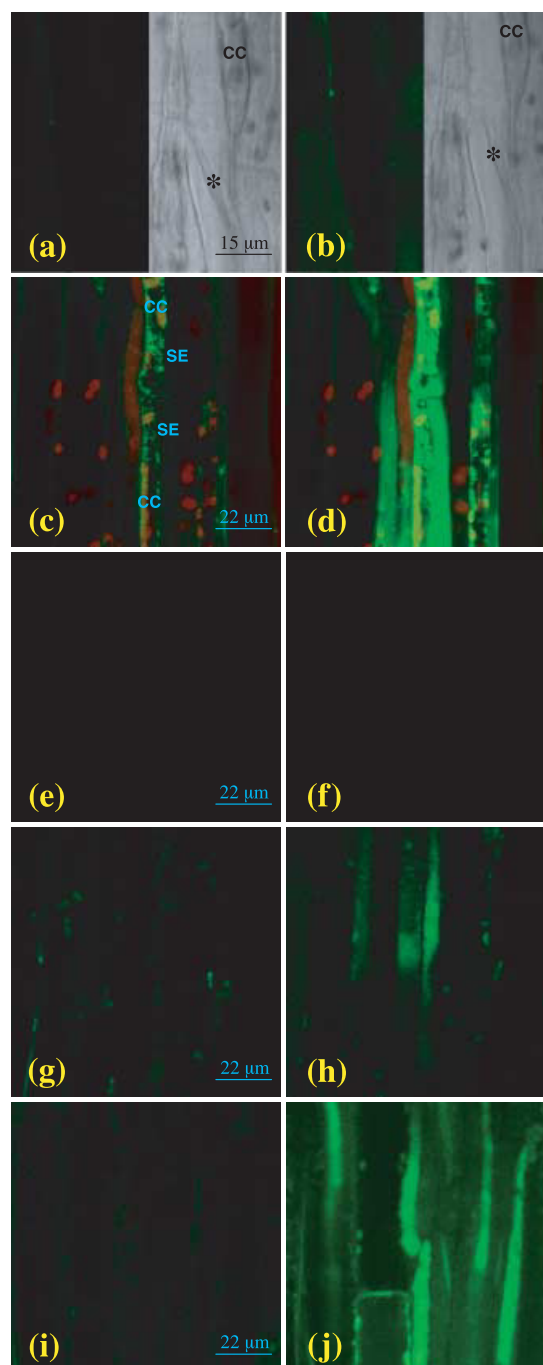
Fig. 3 The emergence of 4,5-diaminofluorescein diacetate (DAF-2 DA) fluorescence in companion cells is dependent on Ca^{2+} and hydrogen peroxide (H_2O_2) and is suppressed by nitric oxide synthase (NOS) inhibitors. (a) Effect of the Ca^{2+} channel blocker $LaCl_3$ (100 μM) and (b) effect of 10 mM H_2O_2/100 μM $LaCl_3$. (c, d) DAF fluorescence (green) (c) 5 min after incubation of phloem tissue in 0.1% Triton X-100 and (d) 1 min 30 s after application of 1 mM H_2O_2. (e, g, i) Control images showing phloem tissue after 30 min of incubation in DAF-2 DA and the NOS inhibitor (e) aminoguanidine (1 mM) or (g) 2-aminoethyl-2-thiopseudurea (AET; 0.2 mM) or (i) the nitrate reductase (NR) inhibitor tungstate (0.1 mM). (f, h, j) Corresponding images taken 10 min after application of 1 mM H_2O_2 together with guanidine (f), AET (h) or tungstate (j).

in plant reactions to fungal elicitors (Neill *et al.*, 2003; Crawford & Guo, 2005). Therefore, the mammalian NOS inhibitors L-NAME, aminoguanidine and 2-aminoethyl-2-thiopseudurea (AET) were employed for characterization of the mode of NO production in CCs. L-NAME turned out to be inappropriate for phloem analyses as both the inhibitor and its inactive enantiomer D-NAME inhibited NO synthesis and impaired forisome dispersal after application of H_2O_2, which is diagnostic for stressed phloem tissue (data not shown). By contrast, 1 mM aminoguanidine blocked H_2O_2-induced DAF fluorescence without affecting the forisome reaction in a total of five experiments (Fig. 3e,f, Table 1), while 0.2 mM AET largely suppressed NO production in CCs in four experiments (Fig. 3g,h). AET was recently shown to be an inhibitor of NO production evoked by treatment of Arabidopsis seedlings with polyamines (Tun *et al.*, 2006). Phloem tissue responded to 1 mM spermine by rapid sieve plate plugging and irreversible forisome dispersal (not shown), whereas 0.2 mM caused dispersal and recondensation of forisomes and DAF fluorescence (Table 1).

To investigate NR as a potential source of NO, the phloem tissue was incubated with 0.1 mM tungstate. The NR inhibitor had no effect on the H_2O_2-induced increase in DAF fluorescence and the forisome reaction (Fig. 3i,j, Table 1). Also, 1 mM sodium nitrite, the substrate of NR, elicited an increase neither in DAF fluorescence nor in forisome dispersal (Table 1), but both could be observed after subsequent addition of 1 mM H_2O_2 (not shown).

Recently, NO production in mitochondria was demonstrated (Guo & Crawford, 2005; Planchet *et al.*, 2005) and NR activity in mitochondria of tobacco was found to be dependent on functional electron transport (Planchet *et al.*, 2005). As we localized an NO source in dot-like structures within CCs (Fig. 2h), inhibitors of mitochondrial electron transport were used to investigate whether these organelles represent mito-chondria. Potassium cyanide (KCN) inhibits the cytochrome *c* and salicylhydroxamic acid (SHAM) alternative oxidase pathway. Surprisingly, the increase in fluorescence not only in dot-like structures but also in whole CCs was completely (SHAM) or largely (KCN) suppressed by preincubation of the phloem tissue in 2.5 mM SHAM or 0.5 or 1 mM KCN before H_2O_2 treatment (Table 1). Hence, functional mito-chondrial electron transport seems to be essential for NO production in CCs.

In summary, the results suggest that the NO source in CCs of *V. faba* is dependent on Ca^{2+} and mitochondrial electron transport and can be suppressed by NOS inhibitors but not by the NR inhibitor tungstate.

Treatment of *Cucurbita maxima* with H_2O_2 induces nitration of phloem proteins

As the specificity of diaminofluorescein for NO has recently been questioned (Planchet & Kaiser, 2006, and references
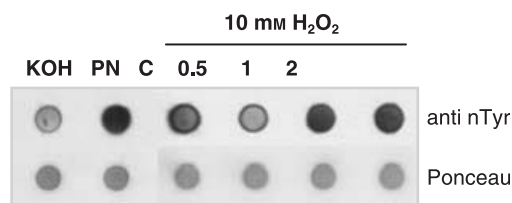

Fig. 4 Detection of nitrated proteins in pumpkin (*Cucurbita maxima*) phloem exudates by western blot analyses using nitrotyrosine antibodies. After watering of pumpkin plants with 10 mM H_2O_2 or water (C, control), phloem exudates were sampled at the indicated time points (hours after treatment). Then 1 μl of exudate was mixed with 50 μl of loading buffer, dotted onto a nitrocellulose membrane and hybridized with nitrotyrosine antibodies (of mouse origin). Detection of nitrated proteins was performed using a peroxidase-conjugated second antibody (anti-mouse) and chemiluminescent peroxidase substrate. One typical result of three western blot analyses is displayed. To test the method, KOH (control) or 2 mM peroxynitrite (PN) was added to phloem samples. anti nTyr, immunodetection of nitrated proteins; Ponceau, Ponceau red staining of the blot membrane.

therein), confirmation of microscopy results by independent methods is required. Unfortunately, the maximal volume of pure sieve tube exudates that can be collected from *V. faba* by aphid stylectomy (Hafke *et al.*, 2005) is too low to allow biochemical measurements of NO content using, for example, Griess and haemoglobin assays. Therefore, we examined NO contents in phloem exudates from pumpkin (*C. maxima*), which produces a significant yield of phloem exudates from cut petioles and stems. In order to elicit NO synthesis, pumpkin plants were watered with 10 mM H_2O_2. In Arabidopsis this treatment induced expression of MAPK (mitogen-activated protein kinase) genes in the shoot (Capone *et al.*, 2004). Although the authors assumed xylem-based transport of H_2O_2 into the shoot, this treatment may act by induced systemic signalling following root-based stress.

Measurements in phloem samples using the Griess assay failed to detect NO in control as well as H_2O_2-treated pumpkin plants (not shown). Recently, protein nitration and nitrosylation in the vascular tissue of salt-stressed olive plants (*Olea europaea*) was demonstrated by CLSM (Valderrama *et al.*, 2007). Hence, rather than being present in sieve tubes in a free form, NO might be rapidly bound to proteins and other phloem com-pounds. In order to test this hypothesis, phloem samples were dotted onto a nitrocellulose membrane and nitrated proteins were detected by western blot analyses with antibodies against nitrotyrosine residues. As shown in Fig. 4, signal intensity, as a cumulative measure for nitration of proteins, was unchanged 0.5 h but increased 1 and 2 h after H_2O_2 treatment. Ponceau staining (Fig. 4) and sodium dodecyl sulphate–polyacrylamide gel electrophoresis (SDS-PAGE; results not shown) confirmed that there was no increase in protein concentration or major changes in protein composition upon application of H_2O_2. In summary, these findings suggest H_2O_2-induced NO accumulation in SEs and subsequent binding to phloem

proteins and thereby corroborate the microscopic detection of NO in the phloem of *V. faba* using DAF-2 DA.

Discussion

Apart from distribution of photoassimilates, the phloem translocates a wide range of molecules, including RNA species, peptides, antioxidants and phytohormones (e.g. SA and jasmonic acid). The nonphotosynthate compounds contribute to sieve tube maintenance, developmental integration and long-distance signalling (Oparka & Santa Cruz, 2000; Ruiz-Medrano *et al.*, 2001; van Bel, 2003; van Bel & Gaupels, 2004).

Recently, NO was detected in the phloem and was suggested to play a role in senescence, lignification of cell walls and the salt stress response (Corpas *et al.*, 2004; Gabaldon *et al.*, 2005, Valderrama *et al.*, 2007). Although plant defences are primarily focused at the site of pathogen challenge, a number of mobile defence signals have been implicated in the partial reiteration of these responses throughout the plant. It has often been presumed (e.g. Ryals *et al.*, 1996) that these have involved the interaction of the mobile signals with the vasculature and more particularly the phloem. To investigate defence signal interactions with the phloem, we exploited the established method of visualizing the responses of living and active phloem through paradermal windows in *V. faba*. For the sake of simplicity, we applied the ubiquitous stress signal H_2O_2, the defence-related hormone SA and the fungal elicitor chitooctaose to the window, assuming that this would mimic the arrival of signals at the phloem from the defences that are localized to the site of attempted pathogen ingress. This study assessed whether NO could be a component in phloem-internal and systemic defence signalling.

H_2O_2 and salicylic acid induce NO synthesis in companion cells

Recent developments have implicated H_2O_2, NO and SA as cooperative components of the defence machinery. Elevated concentrations of H_2O_2 caused SA-dependent defence and resistance gene expression in various plants and cell cultures (Alvarez *et al.*, 1998; Chamnongpol *et al.*, 1998; Mittler *et al.*, 1999). Similarly, H_2O_2 and NO interact in HR induction (Delledonne *et al.*, 1998, 2001; de Pinto *et al.*, 2002). Recently, de Pinto *et al.* (2006) demonstrated that 50 mM H_2O_2 induced NOS activity and programmed cell death in tobacco BY-2 cells, while 10 mM H_2O_2 elicited a rapid NO burst in guard cells of mung bean (*Phaseolus aureus*; Lum *et al.*, 2002). Our current data suggest that the phloem is a significant site of H_2O_2, NO and SA interaction.

Delledonne *et al.* (1998) measured H_2O_2 concentrations of *c*. 1 µM in unstressed cell suspensions and up to 30 µM after elicitation of an oxidative burst by cantharidin and SA. In wounded leaves of tomato (*Lycopersicon esculentum*) plants, H_2O_2 concentrations were estimated to be between 1 and 10 µM (Orozco-Càrdenas & Ryan, 1999). Hence, our treatments of phloem tissue with 10 and 100 µM H_2O_2 were physiological relevant and the rapid increase in NO production in CCs is very likely to occur following the elaboration of a defence response. An important aim for the plant must be to maintain phloem function during such responses, and, accordingly, these low H_2O_2 concentrations do not cause forisome dispersal (Table 1), indicating that the phloem tissue is not severely stressed.

SA is a major signal involved in responses to biotic stress (Ryals *et al.*, 1996) and application of as little as 0.2 mM SA elevated DAF-2 DA fluorescence in 40% of attempts, while with 0.5 and 1 mM SA as many as 80% of attempts exhibited elevated NO production. Fluorescence induced by 0.2 mM SA was lower than after treatment with 0.5 mM SA, whereas there was no difference in fluorescence elicitation among treatments with 0.5, 1 and 10 mM SA. Forisome dispersal suggested that, after application of 10 mM SA, NO production was attributable to cytotoxicity, whereas 0.5 and 1 mM SA did not affect forisome conformation. Zottini *et al.* (2007) noted a greater concentration-dependent induction of NO synthesis in Arabidopsis by an NOS-like enzyme after application of 0.5, 0.75 and 1 mM SA. However, our data are consistent with SA inducing NO production at the phloem, as has also been noted in *V. faba* guard cells (Liu *et al.*, 2003) and soybean (*Glycine max*) leaves (Durner & Klessig, 1999). Further, it seems likely that SA and NO production is under mutual regulation, as application of NO donors was reported to stimulate SA accumulation (Durner *et al.*, 1998; Huang *et al.*, 2004) and the SA-dependent expression of a MAP kinase and *pathogenesis related 1* (*PR1*) gene in tobacco leaves (Durner *et al.*, 1998; Kumar & Klessig, 2000).

Chitosans were found to induce rapid alkalinization of leaf apoplasts and H_2O_2 as well as NO synthesis (Felle *et al.*, 2004; Lin *et al.*, 2005; Zhao *et al.*, 2007). However, although the chitin oligomer chitooctaose elicited NO synthesis in transport phloem tissue, particularly in the CCs, of *V. faba*, as compared with epidermal cells and cell suspensions (Foissner *et al.*, 2000; Modolo *et al.*, 2002; Lamotte *et al.*, 2004; Xu *et al.*, 2005) the reaction was weak. For instance, tobacco epidermal cells responded to the elicitor cryptogein with a strong NO burst within 3 min (Foissner *et al.*, 2000). It may be that epidermal tissue has a higher sensitivity to fungal elicitors than the phloem, as it is the epidermis that is commonly challenged by fungal pathogens.

Subcellular sites of NO production and the nature of the NO-producing enzyme

In experiments with H_2O_2, the CCs were identified as the main sites of NO production, and three subcellular NO sources in CCs could be distinguished; the chloroplast, the cytosol and structures tentatively representing peroxisomes or mitochondria. Nitric oxide synthesis occurred first in chloroplasts of the CCs. Similarly, tobacco leaf segments challenged with cryptogein

displayed early DAF fluorescence in chloroplasts and probably peroxisomes (Foissner *et al.*, 2000). Chloroplasts (Jasid *et al.*, 2006), peroxisomes (Barroso *et al.*, 1999; Corpas *et al.*, 2004) and mitochondria (Guo & Crawford, 2005; Planchet *et al.*, 2005) were previously described as sites of NO synthesis.

NO can be generated by nonenzymatic dismutation of nitrite to NO and nitrate and by activity of the enzymes NR and NOS (Neill *et al.*, 2003; del Río *et al.*, 2004). NOS-like activities are commonly reported in plant reactions to pathogens and elicitors (Crawford & Guo, 2005). Notably, NOS catalyses the Ca^{2+}-dependent transformation of L-arginine into L-citrulline and NO, and we observed that NO generation in the phloem was also Ca^{2+}-dependent. In initial experiments, we used the NOS inhibitor L-NAME and its inactive enantiomer D-NAME for the control treatment. Both compounds impeded NO accumulation and caused stress symptoms, suggesting that L-NAME is not a useful tool for the investigation of phloem NO production. Similarly, Gabaldon *et al.* (2005) found that NO synthesis in the differentiating vascular tissue of *Zinnea elegans* was partly inhibited by L-NAME but also by D-NAME.

However, in the latter study the characterization of the NO source in developing xylem was carried out with stem cross-sections, whereas we analysed inducible NO production in mature intact and unstressed phloem tissue *in planta*. Therefore, the comparability of the results obtained using the two experimental systems is limited. Gabaldon *et al.* (2005) found that 1 mM aminoguanidine did not suppress DAF fluorescence in differentiating xylem, while we found that in CCs this NOS inhibitor effectively blocked the H_2O_2-induced increase in DAF fluorescence. AET – another specific inhibitor of mammalian NOS – also largely prevented the NO burst upon addition of H_2O_2 to the phloem. These results strongly hint at the activity of an NOS-like enzyme in CCs. The rapidity of the reaction to 1 mM H_2O_2 (20–40 s; Supplementary material Movie S1) implies activation of a constitutively present NOS rather than induction of the corresponding gene. The suppressive effects of $LaCl_3$ suggested that Ca^{2+} contributes (directly or indirectly) to its activation. However, the failure of the Triton X-100-induced Ca^{2+} influxes to activate NO generation indicates a requirement for additional factors.

Notably, 0.2 mM spermine elicited forisome dispersal and an increase in DAF fluorescence. This reveals spermine as a potent inducer of phloem stress reactions, similar to H_2O_2 and more effective than SA. Polyamine-induced NO synthesis was detected in Arabidopsis seedlings but the source of NO is still obscure (Tun *et al.*, 2006). It would be interesting to determine whether polyamines, like H_2O_2, act by activating an NOS-like enzyme. Given the rapid induction of NO synthesis by H_2O_2, polyamine treatment might alter H_2O_2 concentrations. In such a scenario, polyamines would be utilized by a phloem polyamine oxidase (PAO) for production of H_2O_2, which in turn would induce NOS activity. Involvement of PAO in the response of maize (*Zea mays*) to wounding and jasmonic acid was described previously (Angelini *et al.*, 2008).

NOS and NR activities were recently detected in mitochondria (Guo & Crawford, 2005; Planchet *et al.*, 2005), and so inhibitors of mitochondrial electron transport were tested for their effects on NO synthesis in CCs. Both KCN, an inhibitor of the cytochrome *c* pathway, and SHAM, an inhibitor of the alternative oxidase pathway, prevented the H_2O_2-induced NO burst. The cytochrome *c* pathway is the main source of ATP in eukariotic cells (Moller, 2001). ATP could be a limiting factor for NO production, as it is essential for the formation of NADPH, which is the electron donor for the conversion of L-arginine to citrullin by NOS (Moller, 2001; Neill *et al.*, 2003). The alternative pathway of electron transport protects mitochondria under oxidative stress conditions (Moller, 2001). Interestingly, Zemojtel *et al.* (2006) hypothesized that *AtNOS1* (renamed to *AtNOA1*) codes for a mitochondrial GTPase and *Atnoa1* mutants might be impaired in NOS activity because of defective mitochondria rather than a lack of the NOS enzyme. Analogously, in CCs functional mitochondria also seem to be essential for NO production catalysed by an NOS-like enzyme.

Application of nitrite evoked NO synthesis by NR in guard cells of Arabidopsis, which could be inhibited by tungstate (Bright *et al.*, 2006). The activity of NR requires NADH as an electron donor but is independent of Ca^{2+} (del Río *et al.*, 2004). Our study suggested that NR was unlikely to be the source of NO in CCs, as treatment with 0.1 mM tungstate did not affect NO generation in response to the treatment with H_2O_2 and, in addition, 1 mM sodium nitrite did not elicit DAF fluorescence. Use of the NR inhibitor sodium azide also had no effect on developmentally regulated NO production in vascular tissue (Gabaldon *et al.*, 2005).

In summary, the described pharmacological approach provides strong evidence implicating NOS activity as a source of inducible NO generation in CCs of *V. faba*. In a future study, the role of mitochondrial electron transport pathways and induction of NO synthesis by polyamines will be further elucidated.

Are SA, H_2O_2 and NO involved in systemic defence signalling via the phloem?

The differing kinetics of NO generation after application of SA or H_2O_2 led us to speculate that H_2O_2 and NO are signals downstream of SA, and this model is supported by findings in the literature: Bright *et al.* (2006) demonstrated that in Arabidopsis ABA-induced NO generation and stomatal closure are mediated by H_2O_2. The ABA-H_2O_2-NO signal cascade regulating stomatal closure could correspond to a hypothetical SA-H_2O_2-NO signal pathway triggered in CCs after pathogen infection. Moreover, studies focusing on defence responses have indicated that SA, H_2O_2 and NO generation are linked, forming part of a potentiating positive feedback loop (Durner & Klessig, 1999). It is therefore especially important that our data and those of Smith-Becker *et al.* (1998) confirm that SA and NO are synthesized in the phloem.

New
Phytologist

Perhaps the simplest model is that the potentiating molecule produced in the phloem is NO, possibly also acting as a mobile signal. After treatment with H_2O_2, weak DAF fluorescence appeared within transporting SEs. Strong H_2O_2-elicited fluorescence was observed when the sieve tubes were occluded, thus preventing removal of DAF by mass flow. DAF fluorescence in SEs could be explained either by influx of NO or fluorescent DAF-T from CCs or by NO synthesis in SEs. The latter possibility is supported by occasional observation of fluorescent SEs next to their nonfluorescent associated CCs (Fig. 1i), but the origin of DAF fluorescence in SEs remains to be established. The pore plasmodesmata units connecting CCs and SEs allow the free exchange of macromolecules (e.g. van Bel & Gaupels, 2004) and an NO-associated molecule could enter the sieve tubes from the SE via mass flow.

Free NO was not detected in SE exudates of pumpkin by the Griess assay; however, using antibodies against nitrotyrosine we found evidence for nitration of phloem proteins upon watering of the plants with 10 mM H_2O_2. Similarly, salt stress induced protein nitration as well as nitrosylation in the vascular tissue of olive plants analysed by CLSM with antibodies and new fluorescent probes (Valderrama et al., 2007). In that study, NO synthesis was induced by growing plants in salt-containing medium for 21 d, whereas we applied salt solutions directly to the phloem tissue, which did not elicit NO production within the 2 h of observation. One mode of NO action in the phloem could be binding of NO to enzymes, thereby modifying their activity, which, in turn, would induce signal synthesis or activation. For instance, NO inhibits the antioxidant enzymes ascorbate peroxidase and catalase (Clark et al., 2000, Igamberdiev et al., 2006) and this has been suggested to facilitate redox signalling by H_2O_2 (Clark et al., 2000; Zeier et al., 2004; de Pinto et al., 2006). In grafting experiments with cucurbits, phloem proteins were shown to move long distances in the sieve tubes (Golecki et al., 1999; van Bel & Gaupels, 2004). Thus, NO-binding proteins and peptides could act as carriers for systemic NO signalling.

Amongst the best candidates for NO-associated molecules are thiols such as glutathione (Durner & Klessig, 1999; Lindermayr et al., 2005). GSNO is known as a vigorous inducer of defence genes (Durner et al., 1998). GSNO or other NO reaction products were speculated to act as a systemic signal (Durner & Klessig, 1999; Foissner et al., 2000; Neill et al., 2003; van Bel & Gaupels, 2004). In support of this idea, injection of NO donors into tobacco leaves reduced the size of lesions caused by tobacco mosaic virus on treated and on systemic nontreated leaves (Song & Goodman, 2001). Also, local treatment with NOS inhibitors or an NO scavenger attenuated SAR in distant leaves (Song & Goodman, 2001). Most significantly, SAR is impaired in GSNOR overexpressing lines and enhanced in antisense lines of Arabidopsis, with GSNOR being mainly localized in CCs (Rusterucci et al., 2007). Together with our finding that NO synthesis in CCs is inducible by resistance-related signals, the collective data

strongly suggest a role of NO and GSNO in systemic signalling via the phloem.

The exact relationship between phloem-localized NO and other, possibly systemic signals is likely to be complex and is under investigation. However, our data have established the phloem as a discrete site of NO generation which may integrate other defence signals and affect the transduction of distal signalling events.

References

Angelini R, Tisi A, Rea G, Chen MM, Botta M, Federico R, Cona A. 2008. Involvement of polyamine oxidase in wound healing. *Plant Physiology* **146**: 162–177.

Alvarez ME, Pennell RI, Meijer PJ, Ishikawa A, Dixon RA, Lamb C. 1998. Reactive oxygen intermediates mediate a systematic signal network in the establishment of plant immunity. *Cell* **92**: 773–784.

Barroso JB, Corpas FJ, Carreras A, Sandalio LM, Valderrama R, Palma JM, Lupianez JA, del Rio LA. 1999. Localization of nitric oxide synthase in plant peroxisomes. *Journal of Biological Chemistry* **274**: 36729–36733.

Baxter-Burrell A, Chang R, Springer P, Bailey-Serres J. 2003. Gene and enhancer trap transposable elements reveal oxygen deprivation-regulated genes and their complex patterns of expression in Arabidopsis. *Annals of Botany (London)* **91**: 129–141.

van Bel AJE. 2003. The phloem, a miracle of ingenuity. *Plant, Cell & Environment* **26**: 125–149.

van Bel AJE, Gaupels F. 2004. Pathogen-induced resistance and alarm signals in the phloem. *Molecular Plant Pathology* **5**: 495–504.

Bright J, Desikan R, Hancock JT, Weir IS, Neill SJ. 2006. ABA-induced NO generation and stomatal closure in *Arabidopsis* are dependent on H_2O_2 synthesis. *Plant Journal* **45**: 113–122.

Capone R, Tiwari BS, Levine A. 2004. Rapid transmission of oxidative and nitrosative stress signals from roots to shoots in *Arabidopsis*. *Plant Physiology and Biochemistry* **42**: 425–428.

Chamnongpol S, Willekens H, Moeder W, Langebartels C, Sandermann H, Van Montagu A, Inzé D, Van Camp W. 1998. Defense activation and enhanced pathogen tolerance induced by H_2O_2 in transgenic tobacco. *Proceedings of the National Academy of Sciences, USA* **95**: 5818–5823.

Clark D, Durner J, Navarre DA, Klessig DF. 2000. Nitric oxide inhibition of tobacco catalase and ascorbate peroxidase. *Molecular Plant–Microbe Interactions* **13**: 1380–1384.

Clarke SM, Mur LA, Wood JE, Scott IM. 2004. Salicylic acid dependent signaling promotes basal thermotolerance but is not essential for acquired thermotolerance in Arabidopsis thaliana. *Plant Journal* **38**: 432–447.

Corpas FJ, Barroso JB, Carreras A, Quiros M, Leon AM, Romero-Puertas MC, Esteban FJ, Valderrama R, Palma JM, Sandalio LM et al. 2004. Cellular and subcellular localization of endogenous nitric oxide in young and senescent pea plants. *Plant Physiology* **136**: 2722–2733.

Crawford NM, Guo FQ. 2005. New insights into nitric oxide metabolism and regulatory functions. *Trends in Plant Science* **10**: 195–200.

Dat JF, Foyer CH, Scott IM. 1998. Changes in salicylic acid and antioxidants during induced thermotolerance in mustard seedlings. *Plant Physiology* **118**: 1455–61.

Delledonne M, Xia Y, Dixon RA, Lamb C. 1998. Nitric oxide functions as a signal in plant disease resistance. *Nature* **394**: 585–588.

Delledonne M, Zeier J, Marocco A, Lamb C. 2001. Signal interactions between nitric oxide and reactive oxygen intermediates in the plant hypersensitive disease resistance response. *Proceedings of the National Academy of Sciences, USA* **98**: 13454–13459.

Durner J, Klessig DF. 1999. Nitric oxide as a signal in plants. *Current Opinion in Plant Biology* **2**: 369–374.

Durner J, Wendehenne D, Klessig DF. 1998. Defense gene induction

in tobacco by nitric oxide, cyclic GMP, and cyclic ADP-ribose. *Proceedings of the National Academy of Sciences, USA* **95**: 10328–10333.

Durrant WE, Dong X. 2004. Systemic acquired resistance. *Annual Review of Phytopathology* **42**: 185–209.

Felle HH, Herrmann A, Hanstein S, Hückelhoven R, Kogel KH. 2004. Apoplastic pH signaling in barley leaves attacked by the powdery mildew fungus *Blumeria graminis* f. sp. *hordei*. *Molecular Plant–Microbe Interactions* **17**: 118–123.

Foissner I, Wendehenne D, Langebartels C, Durner J. 2000. In vivo imaging of an elicitor-induced nitric oxide burst in tobacco. *Plant Journal* **23**: 817–824.

Gabaldon C, Gomez Ros LV, Pedreno MA, Ros Barcelo A. 2005. Nitric oxide production by the differentiating xylem of *Zinnia elegans*. *New Phytologist* **165**: 121–130.

Golecki B, Schulz A, Thompson GA. 1999. Translocation of structural P proteins in the phloem. *Plant Cell* **11**: 127–140.

Gould KS, Lamotte O, Klinguer A, Pugin A, Wendehenne D. 2003. Nitric oxide production in tobacco leaf cells: a generalized stress response? *Plant, Cell & Environment* **26**: 1851–1862.

Guo FQ, Crawford NM. (2005) Arabidopsis nitric oxide synthase 1 is targeted to mitochondria and protects against oxidative damage and dark-induced senescence. *Plant Cell* **17**: 3436–3450.

Guo FQ, Okamoto M, Crawford NM. 2003. Identification of a plant nitric oxide synthase gene involved in hormonal signaling. *Science* **302**: 100–103.

Hafke JB, van Amerongen JK, Kelling F, Furch ACU, Gaupels F, van Bel AJE. 2005. Thermodynamic battle for photosynthate acquisition between sieve tubes and adjoining parenchyma in transport phloem. *Plant Physiology* **138**: 1527–1537.

Hanstein S, Felle HH. 2004. Nanoinfusion: an integrative tool to study elicitor perception and signal transduction in intact leaves. *New Phytologist* **161**: 595–606.

Huang X, Stettmaier K, Michel C, Hutzler P, Mueller MJ, Durner J. 2004. Nitric oxide is induced by wounding and influences jasmonic acid signaling in *Arabidopsis thaliana*. *Planta* **218**: 938–946.

Igamberdiev AU, Stoimenova M, Seregélyes C, Hill RD. 2006. Class-1 hemoglobin and antioxidant metabolism in alfalfa roots. *Planta* **223**: 1041–1046.

Jasid S, Simontacchi M, Bartoli CG, Puntarulo S. 2006. Chloroplasts as a nitric oxide cellular source. Effect of reactive nitrogen species on chloroplastic lipids and proteins. *Plant Physiology* **142**: 1246–1255.

Jih PJ, Chen YC, Jeng ST. 2003. Involvement of hydrogen peroxide and nitric oxide in expression of the ipomoelin gene from sweet potato. *Plant Physiology* **132**: 381–389.

Knoblauch M, van Bel AJE. 1998. Sieve tubes in action. *Plant Cell* **10**: 35–50.

Knoblauch M, Peters WS, Ehlers K, van Bel AJ. 2001. Reversible calcium-regulated stopcocks in legume sieve tubes. *Plant Cell* **13**: 1221–1230.

Kojima H, Nakatsubo N, Kikuchi K, Kawahara S, Kirino Y, Nagoshi H, Hirata Y, Nagano T. 1998. Detection and imaging of nitric oxide with novel fluorescent indicators: diaminofluoresceins. *Analytical Chemistry* **70**: 2446–2453.

Kumar D, Klessig DF. 2000. Differential induction of tobacco MAP kinases by the defense signals nitric oxide, salicylic acid, ethylene, and jasmonic acid. *Molecular Plant Microbe Interactions* **13**: 347–351.

Lamotte O, Gould K, Lecourieux D, Sequeira-Legrand A, Lebrun-Garcia A, Durner J, Pugin A, Wendehenne D. 2004. Analysis of nitric oxide signaling functions in tobacco cells challenged by the elicitor cryptogein. *Plant Physiology* **135**: 516–529.

Levine A, Tenhaken R, Dixon R, Lamb C. 1994. H_2O_2 from the oxidative burst orchestrates the plant hypersensitive disease resistance response. *Cell* **79**: 583–593.

Lin W, Hu X, Zhang W, Rogers WJ, Cai W. 2005. Hydrogen peroxide mediates defence responses induced by chitosans of different molecular weights in rice. *Journal of Plant Physiology* **162**: 937–944.

Lindermayr C, Saalbach G, Durner J. 2005. Proteomic identification of S-nitrosylated proteins in *Arabidopsis*. *Plant Physiology* **137**: 921–930.

Liu X, Zhang SQ, Lou CH. 2003. Involvement of nitric oxide in the signal transduction of salicylic acid regulating stomatal movement. *Chinese Science Bulletin* **48**: 449–452.

Lum HK, Butt YK, Lo SC. 2002. Hydrogen peroxide induces a rapid production of nitric oxide in mung bean (*Phaseolus aureus*). *Nitric Oxide* **6**: 205–213.

Mittler R, Herr EH, Orvar BL, van Camp W, Willekens H, Inzé D, Ellis BE. 1999. Transgenic tobacco plants with reduced capability to detoxify reactive oxygen inter-mediates are hyperresponsive to pathogen infection. *Proceedings of the National Academy of Sciences, USA* **96**: 14165–14170.

Modolo LV, Cunha FQ, Braga MR, Salgado I. 2002. Nitric oxide synthase-mediated phytoalexin accumulation in soybean cotyledons in response to the *Diaporthe phaseolorum* f. sp. *meridionalis* elicitor. *Plant Physiology* **130**: 1288–1297.

Moller IM. 2001. Plant mitochondria and oxidative stress: electron transport, NADPH turnover, and metabolism of reactive oxygen species. *Annual Review of Plant Physiology and Molecular Biology* **52**: 561–591.

Mur LAJ, Carver TLW, Prats E. 2006. NO way to live; the various roles of nitric oxide in plant-pathogen interactions. *Journal of Experimental Botany* **57**: 489–505.

Navarre DA, Wendehenne D, Durner J, Noad R, Klessig DF. 2000. Nitric oxide modulates the activity of tobacco aconitase. *Plant Physiology* **122**: 573–582.

Neill SJ, Desikan R, Clarke A, Hancock JT. 2003. Nitric oxide signalling in plants. *New Phytologist* **159**: 11–35.

Neill SJ, Desikan R, Clarke A, Hurst RD, Hancock JT. 2002. Hydrogen peroxide and nitric oxide as signalling molecules in plants. *Journal of Experimental Botany* **53**: 1237–1247.

Oparka KJ, Santa Cruz S. 2000. The great escape: phloem transport and unloading of macromolecules. *Annual Review of Plant Physiology and Plant Molecular Biology* **51**: 323–347.

Orozco-Càrdenas ML, Narvaez-Vasquez J, Ryan CA. 2001. Hydrogen peroxide acts as a second messenger for the induction of defense genes in tomato plants in response to wounding, systemin and methyl jasmonate. *Plant Cell* **13**: 179–191.

Orozco-Càrdenas ML, Ryan CA. 1999. Hydrogen peroxide is generated systemically in plant leaves by wounding and systemin via the octadecanoid pathway. *Proceedings of the National Academy of Sciences, USA* **96**: 6553–6557.

de Pinto MC, Paradiso A, Leonetti P, De Gara L. 2006. Hydrogen peroxide, nitric oxide and cytosolic ascorbate peroxidase at the crossroad between defence and cell death. *Plant Journal* **48**: 784–795.

de Pinto MC, Tommasi F, De Gara L. 2002. Changes in the antioxidant systems as part of the signaling pathway responsible for the programmed cell death activated by nitric oxide and reactive oxygen species in tobacco Bright-Yellow 2 cells. *Plant Physiology* **130**: 698–708.

Planchet E, Gupta KJ, Sonoda M, Kaiser WM. 2005. Nitric oxide emission from tobacco leaves and suspension cells: rate limiting factors and evidence for the involvement of mitochondrial electron transport. *Plant Journal* **41**: 732–743.

Planchet E, Kaiser WM. 2006. Nitric oxide (NO) detection by DAF fluorescence and chemiluminescence: a comparison using abiotic and biotic NO sources. *Journal of Experimental Botany* **57**: 3043–3055.

Prasad TK, Anderson MD, Martin BA, Stewart CR. 1994. Evidence for chilling-induced oxidative stress in maize seedlings and a regulatory role for hydrogen peroxide. *Plant Cell* **6**: 65–74.

Prats E, Mur LAJ, Sanderson R, Carver TLW. 2005. Nitric oxide contributes both to papilla-based resistance and the hypersensitive response in barley attacked by *Blumeria graminis* f. sp. *hordei*. *Molecular Plant Pathology* **6**: 65–78.

Requena ME, Egea-Gilabert C, Candela ME. 2005. Nitric oxide generation during the interaction with *Phytophtora capsici* of two *Capsicum annuum* varieties showing different degrees of sensitivity. *Physiologia Plantarum* **124**: 50–60.

del Río LA, Corpas FJ, Barroso JB. 2004. Nitric oxide and nitric oxide synthase activity in plants. *Phytochemistry* **65**: 783–792.

Ruiz-Medrano R, Xoconostle-Cazares B, Lucas WJ. 2001. The phloem as a conduit for inter-organ communication. *Current Opinion in Plant Biology* **4**: 202–209.

Rusterucci C, Espunya MC, Diaz M, Chabannes M, Martinez MC. 2007. S-nitrosoglutathione affords protection against pathogens in Arabidopsis, both locally and systemically. *Plant Physiology* **143**: 1282–1292.

Ryals JA, Neuenschwander UH, Willits MG, Molina A, Steiner HY, Hunt MD. 1996. Systemic acquired resistance. *Plant Cell* **8**: 1809–1819.

Scott IM, Clarke SM, Wood JE, Mur LA. 2004. Salicylic acid inhibits growth at chilling temperature in Arabidopsis. *Plant Physiology* **135**: 1040–1049.

Smith-Becker J, Marois E, Huguet EJ, Midland SL, Sims JJ, Keen NT. 1998. Accumulation of salicylic acid and 4-hydroxybenzoic acid in phloem fluids of cucumber during systemic acquired resistance is preceded by a transient increase in phenylalanine ammonia-lyase activity in petioles and stems. *Plant Physiology* **116**: 231–238.

Song FM, Goodman RM. 2001. Activity of nitric oxide is dependent on, but is partially required for function of, salicylic acid in the signaling pathway in tobacco systemic acquired resistance. *Molecular Plant–Microbe Interactions* **14**: 1458–1462.

Stuehr DJ. 1999. Mammalian nitric oxide synthases. *Biochimica et Biophysica Acta* **1411**: 217–230.

Tun NN, Santa-Catarina C, Begum T, Silveira V, Handro W, Floh EIS, Scherer GFE. 2006. Polyamines induce rapid biosynthesis of nitric oxide (NO) in *Arabidopsis thaliana* seedlings. *Plant Cell Physiology* **47**: 346–354.

Valderrama R, Corpas FJ, Carreras A, Fernandez-Ocana A, Chaki M, Luque F, Gomez-Rodriguez MV, Colmenero-Varea P, del Rio LA, Barroso JB. 2007. Nitrosative stress in plants. *FEBS Letters* **581**: 453–461.

Xu MJ, Dong JF, Zhu MY. 2005. Nitric oxide mediates the fungal elicitor-induced hypericin production of *Hypericum perforatum* cell suspension cultures through a jasmonic-acid-dependent signal pathway. *Plant Physiology* **139**: 991–998.

Zeidler D, Zahringer U, Gerber I, Dubery I, Hartung T, Bors W, Hutzler P, Durner J. 2004. Innate immunity in *Arabidopsis thaliana*: lipopolysaccharides activate nitric oxide synthase (NOS) and induce defense genes. *Proceedings of the National Academy of Sciences, USA* **101**: 15811–15816.

Zeier J, Delledonne M, Mishina T, Severi E, Sonoda M, Lamb C. 2004. Genetic elucidation of nitric oxide signaling in incompatible plant-pathogen interactions. *Plant Physiology* **136**: 2875–2886.

Zemojtel T, Fröhlich A, Palmieri MC, Kolanczyk M, Mikula I, Wyrwicz LS, Wanker EE, Mundlos S, Vingron M, Martasek P et al. 2006. Plant nitric oxide synthase: a never-ending story? *Trends in Plant Science* **11**: 524–525.

Zhao J, Fujita K, Sakai K. 2007. Reactive oxygen species, nitric oxide, and their interactions play different roles in *Cupressus lusitanica* cell death and phytoalexin biosynthesis. *New Phytologist* **175**: 215–229.

Zottini M, Costa A, De Michele R, Ruzzene M, Carimi F, Lo Schiavo F. 2007. Salicylic acid activates nitric oxide synthesis in Arabidopsis. *Journal of Experimental Botany* **58**: 1397–405.

Zuppini A, Baldan B, Millioni R, Favaron F, Navazio L, Mariani P. 2003. Hydrogen peroxide is generated systemically in plant leaves by wounding and systemin via the octadecanoid pathway. *New Phytologist* **161**: 557–568.

Supplementary Material

The following supplementary material is available for this article online:

Movie S1 Movie showing the rapid increase in diamino-fluorescence fluorescence upon addition of 1 mM H_2O_2 to bare-lying intact phloem tissue of *Vicia faba*.

This material is available as part of the online article from: http://www.blackwell-synergy.com/doi/abs/10.1111/j.1469-8137.2008.02388.x
(This link will take you to the article abstract.)

Please note: Blackwell Publishing are not responsible for the content or functionality of any supplementary materials supplied by the authors. Any queries (other than about missing material) should be directed to the journal at *New Phytologist* Central Office.

Looking Deep Inside: Detection of Low-Abundance Proteins in Leaf Extracts of Arabidopsis and Phloem Exudates of Pumpkin[1][W]

Andreas Fröhlich[2], Frank Gaupels[2], Hakan Sarioglu, Christian Holzmeister, Manuel Spannagl, Jörg Durner, and Christian Lindermayr*

Institute of Biochemical Plant Pathology (A.F., F.G., C.H., J.D., C.L.), Department of Protein Science (H.S.), and Institute of Bioinformatics and Systems Biology (M.S.), Helmholtz Zentrum München, German Research Center for Environmental Health, D–85764 Neuherberg, Germany

The field of proteomics suffers from the immense complexity of even small proteomes and the enormous dynamic range of protein concentrations within a given sample. Most protein samples contain a few major proteins, which hamper in-depth proteomic analysis. In the human field, combinatorial hexapeptide ligand libraries (CPLL; such as ProteoMiner) have been used for reduction of the dynamic range of protein concentrations; however, this technique is not established in plant research. In this work, we present the application of CPLL to Arabidopsis (*Arabidopsis thaliana*) leaf proteins. One- and two-dimensional gel electrophoresis showed a decrease in high-abundance proteins and an enrichment of less abundant proteins in CPLL-treated samples. After optimization of the CPLL protocol, mass spectrometric analyses of leaf extracts led to the identification of 1,192 proteins in control samples and an additional 512 proteins after the application of CPLL. Upon leaf infection with virulent *Pseudomonas syringae* DC3000, CPLL beads were also used for investigating the bacterial infectome. In total, 312 bacterial proteins could be identified in infected Arabidopsis leaves. Furthermore, phloem exudates of pumpkin (*Cucurbita maxima*) were analyzed. CPLL prefractionation caused depletion of the major phloem proteins 1 and 2 and improved phloem proteomics, because 67 of 320 identified proteins were detectable only after CPLL treatment. In sum, our results demonstrate that CPLL beads are a time- and cost-effective tool for reducing major proteins, which often interfere with downstream analyses. The concomitant enrichment of less abundant proteins may facilitate a deeper insight into the plant proteome.

Proteomics is the large-scale study of proteins and includes the exploration of all proteins present in a cell or an organism under certain conditions and at a certain time point. With each gene giving rise to not only a single protein, complex organisms are thought to produce hundreds of thousands of different proteins that additionally can undergo various posttranslational modifications. Although methods of proteomics, especially mass spectrometry (MS), are constantly improving, we are still seeing only a rather small subset of the total proteome. Another major problem inherent to all proteomic analyses is the enormous dynamic range of protein concentrations within a given sample, which can be up to 12 orders of magnitude (Corthals

et al., 2000). Therefore, most protein samples contain a few high-abundance, dominating proteins and a large number of low-abundance proteins, which often fall below the detection limit of the technique used for analysis. Fractionation of samples reduces the complexity of the protein pool significantly. But high-abundance proteins still lead to masking and suppression effects during analysis with two-dimensional (2D) gel electrophoresis or MS.

Recently, a new technique has emerged that reduces the dynamic range of protein concentrations within a given sample using combinatorial hexapeptide ligand libraries (CPLL; Boschetti et al., 2007; Boschetti and Righetti, 2008a, 2008b, 2009; Fröhlich and Lindermayr, 2011). The CPLL were synthesized on beads by the split-couple-recombine method described in earlier works (Furka et al., 1991; Lam et al., 1991; Buettner et al., 1996). Use of the 20 naturally occurring amino acids theoretically resulted in 64 million different ligands, with each ligand fixed to a single bead (Thulasiraman et al., 2005; Boschetti and Righetti, 2008a). Specific binding of proteins to the CPLL is thought to depend on the physicochemical properties of the protein (e.g. conformation, hydrophobicity, and pI). The native conformation of the proteins, therefore, is preferred during treatment. The interactions between proteins and peptide ligands seem to be mainly stabilized by hydrophobic forces but also by other weak forces such

as ion-ion, dipole-dipole, or hydrogen bonding (Bachi et al., 2008; Righetti and Boschetti, 2008; Keidel et al., 2010). Under capacity-restrained conditions, high-abundance protein species will saturate their ligand quickly, whereas low-abundance species will be bound completely. Unbound proteins will be removed from the matrix by washing, whereas bound proteins will be eluted from the matrix. The resulting protein solution should contain all proteins present in the original sample, albeit with a narrower dynamic range of protein concentrations.

The libraries, commercially available as ProteoMiner (Bio-Rad), have been used to reduce the dynamic range of protein concentrations in various samples, such as *Escherichia coli* crude extract and cell culture supernatant, human serum, and chicken egg white. Furthermore, CPLL have been used for the analysis of human urine, human bile, platelet lysate, red blood cell lysate, chicken egg white and egg yolk, or cow whey (Castagna et al., 2005; Thulasiraman et al., 2005; Guerrier et al., 2006, 2007a, 2007b; D'Ambrosio et al., 2008; Roux-Dalvai et al., 2008; Boschetti and Righetti, 2009; D'Amato et al., 2009; Farinazzo et al., 2009). In all these studies, a much larger number of proteins could be identified when using CPLL, with many of the proteins being described for the first time in the respective sample.

The completion of the Arabidopsis (*Arabidopsis thaliana*) genome sequence revealed the presence of about 30,000 genes in this plant species. However, on the protein level, only a restricted number of different proteins can be detected. The main problem is the presence of some high-abundance proteins, which are limiting the detection of low-abundance proteins (Peck, 2005). In leaves, Rubisco accumulates up to 40% of total leaf protein (Stitt et al., 2010), and in the seed endosperm, storage proteins are present in massive amounts (Li et al., 2008). But even less extreme examples, like many housekeeping proteins, are present in sufficient amounts to hinder the analysis of low-abundance proteins. Recently, CPLL beads were used to identify leaf proteins of spinach (*Spinacia oleracea*). The authors performed capture of proteins at three different pH values and were able to identify 322 proteins, of which 190 could only be found in the CPLL-treated samples (Fasoli et al., 2011a). CPLL were also applied for analyses of some plant-derived products (D'Amato et al., 2010, 2011, 2012; Fasoli et al., 2010a, 2011b, 2012). However, although ProteoMiner has been on the market for 5 years, this technology has still not entered plant research.

Therefore, the overall goal of this study was the establishment of CPLL applications in plant proteomics. Protein extraction protocols were optimized for the incubation of Arabidopsis leaf proteins with CPLL. Subsequent analyses by one-dimensional (1D)-SDS-PAGE, two-dimensional fluorescence difference gel electrophoresis (2D-DIGE), and liquid chromatography-tandem mass spectrometry (LC-MS/MS) showed a reduction of high-abundance proteins in CPLL-treated

leaf extracts. It could also be demonstrated that CPLL allowed the identification of additional proteins that could not be detected in control samples. Currently, two protocols for the application of CPLL are available, and we compared both of them. Capture of Arabidopsis proteins by CPLL at three different pH values and elution from the beads using hot SDS/dithiothreitol (DTT) turned out to yield better results than CPLL treatment according to the manufacturer's protocol. Following the optimized protocol, 1,192 proteins could be identified by LC-MS/MS in control samples but an additional 512 proteins were found only after the application of CPLL. Furthermore, we successfully used this technology to analyze, to our knowledge for the first time, the infectome of *Pseudomonas syringae* DC3000 during infection of Arabidopsis.

In an additional set of experiments, we applied ProteoMiner to liquid pumpkin (*Cucurbita maxima*) phloem samples. Cucurbitaceae species including pumpkin are model plants for phloem biochemistry, because exudates of the unique extrafascicular phloem (EFP) can be easily collected from cut petioles and stems (Van Bel and Gaupels, 2004; Atkins et al., 2011). A main obstacle of protein biochemistry with pumpkin phloem exudates is the high abundance (80% of total protein content) of Phloem Protein1 (PP1) and Phloem Protein2 (PP2). The use of CPLL beads caused a strong reduction in PP1/PP2 levels and facilitated the identification of 320 proteins, including 81 previously unknown phloem proteins.

RESULTS AND DISCUSSION

Protocol I

Application of CPLL to Arabidopsis Leaf Extracts following the Manufacturer's Instructions

Plant proteins are notoriously difficult to extract (Rose et al., 2004). This is mainly due to the low protein content of plant tissue and the low solubility of plant proteins. Furthermore, plants accumulate high levels of diverse metabolites, such as monosaccharides and polysaccharides, phenolic compounds, and oils that may interfere with downstream sample analysis. Our sample preparation protocol addressed these points by polyvinylpolypyrrolidone treatment and the use of size-exclusion columns to remove salts and secondary metabolites as well as NH_4SO_4 precipitation for concentrating proteins without severe denaturation.

In initial experiments, ProteoMiner was applied according to the manufacturer's (Bio-Rad) instructions with some modifications. The ProteoMiner manual recommended the application of 10 mg of protein at concentrations of 50 mg mL^{-1} for incubation with the CPLL beads. However, the maximum protein concentration of Arabidopsis leaf extracts achieved with the described protocol was around 10 mg mL^{-1}. Therefore, the suggested ratio of protein amount to bead slurry volume was maintained, but the sample volume was

increased. Ten milligrams of protein per sample was mixed with 100 μL of bead slurry in a volume of 1 mL. In order to facilitate the binding of diluted proteins to the column, the incubation time was prolonged. Proteins were eluted from the beads with 8 M urea for breaking hydrogen bonds and protein denaturation. CHAPS at 2% was used to disrupt hydrophilic interactions. The average total protein yield per CPLL column was 364 μg, with a coefficient of variation (CV) of 4.7% over four extractions.

A first comparison of the protein pools of the crude extracts, washing fractions, and the CPLL eluates was done by 1D-SDS-PAGE (Fig. 1). Prominent bands representing the large and small subunits of Rubisco were highly abundant in flow-through and washing fractions but strongly reduced in the CPLL eluates. As specified in the manual, unbound proteins were largely removed after four washing steps.

Protein crude extracts and CPLL eluates were also analyzed using the 2D-DIGE technology. 2D-DIGE enables the separation of multiple protein extracts on the same gel by labeling of each protein in the extracts using spectrally resolvable, size- and charge-matched fluorescent dyes. This method adds a highly accurate quantitative dimension to the commonly executed 2D analysis. For reducing biological variation, we used the same Arabidopsis crude extract for four parallel CPLL extractions. A strikingly different protein spot pattern could be observed between CPLL eluates and crude extracts in 2D-DIGE analysis (Fig. 2). The 2D-DIGE overlay image further illustrates the differences between the two sample types. In the Cy3-labeled CPLL
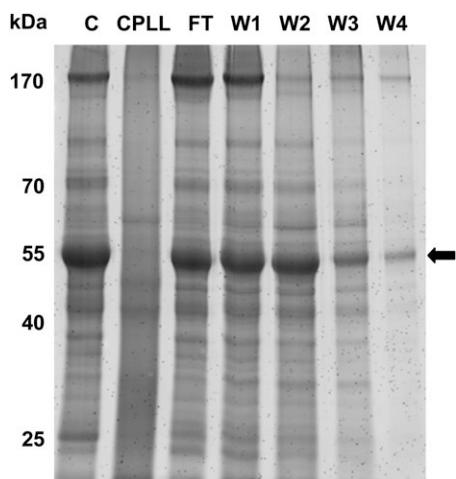

Figure 2. 2D-DIGE analysis of the effect of CPLL fractionation on the Arabidopsis leaf proteome. Each 50-μg protein of crude extract and CPLL eluate was stained with two different probes and separated on the same gel by 2D-DIGE, resulting in strikingly different spot patterns. The top shows spot patterns for both samples separately (DIGE modus black/white). Boxed areas depict selected proteins enriched upon CPLL treatment. The bottom shows a 2D-DIGE fluorescent overlay image of the above CPLL-treated (green) and crude extract (red) samples. A pH gradient of 4 to 7 was used for isoelectric focusing. Results are representative of four independent 2D-DIGE experiments.

sample, new spots appeared, whereas many of the intense spots present in the Cy5-labeled crude extract were missing or reduced in intensity.

In four gel replicates, the DeCyder spot-finding algorithm found approximately 20% more spots in images depicting CPLL-captured proteins than in images of raw extract (data not shown; CV = 20.4%). A total of 305 leaf proteins were statistically significantly enriched and 400 proteins were significantly depleted in the CPLL-treated samples as compared with raw extracts ($P < 0.05$). Reducing the P value to $P < 0.0001$ still resulted in 119 enriched and 178 reduced proteins, pointing toward the high reproducibility of the method. The average CV across all matched spots on four replicate gels was 19.2%.

Figure 1. 1D-SDS-PAGE of CPLL fractionation of Arabidopsis leaf proteins. Ten milligrams of leaf proteins was incubated with CPLL according to the manufacturer's instructions. After four washing steps, proteins were eluted from the CPLL beads. Aliquots of the different fractions were separated by SDS-PAGE, and proteins were stained with Sypro Ruby. The relative masses of protein standards are indicated on the left. C, Crude leaf extract; CPLL, eluate; FT, flow through; W1 to W4, wash fractions. The position of the large subunit of Rubisco is marked with an arrow.
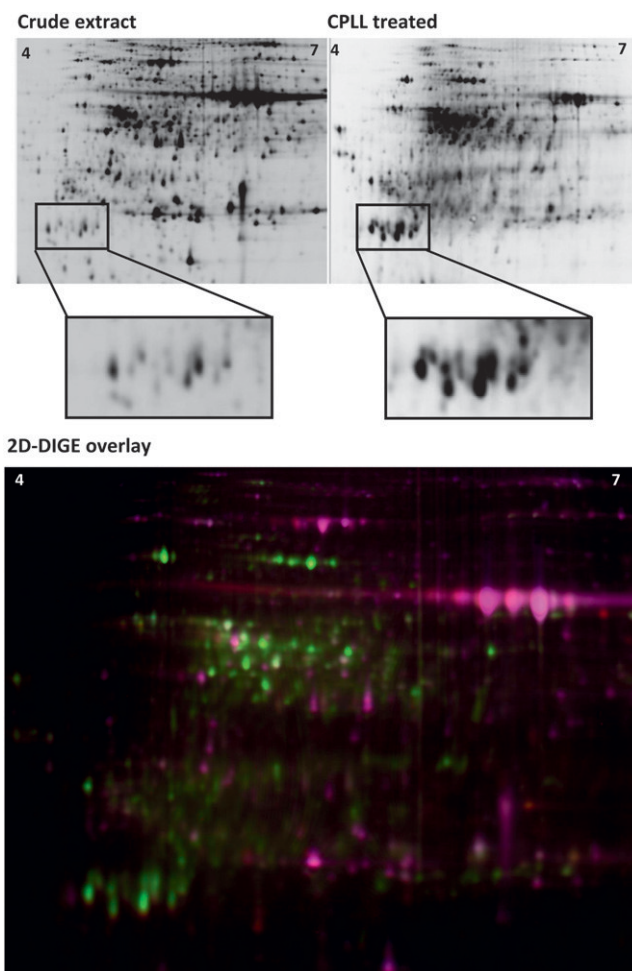
Crude extract and ProteoMiner eluate samples were subjected to LC-MS/MS analysis for protein identification. To reduce the complexity of the different samples, the proteins were separated by 1D-SDS-PAGE and the lanes were cut into 10 subfractions, which were analyzed separately by LC-MS/MS. In total, 1,489 plant proteins could be identified (Supplemental Table S1). A total of 200 proteins could be identified exclusively in the CPLL-treated sample, whereas 675 proteins were identified in both crude extract and CPLL samples. A total of 631 proteins were "lost" due to the ProteoMiner treatment and could be detected only in the crude extract (Fig. 3).

Application of CPLL to Protein Extracts from Infected Leaves

In order to better assess the CPLL effect on a specific protein subpopulation within a given sample, we analyzed bacterial proteins in Arabidopsis leaves infected with virulent *P. syringae* DC3000. Arabidopsis plants were inoculated with virulent *P. syringae* DC3000 and were harvested when typical disease symptoms started to develop (approximately 24 h after inoculation). At that time point, the average bacterial concentration within infected leaves was 5×10^7 colony-forming units cm^{-2}. The samples were subjected to CPLL technology using the ProteoMiner standard protocol (Bio-Rad). In total, 1,598 Arabidopsis and 312 bacterial proteins could be identified (Supplemental Tables S2 and S3). A total of 203 Arabidopsis proteins and 48 bacterial proteins were only found in the CPLL-treated samples, adding 15% and 18% new proteins, respectively, to the proteomes of nonfractionated crude extracts.

To our knowledge, this is the first analysis of an in planta pathogen proteome ("infectome"; Mehta et al., 2008). Approximately 5% of the *P. syringae* DC3000 genes encode for proteins involved in virulence (Rahme et al., 1995; Preston, 2000; Buell et al., 2003). Many of these proteins function in bacterial mobility, the nutrient transport system, reactive oxygen species

Figure 3. The effect of CPLL treatment on Arabidopsis leaf proteins. Leaf extracts were treated with CPLL according to the manufacturer's protocol. The protein composition of the CPLL eluate was analyzed by LC-MS/MS and compared with the protein composition of the corresponding protein crude extract. A total of 1,284 unique proteins were identified in the control sample. Two hundred (15%) additional proteins could be identified by using CPLL for extraction.

detoxification, or biosynthesis of the bacterial polysaccharide capsule (Buell et al., 2003). When analyzing bacterial proteins within leaf extracts, 107 (34%) of the identified 312 *P. syringae* proteins were related to bacterial virulence, including enzymes from coronatine synthesis (coronafacic acid synthase subunits), alginate synthesis (alginate biosynthesis protein [AlgF], alginate lyase), transcriptional regulators (transcriptional regulator, LysR family [LysR], Cys regulon transcriptional activator [Cys regulon], transcriptional regulator AlgQ), ATP-binding cassette (ABC) transporters, outer membrane proteins (outer membrane porin [OprF], outer membrane protein [OmpA]), redox-related proteins (glutathione *S*-transferases, superoxide dismutases, thioredoxin, catalase), and flagellin. Selected bacterial proteins playing a role in *P. syringae* pathogenesis are shown in Table I. The complete lists of identified plant and bacterial proteins are given in Table II and Supplemental Table S1.

Protocol II

Application of CPLL to Arabidopsis Leaf Extracts Using Three pH Values and Hot SDS/DTT Elution

The effect of hexapeptide libraries on animal and human proteins was very pronounced, with a loss of proteins sometimes below 5% but up to 500% additional proteins captured (Di Girolamo et al., 2011). Because we identified only 15% additional leaf proteins when applying ProteoMiner according to the manufacturer's instructions, we tried to further improve the CPLL protocol. Righetti and coworkers (Di Girolamo et al., 2011) reported that a reduction of salt in samples, capture at three pH values, and elution in boiling SDS/DTT strongly improved the efficacy of ProteoMiner in human serum. The rationale behind this study was that the relative affinity of hexapeptide libraries to proteins is defined by the experimental conditions, including pH. The use of three pH values (e.g. pH 4, 7, and 9) reduced the loss of proteins and further increased the total number of identified proteins after CPLL treatment (Fasoli et al., 2010b; Di Girolamo et al., 2011). For elution of captured proteins from the beads, boiling in 4% SDS/50 mM DTT turned out to be most efficient, with a protein recovery of more than 99% as compared with only approximately 50% by 7 M urea/2% CHAPS (Di Girolamo et al., 2011). We now adapted this optimized protocol to the extraction of low-abundance proteins from Arabidopsis leaf extracts. After protein extraction, the sample was split into three aliquots. Each fraction was subjected to size-exclusion chromatography for buffer exchange (pH 4, 7, or 9) and removal of interfering compounds such as salt, carbohydrates, and secondary metabolites. Whereas buffer exchange to pH 7 or 9 had no effect on the proteins, at pH 4 partial precipitation of some proteins could be observed. The acidic conditions are responsible for charge reversal. This breaks hydrogen bonds and results in the irreversible denaturation
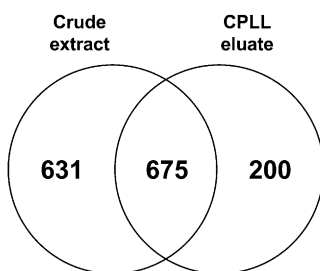
Table I. *Identified proteins in infected Arabidopsis plants*

Organism	Total	Control Only	In Both	CPLL Only
Arabidopsis[a]	1,598	618	777	203
P. syringae[b]	312	168	96	48

[a]Number of identified Arabidopsis proteins in infected plants.
[b]Number of identified *Pseudomonas* proteins in infected plants.

of proteins. Such a loss of proteins due to buffer exchange to pH 4 was also observed for spinach leaf proteins (P.G. Righetti, personal communication). After buffer exchange, samples were treated with CPLL beads and boiling SDS/DTT was used for complete

elution of proteins from the CPLL beads. Nontreated samples served as pH controls.

The different protein fractions of the ProteoMiner experiment were separated by 1D-SDS-PAGE. As shown in Figure 4, the amount of the large subunit of Rubisco was already strongly reduced after adjusting the leaf extract to pH 4. At pH 7 and 9, ProteoMiner treatment caused a depletion of the large Rubisco subunit and a remarkable change in protein composition. Some new bands appeared that were not visible in control extracts, probably representing moderate- to low-abundance proteins. Notably, no obvious difference between control samples at pH 7 and 9 could be observed, whereas after CPLL treatment band patterns were different

Table II. *Selected proteins of the P. syringae DC3000 infectome in leaf crude extracts and CPLL-treated extracts*

Arabidopsis plants were infected with *P. syringae* DC3000, and extracted leaf proteins were analyzed directly by LC-MS/MS or subjected to CPLL before MS analyses. MW, Molecular mass in kD.

| Function	Accession No.	MW	No. of Peptides	Hints to Involvement in Virulence
Proteins identified in CPLL sample only				
Glc-1-P thymidylyltransferase	NP_790913	33	4	Guo et al. (2012)
Gln synthetase	NP_795041	51	2	Si et al. (2009)
Transcriptional regulator, LysR family	NP_795132	33	2	Wharam et al. (1995)
RNA methyltransferase, TrmH family, group 3	NP_794667	27	4	Garbom et al. (2004)
Thr synthase	NP_791307	52	4	Guo et al. (2012)
DNA topoisomerase I	NP_793294	97	2	McNairn et al. (1995)
Amidophosphoribosyltransferase	NP_793585	56	3	Guo et al. (2012)
Phosphate transport system protein PhoU	NP_795207	29	3	Lamarche et al. (2008)
Ribose ABC transporter protein	NP_792188	15	2	Kemner et al. (1997)
Acetyl-CoA carboxylase, biotin carboxylase	NP_794595	49	5	Kurth et al. (2009)
ATP-dependent Clp protease, ATP-binding subunit ClpX	NP_793499	47	4	Ibrahim et al. (2005)
Lysyl-tRNA synthetase	NP_791326	57	3	Navarre et al. (2010)
Phospho*enol*pyruvate carboxykinase	NP_790090	56	2	Liu et al. (2005)
Argininosuccinate synthase	NP_793916	45	4	Ardales et al. (2009)
Coronamic acid synthetase CmaB	NP_794454	35	2	Buell et al. (2003)
dTDP-Glc 4,6-dehydratase	NP_790915	40	3	Sen et al. (2011)
Proteins identified in both crude extract and CPLL sample				
Coronafacic acid synthetase, dehydratase component	NP_794431	18	6/4	Buell et al. (2003)
Coronafacic acid synthetase, ligase component	NP_794429	55	4/12	Buell et al. (2003)
GDP-Man 6-dehydrogenase AlgD	NP_791073	48	9/11	Buell et al. (2003)
Catalase/peroxidase HPI	NP_794283	83	8/2	Jittawuttipoka et al. (2009)
Hfq protein	NP_794675	9	3/3	Schiano et al. (2010)
Translation elongation factor P	NP_791590	21	4/2	Navarre et al. (2010)
ATP-dependent Clp protease, proteolytic subunit ClpP	NP_793500	24	5/3	Ibrahim et al. (2005)
Secreted protein Hcp	NP_795162	19	8/2	Mougous et al. (2006)
Proteins identified in crude extract only				
Alginate biosynthesis protein AlgF	NP_791063	23	6	Buell et al. (2003)
Alginate lyase	NP_791066	42	2	Buell et al. (2003)
Catalase	NP_794994	79	3	Fones and Preston (2012)
Flagellin	NP_791772	29	2	Buell et al. (2003)
Iron ABC transporter, periplasmic iron-binding protein	NP_790164	37	3	Rodriguez and Smith (2006)
Levansucrase	NP_791279	48	2	Li et al. (2006)
Outer membrane porin OprF	NP_792118	37	6	Fito-Boncompte et al. (2011)
Outer membrane protein OmpH, putative	NP_791368	19	5	Fito-Boncompte et al. (2011)
Periplasmic glucan biosynthesis protein	NP_794893	71	5	Buell et al. (2003)
Phosphate ABC transporter	NP_793052	37	8	Buell et al. (2003)
Protein-export protein SecB	NP_795055	18	5	Hueck (1998)
Sugar ABC transporter, periplasmic sugar-binding protein	NP_790728	46	8	Buell et al. (2003)
Superoxide dismutase, iron	NP_794118	21	3	Fones and Preston (2012)
Thiol:disulfide interchange protein DsbA	NP_790191	23	7	Ha et al. (2003)
Transcriptional regulator AlgQ	NP_789993	18	2	Buell et al. (2003)
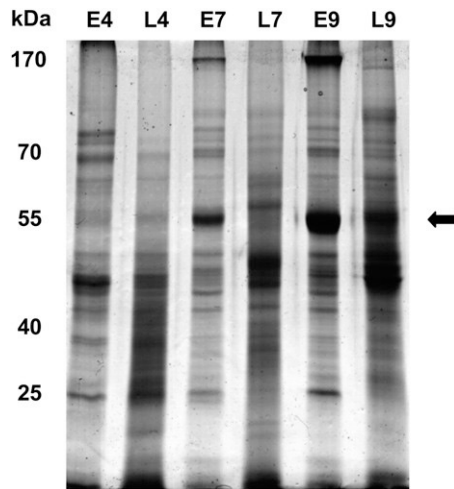
Figure 4. Analysis of a pH-based CPLL fractionation of Arabidopsis leaf proteins by 1D-SDS-PAGE. Protein extracts were adjusted to pH 4, 7, and 9 before application of CPLL. After CPLL fractionation, 15 μg of each fraction was separated by 1D-SDS-PAGE. Proteins were stained with Sypro Ruby. The relative masses of protein standards are indicated on the left. E4, E7, and E9, Protein extract at pH 4, 7, and 9; L4, L7, and L9, corresponding CPLL-treated proteins. The position of Rubisco is marked with an arrow.

between both pH values. Hence, the ProteoMiner effect seems indeed to be dependent on the pH, as reported previously for spinach leaf extracts (Fasoli et al., 2011a).

With the optimized experimental system combining three pH values, a total of 1,704 Arabidopsis leaf proteins were identified. Of these, 1,192 could be detected in control extracts and 512 (43% of control extracts) additional proteins were identified only after the application of ProteoMiner beads (Fig. 5; Supplemental Table S4). There was an overlap of 927 proteins between both data sets. A total of 265 (22%) proteins present in control samples were not found after ProteoMiner treatment, confirming that some proteins were not captured by the hexapeptide libraries or could not be eluted. In comparison with protocol I, the loss of proteins was clearly reduced and significantly more proteins were added to the proteome when protocol II was adopted. This was also true if protocol I was compared with protocol II, considering only the samples adjusted to pH 7. In this case, 15% versus 37% additional CPLL-specific proteins were identified using protocols I and II, respectively (Fig. 3; Supplemental Fig. S1). A major reason for the difference was probably the reduction of salt concentrations in samples and buffers and elution with hot SDS/DTT.

Interestingly, for Arabidopsis leaf extracts, ProteoMiner performed best at pH 7 and 9, whereas only 34 proteins were exclusively detected at pH 4 (data not shown). In contrast, CPLL beads were most effective at pH 4 and 7 with spinach leaf extracts, whereas there was almost no pH effect in coconut (*Cocos nucifera*) milk (Fasoli et al., 2011a; D'Amato et al., 2012). These

results imply that for each experimental system, the most effective pH value(s) must be determined.

In spinach leaf extracts, CPLL caused 18% loss and 79% gain of proteins compared with control samples, whereas for coconut milk, the loss was 78% and the gain was 124% (Fasoli et al., 2011a; D'Amato et al., 2012). In animal and human samples, CPLL was even more effective, with up to 500% additional proteins captured by the beads (Di Girolamo et al., 2011). However, in several of these publications, appropriate pH controls were missing, because CPLL-treated samples adjusted to different pH values were only compared with crude extracts (Di Girolamo et al., 2011; Fasoli et al., 2011a, 2011b; D'Amato et al., 2012). Comparing a single pH 7 control with three ProteoMiner eluates at pH 4, 7, and 9, we obtained results very similar to those reported for spinach, namely, 16% loss and 71% gain (Supplemental Fig. S2), suggesting that ProteoMiner-specific effects were overestimated without correct pH controls.

ProteoMiner-dependent enrichment of protein functional categories was investigated by using Gene Ontology (GO) terms for comparison of the protein sets from control- and ProteoMiner-treated samples (Supplemental Table S5). As recently described for latex proteins of *Hevea brasiliensis* (D'Amato et al., 2010), CPLL beads captured preferentially proteins involved in translation, such as aminoacyl-tRNA ligases (e.g. molecular function GO:0004815, Asp-tRNA ligase activity; GO:0004830, Trp-tRNA ligase activity) and ribosomal or related proteins (e.g. molecular function GO:0008312, 7S RNA binding). Our data also revealed that ProteoMiner had a high affinity to proteins functioning in protein transport to cellular compartments or organelles (e.g. biological process GO:0006886, intracellular protein transport; GO:0006888, endoplasmic reticulum-to-Golgi vesicle-mediated transport; GO:0045038, protein import into chloroplast thylakoid membrane). Significantly, 15 proteins of the vesicle-mediated transport system (GO:0016192) were identified after ProteoMiner
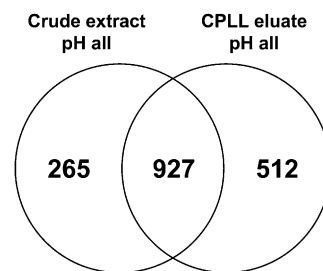
Figure 5. Identification of Arabidopsis leaf proteins by LC-MS/MS after the application of CPLL beads at three different pH values, and elution from the beads using hot SDS/DTT. The protein composition of CPLL eluates captured at pH 4, 7, and 9 was compared with the corresponding pH controls. In total, 1,704 proteins were detected. A total of 1,192 proteins were identified in control samples, whereas 512 (43%) additional proteins were found exclusively after treatment with CPLL at three different pH values.

treatment, but only three proteins of this functional category were found in control samples (Supplemental Table S5).

In sum, the CPLL effect is strongly dependent on the experimental system, probably including some plant-specific complications. However, once established, it is a very useful tool for the depletion of high-abundance proteins. Additionally, the detectable proteome can be extended by about 40%, and ProteoMiner might be a valuable tool for the isolation of proteins involved in translation and (vesicle-mediated) protein transport.

Application of CPLL to Phloem Exudates from Pumpkin

Cucurbitaceae species including pumpkin are model plants for phloem biochemistry, because exudates of the unique EFP can be easily collected from cut petioles and stems (Van Bel and Gaupels, 2004; Atkins et al., 2011; Zhang et al., 2012). The EFP is a unique feature of the Cucurbitaceae (Turgeon and Oparka, 2010; Atkins et al., 2011). In contrast to the fascicular phloem, the EFP does not build effective callose plugs upon wounding, which allows for the sampling of large volumes (50–200 μL plant^{-1}) of spontaneously exuding phloem sap from cut stems and petioles (Van Bel and Gaupels, 2004; Lin et al., 2009; Turgeon and Oparka, 2010). Sugar concentrations in pumpkin phloem exudates are low, implying that the EFP of cucurbits does not function in assimilate transport but rather might be involved in defense and (systemic) signaling (Walz et al., 2004; Zhang et al., 2010). Due to the easy sampling and high protein concentrations of 25 to 50 μg μL^{-1}, cucurbits were frequently used for studying phloem proteins (Atkins et al., 2011). However, proteomic analyses by 2D electrophoresis led to the identification of less than 100 phloem proteins (Walz et al., 2004; Cho et al., 2010; Malter and Wolf, 2011). In these studies, one major pitfall was precipitation of the redox-sensitive PP1 (phloem filament protein) and PP2 (phloem lectin) in the isoelectric focusing, which caused massive streaking and loss of spots in the second dimension (Walz et al., 2004; Malter and Wolf, 2011). These two proteins account for more than 80% of the total protein content, and their gelation during sample preparation under oxidizing conditions is a general problem in downstream applications including MS. Therefore, we tested if CPLL could be used for fast and convenient reduction of PP1/PP2 amounts as well as the enrichment of low-abundance phloem proteins overlooked to this point.

Recently, 1,121 phloem proteins were identified in a groundbreaking proteomic approach (Lin et al., 2009). Protein extracts from as much as 30 mL of pumpkin phloem exudates were fractionated by anion- and cation-exchange chromatography. Afterward, proteins were separated by 1D-SDS-PAGE and analyzed by 345 MS runs. The detected proteins most likely represent the vast bulk of the total protein pool present in pumpkin phloem exudates (Lin et al., 2009). However, tedious fractionation procedures are not feasible if only

low sample volumes are available or many samples must be analyzed in parallel. Therefore, a down-scaled protocol affording minimal hands-on time and preparation steps was established for the prefractionation of pumpkin phloem samples by CPLL. A total of 120 μL of phloem exudate (3 mg of protein content), which can usually be sampled from a single 4- to 5-week-old plant, was used as starting material. Proteins were alkylated with iodoacetamide for preventing gelation of PP1 and PP2. After gel filtration, ProteoMiner beads were added and incubated for 2 h. Unbound proteins were removed by extensive washing, and the captured proteins were eluted at 95°C with Laemmli buffer containing SDS and β-mercaptoethanol.

In a first experiment, two 120-μL aliquots of the same sample pool were adjusted to pH 5.2 and 7.8. A higher pH was not tested, because PP1 and PP2 precipitate at their pI values close to pH 9. After application of ProteoMiner beads, the levels of high-abundance proteins such as PP1 (95 kD) and PP2 (24 kD) were strongly reduced, whereas low- to moderate-abundance proteins were increased in band intensity, as visualized by 1D-SDS-PAGE (Fig. 6). The two pH values resulted in only minor changes in protein pattern, but the total protein amount was somewhat higher at pH 5.2. Similarly, it has been reported for coconut milk that the pH did not significantly influence the CPLL performance (D'Amato et al., 2012), although this was in contrast to our own results with Arabidopsis leaf extracts and to previous findings in spinach leaves and almond (*Prunus dulcis*) milk (Fasoli et al., 2011a, 2011b). The reason for these inconsistent results is unclear but might be related to plant-specific differences in secondary metabolite content (D'Amato et al., 2012). In sum, this experiment demonstrated that
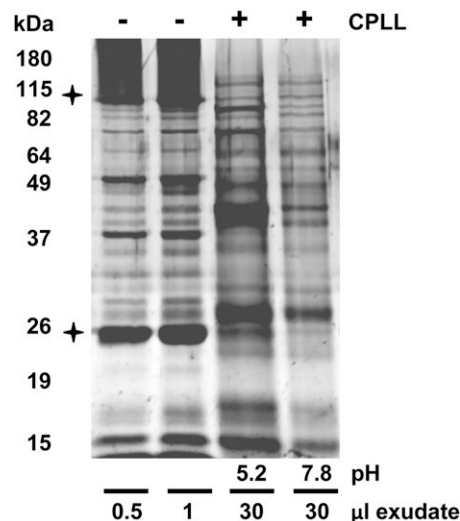

Figure 6. Analysis of CPLL fractionation of pumpkin phloem proteins. Phloem crude extracts and CPLL fractions (pH 5.2 and 7.8) were separated by 1D-SDS-PAGE. Loaded CPLL eluates were equivalent to 30 μL of phloem exudate. The two major phloem proteins PP1 (96 kD) and PP2 (24 kD) are marked with stars.

major phloem proteins, which might interfere with downstream analyses, were strongly depleted, whereas low- to moderate-abundance proteins were enriched.

Next, we investigated the application of CPLL beads in phloem proteomics. We used 1,080 μL of Proteo-Miner-treated samples and 27 μL of control phloem samples and analyzed the extracts in 36 MS runs. Thus, in comparison with Lin et al. (2009), our protocol for phloem proteomics afforded less than 4% of starting material, 10% of MS runs, and was overall more time and cost effective. While Lin et al. (2009) employed elaborate methods for an exploratory genome study, the procedure presented here is compatible with high-throughput approaches. Altogether, 320 proteins could be identified, of which 67 proteins were detected only in ProteoMiner-treated samples (Fig. 7; Supplemental Table S6). Interestingly, 106 proteins were found only in untreated control exudates. Hence, as in leaf extracts of Arabidopsis, the employment of CPLL beads caused a shift rather than an increase in the detectable proteome fraction.

After mapping 305 of the 320 phloem proteins to the cucumber (*Cucumis sativus*) genome for reference (www.icugi.org; version 1 of the cucumber genome; Huang et al., 2009), we found a 73% (224) overlap with pumpkin phloem proteins previously discovered by the group of W.J. Lucas (Huang et al., 2009; Lin et al., 2009; Supplemental Table S6). This result indicates that the current phloem databases might already cover most of the pumpkin extrafascicular proteins. However, 27% (81 proteins) of our data set represent new phloem proteins (Supplemental Table S6), of which 24 could only be revealed by the application of Proteo-Miner beads (Table III). In the past, enucleate sieve elements forming the sieve tubes were thought to be devoid of the protein translation machinery. Our data support the notion of Lin et al. (2009) that many phloem proteins function in transcription and translation, because eight of the 24 phloem proteins captured exclusively by ProteoMiner were related to these functional categories.

Moreover, 13 of the 24 phloem proteins in Table III are involved in transport processes, giving rise to the idea that, at least in the EFP of cucurbits, not only the

companion cells but also sieve elements are able to synthesize, process, and transport proteins. These data also imply that membrane systems such as the Golgi apparatus and endoplasmic reticulum are present within sieve tubes. As in Arabidopsis leaf extracts, Proteo-Miner was particularly effective in capturing proteins related to transport processes, including general protein transport, vesicle transport, and vacuolar targeting. Altogether, 26 of 67 proteins identified only in the CPLL fraction were related to transport processes (data not shown). An additional 25 proteins were functionally annotated to protein synthesis and degradation (data not shown).

The collection of phloem exudates from cut stems and petioles imposes the risk of contaminations from nonphloem tissues. The large subunit of Rubisco is often used for assessing such contaminations, because it is a major enzyme in tissues surrounding the phloem. In the past, only three and seven unique peptides of Rubisco were detected in phloem exudates of rape (*Brassica napus*) and pumpkin, respectively, suggesting that the phloem samples were essentially contamination free (Giavalisco et al., 2006; Lin et al., 2009). In our study, three unique peptides were identified in control samples, but after application of ProteoMiner, the number of unique peptides of Rubisco increased to five (Supplemental Table S6). Thus, ProteoMiner does readily enrich low-abundance contaminating proteins such as Rubisco; therefore, proteins identified by using this tool must be carefully verified for their phloem origin.

CONCLUSION

The CPLL technology is a widely used technique within the human/animal field and was recently applied to some plant-derived products such as spinach leaves from the market, coconut milk, and almond milk (Fasoli et al., 2011a, 2011b; D'Amato et al., 2012). Here, we established the CPLL technology in plant research, performing in-depth analyses of the CPLL-fractionated proteins from Arabidopsis leaf extracts and pumpkin phloem exudates by 2D-DIGE and LC-MS/MS.

The two tested experimental systems are very disparate. On the one hand, extracts from disrupted leaf cells contain mainly proteins involved in photosynthesis and carbohydrate metabolism. On the other hand, in samples from photosynthetically inactive sieve elements, many proteins are related to defense, transport, and protein synthesis. Additionally, the metabolite composition is very different between both plant systems. Therefore, it is remarkable that Proteo-Miner had similar effects in both plant samples. CPLL proved to be an effective tool for diminishing high-abundance proteins such as Rubisco in leaf extracts and PP1 and PP2 in pumpkin phloem exudates. These major proteins interfere with downstream applications such as 2D electrophoresis and western-blot analysis,
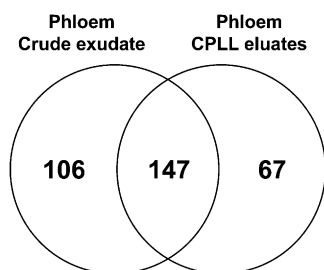

Figure 7. Comparison of the number of identified proteins in crude phloem exudates and CPLL-treated exudates of pumpkin. LC-MS/MS analyses led to the identification of 320 phloem proteins, of which 253 proteins were found in untreated control samples. However, 67 additional proteins could be exclusively detected by using CPLL beads.

Table III. *New phloem proteins of pumpkin identified by utilizing CPLL technology*

MW, Molecular mass in kD.

Function	Accession No.[a]		MW	Unique Peptides
	ICuGI	JGI		
Transport processes				
Tubulin	Csa000342	Cucsa.258870	53	2
Adaptin	Csa000894	Cucsa.285980	96	3
Cofilin/tropomyosin-type actin-binding protein	Csa001107	Cucsa.053580	17	3
Vacuole-sorting protein SNF7	Csa001768	Cucsa.288610	25	2
Nuclear pore complex protein Nup93	Csa002377	Cucsa.338210	54	3
Regulator of Vps4 activity in the MVB pathway	Csa005596	Cucsa.365760	65	2
Dynamin	Csa009772	Cucsa.237630	100	6
Actin binding	Csa012435	Cucsa.165810	47	2
Snare protein synaptobrevin ykt6	Csa016430	Cucsa.350890	23	2
Adaptin	Csa019149	Cucsa.109670	99	3
Importin, Ran-binding protein 6	Csa019530	Cucsa.334860	123	2
Adaptin	Csa021291	Cucsa.240490	98	6
Dynamin	Csa021655	Cucsa.280120	69	2
Protein synthesis and degradation				
Apoptosis inhibitory protein 5 (AIP5)	Csa000645	Cucsa.046470	38	2
U1 small nuclear ribonucleoprotein	Csa000767	Cucsa.048580	30	3
RNA-binding protein, RNA recognition motif	Csa006440	Cucsa.055310	22	2
Translation initiation factor activity	Csa007054	Cucsa.200090	30	2
Structural constituent of ribosome	Csa007533	Cucsa.161150	23	3
Ubiquitin	Csa015756	Cucsa.323030	59	2
Ribosomal protein L16p/L10e	Csa017251	Cucsa.228420	25	2
U1 small nuclear ribonucleoprotein C	Csa019223	Cucsa.084690	21	2
Others				
Calmodulin	Csa002960	Cucsa.094740	17	2
Casein kinase	Csa009196	Cucsa.117110	53	5
Unknown	Csa020629	Cucsa.049570	17	2

[a]Accession numbers are from the cucumber genomes of the ICuGI and the JGI.

because they mask low-abundance proteins, and particularly PP1/PP2 tend to gelate upon oxidation. A significant feature of ProteoMiner, as revealed by 1D and 2D electrophoresis, was that spots or bands representing less abundant and previously undetectable proteins were enriched after CPLL treatment. As a consequence, this technology facilitated the identification of additional proteins by LC-MS/MS. However, the efficacy of ProteoMiner in extending the proteome was dependent on the protocol used. Following the ProteoMiner instruction manual, the 2D pattern changed considerably, but only around 15% new proteins (based on the total number of identified proteins) could be identified. However, when an optimized protocol published by the group of Righetti (Di Girolamo et al., 2011) was employed, more than 40% additional proteins could be identified with the ProteoMiner technology. Noteworthy, even with the optimized protocol, 22% of the proteins present in control extracts were lost due to CPLL treatment. Such a "loss of protein" has been observed previously (Castagna et al., 2005; Thulasiraman et al., 2005) and probably occurs due to following reasons: (1) some proteins do not have binding partners in the hexapeptide library; (2) weak interactions between hexapeptides and proteins can be broken during washing of the columns; and (3) in plant

samples, secondary metabolites might interfere with the binding and elution of proteins, a problem less encountered in human/animal samples.

Importantly, in most experimental approaches, including ours, the ProteoMiner technology did not extend but rather shifted the detectable proteome. A significant increase in the detected proteome was achieved only when results of both crude extracts and ProteoMiner eluates were combined. This way, ProteoMiner increased the number of identified proteins by a maximum of 43% in the leaf experiment and 26% in the phloem experiment. In other papers, the application of CPLL beads to spinach leaves, coconut milk, and almond milk led to a 79% to 124% increase of the detectable proteomes (Fasoli et al., 2011a, 2011b; D'Amato et al., 2012). However, the authors compared three CPLL samples adjusted to different pH values (pH 4, 7, and 9) with a single nontreated control sample (pH 7). In contrast, we compared control samples and CPLL-treated samples both adjusted to pH 4, 7, and 9. Analysis of our data showed that adjustment of the samples to different pH values functions as a kind of prefractionation procedure resulting in a considerable shift in the proteome independent of ProteoMiner application. Therefore, in the past, the ProteoMiner effects on the total protein count might have been often

overestimated. Only by using appropriate pH controls were we able to provide a realistic figure for the specific contribution of ProteoMiner to the proteomic investigation of Arabidopsis leaf extracts and pumpkin phloem exudates. In sum, ProteoMiner is a time- and cost-effective tool with many potential applications in plant protein biochemistry. ProteoMiner is highly effective in reducing high-abundance proteins that might interfere with downstream analyses. It can also be used as an additional easy-to-apply fractionation technique in exploratory proteomics. Targeting a single low-abundance protein of interest, the CPLL technology might be helpful for enriching such proteins, for example, if antibodies for immunoprecipitation are not available. In any case, binding of the candidate protein to hexapeptides in the library must be carefully tested. Last but not least, preferred binding of ProteoMiner beads to proteins of the vesicle transport or translation machinery could facilitate research into these cellular processes.

MATERIALS AND METHODS

Protein Extraction and Treatment with CPLL

For protocol I, 75 g of frozen plant material was ground under liquid nitrogen and suspended in 300 mL of extraction buffer (50 mM Tris-HCl, pH 8.0, 50 mM NaCl, 1 mM EDTA, 0.1% β-mercaptoethanol, and 1× Complete protease inhibitor, EDTA free). Five percent (w/v) polyvinylpolypyrrolidone was added, and the suspension was stirred at 4°C for 30 min. After two centrifugation steps at 4°C (10 min, 4,500g and 15 min, 34,000g), protein was precipitated from the supernatant at 4°C overnight using ammonium sulfate at 95% saturation. After 15 min of centrifugation at 34,000g, the pellet was resuspended in 2 mL of phosphate-buffered saline and protease inhibitor (Complete, EDTA free; Roche). The protein solution was desalted using a PD10 size-exclusion column (GE Healthcare) according to the manual. Treatment of extracts with ProteoMiner was done according to the manual (Bio-Rad) with minor modifications. Because of a lower protein concentration than recommended, a minimum of 10 mg of protein was added to the columns in a volume of 1 mL. Incubation was done at room temperature overnight on a shaker. Complete EDTA-free protease inhibitor (2×) was used during incubation. Elution was done according to the manual with 8 M urea and 2% CHAPS. For protocol II, 5 g of frozen plant material was ground under liquid nitrogen and suspended in 10 mL of extraction buffer (50 mM Tris-HCl, pH 8.0, 50 mM NaCl, 1 mM EDTA, and 0.1% β-mercaptoethanol). The suspension was centrifuged for 15 min (34,000g, 4°C). The supernatant was subjected to buffer exchange using PD10 columns according to the manual. The PD10 columns were equilibrated and eluted using the following buffers: 25 mM Tris-HCl, pH 7.0, 25 mM Tris-HCl, pH 9.0, or 25 mM acetate buffer, pH 4.0. An amount (3.5 mL) of each eluate (pH 4, 7, or 9) was extracted using the batch protocol with 50 μL of equilibrated ProteoMiner slurry. Incubation was done for 3 h at room temperature using an overhead shaker. The CPLL beads were washed two times with 5 mL of the corresponding buffer. The CPLL beads were eluted using 2× 50 μL of hot SDS-DTT solution (4% SDS, 50 mM DTT, 95°C).

2D-DIGE

Fluorescent labeling of protein was done using the Ettan DIGE System (GE Healthcare) according to the manual. Prior to labeling, protein concentration was measured and the required amount of protein (50 μg) was purified using the 2D Cleanup Kit. Four replicates of samples before and after CPLL treatment and an internal standard were labeled, including a dye swap. Isoelectric focusing was done using an IPGphor3 with Immobiline dry strips (24 cm, pH 4–7) and the standard IPGphor3 program for isoelectric focusing of gradients of pH 4 to 7. PAGE was done using an Ettan DALT 6 electrophoresis chamber according to the manufacturer's instructions. 2D-DIGE gels were scanned using a Typhoon variable mode imager. Analysis of scanned gels was done

using DeCyder software. For spot finding, matching, and statistical analysis, standard parameters recommended by the manufacturer were used. Changes in protein amounts were statistically detected by ANOVA ($P < 0.05$) and the application of false discovery rate correction.

Infection of Arabidopsis with *Pseudomonas syringae* DC3000

Four-week-old Arabidopsis (*Arabidopsis thaliana*) ecotype Columbia plants were infected according to Katagiri et al. (2002). Briefly, the plants were grown in pots covered by a fine mesh. Plants were infected by vacuum infiltration with virulent *P. syringae* DC3000 at 10^{-6} colony-forming units mL^{-1} buffer (10 mM MgCl$_2$, 0.004% Silwet). Whole rosettes were harvested 24 h after infection and immediately frozen in liquid nitrogen for proteomic analyses. To determine bacterial growth, surface-sterilized leaf discs were homogenized in 1 mL of 10 mM MgCl$_2$ and different dilutions were plated on King's B medium. After incubating the plates at 28°C for 2 d, the colonies were counted.

CPLL Treatment and Analysis of Pumpkin Phloem Exudates

Phloem samples were collected from cut petioles and stems of 4- to 5-week-old pumpkin (*Cucurbita maxima* 'Gele Centenaar') plants as described previously (Lin et al., 2009). A total of 120 μL of pumpkin phloem exudate (25 mg protein mL^{-1}) was mixed with the same volume of phloem buffer (50 mM Tris-HCl, pH 7.8, 0.1% β-mercaptoethanol; McEuen and Hill, 1982). Redox-sensitive Cys residues of PP1/PP2 were alkylated by adding 25 mM (final concentration) iodoacetamide. Afterward, β-mercaptoethanol and iodoacetamide were removed by gel filtration and proteins were collected in 120 μL of phloem buffer without β-mercaptoethanol. In one experiment, a sodium acetate buffer (100 mM sodium acetate/acetic acid, pH 5.2) was used for elution. ProteoMiner beads were applied according to the manual. The final protein amount was 3 mg at a concentration of 25 mg mL^{-1}. After washing, proteins were eluted from beads by twice applying 50 μL of commercial 4× Laemmli buffer (Roth) at 95°C.

From every plant, 120 μL of the collected phloem sap was used for ProteoMiner experiments and 3 μL served as a control, which was reduced, alkylated, and gel filtrated but not treated with ProteoMiner beads. For SDS-PAGE, Laemmli buffer was added to control phloem exudates whereas ProteoMiner eluates were directly loaded on a 12% SDS-PAGE gel. LC-MS/MS analyses were done in triplicate. For each triplicate assay, three ProteoMiner eluates or corresponding control exudates were combined and proteins were precipitated using the 2D Cleanup Kit (GE Healthcare) and separated by SDS-PAGE. The gel was cut into six pieces per sample and analyzed by LC-MS/MS.

MS Analysis and Data Processing

For the identification of proteins, 1D-SDS-PAGE bands were cut out and samples were prepared using a MS-compatible protocol (Shevchenko et al., 1996). The digested peptides were separated by reverse-phase chromatography (PepMap, 15 cm × 75 μm i.d., 3 μm 100 Å^{-1} pore size; LC Packings) operated on a nano-HPLC device (Ultimate 3000; Dionex) with a nonlinear 170-min gradient using 2% acetonitrile in 0.1% formic acid in water (A) and 0.1% formic acid in 98% acetonitrile (B) as eluents with a flow rate of 250 nL min^{-1}. The gradient settings were subsequently as follows: 0 to 140 min, 2% to 30% B; 140 to 150 min, 31% to 99% B; 151 to 160 min, hold at 99% B. The nano-HPLC device was connected to a linear quadrupole ion-trap-Orbitrap (LTQ Orbitrap XL) mass spectrometer (ThermoFisher) equipped with a nano-electrospray ionization source. The mass spectrometer was operated in the data-dependent mode to automatically switch between Orbitrap-MS and LTQ-MS/MS acquisition. Survey full-scan MS spectra (from mass-to-charge ratio 300 to 1,500) were acquired in the Orbitrap with resolution $r = 60,000$ at a mass-to-charge ratio of 400 (after accumulation to a target of 1,000,000 ions in the LTQ). The method used allowed sequential isolation of the most intense ions, up to 10, depending on signal intensity, for fragmentation on the linear ion trap using collisionally induced dissociation at a target value of 100,000 ions. High-resolution MS scans in the Orbitrap and tandem mass spectrometry (MS/MS) scans in the linear ion trap were performed in parallel. Target peptides already selected for MS/MS were dynamically excluded for 30 s. General MS conditions were as follows: electrospray voltage, 1.25 to 1.4 kV; no

sheath and auxiliary gas flow. The ion selection threshold was 500 counts for MS/MS, and an activation Q value of 0.25 and activation time of 30 ms were also applied for MS/MS.

Database Searching

All MS/MS spectra were analyzed using Mascot version 2.2.06 (Matrix Science). Mascot was set up to search The Arabidopsis Information Resource (TAIR) database (13,434,913 residues, 33,410 sequences) or the National Center for Biotechnology Information *P. syringae* DC3000 protein database (ftp://ftp.ncbi.nih.gov/genomes/Bacteria/Pseudomonas_syringae_tomato_DC3000/) assuming the digestion enzyme trypsin with a fragment ion mass tolerance of 1 D and a parent ion tolerance of 10 ppm. Oxidation of Met and deamidation of Arg and Gln as variable modifications were specified in Mascot as variable modifications. The genome of pumpkin has not yet been sequenced; therefore, we assembled a database for phloem proteomics including among others protein sequences derived from the complete genomes of the Cucurbitaceae species cucumber (*Cucumis sativus*) and *Citrullus lanatus*. We used OrthoMCL software version 1.4 (Li et al., 2003) with default parameters (inflation, 1.5; BLASTP e-value cutoff, 10e-05) to cluster the protein sequences annotated on the complete genome sequences of cucumber (Joint Genome Institute [JGI]; www.phytozome.net/cucumber.php, genome release 1), Arabidopsis (TAIR10 release; www.arabidopsis.org), and *C. lanatus* (International Cucurbit Genomics Initiative [ICuGI] genome version 1; www.icugi.org). Of the resulting 16,877 gene groups, protein sequences were extracted and a high-confidence phloem database was created containing a total of 25,657 sequences.

Additional protein sequences from the National Center for Biotechnology Information Cucurbitaceae database (http://www.ncbi.nlm.nih.gov/sites/entrez?db=protein&cmd=Search&dopt=DocSum&term=txid3650[Organism%3Aexp) and 800 cucumber homologs (ICuGI accessions) of pumpkin phloem proteins from Supplemental Table S18 of Huang et al. (2009) were added. Phloem proteins identified by searching against our homemade protein database were mapped to the JGI and ICuGI cucumber genome accessions using BLASTP with an e-value cutoff of 10e-05 and required more than 90% sequence identity for at least 70% sequence coverage. With nonmapped protein sequences, an additional BLASTP search against the ICuGI genome database was performed, choosing a threshold *P* value of 1e-30. This way, 309 of 320 identified phloem proteins could be annotated to ICuGI identifiers, which were then used for comparison of our data with Supplemental Table S18 of Huang et al. (2009).

Criteria for Protein Identification

Scaffold (version Scaffold_2_02_03; Proteome Software) was used to validate MS/MS-based peptide and protein identifications. Peptide identifications were accepted if they could be established at greater than 95.0% probability as specified by the Peptide Prophet algorithm (Keller et al., 2002). Protein identifications were accepted if they could be established at greater than 99.0% probability and contained at least two identified peptides. Protein probabilities were assigned by the Protein Prophet algorithm (Nesvizhskii et al., 2003). Proteins that contained similar peptides and could not be differentiated based on MS/MS analysis alone were grouped to satisfy the principles of parsimony.

GO Enrichment Analysis

We downloaded GO terms for the gene annotation of Arabidopsis from TAIR. Only GO terms of the categories "molecular function" and "biological process" were evaluated. The GOstats R package from Bioconductor (http://www.bioconductor.org/packages/release/bioc/html/GOstats.html) was used for analyzing the GO terms of the 512 ProteoMiner-specific proteins and the 1,192 proteins derived from the crude extracts shown in Figure 5 and Supplemental Table S4. Supplemental Table S5 lists the GO terms that were significantly ($P < 0.05$) overrepresented in these protein sets as compared with the TAIR10 database.

Supplemental Data

The following materials are available in the online version of this article.

Supplemental Figure S1. pH effect on CPLL performance.

Supplemental Figure S2. pH 7 control versus CPLL capture at pH 4, 7, and 9.

Supplemental Table S1. Identified Arabidopsis proteins using CPLL, protocol 1.

Supplemental Table S2. Identified Arabidopsis proteins in infected leaves.

Supplemental Table S3. Identified *P. syringae* proteins in infected leaves.

Supplemental Table S4. Identified Arabidopsis proteins using CPLL, protocol 2.

Supplemental Table S5. Enriched GO terms after CPLL application.

Supplemental Table S6. Identified pumpkin phloem proteins.

LITERATURE CITED

Ardales E, Moon S-J, Park DS Sr, Byun M-O, Noh TH (2009) Inactivation of argG, encoding argininosuccinate synthetase from Xanthomonas oryzae pv. oryzae, is involved in bacterial growth and virulence in planta. Can J Plant Pathol **31:** 368–374

Atkins CA, Smith PM, Rodriguez-Medina C (2011) Macromolecules in phloem exudates: a review. Protoplasma **248:** 165–172

Bachi A, Simó C, Restuccia U, Guerrier L, Fortis F, Boschetti E, Masseroli M, Righetti PG (2008) Performance of combinatorial peptide libraries in capturing the low-abundance proteome of red blood cells. 2. Behavior of resins containing individual amino acids. Anal Chem **80:** 3557–3565

Boschetti E, Lomas L, Citterio A, Righetti PG (2007) Romancing the "hidden proteome," Anno Domini two zero zero seven. J Chromatogr A **1153:** 277–290

Boschetti E, Righetti PG (2008a) Hexapeptide combinatorial ligand libraries: the march for the detection of the low-abundance proteome continues. Biotechniques **44:** 663–665

Boschetti E, Righetti PG (2008b) The ProteoMiner in the proteomic arena: a non-depleting tool for discovering low-abundance species. J Proteomics **71:** 255–264

Boschetti E, Righetti PG (2009) The art of observing rare protein species in proteomes with peptide ligand libraries. Proteomics **9:** 1492–1510

Buell CR, Joardar V, Lindeberg M, Selengut J, Paulsen IT, Gwinn ML, Dodson RJ, Deboy RT, Durkin AS, Kolonay JF, et al (2003) The complete genome sequence of the Arabidopsis and tomato pathogen Pseudomonas syringae pv. tomato DC3000. Proc Natl Acad Sci USA **100:** 10181–10186

Buettner JA, Dadd CA, Baumbach GA, Masecar BL, Hammond DJ (1996) Chemically derived peptide libraries: a new resin and methodology for lead identification. Int J Pept Protein Res **47:** 70–83

Castagna A, Cecconi D, Sennels L, Rappsilber J, Guerrier L, Fortis F, Boschetti E, Lomas L, Righetti PG (2005) Exploring the hidden human urinary proteome via ligand library beads. J Proteome Res **4:** 1917–1930

Cho WK, Chen XY, Rim Y, Chu H, Kim S, Kim SW, Park ZY, Kim JY (2010) Proteome study of the phloem sap of pumpkin using multidimensional protein identification technology. J Plant Physiol **167:** 771–778

Corthals GL, Wasinger VC, Hochstrasser DF, Sanchez JC (2000) The dynamic range of protein expression: a challenge for proteomic research. Electrophoresis **21:** 1104–1115

D'Amato A, Bachi A, Fasoli E, Boschetti E, Peltre G, Sénéchal H, Righetti PG (2009) In-depth exploration of cow's whey proteome via combinatorial peptide ligand libraries. J Proteome Res **8:** 3925–3936

D'Amato A, Bachi A, Fasoli E, Boschetti E, Peltre G, Sénéchal H, Sutra JP, Citterio A, Righetti PG (2010) In-depth exploration of Hevea brasiliensis latex proteome and "hidden allergens" via combinatorial peptide ligand libraries. J Proteomics **73:** 1368–1380

D'Amato A, Fasoli E, Kravchuk AV, Righetti PG (2011) Mehercules, adhuc Bacchus! The debate on wine proteomics continues. J Proteome Res **10:** 3789–3801

D'Amato A, Fasoli E, Righetti PG (2012) Harry Belafonte and the secret proteome of coconut milk. J Proteomics **75:** 914–920

D'Ambrosio C, Arena S, Scaloni A, Guerrier L, Boschetti E, Mendieta ME, Citterio A, Righetti PG (2008) Exploring the chicken egg white proteome with combinatorial peptide ligand libraries. J Proteome Res **7:** 3461–3474

Di Girolamo F, Boschetti E, Chung MC, Guadagni F, Righetti PG (2011) "Proteomineering" or not? The debate on biomarker discovery in sera continues. J Proteomics **74:** 589–594

Farinazzo A, Restuccia U, Bachi A, Guerrier L, Fortis F, Boschetti E, Fasoli E, Citterio A, Righetti PG (2009) Chicken egg yolk cytoplasmic proteome, mined via combinatorial peptide ligand libraries. J Chromatogr A 1216: 1241–1252

Fasoli E, Aldini G, Regazzoni L, Kravchuk AV, Citterio A, Righetti PG (2010a) Les maîtres de l'orge: the proteome content of your beer mug. J Proteome 9: 5262–5269

Fasoli E, D'Amato A, Citterio A, Righetti PG (2012) Ginger Rogers? No, ginger ale and its invisible proteome. J Proteomics 75: 1960–1965

Fasoli E, D'Amato A, Kravchuk AV, Boschetti E, Bachi A, Righetti PG (2011a) Popeye strikes again: the deep proteome of spinach leaves. J Proteomics 74: 127–136

Fasoli E, D'Amato A, Kravchuk AV, Citterio A, Righetti PG (2011b) In-depth proteomic analysis of non-alcoholic beverages with peptide ligand libraries. I. Almond milk and orgeat syrup. J Proteomics 74: 1080–1090

Fasoli E, Farinazzo A, Sun CJ, Kravchuk AV, Guerrier L, Fortis F, Boschetti E, Righetti PG (2010b) Interaction among proteins and peptide libraries in proteome analysis: pH involvement for a larger capture of species. J Proteomics 73: 733–742

Fito-Boncompte L, Chapalain A, Bouffartigues E, Chaker H, Lesouhaitier O, Gicquel G, Bazire A, Madi A, Connil N, Véron W, et al (2011) Full virulence of Pseudomonas aeruginosa requires OprF. Infect Immun 79: 1176–1186

Fones H, Preston GM (2012) Reactive oxygen and oxidative stress tolerance in plant pathogenic Pseudomonas. FEMS Microbiol Lett 327: 1–8

Fröhlich A, Lindermayr C (2011) Deep insights into the plant proteome by pretreatment with combinatorial hexapeptide ligand libraries. J Proteomics 74: 1182–1189

Furka A, Sebestyén F, Asgedom M, Dibó G (1991) General method for rapid synthesis of multicomponent peptide mixtures. Int J Pept Protein Res 37: 487–493

Garbom S, Forsberg A, Wolf-Watz H, Kihlberg BM (2004) Identification of novel virulence-associated genes via genome analysis of hypothetical genes. Infect Immun 72: 1333–1340

Giavalisco P, Kapitza K, Kolasa A, Buhtz A, Kehr J (2006) Towards the proteome of Brassica napus phloem sap. Proteomics 6: 896–909

Guerrier L, Claverol S, Finzi L, Paye F, Fortis F, Boschetti E, Housset C (2007a) Contribution of solid-phase hexapeptide ligand libraries to the repertoire of human bile proteins. J Chromatogr A 1176: 192–205

Guerrier L, Claverol S, Fortis F, Rinalducci S, Timperio AM, Antonioli P, Jandrot-Perrus M, Boschetti E, Righetti PG (2007b) Exploring the platelet proteome via combinatorial, hexapeptide ligand libraries. J Proteome Res 6: 4290–4303

Guerrier L, Thulasiraman V, Castagna A, Fortis F, Lin SH, Lomas L, Righetti PG, Boschetti E (2006) Reducing protein concentration range of biological samples using solid-phase ligand libraries. J Chromatogr B Analyt Technol Biomed Life Sci 833: 33–40

Guo W, Cui YP, Li YR, Che YZ, Yuan L, Zou LF, Zou HS, Chen GY (2012) Identification of seven Xanthomonas oryzae pv. oryzicola genes potentially involved in pathogenesis in rice. Microbiology 158: 505–518

Ha UH, Wang Y, Jin S (2003) DsbA of Pseudomonas aeruginosa is essential for multiple virulence factors. Infect Immun 71: 1590–1595

Huang S, Li R, Zhang Z, Li L, Gu X, Fan W, Lucas WJ, Wang X, Xie B, Ni P, et al (2009) The genome of the cucumber, Cucumis sativus L. Nat Genet 41: 1275–1281

Hueck CJ (1998) Type III protein secretion systems in bacterial pathogens of animals and plants. Microbiol Mol Biol Rev 62: 379–433

Ibrahim YM, Kerr AR, Silva NA, Mitchell TJ (2005) Contribution of the ATP-dependent protease ClpCP to the autolysis and virulence of Streptococcus pneumoniae. Infect Immun 73: 730–740

Jittawuttipoka T, Buranajitpakorn S, Vattanaviboon P, Mongkolsuk S (2009) The catalase-peroxidase KatG is required for virulence of Xanthomonas campestris pv. campestris in a host plant by providing protection against low levels of H_2O_2. J Bacteriol 191: 7372–7377

Katagiri F, Thilmony R, He S (2002) The *Arabidopsis thaliana-Pseudomonas syringae* interaction. The Arabidopsis Book 1: e0039, doi/10.1199/tab.0039

Keidel EM, Ribitsch D, Lottspeich F (2010) Equalizer technology: equal rights for disparate beads. Proteomics 10: 2089–2098

Keller A, Nesvizhskii AI, Kolker E, Aebersold R (2002) Empirical statistical model to estimate the accuracy of peptide identifications made by MS/MS and database search. Anal Chem 74: 5383–5392

Kemner JM, Liang X, Nester EW (1997) The Agrobacterium tumefaciens virulence gene chvE is part of a putative ABC-type sugar transport operon. J Bacteriol 179: 2452–2458

Kurth DG, Gago GM, de la Iglesia A, Lyonnet BB, Lin TW, Morbidoni HR, Tsai SC, Gramajo H (2009) ACCase 6 is the essential acetyl-CoA carboxylase involved in fatty acid and mycolic acid biosynthesis in mycobacteria. Microbiology 155: 2664–2675

Lam KS, Salmon SE, Hersh EM, Hruby VJ, Kazmierski WM, Knapp RJ (1991) A new type of synthetic peptide library for identifying ligand-binding activity. Nature 354: 82–84

Lamarche MG, Wanner BL, Crépin S, Harel J (2008) The phosphate regulon and bacterial virulence: a regulatory network connecting phosphate homeostasis and pathogenesis. FEMS Microbiol Rev 32: 461–473

Li G, Nallamilli BR, Tan F, Peng Z (2008) Removal of high-abundance proteins for nuclear subproteome studies in rice (Oryza sativa) endosperm. Electrophoresis 29: 604–617

Li H, Schenk A, Srivastava A, Zhurina D, Ullrich MS (2006) Thermo-responsive expression and differential secretion of the extracellular enzyme levansucrase in the plant pathogenic bacterium Pseudomonas syringae pv. glycinea. FEMS Microbiol Lett 265: 178–185

Li L, Stoeckert CJ Jr, Roos DS (2003) OrthoMCL: identification of ortholog groups for eukaryotic genomes. Genome Res 13: 2178–2189

Lin MK, Lee YJ, Lough TJ, Phinney BS, Lucas WJ (2009) Analysis of the pumpkin phloem proteome provides insights into angiosperm sieve tube function. Mol Cell Proteomics 8: 343–356

Liu P, Wood D, Nester EW (2005) Phosphoenolpyruvate carboxykinase is an acid-induced, chromosomally encoded virulence factor in Agrobacterium tumefaciens. J Bacteriol 187: 6039–6045

Malter D, Wolf S (2011) Melon phloem-sap proteome: developmental control and response to viral infection. Protoplasma 248: 217–224

McEuen AR, Hill HAO (1982) Superoxide, hydrogen peroxide, and the gelling of phloem sap from Cucurbita pepo. Planta 154: 295–297

McNairn E, Ni Bhriain N, Dorman CJ (1995) Overexpression of the Shigella flexneri genes coding for DNA topoisomerase IV compensates for loss of DNA topoisomerase I: effect on virulence gene expression. Mol Microbiol 15: 507–517

Mehta A, Brasileiro AC, Souza DS, Romano E, Campos MA, Grossi-de-Sá MF, Silva MS, Franco OL, Fragoso RR, Bevitori R, et al (2008) Plant-pathogen interactions: what is proteomics telling us? FEBS J 275: 3731–3746

Mougous JD, Cuff ME, Raunser S, Shen A, Zhou M, Gifford CA, Goodman AL, Joachimiak G, Ordoñez CL, Lory S, et al (2006) A virulence locus of Pseudomonas aeruginosa encodes a protein secretion apparatus. Science 312: 1526–1530

Navarre WW, Zou SB, Roy H, Xie JL, Savchenko A, Singer A, Edvokimova E, Prost LR, Kumar R, Ibba M, et al (2010) PoxA, yjeK, and elongation factor P coordinately modulate virulence and drug resistance in Salmonella enterica. Mol Cell 39: 209–221

Nesvizhskii AI, Keller A, Kolker E, Aebersold R (2003) A statistical model for identifying proteins by tandem mass spectrometry. Anal Chem 75: 4646–4658

Peck SC (2005) Update on proteomics in Arabidopsis: where do we go from here? Plant Physiol 138: 591–599

Preston GM (2000) Pseudomonas syringae pv. tomato: the right pathogen, of the right plant, at the right time. Mol Plant Pathol 1: 263–275

Rahme LG, Stevens EJ, Wolfort SF, Shao J, Tompkins RG, Ausubel FM (1995) Common virulence factors for bacterial pathogenicity in plants and animals. Science 268: 1899–1902

Righetti PG, Boschetti E (2008) The ProteoMiner and the FortyNiners: searching for gold nuggets in the proteomic arena. Mass Spectrom Rev 27: 596–608

Rodriguez GM, Smith I (2006) Identification of an ABC transporter required for iron acquisition and virulence in Mycobacterium tuberculosis. J Bacteriol 188: 424–430

Rose JK, Bashir S, Giovannoni JJ, Jahn MM, Saravanan RS (2004) Tackling the plant proteome: practical approaches, hurdles and experimental tools. Plant J 39: 715–733

Roux-Dalvai F, Gonzalez de Peredo A, Simó C, Guerrier L, Bouyssié D, Zanella A, Citterio A, Burlet-Schiltz O, Boschetti E, Righetti PG, et al (2008) Extensive analysis of the cytoplasmic proteome of human erythrocytes using the peptide ligand library technology and advanced mass spectrometry. Mol Cell Proteomics 7: 2254–2269

Schiano CA, Bellows LE, Lathem WW (2010) The small RNA chaperone Hfq is required for the virulence of Yersinia pseudotuberculosis. Infect Immun **78:** 2034–2044

Sen M, Shah B, Rakshit S, Singh V, Padmanabhan B, Ponnusamy M, Pari K, Vishwakarma R, Nandi D, Sadhale PP (2011) UDP-glucose 4,6-dehydratase activity plays an important role in maintaining cell wall integrity and virulence of Candida albicans. PLoS Pathog **7:** e1002384

Shevchenko A, Wilm M, Vorm O, Mann M (1996) Mass spectrometric sequencing of proteins silver-stained polyacrylamide gels. Anal Chem **68:** 850–858

Si Y, Yuan F, Chang H, Liu X, Li H, Cai K, Xu Z, Huang Q, Bei W, Chen H (2009) Contribution of glutamine synthetase to the virulence of Streptococcus suis serotype 2. Vet Microbiol **139:** 80–88

Stitt M, Lunn J, Usadel B (2010) Arabidopsis and primary photosynthetic metabolism: more than the icing on the cake. Plant J **61:** 1067–1091

Thulasiraman V, Lin S, Gheorghiu L, Lathrop J, Lomas L, Hammond D, Boschetti E (2005) Reduction of the concentration difference of proteins in biological liquids using a library of combinatorial ligands. Electrophoresis **26:** 3561–3571

Turgeon R, Oparka K (2010) The secret phloem of pumpkins. Proc Natl Acad Sci USA **107:** 13201–13202

Van Bel AJE, Gaupels F (2004) Pathogen-induced resistance and alarm signals in the phloem. Mol Plant Pathol **5:** 495–504

Walz C, Giavalisco P, Schad M, Juenger M, Klose J, Kehr J (2004) Proteomics of cucurbit phloem exudate reveals a network of defence proteins. Phytochemistry **65:** 1795–1804

Wharam SD, Mulholland V, Salmond GPC (1995) Conserved virulence factor regulation and secretion systems in bacterial pathogens of plants and animals. Eur J Plant Pathol **101:** 1–13

Zhang B, Tolstikov V, Turnbull C, Hicks LM, Fiehn O (2010) Divergent metabolome and proteome suggest functional independence of dual phloem transport systems in cucurbits. Proc Natl Acad Sci USA **107:** 13532–13537

Zhang C, Yu X, Ayre BG, Turgeon R (2012) The origin and composition of cucurbit "phloem" exudate. Plant Physiol **158:** 1873–1882

Deciphering Systemic Wound Responses of the Pumpkin Extrafascicular Phloem by Metabolomics and Stable Isotope-Coded Protein Labeling[1][C][W]

Frank Gaupels*, Hakan Sarioglu, Manfred Beckmann, Bettina Hause, Manuel Spannagl, John Draper, Christian Lindermayr, and Jörg Durner

Institute of Biochemical Plant Pathology (F.G., C.L., J.Du.), Department of Protein Science (H.S.), and Institute of Bioinformatics and Systems Biology (M.S.), Helmholtz Zentrum München, German Research Center for Environmental Health, D–85764 Neuherberg, Germany; Institute of Biological Environmental and Rural Sciences, Aberystwyth University, Aberystwyth SY23 3DA, United Kingdom (M.B., J.Dr.); and Department of Cell and Metabolic Biology, Leibniz Institute of Plant Biochemistry, D–06120 Halle/Saale, Germany (B.H.)

In cucurbits, phloem latex exudes from cut sieve tubes of the extrafascicular phloem (EFP), serving in defense against herbivores. We analyzed inducible defense mechanisms in the EFP of pumpkin (*Cucurbita maxima*) after leaf damage. As an early systemic response, wounding elicited transient accumulation of jasmonates and a decrease in exudation probably due to partial sieve tube occlusion by callose. The energy status of the EFP was enhanced as indicated by increased levels of ATP, phosphate, and intermediates of the citric acid cycle. Gas chromatography coupled to mass spectrometry also revealed that sucrose transport, gluconeogenesis/glycolysis, and amino acid metabolism were up-regulated after wounding. Combining ProteoMiner technology for the enrichment of low-abundance proteins with stable isotope-coded protein labeling, we identified 51 wound-regulated phloem proteins. Two Sucrose-Nonfermenting1-related protein kinases and a 32-kD 14-3-3 protein are candidate central regulators of stress metabolism in the EFP. Other proteins, such as the Silverleaf Whitefly-Induced Protein1, Mitogen Activated Protein Kinase6, and Heat Shock Protein81, have known defensive functions. Isotope-coded protein labeling and western-blot analyses indicated that Cyclophilin18 is a reliable marker for stress responses of the EFP. As a hint toward the induction of redox signaling, we have observed delayed oxidation-triggered polymerization of the major Phloem Protein1 (PP1) and PP2, which correlated with a decline in carbonylation of PP2. In sum, wounding triggered transient sieve tube occlusion, enhanced energy metabolism, and accumulation of defense-related proteins in the pumpkin EFP. The systemic wound response was mediated by jasmonate and redox signaling.

A series of elegant experiments have demonstrated recently that phloem samples collected from cut petioles and stems of cucurbits do not represent pure fascicular phloem sap but rather the mixed content of extrafascicular phloem (EFP), xylem, and fascicular phloem (Zhang et al., 2010, 2012). The EFP is a unique feature of Cucurbitaceae. It consists of a complex network of longitudinal perifascicular strands next to the fascicular bundles, lateral commissural strands, and entocyclic as well as ectocyclic sieve tubes (Zhang et al., 2012). In contrast to the fascicular phloem, the EFP does not build effective callose plugs and freely exudes from cut sieve

tubes. Due to easy sampling and its high protein content, cucurbit exudates were frequently used for phloem biochemistry (van Bel and Gaupels, 2004; Turgeon and Oparka, 2010; Atkins et al., 2011). Recently, more than 1,100 phloem proteins were identified in a large-scale proteomic approach with pumpkin (*Cucurbita maxima*; Lin et al., 2009). Interestingly, 67%, 46%, and 62% of the previously identified phloem proteins from rice (*Oryza sativa*), rape (*Brassica napus*), and castor bean (*Ricinus communis*), respectively, were found among the EFP proteins of pumpkin, confirming functional overlap between extrafascicular and fascicular phloem of different plant species (Lin et al., 2009).

Although the EFP is physically and functionally linked to the fascicular phloem, a role in assimilate transport, the major function of fascicular phloem, is still ambiguous. The presence of many defense-related proteins in cucurbit phloem exudates rather pointed toward a role of the EFP in (systemic) stress and defense responses (van Bel and Gaupels, 2004; Walz et al., 2004; Turgeon and Oparka, 2010). In this regard, it has been largely overlooked by phloem biologists that phloem exudates of cucurbits are routinely classified by ecologists as latex-like exudates involved in

defense against herbivorous insects (Carroll and Hoffman, 1980; Tallamy, 1985; Konno, 2011). In fact, the EFP is similar to branched laticifer (latex-containing conduits) networks, which develop from protophloem and/or phloem initials (Hagel et al., 2008). For this reason, and for better differentiation from fascicular phloem samples, hereafter we will use the term phloem latex instead of phloem exudates.

Phloem latex provides two layers of defense. It is a physical barrier for small insects, which can be trapped in large droplets of exudates from wounded veins or sticky compounds that might glue their mouth parts (Konno, 2011). In addition, it was also shown that compounds in phloem latex of squash (*Cucurbita* spp.) such as cucurbitacin steroids deterred beetles from feeding (Carroll and Hoffman, 1980; Tallamy, 1985). Specialist feeders of cucurbits can tolerate toxic compounds in phloem latex or even use them for their own defense. Other herbivores, such as certain species from the genus *Epilachna*, counteract chemical defense by trenching. They isolate a circular leaf area by cutting all tissues except for the lower epidermis, this way avoiding pressure-driven exudation within the feeding area (Carroll and Hoffman, 1980; Tallamy, 1985; Konno, 2011).

Some defense responses were demonstrated to be inducible by herbivore attack both in the local as well as neighbor leaves (Carroll and Hoffman, 1980; Tallamy, 1985). In this report, we analyzed by gas chromatography/mass spectrometry (GC-MS) and stable isotope-coded protein labeling (ICPL) systemic wound responses of the EFP upon leaf wounding. Overall, wounding induced jasmonate accumulation, reprogramming of the metabolism toward increased energy status, and the regulation of proteins related to carbon metabolism, signaling, and defense. This report gives a comprehensive overview of wound-inducible changes in the metabolite and the protein composition of pumpkin phloem latex, thereby providing a framework for future in-depth studies on defense responses of both EFP as well as fascicular phloem.

RESULTS

For a long time, phloem latex has been used in biochemical studies assuming that it is equivalent to fascicular phloem sap. However, separate sampling of EFP and fascicular phloem exudates of pumpkin using microdissection revealed large differences in the sugar and protein composition between both phloem systems (Zhang et al., 2010). In this report, this finding was confirmed by employing aphid stylectomy for the collection of pure phloem sap (Gaupels et al., 2008a, 2008c). Pumpkin stylet exudates were compared with exudates from cut petioles and stems displaying different SDS-PAGE band patterns between the two sample types (Fig. 1). Particularly, the major phloem proteins (PP1 and PP2), which account for more than 80% of the total protein content in phloem latex, are virtually absent in stylectomy exudates, whereas prominent proteins of about 32 and 60 kD in stylectomy samples
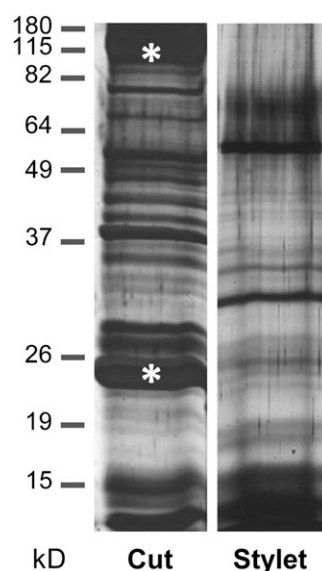

Figure 1. Protein patterns are different between phloem latex collected from cut petioles and stems as compared with phloem sap collected from cut aphid stylets. Each 1.5-μL phloem sample was analyzed by SDS-PAGE and silver staining. Asterisks indicate the major phloem proteins PP1 (96 kD) and PP2 (24 kD).

are not abundant in phloem latex. Together, these and previous results suggest that phloem latex is indeed not equivalent to fascicular phloem sap.

As discussed below, proteins and metabolites in pumpkin phloem latex collected within the first few minutes after cutting the petiole or stem originate predominantly from the EFP. Therefore, we wounded the leaves of pumpkin plants and sampled phloem latex within 2 min after cutting in order to analyze wound-inducible defense mechanisms of the EFP.

Leaf Wounding Induces the Accumulation of Jasmonates in the EFP

Wounding was performed by crushing the edges of all leaves for induction of a uniform and reproducible systemic response in the EFP of petioles and stems (Fig. 2A). The well-known wound signals jasmonic acid (JA) and its conjugate JA-Ile were not found in phloem latex from control plants but were detected at 30 min and peaked at 60 min after wounding, reaching maximum concentrations of 107 nM JA and 49 nM JA-Ile (Fig. 2B). The jasmonate levels strongly decreased again at 3 h after treatment. We also found jasmonate and/or wound-responsive proteins in phloem latex, which is discussed below. These results argue for the onset of a systemic wound response in the EFP.

Transient Reduction of Phloem Exudation Correlates with the Formation of Saccharide Polymers

Leaf damage induced a transient decrease in exudation volume by about 30% at 0.5-, 1-, and 3-h time points (Fig. 3A). The reduced exudation correlated with
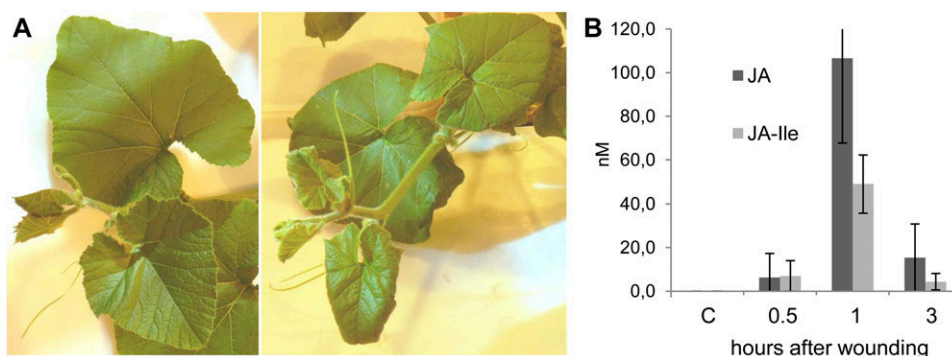
Figure 2. Leaf wounding induced the accumulation of jasmonates in pumpkin phloem latex. A, All leaves of a plant were wounded at the edges for induction of a uniform response throughout the aerial plant parts. A control plant (left) and a wounded plant at 3 h after wounding (right) are shown. B, JA and JA-Ile were not detected in phloem latex from untreated pumpkin plants but accumulated at 0.5, 1, and 3 h after wounding of all leaves. Error bars indicate the SD of three independent replicates. Every replicate was a pool of phloem exudates from seven to 10 plants. C, Control. [See online article for color version of this figure.]

an accumulation of "sticky compounds" in phloem latex, which caused the plugging of pipet tips during the sampling procedure. At 48 h after wounding, the exudate volume increased above control levels and phloem latex was even less sticky than control samples. Results of HPLC fractionation combined with flow injection electrospray ionization (FIE)-MS analysis suggested that the sticky compounds are saccharide polymers (Fig. 3B). The exact nature of the saccharide polymers is not resolved, but they consist of sugar units of 162 mass-to-charge ratio (dehydrated Glc) bound to an unknown conjugate. Most likely, wounding induced the synthesis of glucans such as callose.

Energy Status, Suc Transport, Carbohydrate Metabolism, and Amino Acid Synthesis Are Enhanced after Wounding

The ATP level is a widely used measure for cellular energy status (Geigenberger, 2003). Leaf wounding of pumpkin triggered only a slight, nonsignificant depression at 0.5 and 1 h but a significant 17% rise in ATP concentrations from 6 to 24 h after treatment (Fig. 4).
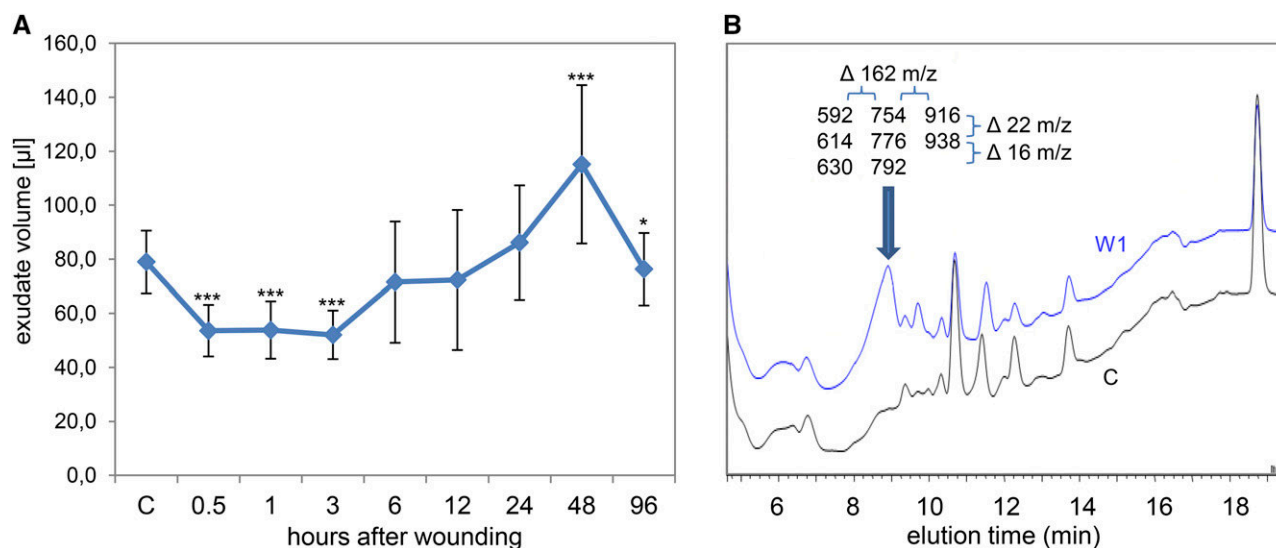

Figure 3. The volume of pumpkin phloem exudates changes concurrent with an accumulation of polysaccharides upon leaf wounding. A, The exudate volume decreased transiently at 0.5, 1, and 3 h after wounding of all leaves. Error bars indicate the SD of 13 replicates. Asterisks indicate statistically significant differences from control samples from untreated plants (Student's t test, $*P < 0.05$; $***P < 0.001$). B, The decrease in volume correlated with an accumulation of polysaccharides in the exudates at 1 h after wounding (W1; top curve), probably representing callose formation. The HPLC fractions containing the peak marked by the arrow were analyzed by FIE-MS. Resulting masses (mass-to-charge ratio [m/z]) are shown. Note the mass differences of 162 (one sugar unit) between columns and 22 (protonated versus sodium adduct) or 16 (sodium versus potassium adduct) between rows of displayed masses. C, Control. [See online article for color version of this figure.]
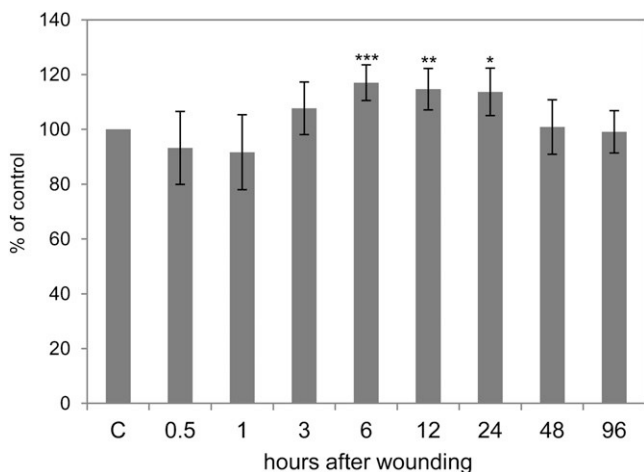
Figure 4. ATP levels as a measure of cellular energy status increase after wounding. Error bars indicate the SD of six replicates. Asterisks indicate statistically significant differences from control samples from untreated plants (Student's *t* test, *$P < 0.05$; **$P < 0.01$; ***$P < 0.001$). C, Control.

Energy metabolism is fueled by Suc, which is the major transport sugar in most plants. ATP is then generated during glycolysis, the citrate cycle, and mitochondrial electron transport. GC-MS data imply that Suc accumulates in the EFP after wounding (Fig. 5). Also, intermediates of glycolysis (Glc-6-P) and the citrate cycle (pyruvate, citrate, and malate) increased. Phosphate, which is released during glycolysis and the citrate cycle, shows kinetics remarkably similar to citrate, malate, and Glc-6-P, with an early peak at 3 h after wounding, confirming the functional link between these metabolites. 3-hydroxypropionate levels are also strongly elevated after wounding, whereas the closely related lactate (2-hydroxypropionate) is not consistently regulated (Fig. 5; Supplemental Fig. S1). Myoinositol decreased after wounding. In sum, the elevated ATP levels in response to crushing of the leaf edges most likely arose from stimulated glycolysis, the citrate cycle, and mitochondrial electron transport.

Under stress conditions, energy/ATP is utilized for the production of defensive compounds such as callose, various stress signals, and defense-related proteins. Accordingly, after wounding, we observed a general increase in amino acids, which probably served as building blocks for enhanced protein and secondary metabolite synthesis (Supplemental Fig. S2).

Proteins Related to Signaling, Defense, Protein Metabolism, and Transport Processes Are Wound Regulated

In initial experiments, two-dimensional electrophoresis was applied for the identification of wound-regulated phloem latex proteins. However, results obtained with this method were unreliable, mainly due to uncontrolled precipitation of PP1/PP2 during isoelectric focusing, which caused heavy streaking, as also observed

previously by others (Walz et al., 2004; Malter and Wolf, 2011). Specific problems related to electrophoresis can be avoided by gel-free techniques such as ICPL combined with MS. A principal problem with this approach was masking of less-abundant proteins by a few major proteins, resulting in poor labeling efficiency and a very restricted number of protein identifications. Recently, combinatorial hexapeptide ligand libraries bound to chromatographic beads (ProteoMiner) were used for the depletion of high-abundance proteins and the enrichment of low-abundance proteins in plant extracts (Fröhlich and Lindermayr, 2011; Fröhlich et al., 2012). Application of ProteoMiner to phloem latex caused a considerable change in protein pattern (Supplemental Fig. S3; Fröhlich et al., 2012). Major proteins such as PP1 and PP2 and total protein concentrations were strongly reduced, while new bands probably representing less abundant proteins appeared on the gel.

Combining ProteoMiner pretreatment with ICPL, we found that wounding induced a reprogramming of the phloem latex proteome, with altogether 51 proteins being modulated after leaf crushing (Table I; Supplemental Table S1). Six proteins were part of the carbohydrate and energy metabolism. For instance, GDP-L-Fuc synthase and UDP-L-Rha synthase, which both use nucleotide sugars for cell wall synthesis, were repressed after wounding. Also, Glc-6-P dehydrogenase, which synthesizes the first step of the pentose phosphate pathway, displayed a 3-fold decrease in abundance. The proteomic approach uncovered three proteins that might be key
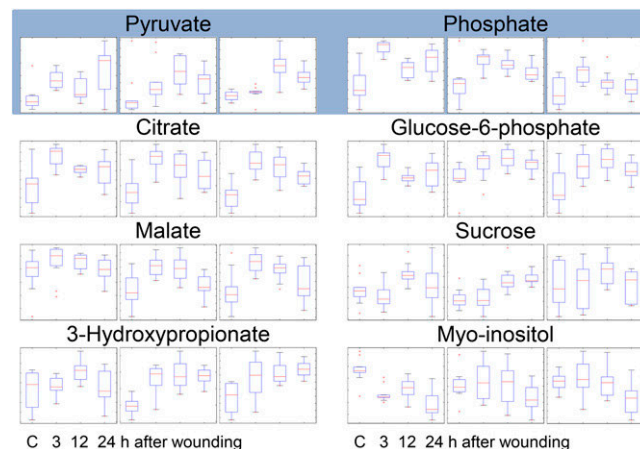

Figure 5. Energy and carbohydrate metabolism are enhanced after wounding. Phloem latex from untreated control and wounded plants at time points 3, 12, and 24 h after wounding were analyzed by GC-MS/MS. The results of three independent experiments with 11 biological replicates are shown. Box plots derived from ANOVA represent relative signal intensity ratios. Pyruvate and phosphate species (shaded) are central metabolites of the citric acid cycle (citrate and malate) and glycolysis/gluconeogenesis (Glc-6-P, Suc, and myoinositol). 3-hydroxypropionate is related to pyruvate (2-oxoproprionate) and lactate (2-hydroxypropionate) and is involved in energy metabolism, glycolysis, and Ala synthesis. C, Control. [See online article for color version of this figure.]

Table I. *Wound-regulated proteins in phloem latex identified by isotope-coded protein labeling*

MW, Molecular mass in kD.

Accession[a]	MW	W3/C[b]	W24/C[b]	Description
Carbohydrate and energy metabolism				
429162	31.1	2.21	2.49	14-3-3 protein 32-kD endonuclease
Cucsa.089980	35.9	0.72	0.58	GDP-L-Fuc synthase
Cucsa.302670	33.6	0.33	0.33	UDP-L-Rha synthase
Csa022482	59.2	0.33	0.43	Glc-6-P dehydrogenase
Cucsa.170120	40.9	0.59	0.62	SNF1-related protein kinase2
1743009	57.8	0.09	0.09	SNF1-related protein kinase1
Signaling, defense				
10998336	48.1	3.25	4.06	Silverleaf whitefly-induced protein1
113045960	17.9	1.09	1.69	MAPK6
319439585	33.8	0.79	1.70	Cyclin-dependent kinase A
110748608	42.7	1.07	1.63	NO_3^- stress-induced MAPK
117573664	16.5	1.82	4.13	16-kD phloem protein1, PP16-1
1753099	95.3	1.06	2.09	Phloem filament protein, PP1
508445	24.5	0.47	1.09	Dimeric phloem-specific lectin, PP2
99906997	35.6	0.59	1.15	Class III peroxidase precursor
20453013	64.0	0.61	0.90	Phloem calmodulin-like domain protein kinase
Cucsa.142500	16.9	0.83	0.56	Calmodulin
50262213	7.6	0.50	1.09	Putative chymotrypsin protease inhibitor
Chaperones				
Csa001697	79.9	2.24	2.67	HSP81
Cucsa.142610	60.5	1.78	2.27	Chaperonin-containing complex protein1
Csa009634	59.0	1.43	2.00	T-complex protein1 subunit ζ-like
62728587	18.1	1.08	1.73	Cyclophilin
Cucsa.106590	13.2	0.96	0.59	Peptidyl-prolyl cis-trans-isomerase Pin1
51477394	63.8	0.57	1.21	Protein disulfide isomerase (PDI)-like protein3
Protein synthesis and degradation				
Cucsa.153230	67.1	3.23	1.38	DEAD box RNA helicase
Cucsa.162420	53.5	1.42	1.72	DEAD box RNA helicase
Cucsa.345110	85.1	2.04	2.42	Elongation factor2-like
Cucsa.201940	16.6	2.40	1.66	Ubiquitin-conjugating enzyme E2
Cucsa.181800	48.0	2.11	2.64	26S protease subunit 6A-like
81076307	16.5	1.63	2.00	Putative translation initiation factor eIF-1A-like
224110244	17.5	0.98	1.81	Proteasome subunit α type 2
224085688	26.6	1.05	1.79	Proteasome subunit α type 1
Csa011709	86.7	1.58	1.77	Cullin-1
147800085	66.7	0.53	1.26	E3 ubiquitin ligase ARI7-like
224095561	97.6	0.58	1.13	26S proteasome regulatory complex component
Cucsa.018140	51.2	0.60	0.78	Eukaryotic translation initiation factor3 subunit 6N
Cucsa.342220	45.3	0.64	0.48	COP9 signalosome subunit4-like
307136429	25.5	0.41	0.34	COP9 signalosome subunit7a
298352997	17.2	0.31	0.36	Putative ubiquitin-conjugating enzyme
Transport, cytoskeleton				
495731	23.0	2.38	1.79	Small ras-related
6097869	13.8	0.93	3.52	Actin
Csa010390	41.7	1.71	1.26	Actin
Cucsa.053580	17.1	2.18	1.59	Actin-depolymerizing factor
157467219	18.5	2.44	1.73	GTP-binding nuclear protein Ran3-like
307135957	49.5	0.61	1.81	Tubulin α-chain
123192431	25.3	1.43	1.89	Ran1
137460	68.8	0.83	1.73	V-type proton ATPase catalytic subunit A
255570599	96.4	0.53	1.01	Importin β-1, putative
51477379	99.8	0.52	1.26	DRP, dynamin
Others				
Cucsa.328440	43.2	1.53	1.71	*S*-Adenosyl-Met synthetase
307135934	32.9	1.70	1.06	Pyridoxal biosynthesis protein
168049525	89.6	0.55	1.18	Cell division control protein48, CDC48

[a]Accession numbers from the National Center for Biotechnology Information, International Cucurbit Genomics Initiative (Csa identifiers), and the Joint Genome Institute (Cucsa identifiers). [b]C, W3, W24 indicate phloem latex from untreated control plants or wounded plants at 3- and 24-h time points.

regulators of energy and carbohydrate metabolism. Two Sucrose-Nonfermenting1 (SNF1)-related protein kinases, SnRK1 and SnRK2, were 11- and 1.67-fold repressed upon the stress treatment, while the 14-3-3 protein 32-kD endonuclease present in phloem latex was 2-fold induced by wounding.

Proteins with roles in signaling and defense included the Silverleaf Whitefly-Induced Protein1 (SLW1), which was 3- and 4-fold induced at 3 and 24 h after wounding, respectively. Also, three kinases related to stress signaling, namely the NO_3^- stress-induced mitogen-activated protein kinase (MAPK), cyclin-dependent kinase A, and MAPK6, were induced at the later time point. Among the major phloem proteins, PP2 was 2-fold downregulated at 3 h, whereas the 16-kD Phloem Protein1 (PP16-1) and PP1 were up-regulated. Chaperones modify protein structure and function and are often involved in signaling processes. Heat Shock Protein81 (HSP81) belongs to the HSP90 family and is 2- and 3-fold induced at the two sampling time points. Moreover, an 18-kD cyclophilin (CYP18) was more abundant at 24 h after

wounding as compared with the control. CYP18 turned out to be an excellent marker for stress responses of the EFP, as detailed below.

Fifteen wound-regulated proteins are related to protein synthesis and degradation (Table I), consistent with previous reports that pumpkin phloem latex contains the complete machinery for protein turnover (Lin et al., 2009; Fröhlich et al., 2012). In general, regulation of these proteins mainly reflects proteomic reprogramming under stress conditions. Enhanced metabolism and protein turnover correlated with an increase in transport processes, as indicated by the accumulation of transport-related proteins such as the small GTPases Ran1, Ran3, and small Ras-related, a vacuolar-type proton ATPase, and elements of the cytoskeleton, including two actin isoforms, an actin-depolymerizing factor, and tubulin. Dynamin, which is involved in the scission of vesicles from membranes, decreased after wounding.

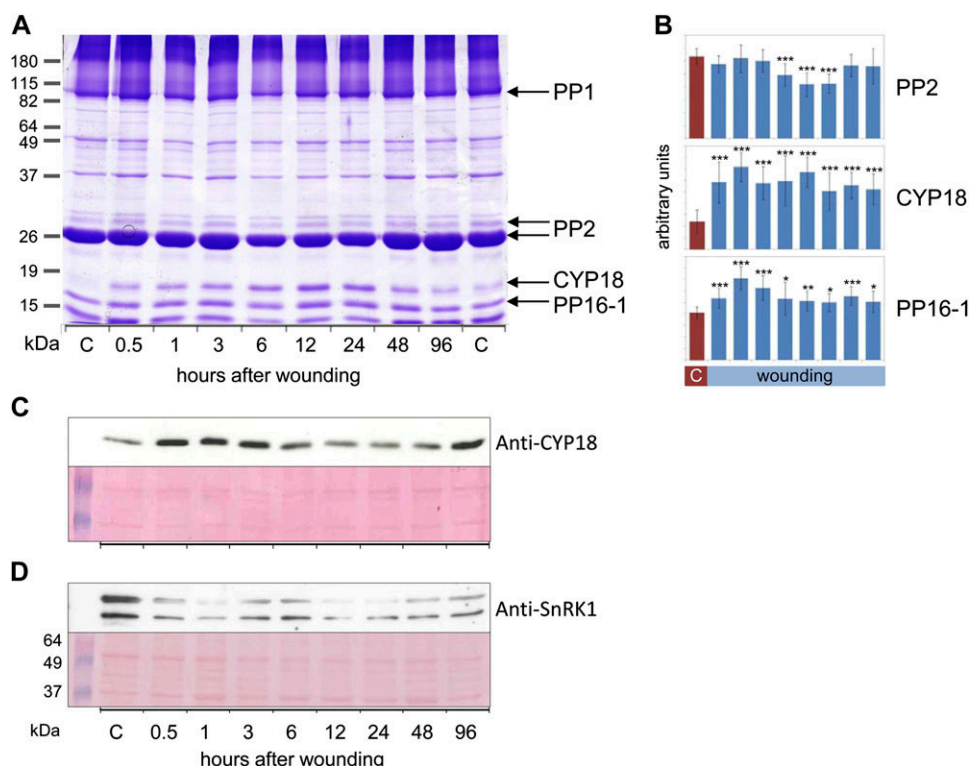Some proteome changes were readily visible after SDS-PAGE separation of phloem latex proteins (Fig. 6). PP2

Figure 6. PP2, CYP18, PP16-1, and SnRK1 are wound-regulated phloem proteins. A, Representative Coomassie blue-stained polyacrylamide gel displaying phloem proteins from untreated (two controls shown) or wounded pumpkin plants. Major phloem proteins PP1 and PP2, PP16-1, and CYP18 were labeled. CYP18 and PP16-1 were cut from the gel and identified by LC-MS/MS. B, Quantification of PP2 (major isoform), CYP18, and PP16-1 band intensities by ImageJ. Note the transient reduction in PP2 band intensity at 6 to 24 h after wounding, whereas CYP18 and PP16-1 were significantly induced from 0.5 to 96 h after wounding. Error bars indicate SE ($n = 9$). Asterisks indicate statistically significant differences from the control (Student's t test, *$P < 0.05$; **$P < 0.01$; ***$P < 0.001$). C, Western-blot analysis of phloem proteins with anti-CYP18 antibodies confirmed the wound induction of CYP18, although the kinetics is induction are somewhat variable. D, Western-blot analysis of phloem proteins with anti-SnRK1 antibodies. The western-blot signal corresponds to the expected protein mass of approximately 57 kD. The identity of the bottom band is unknown. The nitrocellulose membrane was stained with Ponceau red for confirmation of equal loading. C, Control. [See online article for color version of this figure.]

levels decreased between 6 and 24 h after wounding (Fig. 6, A and B). Intraexperimental variability might explain why in the ICPL approach, PP2 decreased already at 3 h but not at 24 h. However, the general tendency of regulation was the same with both techniques. Another major phloem protein, PP16-1, was found by ICPL to be induced after wounding, and this was confirmed by quantification of SDS-PAGE results (Fig. 6B). The most prominent wound-responsive protein was unequivocally identified by SDS-PAGE, liquid chromatography-tandem mass spectrometry (LC-MS/MS), and western-blot analyses to be an 18-kD cyclophilin (Fig. 6, A–C). CYP18 abundance increased already at 0.5 h and was still higher than the control level at 96 h. This is in accordance with the results of the ICPL experiment, in which CYP18 was also up-regulated, although only at 24 h after wounding. Additionally, we confirmed the regulation of SnRK1, which was shown to be strongly down-regulated both by ICPL and western-blot analyses (Fig. 6D). In sum, we were able to validate the results of the ProteoMiner/ICPL experiment by SDS-PAGE and western-blot analyses with nonpretreated phloem latex. Although the extent and timing were somewhat variable, the general tendencies of the regulation of the tested candidate wound-responsive proteins were consistent between the different experimental approaches.

Wounding Triggers Redox Modifications of Phloem Proteins

If phloem latex is exposed to air oxygen, it will gelate within a few hours. This special feature of cucurbit phloem latex is mediated by the redox-sensitive PP1 and PP2, which polymerize upon oxidation of Cys residues (Read and Northcote, 1983). Gelation can be artificially induced by 4-fold dilution of phloem latex with alkaline buffer (Alosi et al., 1988). By using this assay, we found that sample gelation was significantly delayed at 6 to 48 h after leaf crushing (Fig. 7). The average gelation time rose from 5 min in control samples to 22 min at 12 h after treatment. In order to investigate if PP1 and PP2 were altered in their redox state, western-blot analysis for the detection of carbonylated proteins was performed (Fig. 8). PP1 was not carbonylated, whereas PP2, CYP18, and PP16-1 produced strong signals on the western blot. Surprisingly, the signals for two PP2 isoforms were already strong in control samples but weakened from 6 to 96 h after wounding, with minimum signal intensity at the 12-h time point. However, only weak changes in protein abundance of PP2 were observed by Ponceau staining, implying that the western-blot signals decreased due to decarbonylation of PP2 rather than reduction in PP2 protein levels. For CYP18 and PP16-1, we observed a good correlation between the intensities of western-blot signals and Ponceau staining, suggesting that the oxidation status of these proteins did not change after wounding.
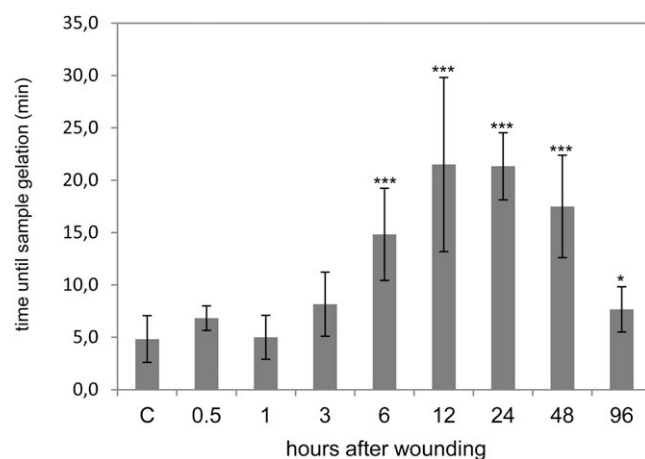
Figure 7. The gelation of phloem latex due to redox-dependent polymerization of PP1 and PP2 is delayed after wounding. The time until sample gelation was measured after the addition of 3 volumes of alkaline buffer (pH 7.8). In this assay, samples were assumed to be gelated when they could not be mixed by vortexing anymore. Error bars indicate SE ($n = 9$). Asterisks indicate statistically significant differences from the control (Student's t test, $*P < 0.05$; $***P < 0.001$). C, Control.

DISCUSSION

Pumpkin Phloem Latex Mainly Originates from the EFP

Phloem latex does not represent pure EFP exudates, since it is blended with fascicular phloem and xylem/apoplastic fluids (Zhang et al., 2012). The contribution of the vascular systems to the latex composition varies between cucurbit species. For example, a major proportion of initial phloem exudates from cucumber (*Cucumis sativus*) originated from the fascicular phloem (Zhang et al., 2012). On the other hand, pumpkin phloem exudates collected within the first minutes after cutting of stems and petioles mainly consisted of EFP content. This was suggested by several observations. (1) Microscopy revealed that phloem sap exuded freely from the EFP but only a little from the fascicular phloem, which was shown to be rapidly occluded by callose formation (Zhang et al., 2010, 2012). (2) Nonmobile hexoses, which are not present in pure fascicular phloem sap, were detected in phloem latex, whereas levels of the major phloem-mobile carbohydrates stachyose and Suc were exceptionally low (Zhang et al., 2010, 2012). (3) Protein concentration and composition were disparate between fascicular phloem exudates and phloem latex (Fig. 1; Zhang et al., 2010). The above-mentioned facts would argue against an important contribution of fascicular phloem sap to pumpkin phloem latex.

Feeding experiments with xylem-mobile silicon showed that phloem latex was diluted by xylem fluid (Zhang et al., 2012). According to a current model, cutting releases the pressurized EFP content, and exudation of phloem latex is driven by diffusion of water into the EFP, causing an increase in turgor pressure (Zhang et al., 2012; Zimmermann et al., 2012). However,
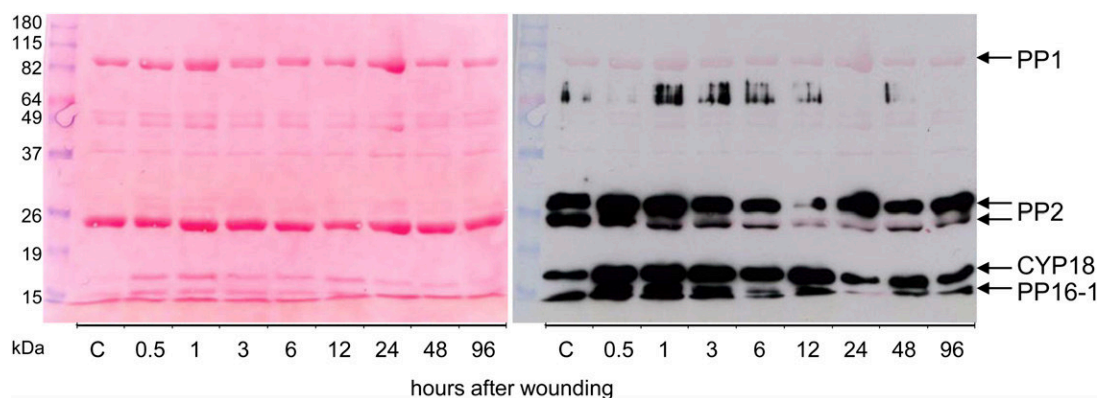
Figure 8. Leaf wounding triggers a specific decline in carbonylation of PP2. Carbonylated (oxidized) phloem proteins were labeled with DNP for immunodetection by anti-DNP antibodies. The left image shows Ponceau red-stained proteins after blotting to a nitrocellulose membrane. The right image is a digital overlay of the western-blot signals with Ponceau red-stained proteins. Note that CYP18, PP16-1, and PP2 isoforms but not PP1 cross reacted with anti-DNP antibodies. C, Control. [See online article for color version of this figure.]

translocation of water from the xylem (i.e. apoplast) through membranes or aquaporins into the EFP sieve tubes would probably not permit the exchange of large solutes between both vascular systems. Therefore, xylem proteins and metabolites are most likely only trace constituents of phloem latex. This is also inferred from the low protein concentrations of 0.05 to 0.1 μL mL^{-1} in xylem sap (Buhtz et al., 2004) as compared with more than 20 μL mL^{-1} in phloem latex. Efflux of phloem latex will cease after some minutes, and subsequently, xylem sap will exude if the root pressure is high enough (Zhang et al., 2012; Zimmermann et al., 2012). On these grounds, we sampled EFP-enriched phloem latex by immediate blotting of the cut surface with lint-free paper (to remove the content of damaged nonvascular cells and fascicular phloem sap) and collection of exudates within less than 2 min after cutting (to avoid further sample dilution by xylem exudation). In sum, phloem latex from pumpkin consists predominantly of diluted EFP content with trace materials from other sources and can be employed for analyzing the EFP wound response.

Is the Systemic Wound-Induced Accumulation of Saccharide Polymers in Phloem Latex Related to Sieve Tube Occlusion?

Sieve tubes of the fascicular phloem contain valuable nutrients. To avoid loss of phloem content from wounded veins, most plants have developed rapid and reversible sieve tube occlusion by callose formation. The EFP was presumed to be devoid of this defense mechanism, since it exudes large volumes of phloem latex from cuts (van Bel and Gaupels, 2004; Turgeon and Oparka, 2010; Atkins et al., 2011). However, during sampling, we observed a transient reduction by about 30% in phloem latex exudation at 0.5 to 3 h after wounding, concurrent with an

accumulation of sticky compounds, which were identified as saccharide polymers. Similar compounds were previously detected in pumpkin phloem latex, without biological functions being investigated (Tolstikov and Fiehn, 2002). Taken together, these observations are reminiscent of callose formation in the fascicular phloem. It remains to be answered why, in the EFP wound-induced sieve tube, occlusion is obviously ineffective.

One possible explanation is that sieve tubes as well as sieve plates of the EFP are exceptionally wide and, therefore, are difficult to seal by callose (Mullendore et al., 2010; Zhang et al., 2012). More likely, however, exudation of copious amounts of phloem latex is a defensive trait (Turgeon and Oparka, 2010; Konno, 2011). In general, latex is particularly effective in defense against small insects, which are confronted at the site of feeding with relatively large droplets of the toxic and sticky liquid (Konno, 2011). Insects can counteract this defense by trenching and vein cutting. The resulting release of pressure from laticifers allows the insects to feed in the now unprotected parts of the leaf for a certain time interval. Only after occlusion and reestablishment of high-pressure conditions can damaged laticifers exude latex again (Konno, 2011).

EFP sieve tubes have typical features of laticifers in that they are under high pressure and exude large volumes of cucurbitacin-containing phloem latex from cuts. Therefore, it can be hypothesized that, analogous to laticifers, EFP sieve tube occlusion also is only effective after pressure release by exudation and is necessary for reloading the EFP's defensive arsenal. Systemic polysaccharide accumulation induced by leaf wounding did not prevent pressure-driven exudation but rather might function in clogging of an insect's mouth parts. Accordingly, sticky compounds in phloem latex, which accumulated after leaf wounding but were present also in control samples, effectively plugged pipette tips during the sampling procedure.

Stress-Induced Energy Metabolism in the Phloem Is Controlled by SNF1-Related Kinases and a 32-kD 14-3-3 Protein and Is Not Limited by Oxygen Availability

Phloem is largely isolated from air oxygen by many layers of surrounding cells. Using microelectrodes, the oxygen tension was determined to be 15% at the epidermis but only 5% to 6% in the phloem region of castor bean stems (van Dongen et al., 2003). Exposure of stem tissue to 21%, 10%, and 5% oxygen caused a gradual decline in ATP levels of phloem samples, indicative for oxygen limitation of energy metabolism in the fascicular phloem under natural conditions (van Dongen et al., 2003). Geigenberger (2003) proposed that under stress conditions, a rise in mitochondrial oxygen-consuming respiration would cause hypoxia or even anoxia and, consequently, energy deficiency in the phloem. Accordingly, in phloem exudates from castor bean stem sections, which were incubated in zero-oxygen atmosphere for 90 min, ATP dropped to 50% of the ambient air control (van Dongen et al., 2003). As a consequence, energy-dependent Suc transport was inhibited and other markers of energy metabolism such as pyruvate, Glc-6-P, citrate, and malate were also diminished, whereas lactate and ethanol levels increased under severe oxygen deficiency.

However, in the EFP of pumpkin plants, the energy status as determined by ATP levels did not change strongly in response to stress. After an initial insignificant depression, ATP concentrations even increased by about 17% at 6 to 24 h upon wounding. ATP was most likely derived from enhanced glycolysis and the citrate cycle, because Suc, Glc-6-P, pyruvate, as well as the citrate cycle intermediates citrate, malate, and phosphate were strongly elevated after wounding. The intermediates of the citrate cycle displayed very similar kinetics, with an early rise at 3 h and a decline toward control levels at 24 h after leaf damage. Lactate was not consistently regulated, indicating that, in contrast to oxygen-deficient fascicular phloem of castor bean, fermentation of pyruvate is not an essential pathway for energy production in the stressed EFP. Collectively, these results imply that either stress does not cause hypoxia in the EFP or the energy-consuming stress response is at least not limited by oxygen availability. In comparison with the fascicular phloem, the EFP consists of a network of sieve elements (Turgeon and Oparka, 2010) connecting well-oxygenated outer tissues with oxygen-deficient inner tissues. Hence, the EFP is probably better supplied with oxygen than the fascicular phloem. It would be interesting to learn if the EFP even plays a role in "ventilation" of the fascicular phloem and other internal tissues.

Glc-6-P and Fru-6-P are central metabolites at the interface between glycolysis and gluconeogenesis and are involved in nucleotide sugar metabolism and cell wall synthesis (Seifert, 2004; Schluepmann et al., 2012). Immediately after wounding, Glc-6-P was probably used for callose formation, since polysaccharides strongly accumulated at the 0.5- to 3-h time points (Fig. 2B). From 3 h

on, EFP metabolism switched toward increased energy supply. The observed accumulation of Glc-6-P at 3 h after wounding could originate from different sources, including (1) digestion of Suc or other carbohydrates in the course of glycolysis, (2) breakdown of callose/polysaccharides after transient partial sieve tube occlusion, or (3) either/both of these two sources in conjunction with inhibition of Glc-6-P-consuming pathways. Our results provide evidence for a tightly controlled channeling of Glc-6-P into glycolysis and the citrate cycle (Supplemental Fig. S4), because intermediates of the citrate cycle increased with similar kinetics like Glc-6-P. One metabolic checkpoint seems to be Glc-6-P dehydrogenase, which is the first enzyme of the oxidative pentose phosphate pathway. This pathway mainly provides reducing power in the form of NADPH for metabolic processes but not the energy equivalents NADH and ATP. Glc-6-P dehydrogenase was strongly inhibited at 3 and 24 h after leaf wounding, suggesting that the pentose phosphate pathway is down-regulated under high energy demand.

Cell wall synthesis consumes most of the carbon in plant cells, main components being the nucleotide sugars Glc-6-P, Glc-1-P, UDP-Glc, and GDP-L-Fuc (Seifert, 2004). In wound-induced stress conditions, the EFP down-regulated the cell wall-synthesizing enzymes GDP-L-Fuc synthase and UDP-L-Rha synthase (Supplemental Fig. S4). As mentioned above, callose synthase is probably also inactivated after transient sieve tube occlusion. If the same applies for cellulose synthase remains to be answered in a future study. Moreover, the cell wall component Hyp, which is used for the synthesis of Hyp-rich glycoproteins, and myoinositol declined in phloem latex from wounded plants. Inhibition of myoinositol synthesis could also contribute to the accumulation of its precursor Suc. The latter disaccharide is probably both a substrate for glycolysis as well as a product of gluconeogenesis. Alternatively, increased Suc levels could indicate enhanced phloem transport/sugar uptake (van Dongen et al., 2003). Amino acids accumulate late, suggesting that in the early phase of the stress response energy metabolism is preferred and, later, energy and carbon are used for amino acid and protein synthesis. Collectively, these results demonstrate that a major part of the EFP stress response is dedicated to metabolic reprogramming toward an increase in energy production by enhanced glycolysis and the citrate cycle.

SNF1-Related Protein Kinases and the 14-3-3 32-kD Endonuclease

The two SNF1-related protein kinases SnRK1 and SnRK2 are currently emerging as central regulators of energy and carbon metabolism under stress conditions (Boudsocq and Laurière, 2005; Polge and Thomas, 2007; Baena-González and Sheen, 2008). Sugar or energy depletion during hypoxia, long darkness, and phosphate starvation were shown to activate SnRK1, which then

triggered the degradation of alternative energy sources such as Suc, starch, cell wall compounds, amino acids, and storage lipids (Baena-González et al., 2007; Lee et al., 2009; Bailey-Serres et al., 2012; Schluepmann et al., 2012). Accordingly, overexpression of the Arabidopsis (*Arabidopsis thaliana*) SnRK1 subunit KIN10 induced the expression of genes related to catabolism, but genes related to energy-consuming processes and anabolism were repressed (Baena-González et al., 2007). Exogenously supplied Suc was more efficiently used for energy production by KIN10-silenced plants as compared with KIN10 overexpressors (Baena-González et al., 2007). Based on these findings, the observed wound-induced reduction of SnRK1 protein levels in phloem latex would provoke a rise in energy metabolism in the course of the EFP stress response. Basal levels of SnRK1 in control samples might fine-tune the energy economy by establishing a low metabolic rate at rest.

In line with this hypothesis, the SnRK1 subunit GAL83 of *Nicotiana attenuata* was down-regulated in gene expression after leaf wounding, which was associated with the allocation of carbohydrates from leaves to the roots for improved herbivore tolerance (Schwachtje et al., 2006). Moreover, Coello et al. (2012) found a drastic decline in SnRK1 levels at 6 to 10 h after abscisic acid (ABA) treatment of wheat (*Triticum aestivum*) roots, but the total SnRK1 activity was weakly enhanced due to a simultaneous ABA-induced increase in phosphorylation/activation. If the wound-induced down-regulation of SnRK1 in the EFP is mediated by the well-known wound signal ABA remains to be investigated. Notably, SnRK1 activity is allosterically inhibited by Glc-6-P (Toroser et al., 2000). Given the strong down-regulation of SnRK1 protein abundance and the accumulation of inhibitory levels of Glc-6-P in phloem latex, it can be assumed that SnRK1 activity is reduced in the EFP after leaf wounding.

In phloem latex, the 14-3-3 32-kD endonuclease was induced at 3 and 24 h after leaf wounding. 14-3-3 proteins interact with phosphorylated target proteins, thereby modulating their conformation and/or activity. Originally, they were thought to mainly regulate metabolic enzymes (Huber et al., 2002) but are now recognized as central mediators of signal transduction (Gökirmak et al., 2010; Jaspert et al., 2011). The EFP 14-3-3 32-kD endonuclease is highly similar to potato (*Solanum tuberosum*) 14-3-3 proteins (Aksamit et al., 2005; Zuk et al., 2005). In the context of phloem signaling, it is of particular interest that expression of the potato 14-3-3 16R and 20R isoforms is restricted mainly to vascular tissues and adjacent parenchyma cells (Aksamit et al., 2005). Both 14-3-3-coding genes were inducible by ABA, which was mediated by promoters containing Myc-binding sites, but were differentially expressed in response to various abiotic stresses and phytohormones (Aksamit et al., 2005).

The promoter of the 14-3-3 isoform 16R was inducible by Suc. Moreover, transgenic potato plants silenced in 14-3-3 genes displayed reduced nitrate reductase, Suc phosphate synthase, and Suc synthase activities accompanied by increases in starch, Suc, and protein levels (Zuk et al., 2005). This phenotype could be complemented by overexpressing the 14-3-3 32-kD endonuclease from zucchini (*Cucurbita pepo*). In *Hevea brasiliensis* latex, 14-3-3 proved to be inducible by JA, corroborating a possible role of this protein in defense responses (Yang et al., 2012). Thus, 14-3-3 proteins might, like SnRKs, act as integrators of carbohydrate, energy, and (ABA- or JA-controlled) stress metabolism. If the 14-3-3 endonuclease and SnRK1/2 are antagonists in the same signaling pathways will be deciphered in future studies.

JA Signaling and the Accumulation of Defense-Related Proteins during Systemic Wound Responses of the EFP

Leaf damage simulating herbivore attack triggers systemic signaling cascades in plants, and JA derivatives were hypothesized to act as phloem-mobile signals in the systemic wound response (Li et al., 2002; Ryan and Moura, 2002; Koo and Howe, 2009; Sun et al., 2011; Gaupels and Vlot, 2012). Accordingly, wounding triggered JA synthesis in the tomato (*Solanum lycopersicum*) sieve elements (Hause et al., 2000, 2003), and isotope-labeled JA was found to be systemically transported in the sieve tubes (Zhang and Baldwin, 1997; Thorpe et al., 2007). However, to date, few data are available on the actual concentrations of this hormone in phloem exudates. We measured the JA and JA-Ile contents in phloem latex from wounded pumpkin. Jasmonates were not detectable in samples from untreated plants but accumulated rapidly at 0.5, 1, and 3 h after wounding. Maximum concentrations were measured at the 1-h time point, when JA and JA-Ile reached 107 and 49 nM, respectively. The kinetics is very similar to previously reported jasmonate accumulation in wounded and systemic leaves of tomato and is indicative for the induction of a systemic wound response (Koo et al., 2009). Interestingly, declining jasmonate levels at 3 h after leaf damage coincided with the down-regulation of two proteins of the COP9 signalosome, which is required for the expression of JA biosynthesis-related genes (Feng et al., 2003).

In the EFP, jasmonates could elicit the local accumulation of defense-related proteins such as SLW1. *SLW1* was expressed in response to infestation of squash with the phloem-feeding silverleaf whitefly and upon treatment with methyl jasmonate but not wounding (van de Ven et al., 2000). The most prominent wound-induced protein in pumpkin phloem latex was identified by ICPL, SDS-PAGE, LC-MS, and western-blot analyses to be an 18-kD cyclophilin. CYP18 is highly similar to Arabidopsis ROC1/AtCYP18-3, which was shown to be 3.5-fold induced in expression by wounding (Chou and Gasser, 1997). We used anti-AtCYP18-3 antibodies for the detection of CYP18 in phloem latex. Previously, these antibodies were applied for demonstrating the presence of cyclophilins in phloem latex from pumpkin as well as phloem exudates from six monocotyledonous and

dicotyledonous plant species, including castor bean (Schobert et al., 1998; Gottschalk et al., 2008). Hence, 18-kD cyclophilins are conserved constituents of EFP as well as fascicular phloem and probably fulfill essential functions in the phloem. In castor bean, phloem cyclophilin displayed high peptidyl-prolyl cis-trans-isomerase activity, interacted with plasmodesmata, and trafficked from cell to cell (Gottschalk et al., 2008). Based on these findings, phloem cyclophilins may act as molecular chaperones modulating the import, mobility, and function of target proteins in the phloem.

Further wound-elicited chaperones, such as HSP81 and Chaperonin-Containing Complex Protein1, could have similar functions in the EFP. PP16-1 is yet another protein in phloem latex related to transport and signaling. The protein is a paralog to a movement protein of the *Red clover necrotic mosaic virus* and acts as mRNA carrier within the phloem of pumpkin (Xoconostle-Cázares et al., 1999). Aoki et al. (2005) uncovered destination-selective transport of PP16-1 and PP16-2 against the mass flow from shoot to roots of rice. To date, no further details about the role of PP16-1 in stress signaling processes are known. However, PP16-1 is regulated with similar kinetics to CYP18, suggesting common upstream signals or even a functional link between both proteins.

Protein kinases, particularly MAPKs, are often activated by phosphorylation in the course of kinase signaling cascades. However, some kinases, including MAPKs, were also found to be regulated in gene expression after stress treatments (Mizoguchi et al., 1996). In pumpkin phloem latex, the three protein kinases cyclin-dependent kinase A, NO_3^- stress-induced MAPK, and MAPK6 were increased in protein levels at 24 h after leaf wounding. Supportive of these results, CDC2a, a cyclin-dependent kinase A of Arabidopsis, was strongly induced at the transcriptional level by wounding (Hemerly et al., 1993). In cucumber plants, the NO_3^- stress-induced MAPK was also inducible by root infection with *Trichoderma asperellum*. A more detailed characterization revealed that this cucumber MAPK is highly homologous to the tobacco wound-induced protein kinase, and gene expression was actually inducible within 10 min in the wounded leaves and after 24 but not 3 h in systemic leaves (Shoresh et al., 2006). Similarly, the NO_3^-/*T. asperellum*-induced MAPK in the EFP accumulated at 24 h but not 3 h after leaf wounding. It was recently reported that MAPK6 is an important component of the JA signaling pathway in Arabidopsis (Takahashi et al., 2007). If the regulation of MAPK6 in the EFP is linked to JA signaling is not yet known.

Indications for Redox Signaling in the Phloem

Recently, a microscopic study using the nitric oxide (NO)-sensitive dye diaminofluorescein revealed interaction of the redox signals hydrogen peroxide and NO in the phloem (Gaupels et al., 2008b). Hydrogen peroxide applied to the bare-lying phloem of *Vicia faba* elicited rapid NO synthesis in companion cells, whereas watering of pumpkin with hydrogen peroxide induced

NO-dependent Tyr nitration of proteins in the EFP. A further hint toward redox signaling in the EFP could be the increase in MAPK6 levels upon leaf wounding, as reported in this study. The Arabidopsis homolog of this enzyme was shown to mediate the hydrogen peroxide-stimulated production of NO in lateral root formation (Wang et al., 2010).

PP1 and PP2 are well-known redox sensors in phloem latex. They were shown to interact via the formation of intermolecular disulfide bridges between Cys residues (Read and Northcote, 1983). Under oxidizing conditions, extensive polymerization turns PP1/PP2 complexes insoluble, causing gelation of EFP exudates (Read and Northcote, 1983). In the air, this process takes several hours, but if exudates are diluted in neutral or alkaline buffers, Cys residues get exposed, facilitating oxidation and consequently sample gelation within minutes (Alosi et al., 1988). After leaf wounding, we observed a delay in sample gelation at 6 to 48 h, which could reflect redox modifications of PP1/PP2 during the wound response.

Therefore, oxidation/carbonylation of phloem proteins was investigated by anti-dinitrophenol (DNP) western-blot analyses. By this method, the carbonylated proteins PP16-1, CYP18, and two isoforms of PP2 were immunodetected. Notably, PP1 was not carbonylated. In contrast, PP2 was strongly carbonylated even in EFP exudates from untreated control plants, suggesting that PP2 is oxidized under nonstress conditions. At 6-, 12-, and 24-h time points, PP2 signal intensity decreased, but it increased again at 48 and 96 h after wounding. This decline in carbonylation
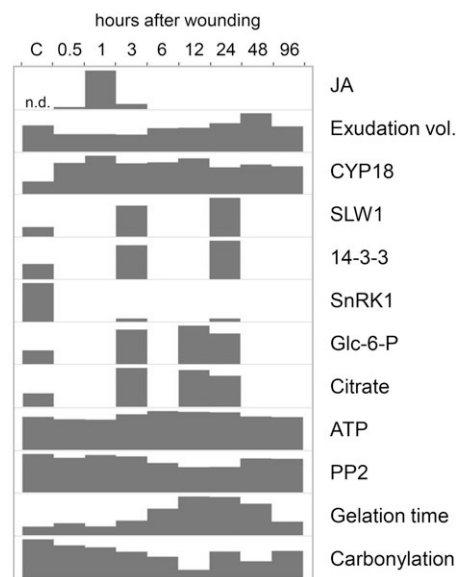
Figure 9. Summary of main results. Responses of the pumpkin EFP to leaf wounding are shown. Glc-6-P and citrate are given in relative signal intensity ratios (only one representative replicate is shown). For all other parameters, the height of the bars is proportional to control levels. Carbonylation is visualized by ImageJ quantification of the anti-DNP western blot. C, Control; n.d., not detected.

correlated well with the observed delay in sample gelling at 6 to 48 h (Fig. 9), suggesting that the increase in the reduction of PP2 hinders oxidation-dependent polymerization of PP2/PP1. The decrease in carbonylation of PP2 but not CYP18 and PP16-1 after wounding could be explained by enhanced turnover of oxidized PP2, the activity of antioxidant enzymes interacting specifically with PP2, or a redox-dependent change in conformation of PP2 potentially hiding amino acids that are prone to carbonylation.

Decreased carbonylation could even be involved in the observed decline in PP2 levels in response to leaf wounding, which could be caused by redox-regulated protein mobilization in the phloem in the course of signaling or defense events. It was proposed previously that PP2 might then occlude sieve plates (Furch et al., 2010). However, the data presented here do not support this hypothesis, because transient sieve tube occlusion occurs earlier than the reduction in PP2 levels (Fig. 9). Alternatively, PP2, PP1, and callose might cover the wounded tissue to protect the plant from insect and pathogen ingress. In this model, the lectin PP2 would interfere in an unknown mode with surface or internal GlcNAc of the attackers, while the filamentous PP1 in conjunction with callose could clog the mouth parts of insects or affect the motility of pathogens (Read and Northcote, 1983; Beneteau et al., 2010; Konno, 2011). PP2 was also identified as an RNA-transporting protein in melon (*Cucumis melo*) EFP, and as a lectin it showed affinity for phloem-internal glycoproteins (Gomez et al., 2005; Beneteau et al., 2010). Neither RNAs nor glycoproteins carried by PP2 could be identified to date. Thus, the functions of PP1 and PP2 in stress defense or signaling remain ambiguous.

CONCLUSION

This study was aimed at deciphering responses of the EFP to leaf wounding by metabolomic and proteomic approaches. As summarized in Figure 9, the EFP launched within 3 h a systemic wound response including JA accumulation, partial sieve tube occlusion, a rise in defensive protein levels, and adaptation of carbon metabolism to the higher energy demand. Later wounding caused a decline in the oxidation of PP2, which correlated with a decrease in PP2 protein level and a delay in redox-dependent sample gelation. Some of our findings for the EFP could apply also to the fascicular phloem. For instance, the major phloem proteins CYP18 and PP2 might be valuable markers for stress responses and redox signaling in both phloem systems.

MATERIALS AND METHODS

Plant Material, Sampling, and Sample Gelation Assay

Leaf edges of 4- to 5-week-old pumpkin plants (*Cucurbita maxima* 'Gele Centenaar') grown under greenhouse conditions were crushed between the lids of two 50-mL polypropylene reaction tubes. Phloem samples were

collected in the greenhouse as follows. Petioles and stems were cut using a razor blade, and the basal side of the cut was immediately blotted with Kimtech Science paper (Kimberly-Clark) to remove the content of damaged nonvascular cells and fascicular phloem sap. Exuding phloem latex was subsequently collected by a micropipette for less than 2 min. Control plants were left untreated. Pumpkin phloem latex was either snap frozen in liquid N_2 for metabolite analyses or mixed with the same volume of phloem buffer if not otherwise stated (50 mM Tris-HCl, pH 7.8, 0.1% β-mercaptoethanol; McEuen and Hill, 1982). Aphid stylectomy was used for phloem sampling according to Gaupels et al. (2008a, 2008c) with the aphid *Macrosiphum euphorbiae*. The time until sample gelation was measured after the addition of 3 volumes of alkaline buffer (25 mM HEPES/NaOH, pH 7.8) to the phloem latex (80 μL). Samples were assumed to be gelated when they could not be mixed by vortexing anymore.

Jasmonate Measurements

JA and JA-Ile in 1 mL of phloem latex from seven to 10 plants were determined as described by Hause et al. (2000).

ATP Assay

Five microliters of phloem latex was frozen in liquid nitrogen and stored at $-80°C$. Immediately before the measurements, 5 μL of phloem buffer and 40 μL of water were added, and ATP was determined using the ATP Bioluminescence Assay Kit CLSII (Roche) according to the manufacturer's instructions.

Metabolomics

GC-Time of Flight-MS

The sample extraction process involved the use of a single-phase solvent (chloroform-methanol-water) that was optimized for recovery of a wide range of metabolites (Beckmann et al., 2007). Metabolites were extracted by mixing 9 μL of phloem latex with 81 μL of chilled $CHCl_3$:methanol:water (1:2.5:1, v/v/v), and samples were stored at $-18°C$. After the addition of 90 μL of chilled methanol, samples were centrifuged (18,000g for 3 min at 0°C), and the resulting supernatant was dried in vacuo. GC-time of flight-MS analysis was performed as described previously (Catchpole et al., 2005; Beckmann et al., 2007) using tetramethylsilane derivatization and a Pegasus III GC-time of flight-MS system (Leco; http://www.leco.com/) fitted with a 20 m DB5 MS column. Peak finding and peak deconvolution were performed using ChromaTof software (Leco). Mass spectra of all detected compounds were compared with spectra in the National Institute of Standards and Technology library and with in-house and publicly available databases. Targeted peak lists were generated, and the peak apex intensity of a characteristic mass in a retention time window for each GC-MS data set (using Matlab; The Mathworks) was saved in the form of an intensity matrix (run × metabolite) for further statistical analysis.

Data Analysis

Due to the three-dimensional data structure, peak aligned and log_{10}-transformed GC-MS intensity data were first filtered by univariate data analysis using ANOVA (function ANOVA1 in Matlab; The Mathworks) to reduce their size. Metabolite signals with ANOVA $P > 5 \times 10^{-4}$ were removed from each data set. The main criterion for good model selection (i.e. discriminatory metabolites) in multidimensional GC-MS metabolomics data sets is $P < 1 \times 10^{-10}$ (ANOVA). However, a P value threshold of 1×10^{-6} is acceptable, considering a false discovery rate level of 0.001. In the second step, 80 metabolites, including all unique metabolites showing significant differences between treatment groups ($n = 10$ biological replicates for each group and experiment), were targeted in the three GC-MS raw data sets of replicated experiments. ANOVA was performed on log_{10}-transformed and normalized data. Results are shown for metabolites that were significantly regulated ($P < 0.05$) in at least two of three experiments.

HPLC and FIE-MS

Metabolites of 120 μL of phloem latex were extracted by mixing with 180 μL of chilled $CHCl_3$:methanol:water (1:2.5:1, v/v/v), and samples were stored at $-18°C$. After the addition of 300 μL of chilled methanol, samples

were centrifuged (18,000g for 3 min at 0°C), the resulting supernatant was dried in vacuo, and the metabolites were redissolved in 60 μL of 0.1% trifluoroacetic acid (TFA)/60% methanol. A Dionex HPLC system consisting of an Automated Sample Injector (ASI 100), P580 pump, column oven, and PDA-100 photodiode array detector was controlled by Chromeleon version 6.5 software. Ten microliters was injected onto a CC 250 × 4.6 Nucleodur C18 Gravity 5-μm column (Macherey-Nagel). A binary gradient (mobile phase A, water and 0.1% TFA; mobile phase B, methanol and 0.1% TFA) from 0% B (held for 2 min) to 100% B (held for 6 min) within 10 min followed by a 10-min equilibration period at 0% B was used to separate metabolites. A flow of 1 mL min^{-1} was maintained at 40°C. HPLC fractions containing the peak that eluted from 8 to 10 min of elution time were collected and analyzed by FEI-MS as described (Parker et al., 2009). FIE-MS and MS experiments were performed on a linear ion trap (LTQ; Thermo).

Proteomics

ProteoMiner Treatment and ICPL

A 120-μL pumpkin phloem exudate (25 mg protein mL^{-1}) was mixed with the same volume of phloem buffer. Redox-sensitive Cys residues of PP1/PP2 were alkylated by adding 25 mM (final concentration) iodoacetamide. Afterward, β-mercaptoethanol and iodoacetamide were removed by gel filtration, and proteins were collected in 120 μL of phloem buffer without β-mercaptoethanol. ProteoMiner beads were applied according to the manual. Final protein amount was 3 mg at a concentration of 25 mg mL^{-1}. After washing, proteins were eluted from beads by twice applying 50 μL of commercial 4× Laemmli buffer (Roth) at 95°C. Proteins were precipitated using the 2D Clean-up Kit (GE Healthcare) and dissolved in 40 μL of 100 mM HEPES, pH 8.5. Stable isotope labeling of the phloem proteins was done with the ICPL Triplex Kit (Serva) according to the manual with doubled volumes of all kit reagents. For each triplicate, isotope-labeled phloem proteins from control and wounded plants, time points 3 and 24 h after wounding, were combined. Proteins were again precipitated using the 2D Clean-up Kit and separated by SDS-PAGE. The gel was cut in six pieces per sample and analyzed by LC-MS/MS.

MS Analysis and Data Processing

After Coomassie blue staining, gel slices from one-dimensional ICPL gels were excised and subjected to in-gel digestion before MS analysis. Digested peptides were analyzed by nano-HPLC (Ultimate 3000; Dionex) coupled to a linear quadrupole ion trap-Orbitrap (LTQ Orbitrap XL) mass spectrometer (Thermo Fisher) equipped with a nano-electrospray ionization source. A nonlinear gradient using 2% acetonitrile in 0.1% formic acid in water (A) and 0.1% formic acid in 98% acetonitrile (B) was used with a flow rate of 300 nL min^{-1}. The mass spectrometer was operated in the data-dependent mode to automatically switch between Orbitrap-MS and LTQ-MS/MS. General MS conditions were as follows: ion selection threshold was 500 counts for MS/MS, an activation default instrument setting in Q text box of 0.25, and activation time of 30 ms was also applied for MS/MS. The MS/MS spectra were searched against a customized database (Fröhlich et al., 2012) by using MASCOT (version 2.3.02; Matrix Science) with the following parameters: a precursor mass error tolerance of 10 ppm and a fragment tolerance of 0.6 D. One missed cleavage was allowed. Carbamidomethylation was set as a fixed modification. Oxidized Met and ICPL_0, ICPL_4, and ICPL_6 for Lys were set as variable modifications.

Data processing for the identification and quantitation of ICPL-labeled protein triplex pairs was performed using Proteome Discoverer version 1.3 (Thermo Fisher) as described in Supplemental Information S1. Proteins with ratios of heavy/light label greater or less than 1.6-fold change were defined as being differentially expressed ($P < 0.05$; Perseus statistical tool). Proteins identified by at least two unique constituent peptides in at least two of the three biological replicates were taken into consideration.

SDS-PAGE and Western-Blot Analyses

SDS-PAGE, Coomassie blue staining, and silver staining were performed according to Gaupels et al. (2008b, 2008c). ImageJ was applied for the quantification of SDS-PAGE bands. The generation and application of anti-CYP18-3 was described previously (Lippuner et al., 1994). Anti-OsSnRK1A/B antiserum was raised against the synthetic peptide N'-RKWALGLQSRAHPRE-C',

which represents amino acid residues 383 to 397 of rice (*Oryza sativa*) SnRK1A and SnRK1B. The antibodies were a generous gift of Su-May Yu and Kuo-Wei Lee (Institute of Molecular Biology, Academia Sinica). The OxyBlot Protein Oxidation Detection Kit (Millipore) was employed for the detection of carbonylated proteins in 2.5 μL of phloem latex/2.5 μL of phloem buffer following the manufacturer's instructions.

Supplemental Data

The following materials are available in the online version of this article.

Supplemental Figure S1. Lactate levels in phloem latex.

Supplemental Figure S2. Amino acids and primary amines.

Supplemental Figure S3. ProteoMiner effect.

Supplemental Figure S4. Regulation of carbohydrate and energy metabolism after wounding.

Supplemental Table S1. Labeled and identified phloem latex proteins.

LITERATURE CITED

Aksamit A, Korobczak A, Skala J, Lukaszewicz M, Szopa J (2005) The 14-3-3 gene expression specificity in response to stress is promoter-dependent. Plant Cell Physiol **46:** 1635–1645

Alosi MC, Melroy DL, Park RB (1988) The regulation of gelation of phloem exudate from *Cucurbita* fruit by dilution, glutathione, and glutathione reductase. Plant Physiol **86:** 1089–1094

Aoki K, Suzui N, Fujimaki S, Dohmae N, Yonekura-Sakakibara K, Fujiwara T, Hayashi H, Yamaya T, Sakakibara H (2005) Destination-selective long-distance movement of phloem proteins. Plant Cell **17:** 1801–1814

Atkins CA, Smith PM, Rodriguez-Medina C (2011) Macromolecules in phloem exudates: a review. Protoplasma **248:** 165–172

Baena-González E, Rolland F, Thevelein JM, Sheen J (2007) A central integrator of transcription networks in plant stress and energy signalling. Nature **448:** 938–942

Baena-González E, Sheen J (2008) Convergent energy and stress signaling. Trends Plant Sci **13:** 474–482

Bailey-Serres J, Fukao T, Gibbs DJ, Holdsworth MJ, Lee SC, Licausi F, Perata P, Voesenek LA, van Dongen JT (2012) Making sense of low oxygen sensing. Trends Plant Sci **17:** 129–138

Beckmann M, Enot DP, Overy DP, Draper J (2007) Representation, comparison, and interpretation of metabolome fingerprint data for total composition analysis and quality trait investigation in potato cultivars. J Agric Food Chem **55:** 3444–3451

Beneteau J, Renard D, Marché L, Douville E, Lavenant L, Rahbé Y, Dupont D, Vilaine F, Dinant S (2010) Binding properties of the *N*-acetylglucosamine and high-mannose *N*-glycan PP2-A1 phloem lectin in Arabidopsis. Plant Physiol **153:** 1345–1361

Boudsocq M, Laurière C (2005) Osmotic signaling in plants: multiple pathways mediated by emerging kinase families. Plant Physiol **138:** 1185–1194

Buhtz A, Kolasa A, Arlt K, Walz C, Kehr J (2004) Xylem sap protein composition is conserved among different plant species. Planta **219:** 610–618

Carroll CR, Hoffman CA (1980) Chemical feeding deterrent mobilized in response to insect herbivory and counteradaptation by *Epilachna tredecimnotata*. Science **209:** 414–416

Catchpole GS, Beckmann M, Enot DP, Mondhe M, Zywicki B, Taylor J, Hardy N, Smith A, King RD, Kell DB, et al (2005) Hierarchical metabolomics demonstrates substantial compositional similarity between

genetically modified and conventional potato crops. Proc Natl Acad Sci USA **102:** 14458–14462

Chou IT, Gasser CS (1997) Characterization of the cyclophilin gene family of *Arabidopsis thaliana* and phylogenetic analysis of known cyclophilin proteins. Plant Mol Biol **35:** 873–892

Coello P, Hirano E, Hey SJ, Muttucumaru N, Martinez-Barajas E, Parry MA, Halford NG (2012) Evidence that abscisic acid promotes degradation of SNF1-related protein kinase (SnRK) 1 in wheat and activation of a putative calcium-dependent SnRK2. J Exp Bot **63:** 913–924

Feng S, Ma L, Wang X, Xie D, Dinesh-Kumar SP, Wei N, Deng XW (2003) The COP9 signalosome interacts physically with SCF COI1 and modulates jasmonate responses. Plant Cell **15:** 1083–1094

Fröhlich A, Gaupels F, Sarioglu H, Holzmeister C, Spannagl M, Durner J, Lindermayr C (2012) Looking deep inside: detection of low-abundance proteins in leaf extracts of Arabidopsis and phloem exudates of pumpkin. Plant Physiol **159:** 902–914

Fröhlich A, Lindermayr C (2011) Deep insights into the plant proteome by pretreatment with combinatorial hexapeptide ligand libraries. J Proteomics **74:** 1182–1189

Furch AC, Zimmermann MR, Will T, Hafke JB, van Bel AJ (2010) Remote-controlled stop of phloem mass flow by biphasic occlusion in *Cucurbita maxima*. J Exp Bot **61:** 3697–3708

Gaupels F, Buhtz A, Knauer T, Deshmukh S, Waller F, van Bel AJ, Kogel KH, Kehr J (2008a) Adaptation of aphid stylectomy for analyses of proteins and mRNAs in barley phloem sap. J Exp Bot **59:** 3297–3306

Gaupels F, Furch AC, Will T, Mur LA, Kogel KH, van Bel AJ (2008b) Nitric oxide generation in *Vicia faba* phloem cells reveals them to be sensitive detectors as well as possible systemic transducers of stress signals. New Phytol **178:** 634–646

Gaupels F, Knauer T, van Bel AJ (2008c) A combinatory approach for analysis of protein sets in barley sieve-tube samples using EDTA-facilitated exudation and aphid stylectomy. J Plant Physiol **165:** 95–103

Gaupels F, Vlot AC (2012) Plant defense and long-distance signaling in the phloem. *In* GA Thompson, AJE van Bel, eds, Phloem: Molecular Cell Biology, Systemic Communication, Biotic Interactions, Vol 1. Wiley-Blackwell, Hoboken, NJ, pp 227–247

Geigenberger P (2003) Response of plant metabolism to too little oxygen. Curr Opin Plant Biol **6:** 247–256

Gökirmak T, Paul AL, Ferl RJ (2010) Plant phosphopeptide-binding proteins as signaling mediators. Curr Opin Plant Biol **13:** 527–532

Gomez G, Torres H, Pallas V (2005) Identification of translocatable RNA-binding phloem proteins from melon, potential components of the long-distance RNA transport system. Plant J **41:** 107–116

Gottschalk M, Dolgener E, Xoconostle-Cázares B, Lucas WJ, Komor E, Schobert C (2008) *Ricinus communis* cyclophilin: functional characterisation of a sieve tube protein involved in protein folding. Planta **228:** 687–700

Hagel JM, Yeung EC, Facchini PJ (2008) Got milk? The secret life of laticifers. Trends Plant Sci **13:** 631–639

Hause B, Hause G, Kutter C, Miersch O, Wasternack C (2003) Enzymes of jasmonate biosynthesis occur in tomato sieve elements. Plant Cell Physiol **44:** 643–648

Hause B, Stenzel I, Miersch O, Maucher H, Kramell R, Ziegler J, Wasternack C (2000) Tissue-specific oxylipin signature of tomato flowers: allene oxide cyclase is highly expressed in distinct flower organs and vascular bundles. Plant J **24:** 113–126

Hemerly AS, Ferreira P, de Almeida Engler J, Van Montagu M, Engler G, Inzé D (1993) cdc2a expression in *Arabidopsis* is linked with competence for cell division. Plant Cell **5:** 1711–1723

Huber SC, MacKintosh C, Kaiser WM (2002) Metabolic enzymes as targets for 14-3-3 proteins. Plant Mol Biol **50:** 1053–1063

Jaspert N, Throm C, Oecking C (2011) Arabidopsis 14-3-3 proteins: fascinating and less fascinating aspects. Front Plant Sci **2:** 96

Konno K (2011) Plant latex and other exudates as plant defense systems: roles of various defense chemicals and proteins contained therein. Phytochemistry **72:** 1510–1530

Koo AJ, Gao X, Jones AD, Howe GA (2009) A rapid wound signal activates the systemic synthesis of bioactive jasmonates in Arabidopsis. Plant J **59:** 974–986

Koo AJ, Howe GA (2009) The wound hormone jasmonate. Phytochemistry **70:** 1571–1580

Lee KW, Chen PW, Lu CA, Chen S, Ho TH, Yu SM (2009) Coordinated responses to oxygen and sugar deficiency allow rice seedlings to tolerate flooding. Sci Signal **2:** ra61

Li L, Li C, Lee GI, Howe GA (2002) Distinct roles for jasmonate synthesis and action in the systemic wound response of tomato. Proc Natl Acad Sci USA **99:** 6416–6421

Lin MK, Lee YJ, Lough TJ, Phinney BS, Lucas WJ (2009) Analysis of the pumpkin phloem proteome provides insights into angiosperm sieve tube function. Mol Cell Proteomics **8:** 343–356

Lippuner V, Chou IT, Scott SV, Ettinger WF, Theg SM, Gasser CS (1994) Cloning and characterization of chloroplast and cytosolic forms of cyclophilin from *Arabidopsis thaliana*. J Biol Chem **269:** 7863–7868

Malter D, Wolf S (2011) Melon phloem-sap proteome: developmental control and response to viral infection. Protoplasma **248:** 217–224

McEuen AR, Hill HAO (1982) Superoxide, hydrogen peroxide, and the gelling of phloem sap from *Cucurbita pepo*. Planta **154:** 295–297

Mizoguchi T, Irie K, Hirayama T, Hayashida N, Yamaguchi-Shinozaki K, Matsumoto K, Shinozaki K (1996) A gene encoding a mitogen-activated protein kinase kinase kinase is induced simultaneously with genes for a mitogen-activated protein kinase and an S6 ribosomal protein kinase by touch, cold, and water stress in *Arabidopsis thaliana*. Proc Natl Acad Sci USA **93:** 765–769

Mullendore DL, Windt CW, Van As H, Knoblauch M (2010) Sieve tube geometry in relation to phloem flow. Plant Cell **22:** 579–593

Parker D, Beckmann M, Zubair H, Enot DP, Caracuel-Rios Z, Overy DP, Snowdon S, Talbot NJ, Draper J (2009) Metabolomic analysis reveals a common pattern of metabolic re-programming during invasion of three host plant species by *Magnaporthe grisea*. Plant J **59:** 723–737

Polge C, Thomas M (2007) SNF1/AMPK/SnRK1 kinases, global regulators at the heart of energy control? Trends Plant Sci **12:** 20–28

Read SM, Northcote DH (1983) Chemical and immunological similarities between the phloem proteins of three genera of the Cucurbitaceae. Planta **158:** 119–127

Ryan CA, Moura DS (2002) Systemic wound signaling in plants: a new perception. Proc Natl Acad Sci USA **99:** 6519–6520

Schluepmann H, Berke L, Sanchez-Perez GF (2012) Metabolism control over growth: a case for trehalose-6-phosphate in plants. J Exp Bot **63:** 3379–3390

Schobert C, Baker L, Szederkenyi J, Grossmann P, Komor E, Hayashi H, Chino M, Lucas WJ (1998) Identification of immunologically related proteins in sieve-tube exudate collected from monocotyledonous and dicotyledonous plants. Planta **206:** 245–252

Schwachtje J, Minchin PE, Jahnke S, van Dongen JT, Schittko U, Baldwin IT (2006) SNF1-related kinases allow plants to tolerate herbivory by allocating carbon to roots. Proc Natl Acad Sci USA **103:** 12935–12940

Seifert GJ (2004) Nucleotide sugar interconversions and cell wall biosynthesis: how to bring the inside to the outside. Curr Opin Plant Biol **7:** 277–284

Shoresh M, Gal-On A, Leibman D, Chet I (2006) Characterization of a mitogen-activated protein kinase gene from cucumber required for trichoderma-conferred plant resistance. Plant Physiol **142:** 1169–1179

Sun JQ, Jiang HL, Li CY (2011) Systemin/jasmonate-mediated systemic defense signaling in tomato. Mol Plant **4:** 607–615

Takahashi F, Yoshida R, Ichimura K, Mizoguchi T, Seo S, Yonezawa M, Maruyama K, Yamaguchi-Shinozaki K, Shinozaki K (2007) The mitogen-activated protein kinase cascade MKK3-MPK6 is an important part of the jasmonate signal transduction pathway in *Arabidopsis*. Plant Cell **19:** 805–818

Tallamy DW (1985) Squash beetle feeding behavior: an adaptation against induced cucurbit defenses. Ecology **66:** 1574–1579

Thorpe MR, Ferrieri AP, Herth MM, Ferrieri RA (2007) 11C-imaging: methyl jasmonate moves in both phloem and xylem, promotes transport of jasmonate, and of photoassimilate even after proton transport is decoupled. Planta **226:** 541–551

Tolstikov VV, Fiehn O (2002) Analysis of highly polar compounds of plant origin: combination of hydrophilic interaction chromatography and electrospray ion trap mass spectrometry. Anal Biochem **301:** 298–307

Toroser D, Plaut Z, Huber SC (2000) Regulation of a plant SNF1-related protein kinase by glucose-6-phosphate. Plant Physiol **123:** 403–412

Turgeon R, Oparka K (2010) The secret phloem of pumpkins. Proc Natl Acad Sci USA **107:** 13201–13202

van Bel AJE, Gaupels F (2004) Pathogen-induced resistance and alarm signals in the phloem. Mol Plant Pathol **5:** 495–504

van de Ven WT, LeVesque CS, Perring TM, Walling LL (2000) Local and systemic changes in squash gene expression in response to silverleaf whitefly feeding. Plant Cell **12:** 1409–1423

van Dongen JT, Schurr U, Pfister M, Geigenberger P (2003) Phloem metabolism and function have to cope with low internal oxygen. Plant Physiol **131:** 1529–1543

Walz C, Giavalisco P, Schad M, Juenger M, Klose J, Kehr J (2004) Proteomics of curcurbit phloem exudate reveals a network of defence proteins. Phytochemistry **65:** 1795–1804

Wang P, Du Y, Li Y, Ren D, Song CP (2010) Hydrogen peroxide-mediated activation of MAP kinase 6 modulates nitric oxide biosynthesis and signal transduction in *Arabidopsis*. Plant Cell **22:** 2981–2998

Xoconostle-Cázares B, Xiang Y, Ruiz-Medrano R, Wang HL, Monzer J, Yoo BC, McFarland KC, Franceschi VR, Lucas WJ (1999) Plant paralog to viral movement protein that potentiates transport of mRNA into the phloem. Science **283:** 94–98

Yang ZP, Li HL, Guo D, Tian WM, Peng SQ (2012) Molecular characterization of a novel 14-3-3 protein gene (Hb14-3-3c) from *Hevea brasiliensis*. Mol Biol Rep **39:** 4491–4497

Zhang B, Tolstikov V, Turnbull C, Hicks LM, Fiehn O (2010) Divergent metabolome and proteome suggest functional independence of dual phloem transport systems in cucurbits. Proc Natl Acad Sci USA **107:** 13532–13537

Zhang CK, Yu XY, Ayre BG, Turgeon R (2012) The origin and composition of cucurbit "phloem" exudate. Plant Physiol **158:** 1873–1882

Zhang ZP, Baldwin IT (1997) Transport of [2-^{14}C]jasmonic acid from leaves to roots mimics wound-induced changes in endogenous jasmonic acid pools in *Nicotiana sylvestris*. Planta **203:** 436–441

Zimmermann MR, Hafke JB, van Bel AJ, Furch AC (2012) Interaction of xylem and phloem during exudation and wound occlusion in *Cucurbita maxima*. Plant Cell Environ (in press)

Zuk M, Weber R, Szopa J (2005) 14-3-3 protein down-regulates key enzyme activities of nitrate and carbohydrate metabolism in potato plants. J Agric Food Chem **53:** 3454–3460

The extrafascicular phloem is made for fighting

Frank Gaupels[1]* and Andrea Ghirardo[2]

[1] Helmholtz Zentrum München, German Research Center for Environmental Health, Department of Environmental Sciences, Institute of Biochemical Plant Pathology, Neuherberg, Germany

[2] Helmholtz Zentrum München, German Research Center for Environmental Health, Department of Environmental Sciences, Institute of Biochemical Plant Pathology, Research Unit Environmental Simulation, Neuherberg, Germany

*Correspondence: frank.gaupels@helmholtz-muenchen.de

Edited by:
Sylvie Dinant, Institut National de la Recherche Agronomique, France

Reviewed by:
Biao Ding, The Ohio State University, USA

The fascicular (bundle) phloem (FP) distributes assimilates from photosynthetic active source leaves to sinks such as young leaves, meristems and roots. It is also involved in long-distance signaling and defence responses (Van Bel and Gaupels, 2004; Walz et al., 2004; Lough and Lucas, 2006). In the past, cucurbits were frequently used as model plants for phloem biochemistry because large quantities of phloem exudates can be easily sampled from incisions into petioles and stems. Analysing pumpkin (*Cucurbita maxima*) exudates more than 1100 phloem proteins and about 100 metabolites could be identified providing some insight into phloem functions (Fiehn, 2003; Lin et al., 2009).

However, recent publications convincingly demonstrated that cucurbit exudates do not represent pure FP sap but rather originate mainly from the extrafascicular phloem (EFP) blended with xylem fluid (Zhang et al., 2010, 2012; Gaupels et al., 2012; Zimmermann et al., 2013). The EFP is a network of sieve tubes outside of the vascular bundles found only in *Cucurbitaceae*. Due to this unique characteristic, knowledge obtained from analyses of EFP exudates must be carefully verified to apply also for the FP of other plants (Turgeon and Oparka, 2010).

These findings settled a long-standing debate on the origin and purity of cucurbit phloem exudates, but one important question is still not resolved: what is actually the main function of EFP and EFP-derived exudates in cucurbits? We will discuss here the hypothesis that the EFP functions in herbivore and pathogen defence similar to laticifers in other plant species. Consequently, for better differentiation from FP sap and owing to the latex-like properties EFP exudates will be termed phloem latex hereafter.

EXTRAFASCICULAR PHLOEM vs. FASCICULAR PHLOEM

The EFP consists of a complex network of perifascicular strands next to the vascular bundles, lateral commissural strands, entocyclic sieve tubes within the pit and ectocyclic sieve tubes in the cortex (Crafts, 1932). The companion cell/sieve element complexes of the EFP strands are similar in shape and diameter to the FP (Golecki et al., 1999). However, absence of the EFP from minor veins of source leaves suggests that this particular phloem is not involved in sugar loading (Turgeon and Oparka, 2010). The fact that the EFP does not connect sink and source tissues would generally argue against an important role of the EFP in assimilate distribution.

A detailed analysis of the sugar composition revealed low sugar concentrations in phloem latex due to dilution of EFP content with xylem fluid (Zhang et al., 2012; Zimmermann et al., 2013). A similar dilution effect was also observed for FP exudates suggesting similar sugar concentration and osmotic pressure within both phloem systems. However, the sugar composition differed considerably between FP and the various elements of the EFP. In the perifascicular phloem—like in the FP—the transport sugars stachyose and sucrose were most abundant whereas in ento- and ectocyclic sieve tubes non-mobile hexoses were most prominent (Zhang et al., 2012). These findings indicate that the perifascicular but not other elements of the EFP contribute to assimilate transport. Further studies e.g., using ^{13}C- or ^{14}C-labeling techniques (Ghirardo et al., 2011; Zhang et al., 2012) are needed to gain more detailed information of assimilate transport in the EFP.

Notably, the different types of extrafascicular sieve tubes are all involved in transport processes as evidenced by translocation of the phloem-mobile tracer 5(6)-carboxyfluorescein (Zhang et al., 2010) and graft-transmission of several phloem proteins including the major Phloem protein1 (PP1) and Phloem protein2 (PP2) (Golecki et al., 1999) within the EFP. PP1 and PP2 were also immuno-localized in the FP although the corresponding genes were mainly expressed in companion cells of the EFP, which would hint at plasmodesmal connections between the two phloem systems of cucurbits (Golecki et al., 1999).

Apart from symplasmic continuity, the ~50% overlap of so-far identified FP proteins from rice (*Oryza sativa*), rape (*Brassica napus*) and castor bean (*Ricinus communis*) with phloem latex proteins from pumpkin also suggested some degree of functional similarity between EFP and FP (Lin et al., 2009). On the other hand, the same comparison revealed that the EFP contained the complete machinery for protein translation, which is not present in the FP probably as an adaptation to assimilate transport functions (Lough and Lucas, 2006; Lin et al., 2009). Even within one plant—namely pumpkin—the protein composition was found to be disparate between exudates from EFP and FP (Zhang et al., 2010; Gaupels et al., 2012). Particularly, PP1 and PP2 make up to 80% of total protein content in phloem latex but were not detected by 1- and 2-dimensional polyacrylamid gel electrophoresis in FP sap of pumpkin.

In sum, the discussed data support the notion that EFP and FP are physically and functionally connected. This applies particularly to the perifascicular sieve tubes of the EFP. Given the reported differences in structure as well as sugar and protein composition it seems, however,

likely that the EFP network is at least partially separated from FP and probably has other functions than assimilate transport.

EXTRAFASCICULAR PHLOEM vs. LATICIFERS

Laticifers are specialized cells forming tubular systems with a distinct cytoplasmic content known as latex. A proposed function of laticifers is the synthesis and storage of compounds involved in herbivore and pathogen defence (Hagel et al., 2008; Konno, 2011). Here, we define latex as a plant exudate from intracellular stores with primarily defensive functions (Konno, 2011), which may but must not contain rubber particles (but cf. Pickard, 2008). Eminent examples of economically relevant latex-producing plants are opium poppy (*Papaver somniferum*) and para rubber tree (*Hevea brasiliensis*). Depending on the species laticifers can originate from various cell types. Interestingly, anastomosing (net-like) laticifers develop from phloem initials and are tightly associated with the vascular tissue (Hagel et al., 2008). Here, we hypothesize that the anastomosing EFP system shares common functions with anastomosing laticifers.

An important feature of laticifers is the secretion of copious amounts of latex from wounds. This way, insects are confronted with large droplets of the sticky and toxic fluid. Similarly, cucurbits bleed profoundly upon wounding. The exudation is driven by the high osmotic pressure in the EFP and by diffusion of xylem water into the EFP after wound-induced pressure release (Zhang et al., 2012; Zimmermann et al., 2013). The EFP content was estimated to be ~100-fold diluted by xylem fluid (Zhang et al., 2012). If the FP, which is rapidly plugged by callose, contributes considerably to phloem latex is still ambiguous and might vary between species (Zhang et al., 2012).

Previously, the EFP was assumed to be devoid of efficient sieve tube plugging by callose (Turgeon and Oparka, 2010; Zhang et al., 2012). However, wound-inducible polysaccharide synthesis reminiscent of callose formation (Gaupels et al., 2012) as well as SIEVE ELEMENT OCCLUSION proteins (Lin et al., 2009) were detected

in pumpkin phloem latex. These findings would imply that EFP occlusion is delayed or suppressed for facilitating unrestricted exudation from cuts. Only after unloading of the phloem latex the occlusion mechanisms are probably essential for reestablishment of the EFPs osmotic pressure and defensive arsenal (Gaupels et al., 2012).

Callose or other carbohydrates and proteins such as PP1 and PP2 which coagulate upon exudation could have dual functions (1) by causing the observed stickiness of phloem latex (Gaupels et al., 2012), which is essential for clogging insect mouth parts as was reported for the defence strategy of cucurbits against squash beetle (*Epilachna borealis*) (McCloud et al., 1995). (2) Additionally, callose and PP1/PP2 polymers could be involved in covering the wound site for sealing and protection from microbial ingress into the vascular system (Read and Northcote, 1983; Turgeon and Oparka, 2010).

The pressure-driven exudation of both laticifers and EFP can be circumvented by trenching (**Figure 1A**). Some beetle species isolate a circular leaf area through cutting all tissues except for the lower epidermis. Through this adaptive behavior the beetles clear the feeding area from harmful latex (Carroll and Hoffman, 1980; Tallamy, 1985; Konno, 2011).

DEFENCE-RELATED MOLECULES IN PHLOEM LATEX

To date, cucurbitacins are the best studied defensive metabolites in cucurbit phloem latex. They constitute a heterologous family of tetracyclic triterpenoids with a bitter taste and high cytotoxicity (Chen et al., 2005). Some cucurbitacins display antibacterial and antifungal activities. Others were shown to be involved in insect defence by acting as an antifeedant or antagonizing the effect of insect steroid hormones (Chen et al., 2005). For instance, when host leaves were painted with cucurbitacin B (**Figure 1B**) all six tested species of non-specialist herbivorous insects were deterred from feeding and two species were deterred from oviposition (Tallamy et al., 1997). However, specialist feeders of cucurbits can tolerate cucurbitacins or even use them for their own defence system (Carroll and Hoffman, 1980; Agrawal et al., 1999). Cucurbitacins are constitutively present

in phloem latex but levels further increase locally and systemically after herbivore attack (Carroll and Hoffman, 1980; Tallamy, 1985; Agrawal et al., 1999).

Inducible defence responses against herbivores and certain pathogens are under control of the plant hormone jasmonic acid (JA). After leaf wounding JA and its bioactive conjugate JA-isoleucine rapidly accumulated within 30 min in pumpkin phloem latex collected from distant petioles and stems indicating the onset of a systemic wound response (SWR) (Gaupels et al., 2012). During SWR JA is synthesized in the phloem and is transported as a systemic phloem-mobile signal (Li et al., 2002; Gaupels et al., 2012; Gaupels and Vlot, 2012).

Downstream-targets of JA in the EFP remain to be elucidated but could include amongst others the phloem latex proteins SILVERLEAF-WHITEFLY-INDUCED PROTEIN1, 18-kD CYCLOPHILIN, 16-kD PHLOEM PROTEIN1 and MITOGEN-ACTIVATED PROTEIN KINASE6, which were all increased in protein level after leaf damage (Gaupels et al., 2012). Further abundant proteins in cucurbit exudates are elements of the constitutive defence such as peroxidases, proteinases as well as PHLOEM SERPIN1 and other proteinase inhibitors (Walz et al., 2004; Frohlich et al., 2012; Gaupels et al., 2012). Similar defence proteins are also widespread in latex from laticifers (Konno, 2011).

The most remarkable protein in phloem latex is PP2. This protein has several proposed functions in defence and signaling. First of all, PP2 is a lectin. AtPP2-A1—the closest Arabidopsis homolog of cucurbit PP2—was shown to bind N-acetylglucosamine and glycans (Beneteau et al., 2010). The corresponding gene is inducible by the bacterial elicitor hairpin and transgenic overexpression of AtPP2-A1 induced resistance against the aphid *Myzus persicae* without exact mechanisms of resistance known (Zhang et al., 2011). Hence, PP2 could be involved both in defence against bacterial pathogens and phloem-sucking insects. Moreover, upon exposure to air oxygen the redox-sensitive PP2 and PP1 are responsible for stickiness and gelation of phloem latex as a defence trait against herbivorous beetles (McCloud et al., 1995).
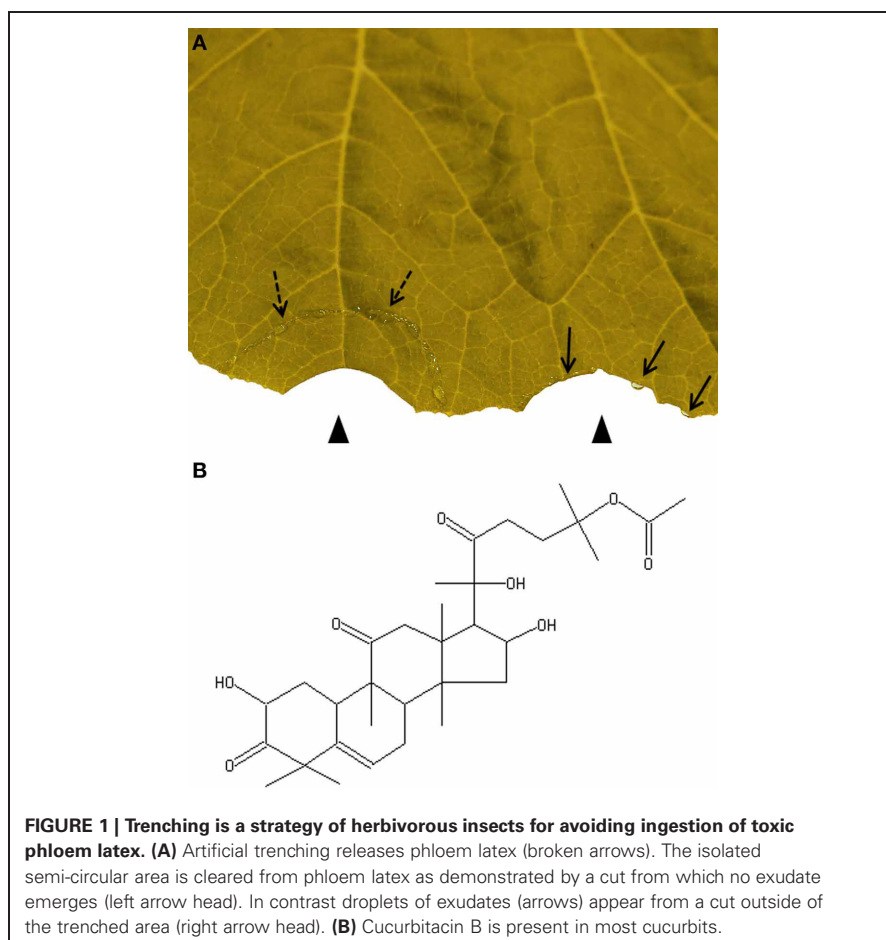
FIGURE 1 | Trenching is a strategy of herbivorous insects for avoiding ingestion of toxic phloem latex. (A) Artificial trenching releases phloem latex (broken arrows). The isolated semi-circular area is cleared from phloem latex as demonstrated by a cut from which no exudate emerges (left arrow head). In contrast droplets of exudates (arrows) appear from a cut outside of the trenched area (right arrow head). **(B)** Cucurbitacin B is present in most cucurbits.

In sum, the accumulation of cucurbitacins and major proteins related to signaling and defence responses in phloem latex further supports a protective role of the EFP system against herbivore attack and subsequent microbial infection.

CONCLUSIONS

The main function of phloem is distributing assimilates. Because the phloem contains highly nutritive molecules, which appeal insects and pathogens, it was evolutionary forced to develop efficient defence measures. In cucurbits the tasks of transporting assimilates and defending against attackers are shared by two specialized phloem systems. The FP is a linear and simply branched tubular system optimized for unhindered sugar translocation. In contrast, the structure of the EFP is net-like for better coverage of all tissues and improved resistance against insect counter-defences e.g., by vein cutting. The content of the EFP is highly enriched in proteins (PP1/PP2) and compounds with viscous, sticky and toxic properties. These features all resemble laticifers and would severly interfere with assimilate transport functions of phloem. Collective evidence rather supports the view that the EFP acts similar to laticifers as a pressure-driven defence mechanism against insects and pathogens.

PP2 and PP1 interact via intermolecular disulfide bridges between cysteine residues forming insoluble gel-like polymers under oxidizing conditions (Read and Northcote, 1983). However, even under non-stress conditions PP1 and PP2 self-assemble to filaments in the EFP while only a small proportion of the proteins is mobile (Smith et al., 1987; Golecki et al., 1999). At high levels mobile PP1 and PP2 would probably interfere with assimilate transport and therefore, filaments are stored in the EFP until pressure-released from cuts. After leaf wounding pumpkin PP2 abundance decreased transiently concomitant with a decline in protein carbonylation/oxidation suggesting that PP2 might be redox-modified under stress conditions (Gaupels et al., 2012). This redox-modification might trigger a monomerization and mobilization of PP2 in the phloem. PP2 monomers could act as defensive lectins or carriers of mRNA signals like recently shown in melon (*Cucumis melo*)

(Gomez et al., 2005; Beneteau et al., 2010).

Other defensive proteins in phloem latex typically also found in latex from other plants include a large set of protease inhibitors, proteases, peroxidases, and lipoxygenase (Walz et al., 2004; Konno, 2011). Although not directly related to herbivore defence it is significant that both in latex from *Hevea brasiliensis* as well as in pumpkin phloem latex, proteins of the translation and proteasome complexes including ribosomal proteins, eukaryotic translation initiation factors and elements of the proteasome constitute major functional categories whereas these proteins are largely missing in the FP (Lin et al., 2009; D'Amato et al., 2010; Frohlich et al., 2012; Gaupels et al., 2012). We speculate here that this finding reflects the special laticifer-like functions of the EFP, which necessitate extensive biosynthesis of defensive proteins and enzymes involved in the production of secondary metabolites.

REFERENCES

Agrawal, A. A., Gorski, P. M., and Tallamy, D. W. (1999). Polymorphism in plant defense against herbivory: constitutive and induced resistance in *Cucumis sativus*. *J. Chem. Ecol.* 25, 2285–2304. doi: 10.1023/A:1020821823794

Beneteau, J., Renard, D., Marche, L., Douville, E., Lavenant, L., Rahbe, Y., et al. (2010). Binding properties of the N-acetylglucosamine and high-mannose N-glycan PP2-A1 phloem lectin in Arabidopsis. *Plant Physiol.* 153, 1345–1361. doi: 10.1104/pp.110.153882

Carroll, C. R., and Hoffman, C. A. (1980). Chemical feeding deterrent mobilized in response to insect herbivory and counteradaptation by *Epilachna tredecimnotata*. *Science* 209, 414–416. doi: 10.1126/science.209.4454.414

Chen, J. C., Chiu, M. H., Nie, R. L., Cordell, G. A., and Qiu, S. X. (2005). Cucurbitacins and cucurbitane glycosides: structures and biological activities. *Nat. Prod. Rep.* 22, 386–399. doi: 10.1039/b418841c

Crafts, A. S. (1932). Phloem anatomy, exudation, and transport of organic nutrients in cucurbits. *Plant Physiol.* 7, i4–i225. doi: 10.1104/pp.7.2.183

D'Amato, A., Bachi, A., Fasoli, E., Boschetti, E., Peltre, G., Senechal, H., et al. (2010). In-depth exploration of *Hevea brasiliensis* latex proteome and "hidden allergens" via combinatorial peptide ligand libraries. *J. Proteomics* 73, 1368–1380. doi: 10.1016/j.jprot.2010.03.002

Fiehn, O. (2003). Metabolic networks of *Cucurbita maxima* phloem. *Phytochemistry* 62, 875–886. doi: 10.1016/S0031-9422(02)00715-X

Frohlich, A., Gaupels, F., Sarioglu, H., Holzmeister, C., Spannagl, M., Durner, J., et al. (2012). Looking deep inside: detection of low-abundance proteins in leaf extracts of Arabidopsis and Phloem exudates of pumpkin. *Plant Physiol.* 159, 902–914. doi: 10.1104/pp.112.198077

Gaupels, F., Sarioglu, H., Beckmann, M., Hause, B., Spannagl, M., Draper, J., et al. (2012). Deciphering systemic wound responses of the pumpkin extrafascicular phloem by metabolomics and stable isotope-coded protein labeling. *Plant Physiol.* 160, 2285–2299. doi: 10.1104/pp.112.205336

Gaupels, F., and Vlot, A. C. (2012). "Plant defense and long-distance signaling in the phloem," in *Phloem: Molecular Cell Biology, Systemic Communication, Biotic Interactions*, 1st Edn., eds G. A. Thompson and A. J. E. Van Bel (Hoboken, NJ: Wiley-Blackwell), 227–247.

Ghirardo, A., Gutknecht, J., Zimmer, I., Bruggemann, N., and Schnitzler, J. P. (2011). Biogenic volatile organic compound and respiratory CO2 emissions after 13C-labeling: online tracing of C translocation dynamics in poplar plants. *PLoS ONE* 6:e17393. doi: 10.1371/journal.pone.0017393

Golecki, B., Schulz, A., and Thompson, G. A. (1999). Translocation of structural P proteins in the phloem. *Plant Cell* 11, 127–140. doi: 10.1105/tpc.11.1.127

Gomez, G., Torres, H., and Pallas, V. (2005). Identification of translocatable RNA-binding phloem proteins from melon, potential components of the long-distance RNA transport system. *Plant J.* 41, 107–116. doi: 10.1111/j.1365-313X.2004.02278.x

Hagel, J. M., Yeung, E. C., and Facchini, P. J. (2008). Got milk? The secret life of laticifers. *Trends Plant Sci.* 13, 631–639. doi: 10.1016/j.tplants.2008.09.005

Konno, K. (2011). Plant latex and other exudates as plant defense systems: roles of various defense chemicals and proteins contained therein. *Phytochemistry* 72, 1510–1530. doi: 10.1016/j.phytochem.2011.02.016

Li, L., Li, C., Lee, G. I., and Howe, G. A. (2002). Distinct roles for jasmonate synthesis and action in the systemic wound response of tomato. *Proc. Natl. Acad. Sci. U.S.A.* 99, 6416–6421. doi: 10.1073/pnas.072072599

Lin, M. K., Lee, Y. J., Lough, T. J., Phinney, B. S., and Lucas, W. J. (2009). Analysis of the pumpkin phloem proteome provides insights into angiosperm sieve tube function. *Mol. Cell. Proteomics* 8, 343–356. doi: 10.1074/mcp.M800420-MCP200

Lough, T. J., and Lucas, W. J. (2006). Integrative plant biology: role of phloem long-distance macro-molecular trafficking. *Annu. Rev. Plant Biol.* 57, 203–232. doi: 10.1146/annurev.arplant.56.032604.144145

McCloud, E. S., Tallamy, D. W., and Halaweish, F. T. (1995). Squash beetle trenching behaviour: avoidance of cucurbitacin induction or mucilaginous plant sap? *Ecol. Entomol.* 20, 9. doi: 10.1111/j.1365-2311.1995.tb00428.x

Pickard, W. F. (2008). Laticifers and secretory ducts: two other tube systems in plants. *New Phytol.* 177, 877–888. doi: 10.1111/j.1469-8137.2007.02323.x

Read, S. M., and Northcote, D. H. (1983). Chemical and immunological similarities between the phloem proteins of three genera of the Cucurbitaceae. *Planta* 158, 119–127. doi: 10.1007/BF00397704

Smith, L. M., Sabnis, D. D., and Johnson, R. P. C. (1987). Immunochemical localisation of phloem lectin from *Cucurbita maxima* using peroxidase and colloidal-gold labels. *Planta* 170, 10. doi: 10.1007/BF00402980

Tallamy, D. W. (1985). Squash beetle feeding behavior: an adaptation against induced cucurbit defenses. *Ecology* 66, 1574–1579. doi: 10.2307/1938019

Tallamy, D. W., Stull, J., Ehresman, N. P., Gorski, P. M., and Mason, C. E. (1997). Cucurbitacins as feeding and oviposition deterrents to insects. *Environ. Entomol.* 26, 678–683.

Turgeon, R., and Oparka, K. (2010). The secret phloem of pumpkins. *Proc. Natl. Acad. Sci. U.S.A.* 107, 13201–13202. doi: 10.1073/pnas.1008134107

Van Bel, A. J. E., and Gaupels, F. (2004). Pathogen-induced resistance and alarm signals in the phloem. *Mol. Plant Pathol.* 5, 495–504. doi: 10.1111/j.1364-3703.2004.00243.x

Walz, C., Giavalisco, P., Schad, M., Juenger, M., Klose, J., and Kehr, J. (2004). Proteomics of curcurbit phloem exudate reveals a network of defence proteins. *Phytochemistry* 65, 1795–1804. doi: 10.1016/j.phytochem.2004.04.006

Zhang, B., Tolstikov, V., Turnbull, C., Hicks, L. M., and Fiehn, O. (2010). Divergent metabolome and proteome suggest functional independence of dual phloem transport systems in cucurbits. *Proc. Natl. Acad. Sci. U.S.A.* 107, 13532–13537. doi: 10.1073/pnas.0910558107

Zhang, C., Shi, H., Chen, L., Wang, X., Lu, B., Zhang, S., et al. (2011). Harpin-induced expression and transgenic overexpression of the phloem protein gene AtPP2-A1 in Arabidopsis repress phloem feeding of the green peach aphid *Myzus persicae*. *BMC Plant Biol.* 11:11. doi: 10.1186/1471-2229-11-11

Zhang, C. K., Yu, X. Y., Ayre, B. G., and Turgeon, R. (2012). The origin and composition of cucurbit "phloem" exudate. *Plant Physiol.* 158, 1873–1882. doi: 10.1104/pp.112.194431

Zimmermann M. R., Hafke J. B., van Bel A. J., and Furch A. C. (2013). Interaction of xylem and phloem during exudation and wound occlusion in *Cucurbita maxima*. *Plant Cell Environ.* 36, 237–247. doi: 10.1111/j.1365-3040.2012.02571.x